Multiscale characterisation of biodegradable flax composites through structural, mechanical and ageing investigations

Delphin Pantaloni

DOCTORAT BRETAGNE LOIRE SCIENCES POUR L'INGENIEUR

Université Bretagne Sud

Thèse de doctorat de

L'UNIVERSITE BRETAGNE SUD

ECOLE DOCTORALE N° 602

Sciences pour l'Ingénieur

Spécialité : Génie des Matériaux

Par

Delphin PANTALONI

Multiscale characterisation of biodegradable flax composites through structural, mechanical and ageing investigations

Caractérisation multi-échelle de composites de lin biodégradables par le biais d'études structurelles, mécaniques et de vieillissement

Thèse présentée et soutenue à Lorient, le 8 Décembre 2021
Unité de recherche : IRDL UMR CNRS 6027

N° ordre 609

Rapporteurs avant soutenance :

Patrick PERRE	Professeur des Universités, Centrale Supélec, Saclay
Peter DAVIES	Ingénieur de Recherche, HDR, IFREMER Brest

Composition du Jury :

Examinateurs :

Nina GRAUPNER	Research Associate, City University of Applied Sciences
Pierre OUAGNE	Professeur des Universités, École Nationale d'Ingénieurs de Tarbes
Johnny BEAUGRAND	Directeur de Recherche, INRAE Nantes

Dir. de thèse :	Alain BOURMAUD	Ingénieur de Recherche, HDR, Université de Bretagne Sud
Co-dir. de thèse :	Christophe BALEY	Professeur des Universités, Université de Bretagne Sud
Co-dir. de thèse :	Darshil U. SHAH	University Lecturer, University of Cambridge

"We are the first generation to feel the effect of climate change

and certainly the last to be able to do anything about it."

Cyril Dion

Acknowledgements

The work presented in this thesis was carried out at the Institut Dupuy De Lôme (IRDL), from the Université de Bretagne Sud, Lorient, France. It is the achievement of three years of research taking place in the FLOWER (Flax composites, for LOW weight, End of life and Recycling) project. It associated four academics institutions (Université de Bretagne Sud in Lorient, INRA in Nantes, University of Cambridge and University of Portsmouth) and four industries (Kaïros, Teillage Vandecandelaère, EcoTechnilin and Howa-Tramico). I wish to thank all involved partners for the meaningful and instructive discussions generated by the project. A special thanks to Chloé Joly (and then Lise Dugor) for coordinating the project and organising all the meetings and conferences.

My acknowledgement is attributed to Patrick PERRE, Professor at Centrale Supélec, and Peter DAVIES, Research engineer – HDR at Ifremer Brest, for evaluating this PhD thesis and accepting to be reporter. I also thank Nina Graupner, Pierre Ouagne and Johnny Beaugrand for being a part of this PhD evaluation jury as examiners. I look forward to fruitful exchanges regarding this PhD work thanks to your expertise in your respective fields.

These three years were full of learning experiences, rich scientific exchanges and exciting findings. It was an absolute pleasure to be under the supervision of Alain Bourmaud, Christophe Baley and Darshil U. Shah. Alain, thank you a lot for your implication on my PhD thesis, your numerous feedback and your positive point of view. A special point for your legendary reactivity and tranquillity, even when I forgot my luggage. I want to thank you, Christophe, for all the knowledge you shared with me, from composites to mechanics. Your scientific rigour and your storytelling skills were always appreciated before finalising our writing, and it was always a pleasure to discuss ecology with you. It was also a pleasure to be supervised by you, Darshil. Thank you so much for your innovative ideas, your motivation and your kindness. Furthermore, thank you for your hospitality. The two months spent in your lab at Cambridge were scientifically and personally very much appreciated. The eagle is waiting.

This two-month exchange was not possible without the agreement of Michael Ramage and Pierre-Yves Manach. Thank you for your positive answer. A special thanks to Mutsuko Grant, who worked hard for my exchange arrival and made sure I felt at home in this new lab.

Back to France, I would love to thank all the technical support I had during these three years, more specifically Anthony, Isabelle, Hervé, Lénaïck, Sylvie and Antoine. Thank you Sylvie for all the time spent on carried out experiments. Unfortunately, sometimes a protocol is much more complex than

expected. Many thanks to Antoine K. for all your advice on experimental setups. I did not listen to them each time, but it would have been time-saving if I had done it more often. Thanks also for the time spent on sharing our intuition or experience on many subjects.

During this thesis, I had the opportunity to meet and collaborate with several researchers, which was always a great pleasure. A special thank you to Johnny Beaugrand, Sofiane Guessasma and Eric Rondet, for our exciting talks, debates and shared knowledge.

It is time to acknowledge all my colleagues. Thank you all for the coffee discussions, it was a pleasure to share these good times in the office with all of you. A big thanks to the three of you, Lucile, Victor P. and Victor G. What a team! Many times spent together, working and thinking hard about flax composites. It was a great thesis adventure spent at your side. Be careful Mother Nature, we are coming for you! Our crew has grown since the arrival of Maïalen, Lata, Guillaume, and Elouan. I shared a lot of great moments around perfect meals, delicious beverages or camping adventures with all of you. I hope many others will come, with some slackline around. It is now time to leave the next generation be in charge of the office. Roxane, Thomas and Elouan, I wish you all the best for your remaining PhD years. Please take care of my plants and my mentees.

I want to make a special mention to all my family, without whom I would not be here today. Thanks for accompanying me in my decisions all along my university education. Sorry for the time spent speaking about science during family meetings! Finally, a big thank you, Lulu, for supporting me in the good and more complicated moments. Your optimism and energy were always here to remind me of the importance of a relaxed mind, thank you!

Table of contents

General Introduction

In August 2021, the Intergovernmental Panel on Climate Change (IPCC) released its latest report on climate change, affirming that humans are undeniably responsible for climate change, with many of the impacts irreversible. The global surface temperature has already risen by 1.1°C between 1850 - 1900 and 2011 – 2020, calculated as the difference between the mean value of both periods. Depending on the future greenhouse gas (GHG) emission, the IPCC concluded that this increase in temperature would keep rising during the current century to a value in 2100 between 1.6°C (CO_2 emission declined to net-zero by 2050) and 4.4°C (CO_2 emission double by 2050 before decreasing). This increase is not homogenous in the earth, with a higher increase over land (up to +0.7°C) than over the oceans. One way to grasp the impact of these global surface temperature modifications is to look at the frequency of rare meteorological events. IPCC estimates the modification in frequency and intensity of extreme heat waves appearing once during ten years in a climate without human influence. With the present increase of temperature of +1°C, this heatwave appears 2.8 times and are 1.2°C hotter than a heatwave occurring between 1850-1900 (reference used by IPCC). Switching from a scenario of +1.6°C to +4.4°C, the frequency increases from 4.1 times to 9.4 times. Additionally, the heatwave will be +1.9°C to +5.1°C hotter. This highlights the necessity for humanity to do its best to be in a scenario with a moderate temperature rise.

This temperature rise is mainly due to GHG. Therefore, it is vital to reduce emissions drastically. Transportation is responsible for a quart of the European GHG emission and 31% of the French GHG emission. Composite materials appear to be a solution for lightning transport means, thereby decreasing their in-use GHG emissions. However, these materials present critical environmental impacts due to the raw materials used - synthetic fibres and petro-sourced matrix - and their limited end-of-life disposal scenario - principally landfill. Recycling is practical for thermoplastic composites, though not mandatory in all transport sectors.

Flax fibres are a credible alternative to synthetic fibres, especially glass, due to their low density and remarkable mechanical properties. They are already used in the automotive area for interior parts of cars and have started to be used in motorsports (car body/seat) and sailing (hull). However, there is a notable lack of low areal-density flax preforms in the market. Such preforms could lead to more versatile composites for transport materials. The INTERREG “Flax composites, LOW weight, End of life and Recycling” (FLOWER) project aims to fill in this gap. Four academic institutions (Université de Bretagne Sud, University of Cambridge, INRAE, University of Portsmouth) and four industrial

companies (Ecotechnilin, Kaïros, Howa-Tramico, Depestele) have been working together to develop new light-weight flax preforms for composite industry, including a bi-axial flax preform and an oriented non-woven flax preform. This thesis is a part of the FLOWER project, focussing principally on the oriented non-woven flax preform and its potential to be reinforced by bio-degradable polymers. Indeed, one prototype developed in the project is a panel made of flax and biodegradable polymer (PLA) for Point Of Purchase (POP) application.

The recent enlargement of biodegradable thermoplastics is able to tackle the second drawback of composite materials: end-of-life management. Thanks to the use of a thermoplastic matrix, the composite is also recyclable. This allows reusing the material of a product as new raw material for similar or another application, spreading the environmental impacts between the different life of the materials. Furthermore, the biodegradability behaviour of the composite suggests compostability as another end-of-life solution.

This thesis aims first to investigate the mechanical potential of three biodegradable thermoplastics (poly-(lactide) (PLA), poly-(butylene-succinate) (PBS), poly-(hydroxy alkanoates) (PHAs)) as a matrix for flax composite materials. The second part focuses on the ageing behaviour of these materials.

In chapter 1, a state-of-the-art review discusses the current knowledge on developing biodegradable flax composites. Following a clarification on terminology, the origins, properties and biodegradation of biodegradable polymers are then discussed. Additionally, a structural and mechanical description of flax fibres is presented. Before dealing with the composite, the notion of the interface is addressed. Then, the manufacturing of thermoplastic flax composites is developed and its influence on the flax and the composite. Other parameters influencing the mechanical properties of flax composites are then presented, from microstructure to heterogeneity at the microscale. The ageing behaviour of flax composite and biodegradable flax composite in several environments is discussed. Finally, a discussion on the environmental impact of biodegradable composite systems is proposed.

The reinforcement of a matrix by flax fibres depends on their affinity; strong adherence between the composite’s constituents allows to exploit the potential of reinforcement of the fibres fully. Knowing the interfacial strength of several formulations is a first approach to understanding the composite's mechanical efficiency. That is why chapter 2 focuses on the interfacial characterisation of a range of biodegradable polymers and flax fibres systems. Thanks to a microscale level investigation, the adhesion between biopolymers and elementary flax fibres is measured and compared to industrial references. Unidirectional and bi-axial composites are then tensile tested to obtain their mechanical

properties. The importance of the flax/matrix interfacial properties and the matrix mechanical values help to discuss and understand the mechanical properties of the biobased composite materials developed in this chapter.

Chapter 3 studies the influence of the orientation of the non-woven preform developed in the project. It is made through a simple carding process, mixing PLA fibres and flax fibres at a weight ratio of 50%. The porosity, as well as the shives, are quantified. Thanks to a tomography analysis, the microstructure of the composite is observed. Furthermore, the distribution of the orientation inside the composite is explored. The anisotropy of mechanical properties is investigated thanks to off-axis tensile tests. The modulus of the composite at several angles is correlated to the orientation of the fibres. The possibility of using mechanical characterisation for fast and cheap composite fibre orientation analysis is finally discussed.

During the service life of a composite, its surrounding environment may evolve. As flax/PLA composites are sensitive to moisture, the influence of relative humidity on their mechanical and structural properties should be tackled. Chapter 4 brings answers to the impact of water (in liquid or vapour form) on the microstructure and the mechanical properties of a flax/PLA non-woven composite. First, the sorption of the composite submitted to hygroscopic (50RH/75RH/98RH/immersion) conditions is measured. Composites are then dried to focus on the irreversible impact of these environments. Next, the evolution of the composite constituent (flax and PLA) is studied at the micro-scale level. Then, the structural evolution (porosity/interface deterioration/microcracks) inside the composite is investigated and correlated to the decrease of mechanical properties observed.

Finally, chapter 5 suggests a harsh ageing condition, garden compost, to compare the evolution of the mechanical properties of biodegradable flax composites (flax/PLA, flax/PBS, flax/PHA) with flax/PP reference. The compost is not controlled, but the temperature and meteorological data are recorded. The degradation is investigated through weight loss and mechanical properties, highlighting two degradation behaviour depending on the biodegradable matrix used. The microstructure evolution is observed thanks to SEM and Micro-CT investigations and used to discuss the evolution of the mechanical properties.

The organisation of the thesis work is summarised in Figure 0-1.

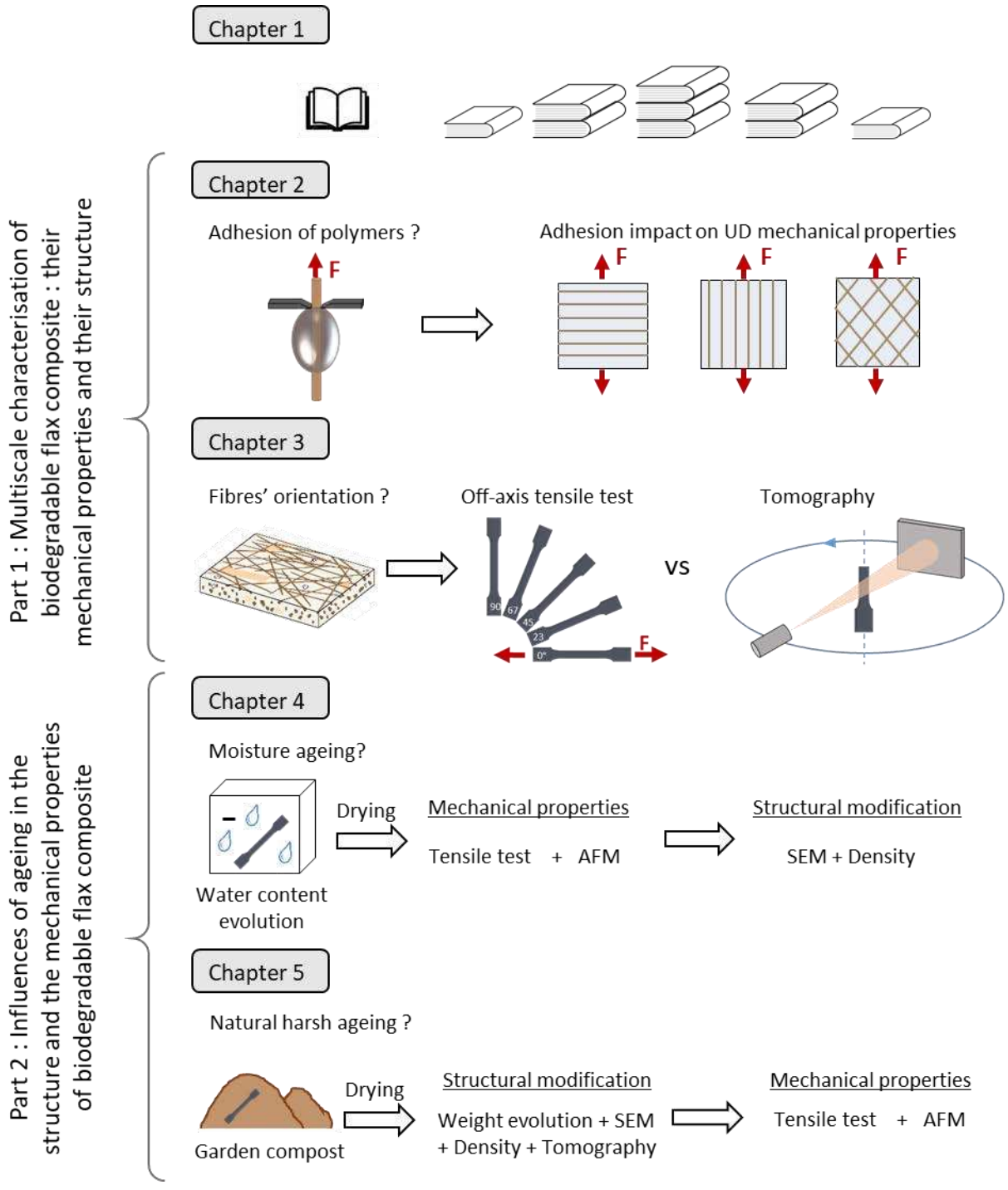

Figure 0-1: Schematic sum-up of work presented in the thesis

Scientific contributions

All chapters have been or will be submitted for publications in the form of international peer-reviewed journal papers.

I. Accepted Paper

Pantaloni D, Shah D, Baley C, Bourmaud A. Monitoring of mechanical performances of flax non-woven biocomposites during a home compost degradation. Polymer Degradation and Stability, 2020, https://doi.org/10.1016/j.polymdegradstab.2020.109166

Pantaloni D, Bourmaud A, Baley C, Clifford MJ, Ramage MH, Shah D. A Review of Permeability and Flow Simulation for Liquid Composite Moulding of Plant Fibre Composites. Materials, 2020, https://doi.org/10.3390/ma13214811

Pantaloni D, Rudolph AL, Shah D, Baley C, Bourmaud A. Interfacial and mechanical characterisation of biodegradable polymer-flax fibre composites. Composites Science and Technology, 2021, https://doi.org/10.1016/j.compscitech.2020.108529

Melelli Alessia, **Pantaloni D**, Balnois E, Arnould O, Jamme F, Baley C, Beaugrand J, Shah D, Bourmaud A. Investigations by AFM of Ageing Mechanisms in PLA-Flax Fibre Composites during Garden Composting. Polymers, 2021, https://doi.org/10.3390/polym13142225

II. Under review

Pantaloni D, Ollier L, Shah D, Baley C, Rondet E, Bourmaud A. Can we predict the microstructure of a non-woven flax/PLA composite through assessment of anisotropy in tensile properties? Composites Science and Technology.

III. In writing

Pantaloni D, Ollier L, Shah D, Baley C, Rondet E, Beaugrand J, Bourmaud A. Irreversible structural modification of flax/PLA composite after hygro and hydro-ageing and its impacts on mechanical properties

IV. International conferences

Pantaloni D, Shah D, Baley C, Bourmaud A. Humidity impact on the mechanical and microstructural properties of flax/PLA non-woven composite materials. Biobased Composites in Marine Environment Conference 2021, Lorient, France

Pantaloni D, Shah D, Baley C, Bourmaud A. Durability of biodegradable non-woven composites reinforced with flax fibres: evolution of mechanical properties during harsh ageing. 5th International Conference on Natual Fibers 2021, Online

Pantaloni D, Shah D, Baley C, Bourmaud A. Are biodegradable polymers suitable as matrix for biodegradable flax composites? 1st European Summer School on Bio-Based Composites 2021 (3rd best flash presentation award), Online

V. National conferences

Pantaloni D, Shah D, Baley C, Bourmaud A. Development of compostable composites reinforced with non-woven flax fibres: a study of mechanical properties and biodegradability (poster). 21ème Journée Nationales sur les composites 2019, Bordeaux, France

Pantaloni D, Shah D, Baley C, Bourmaud A. Durabilité de composites non-tissés biodégradables renforcés par des fibres de lin : évolution des performances mécaniques après un vieillissement sévère. JST AMAC : Durabilité des Matériaux Composites à Matrice Thermoplastique 2021, Online

Chapter 1: Literature review

This chapter presents a literature review on biodegradable thermoplastic polymers reinforced by flax fibres to obtain biodegradable composites. First, the notion of biodegradation is explained with some clarification of key terminology. Biodegradable thermoplastics and their characteristics are then explored thereafter. Then, the specificities of flax fibres as reinforcements are explored through the flax's chemical composition, structural architecture, and no-linearity behaviour. These parts aim to present in detail the composite's raw materials used in this thesis. Next, the notion of the interface is developed, as it is investigated in chapter 2 to discuss the feasibility of flax/biodegradable thermoplastics composite. Indeed, the interface is the critical stress transfer zone between reinforcement and matrix, especially for flax fibres that present several interfaces. Before dealing with the manufacturing process for thermoplastic composite, the flax fibres extraction and the typical flax preforms are presented. This help to understand the manufacturing choices made in the thesis and the varieties of preform used. Finally, the importance of the ply structure in its mechanical properties is developed, as it is the baseline of the results' discussion in chapters 3, 4 and 5. To conclude, the environmental impacts of flax composite are discussed as well as several end-of-life scenarios. It allows the environmental impact discussion of the biodegradable flax composite, highlighting the advantages and inconveniences of biodegradable flax composites.

I. General understanding of biodegradation

I.a. Biodegradation: a fuzzy term for a complex phenomenon

As an indicator of human pollution, plastic waste invasion is considered the second-biggest environmental concern after climate change [1]. According to Ellen MacArthur, *"[…], there could be more plastic than fish by weight in the oceans by 2050."*[2]. A recent study [3] claims that in 2020, there is more plastic on earth than the total mass of animals combined. As a response, commonly called "bioplastics" appear in the media as ecological alternatives, initially developed for packaging and mulching. However, it is more nuanced than that. First, the term "bioplastics" has to be more precise as it incorporates two different notions: bio-sourced and bio-degradable [4].

Bio-sourced polymers use biomass as source materials. Standards exist to quantify the proportion of biomass in a plastic without defining a limit to consider a plastic as bio-sourced [5]. However, one Japanese certification (JBPA BiomassPla Certification) defines this limit as 25% of the "biomass-based plastic ratio".

A simple definition of biodegradable polymers suggested by Dommergues et al. [6] is that polymers can undergo chemical reactions via natural ageing (environment, temperature, microorganism) to convert to water, carbon dioxide and biomass.

As presented in Figure 1-1, one notion (e.g. bio-sourced) does not imply the other (biodegradation). In this thesis, we will use the bioplastics poly-(lactide) (PLA), poly-(hydroxy alkanoates) (PHAs) and poly-(butylene-succinate) (PBS) as composite matrices, all of which are both bio-sourced and biodegradable.

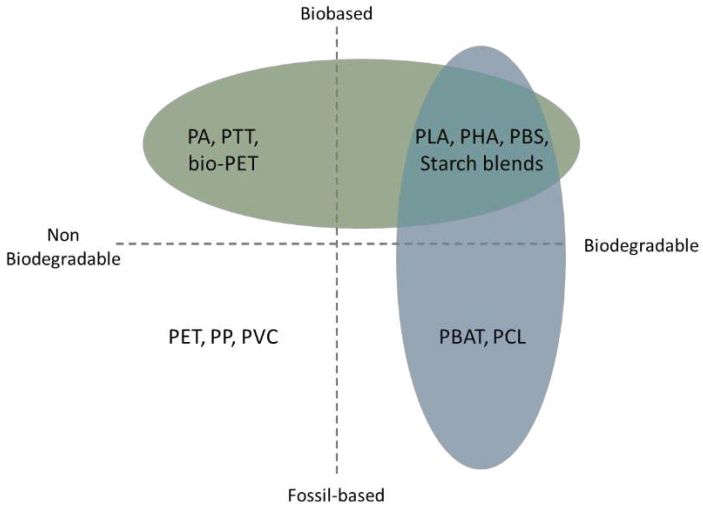

Figure 1-1: Classification of common thermoplastic polymers regarding their bio-sourced and/or bio-degradation behaviour, inspired by [4]

Nevertheless, bio-degradation is more complex than the definition proposed by Dommergues et al. [6]. Many reviews focus on explaining all the phenomena englobed under this notion [7–10]. As summarised in Figure 1-2, polymer degradation must first occur to reduce their size to an assimilable scale for microorganisms. The degradation of polymers (un-bio-degradable ones included) can be due to abiotic phenomena such as mechanical degradation, light degradation, thermal degradation and chemical degradation (mainly oxidation) [7]. In the specific case of biodegradable polymers, the colonisation by microorganisms at the macro-scale adds on to the list of degradation mechanisms. This bio-film secretes enzymes that catalyse chemical degradation. Furthermore, these polymers tend to be hydrophilic. The uptake of water impacts polymer micro-structure through plastification [11] and swelling [12]. In addition to oxidation, they undergo mainly hydrolysis [13]. Depending on water diffusion and kinetics of hydrolysis, the degradation occurs in the bulk or at the surface of the polymer [8,14]. The oligomers and monomers generated by the degradation can then be bio-assimilated by microorganisms, leading to mineralisation (HO_2, CO_2, CH_4, N_2 release) and new biomass. This bio-

assimilation was recently clearly observed on ^{13}C-labeled PBAT, where after six months in soil, ^{13}C was found in fungal hyphae and unicellular organisms attached to the PBAT surface [15].

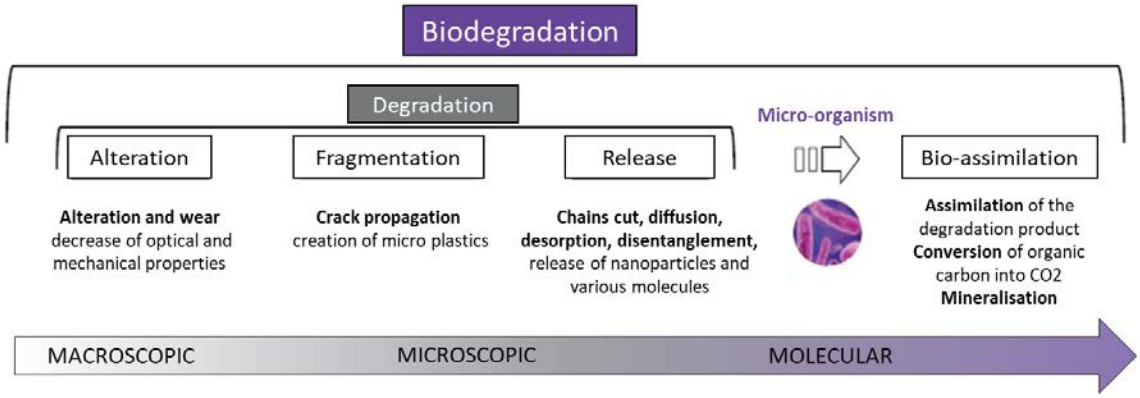

Figure 1-2: Following step for the biodegradation of polymers, inspired by Galgani et al. [13].

I.b. Standards and labels

Biodegradation englobes many phenomena, each one being environmentally dependent. Microorganisms will not be identical in compost, soil, nor sea. Light and oxygen also impact their population. The temperature differs in all these environments, influencing the microorganism activity and the polymeric chain mobility. Another critical parameter that should be specified speaking about biodegradation is the timescale considered. That is why several norms exist to oversee the biodegradation designation in the polymer industry. The ones focussing on compost biodegradation are NF T 51-800 and NF EN 13432, respectively, for domestic and industrial compost. Both are based on the same criteria: characterization of samples before testing, biodegradability, disintegration, compost quality and identification.

The biodegradability criterion is based on the quantity of carbon dioxide released (NF EN ISO 14855-1). The main differences are test environment and time considered. Material has to biodegrade in 6 months in compost at 58 ± 2°C to be considered as industrially compostable, where for a domestic compostable criterion, it should biodegrade under 25 ± 5°C in 1 year. For these two norms, labels delivered by TUV Austria exists: “OK compost industrial” and “OK compost home”. This same institution delivers equivalent labels for soil, water and seawater biodegradation based on the same tests as previously quoted norms. They use a temperature of 20 ± 5°C and a time consideration respectively of 2 years, 56 days and 6 months for soil, water and seawater. One standard (ISO 19679:2020), effective since 2020, is to quantify the aerobic biodegradability of a plastic film at seawater/sand interface. However, no critical value is given to consider the film as biodegradable in this environment.

II. Biodegradable polymers

II.a. Bio-sourced manufacturing

As previously said, the polymers investigated in this thesis are all bio-sourced (and biodegradable). However, different processes are used to obtain PHAs, PLA and PBS. For PBS, the grade used in this thesis is bio-sourced, but this polymer can also be petro-chemically synthesized.

PHAs are naturally produced by bacteria as energy reserves. Its production is now well understood and mastered [16–18]. Firstly, the bacteria population grow thanks to fermentation with carbon sources (sugar, fatty acid, renewable resources: cellulose, starch) and nutrient (nitrogen, phosphor, oxygen, amino acids, B-vitamins). Then, nutrients are reduced, leading to a C/N ratio too high for the bacteria. As a response to this stress, they convert the excess carbon in PHAs, stocked inside bacteria cells as energy reserves, as shown in Figure 1-3. The final step is to extract the PHAs from the cells, usually using solvents, following by purification to eliminate the organic residue. Depending on the bacteria, the carbon sources and nutrients, various types of PHAs are obtained.

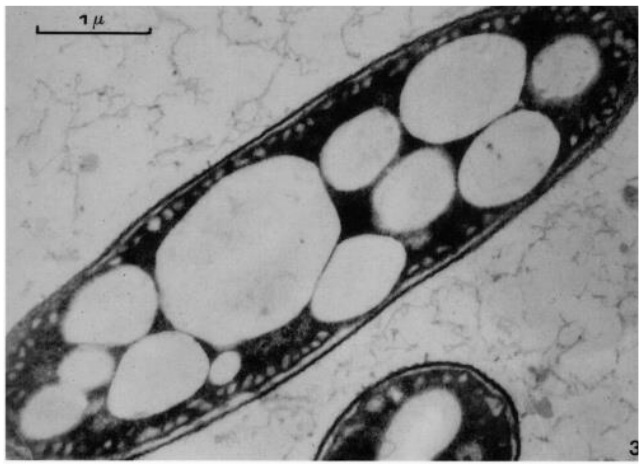

Figure 1-3: MET observation of PHB granulates inside a bacteria cell [18]

As presented in Figure 1-4, PHAs refer to a family of polymers with a specific monomeric sequence. It is commonly separated into three classes depending on the number of carbon in the alkyl group (R). The short-chain length PHAs are characterised by R = 1 or 2, medium-chain length PHAs by 3 to 13 and long-chain length PHAs for R > 13. This classification is described in Figure 1-4.

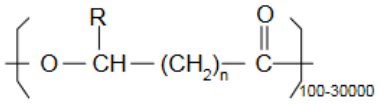

n =1	R =	hydrogen	poly (-3-hydroxypropionate)
		methyl	poly (-3-hydroxybutyrate)
		ethyl	poly(3-horoxyvalerate)
		propyl	poly (-3-hydroxyhexanoate)
		pentyl	poly (-3-hydroxyoctanoate)
		nonyl	poly (-3-hydroxydodecanoate)
n = 2	R =	hydrogen	poly (-4-hydroxybutyrate)
n = 3	R =	hydrogen	poly (-5-hydroxyvalerate)

Figure 1-4: Classification of polyhydroxyalkanoates according to their structure, extracted from [19].

On the other hand, PLA and PBS are chemically synthesized. Regarding PLA, a bacteria fermentation of carbohydrates forms lactic acid [20]. These carbohydrates can be extracted from corn/potato starch (glucose, maltose, dextrose) or beet sugar/cane (sucrose). Once the monomers are synthesized, several processes are available to obtain PLA [20,21]. The most efficient and widely used is the ring-open-polymerisation of the lactide, created by the natural condensation of the lactic acid, represented in Figure 1-5. As lactic acid is asymmetric, it is present under two enantiomeric forms: L(+) and D(-). L(+) lactic acid is the natural enantiomer, so it is the major one synthesized by the fermentation process (99,5%). Thanks to the ring-opening-polymerisation[21], the enantiomeric concentration could be controlled, leading PLA with various properties [22,23]. A pure L(+) PLA or D(-) PLA is called PLLA and PDLA, respectively, whereas PDLLA refers to a mixture of L(+) and D(-) PLA.

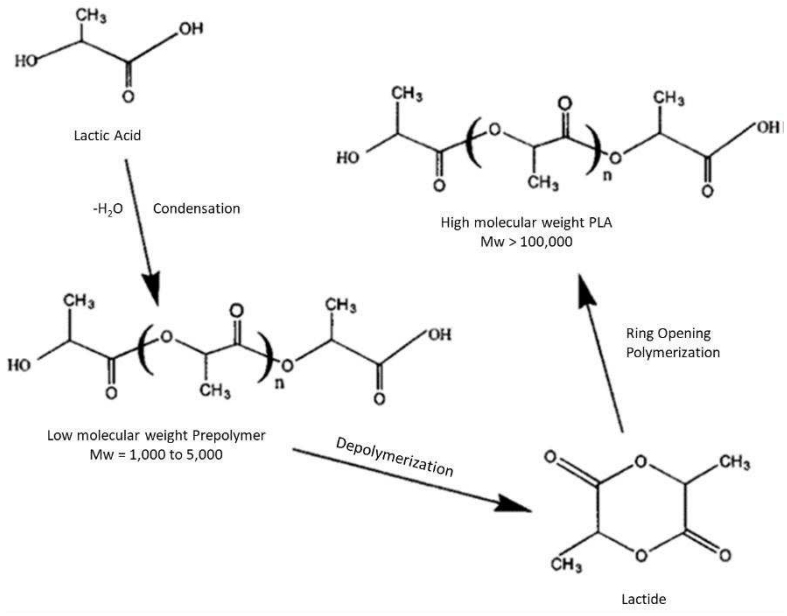

Figure 1-5: Ring-opening-polymerisation of the Lactide to synthesize high molecular weight PLA [20].

PBS are commonly petro-sourced, but all its precursors can now be synthesized from biomass [24]. That is why recently commercialised PBS are partially bio-based [25], with up to 50% of bio-sourced

carbon (Serpbio intern report). The succinic acid could be produced from the fermentation of renewable feedstock [24]. Cooper et al. [26] succeeded to catalytically reduce this succinic acid into 1,4-butanediol. Then, the esterification of these two precursors leads to PBS oligomers. A polycondensation of these oligomers is required to increase the molecular weight of PBS, as shown in Figure 1-6. However, this reaction is long, and the high temperature could cause side reactions, decreasing the molecular weight. This is why catalysts are often used in industry to accelerate the main reaction and avoid side ones [25].

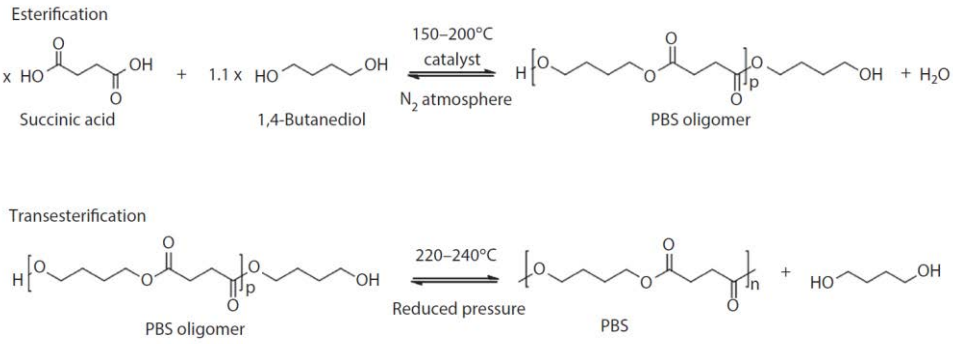

Figure 1-6: Polymerization process of PBS from succinic acid and 1,4-Butanediol. [25]

II.b. Mechanical properties

As they could be synthesized by many bacterial species [27], the short-chain length PHAs are the more commonly studied, especially the poly-(3-hydroxybutyrate) (PHB). However, its high crystallinity, between 60% and 90% [28], makes it a brittle polymer. One strategy to overcome this high crystallinity is to create a copolymer with PHB and a mcl-PHA, poly-(3-hydroxybutyrate)-co-(3-hydroxy valerate) (PHBV) being the most studied. Increasing the amount of PHV in the copolymer decreases its crystallinity and stiffness [29–31]. Depending on the amount of PHV, PHBV modulus evolves from 3.8 GPa (0 mol% of PHV) to 1.2 GPa (34 mol% of PHV) [32]. In this thesis, the PHBV used (PHI 002) contains 2 mol % of PHV [33]. In the next chapters, it will be called PHA as it is the only PHBV used in this work.

As previously discussed, PLA could undergo several enantiomeric conformations, which will modify its crystallinity, structure, and mechanical properties. For example, Perego et al. [34] observed a 20 % modulus decrease between a PLLA and a PDLLA. Indeed, PLLA (or PDLA) is a semi-crystalline polymer. Therefore, incorporating PDLA (or PLLA) greater than 7% in the PDLLA formulation leads to a completely amorphous polymer [22]. Interestingly, a 1:1 ratio of L(+) and D(-) leads to racemic crystallite and a polymer with higher glass transition and mechanical properties [20]. Thus, PLA could be found commercially in many grads depending on the PLLA/PDLA ratio and the polymer chain length. For example, the 2002D PLA (a PDLLA from Natureworks™) exhibits a tensile modulus of 3.5 GPa and a

strength of 53 MPa [35] for a 4.2 mol% of D(-) Lactic isomer content [36]. In this thesis, the PLA 3001D (from Natureworks™) is used, which is a PDLLA containing 1.4 mol% of D(-) Lactic isomer [37].

In contrast to both previous polymers, PBS is a less stiff polymer with mechanical properties comparable to low-density polyethene (LDPE) [38] with a tensile modulus of ≈ 0.6 GPa [38,39] and a strength of ≈ 35 MPa [24,25,40]. Once again, molecular weight and so crystallinity influence these properties [24]. Xu and Guo [40] focus on the crystallisation behaviour of PBS, finding that it acts like polyethene. For information only, Figure 1-1 compares mechanical properties of PLA, PHBV, PBS and three commonly used petrol-sourced thermoplastics, polypropylene (PP), LDPE and polyamide (PA11).

Table 1-1: Comparison of thermal and mechanical properties of biodegradable as well as conventional polymers. Data is extracted from literature [19,25,32,38,41–46]

	PLA	PBS	PHBV (%HV < 20%)	PP	LDPE	PA11
Glass transition temperature [°C]	60 – 65	-40 – -30	-10 – 10	-10 – 0	-120	-40
Melting temperature [°C]	160 – 200	110 –115	115 – 175	160 – 170	110	190
Tensile modulus [GPa]	2 – 4	0.5 – 0.700	1.5 – 4	1 – 1.7	0.3 – 0.4	1 – 1.2
Ultimate strength [MPa]	50 – 65	20 – 40	20 – 45	25 – 40	20 – 45	45
Ultimate failure strain [%]	2.4 - 5.4	150 – 500	4 – 30	4 – 500	300 – 400	250 – 300

In this thesis, the three biopolymers are compared to PP as it is the industrial standard for flax composite in the automotive sector [47]. Indeed, the automotive sector is currently the more developed market concerning flax/thermoplastic composites. They commonly thermos-compress flax/PP non-wovens to make interior parts of cars, such as dashboard and internal part of doors [48].

II.c. Differences in biodegradation behaviour of biodegradable polymers

As previously discussed, biodegradation of polymers depends on complex phenomena acting altogether. Despite its complexity, several reviews present a deep understanding of polymer biodegradation [7–10]. A focus is made here on differences between the three polymers investigated in this thesis, the first major one being the environment suitable for their biodegradation. First of all, due to its high glass transition temperature, PLA needs a temperature around 60°C to start its degradation process [49], occurring by abiotic hydrolysis [8]. With glass transition temperatures lower than ambient temperature, the temperature limit criterion is less restrictive for PHBV and PBS. Microorganisms present in the degrading environment are of importance too. The enzyme biodegrading PHAs (called depolymerases) are carboxylesterases [8], which can be created by many

bacterias and filamentous fungi present in nature, from seawater to compost. PLA needs more precise micro-organisms [50]. On the other hand, microorganisms degrading PBS are mainly present in soil or compost [51,52]. The presence and the activity of these microorganisms are primordial to the bio-assimilation step. Therefore, the biodegradation of biodegradable polymers in areas with low microbial activity (low humidity or low temperature) or low population (deep ocean) is more difficult. To summarise this, a biodegradation scale is presented in Figure 1-7.

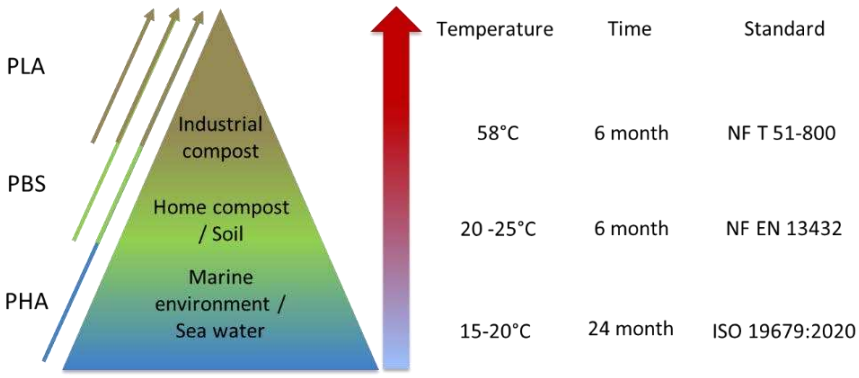

Figure 1-7: Schematic representation of the environment biodegrading the investigated polymers.

A second significant difference is the mechanism of erosion before bio-assimilation, specifically, the mechanisms of bulk erosion and surface erosion, described clearly by Laycock et al. [8] in Figure 1-8. The polymer properties evolve according to erosion type. PLA is known to undergo mainly bulk erosion [8,14], where PHAs are more subject to surface erosion [8,53,54]. For PBS, some studies have noted surface erosion [51], while others have highlighted bulk erosion [55]. These mechanisms compete, and many factors can influence which one is dominant [14,56], including the thickness of the sample (L) [57]. Indeed, as reported in Figure 1-8, there exists a critical thickness (L_{crit}), depending on the diffusion coefficient of water (D) and the pseudo-first-order hydrolysis rate constant (λ').

II.d. Biodegradation of plant fibres

Plant fibres are mainly constituted of polysaccharidic parietal polymers such as cellulose, hemicelluloses, lignin and pectins. Enzymes breaking down these complex polysaccharides can be secreted by many fungi and bacteria [58,59]. Both act in synergy to degrade efficiently plant fibres [59]. This microorganism is present and active in water and soil [60]. Van den Brink et al. [61] develops which fungal enzymes are responsible for the biodegradation of each polysaccharide. Plants fibres can also be digested by animals thanks to their rumen microorganism [62]. As all plant fibres constituents are biodegradable, using them to reinforce biodegradable polymers offers a new end-of-life scenario for the composite field: biodegradation. However, many plant fibres exist with their own structures and characteristics.

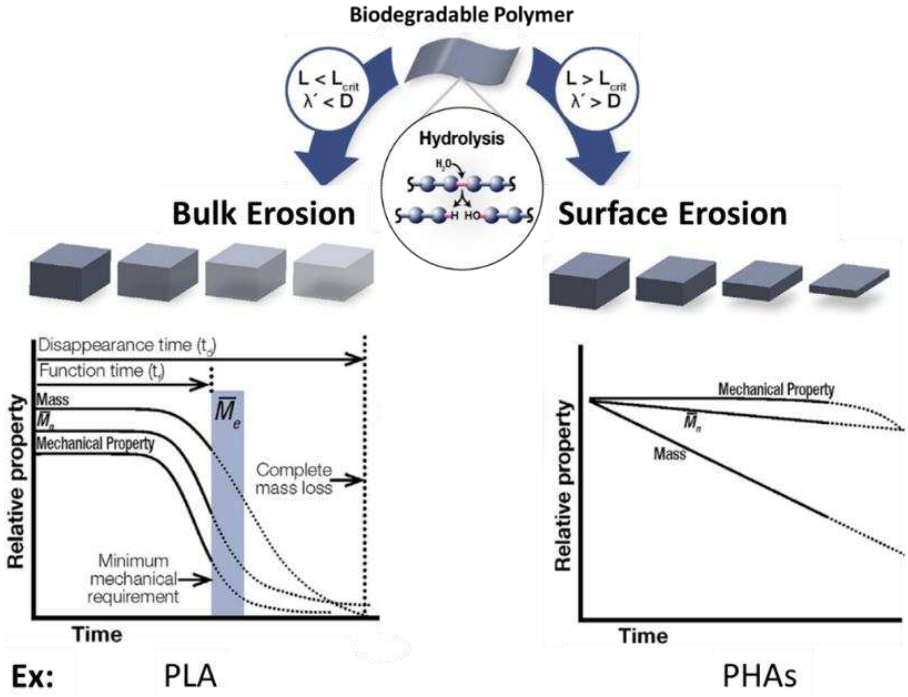

Figure 1-8: Schematic description of polymer degradation through hydrolysis, focusing on the erosion phenomenon and its impact on polymer properties. L is the thickness of the specimen, L_{crit} is the critical thickness where polymers erosion swishing from bulk to surface erosion. D is the diffusion coefficient of water of the polymers, and λ' is the pseudo-first-order hydrolysis rate constant, both parameters influencing $L_{crit.}$ Inspired by [8]

III. Flax fibres as a potential reinforcement for biodegradable polymers

III.a. Why flax?

A standard classification of plant fibres is based on their origin in the plant. Figure 1-9 represents this classification, giving some examples for each class and splitting each class into primary fibres (the aim of plant cultivation) and secondary fibres (a by-product of plant cultivation).

The agro-polymer composition found in fibres plants depends on many factors such as species [63], growth condition [60] and the fibre function inside the plant [63]. Table 1-2 presents this repartition for some common plant fibres.

Table 1-2: Biochemical composition of several plant fibres, according to [63].

	Cellulose [%]	Hemicellulose [%]	Lignin [%]	Pectin [%]	Other [%]
Flax	60 - 85	14 - 21	1 - 3	2 - 15	1 - 6
Sisal	53 - 65	19	11 - 14	10 - 14	<1
Cotton	83 - 98	4 - 6	1	4	2 - 3
Bamboo	36 - 55	11 - 17	21 - 29	<1	1 - 4

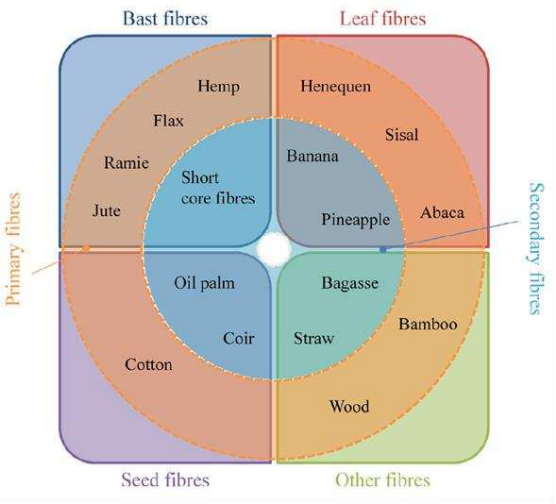

Figure 1-9: Plant fibre classification based on their origin in the plant. Extracted from [64]

The fibre's function in the plant, governed by its location in the plant, directly impacts their mechanical properties, represented in Table 1-3. For example, cotton fibres are seed hair used by the plant to enrobe the seed and support its dissemination. This function does not require specific mechanical properties, explaining the low stiffness of cotton fibres. On the other hand, flax fibres support the stem structurally, explaining its remarkable mechanical properties [65]. These properties come from a high proportion of cellulose, highly oriented in the direction of the fibres due to a slight microfibril angle (MFA) [66,67]. The hierarchical architecture of flax fibre is discussed in the following section.

Table 1-3: Mechanical properties of several plants fibres [63]. [1] referee to elementary fibres and [2] to bundles.

	Stiffness [GPa]	Ultimate strength [MPa]	Ultimate strain [%]	MFA (°)	Length [mm]
Flax[1]	37.2 – 75.1	595 – 1510	1.6 – 3.6	8.3 – 11.0	6 - 80
Sisal	9.0 – 25.0 [2]	347 – 577 [2]	2.3 – 5.45 [2]	20 [1]	0.5 – 8 [1]
Cotton[1]	5.5 – 13.0	287 – 800	3 – 10	20 – 30	10 - 60
Bamboo[1]	32.0 – 43.7	1200 – 1610	3.8 – 5.8	8 – 10.7	0.5 - 50

Additionally, flax is a major local product of France, accounting for 68% of the world flax production with a surface coverage of 122 000 ha [68]. Due to the textile background of flax, there is knowledge on flax fibres extraction and flax fabric manufacturing for textile but also composite with unidirectional and non-woven preforms now available. This is not the case for other plant fibres. That is why, in Europe, flax fibre is commonly chosen among plant fibres to be used in composite materials, from car dashboards [44] to hulls of boats [69]. However, flax appears to be more expensive (1 700 to 2600 $/ton) than other plant fibres such as sisal (700 to 1800 $/ton) or bamboo (250 to 500 $/ton) [63] as they are long fibres and used in textile. The following sections will only focus on flax fibres which are the only plant reinforcement used in the experimental work of this thesis.

III.b. Multi-scale structure of flax fibres

The localisation of flax fibres inside the flax stem and the multi-scale structure of flax fibres are represented in Figure 1-10. Thanks to retting and extraction processes [70], and due to the architecture of the fibre region *in planta*, extracted fibres are mainly present in the bundle form, which are an assembly of elementary fibres. Elementary fibres are glued together with a middle lamella, mainly composed of pectins [71] and calcium pectate, the latter being located explicitly on tricellular junctions [72]. A bundle is made in its section of between 30 and 60 elementary fibres [73]. Thanks to the intrusive growth, the number of fibres in length reach hundred elementary flax fibres [74]. The extraction process aims to individualised as much as possible the bundles present in stems to obtain smaller bundles counting only a few elementary flax fibres or ideally to split them into single flax fibres.

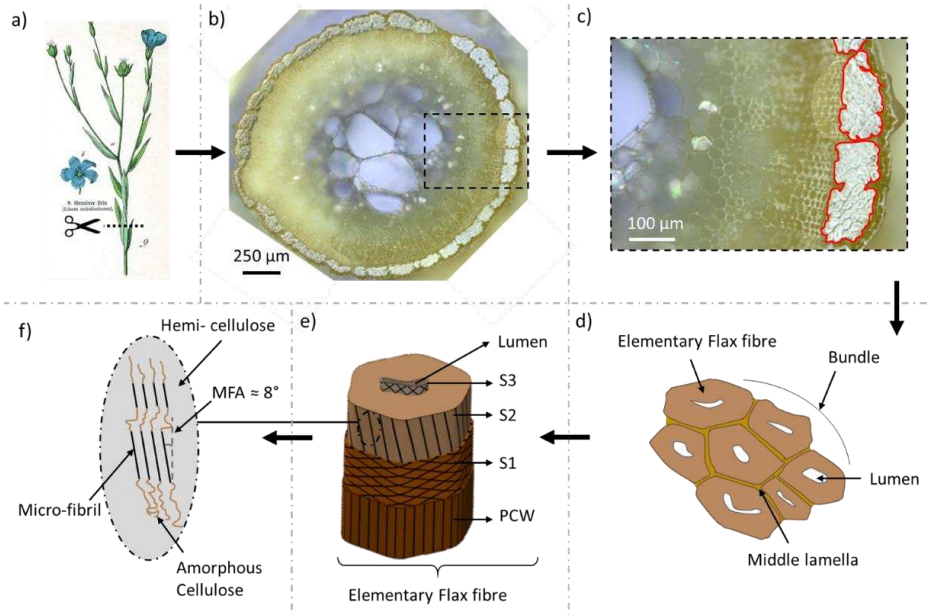

Figure 1-10: Flax fibres architecture, from the stem to the micro-fibril of cellulose, a) representation of a flax plant, b) cross observation of an Aramis flax stem (extracted from [75]), c) zoom on bundles inside the flax stem circled in red, d) schematic representation of the bundle constituent, e) micro-structure of an elementary flax-fibres, f) ultrastructure and microfibril of cellulose layout inside the secondary cell-wall.

Elementary flax fibre has a length of 35 ± 15 mm [71] and an apparent diameter of 17 ± 3 µm [72] typically. The fibre cross-section appears to be polygonal due to the intrusive growth of flax fibres inside bundles. Furthermore, the apparent diameter evolves along the fibres' length [74,76,77]. This diameter is lower for fibres extracted from the top of the stem [74]. The fibre length also depends on the location within the stem. Indeed, fibre length of 16 mm is measured at stem extremities against 35 mm in the middle [74].

Looking closer to elementary flax fibres, a complex architecture is observed with a primary cell wall (PCW) and three secondary cell walls called S1, S2 (or G-layer) and S3 (or Gn-layer)[78]. In the centre of the fibre, a hole called the lumen represents from 0.5% to 7% of a mature flax fibres cross-section [77,79]. Furthermore, the size of the lumen varies along fibres length and can be closed during few micrometres [79]. Its biochemical composition and its thickness characterise each cell wall. It appears that S2 is the predominant one with 90% of the global cell walls of a mature flax fibre [80]. It is composed mainly of cellulose micro-fibril, linked with hemicelluloses (galactan chains) [78,80]. In S2, these micro-fibrils are aligned together, making an angle estimated between 5° and 10° with the axial fibre direction [66,67]. This angle is called the microfibrillar angle (MFA). The MFA value impacts plant fibre mechanical properties as the micro-fibrils are more solicited with a low MFA [81]. Due to its large thickness, its high content of cellulose, mainly under micro-fibril shape and the low MFA, the S2 cell wall is mainly responsible for the apparent mechanical properties of flax fibres.

III.c. Mechanical behaviour of flax fibres

Micro-fibrils of cellulose are responsible for the mechanical properties of S2 cell-wall and so of flax fibres. They present high mechanical properties, with a stiffness estimated between 120 GPa and 140 GPa [82]. However, due to the complex internal structure of elementary flax fibres, including the MFA and other polysaccharidic parietal polymers, the stiffness of flax fibres is reduced. Baley and Bourmaud [83] estimate its average value to be 52.5 ± 8.6 GPa, based on 50 different flax batches tested in a period of 18 years. They reported tensile strength of 945 ± 200 MPa and a failure strain of 2.1 ± 0.5%. They explain the high scattering by the natural origin of flax, which is influenced by soil composition, meteorological conditions, and extraction processes (responsible for different densities of defects).

Furthermore, flax fibres have a density estimated between 1.45 and 1.50 $g.cm^{-3}$ [84], much lower than the 2.55 $g.cm^{-3}$ value of glass fibres [85]. This density difference induces a specific stiffness 31% higher for flax fibres than for glass fibres [86]. This clearly shows the potential of flax fibres to replace glass fibres when stiffness is of high interest for the applications.

As reported in Figure 1-11, flax fibres can present three different tensile behaviours. Type I (TI) is linear, type II (TII) appears to be bi-linear, where type III (TIII) is non-linear with a loss of stiffness at the beginning followed by an increase, TIII being the predominant behaviour [87]. The origin of this non-linear behaviour is still discussed in the literature.

One scenario proposed by Placet et al. [88] is represented in Figure 1-12 to explain the behaviour of elementary hemp fibres, which is similar to flax fibres.

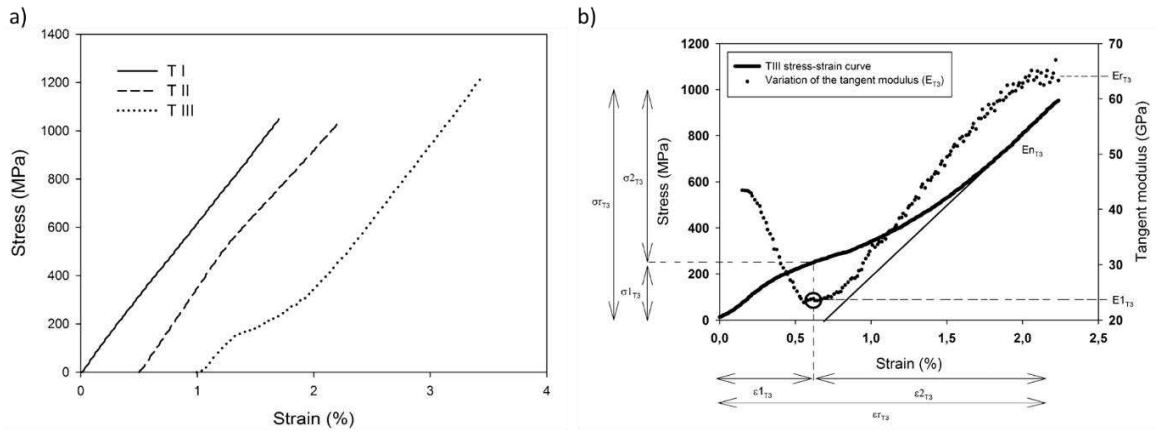

Figure 1-11: a) Several mechanical behaviours of elementary flax fibres, b) focus on the third behaviour (T III) and the stiffness evolution during the tensile test. [87]

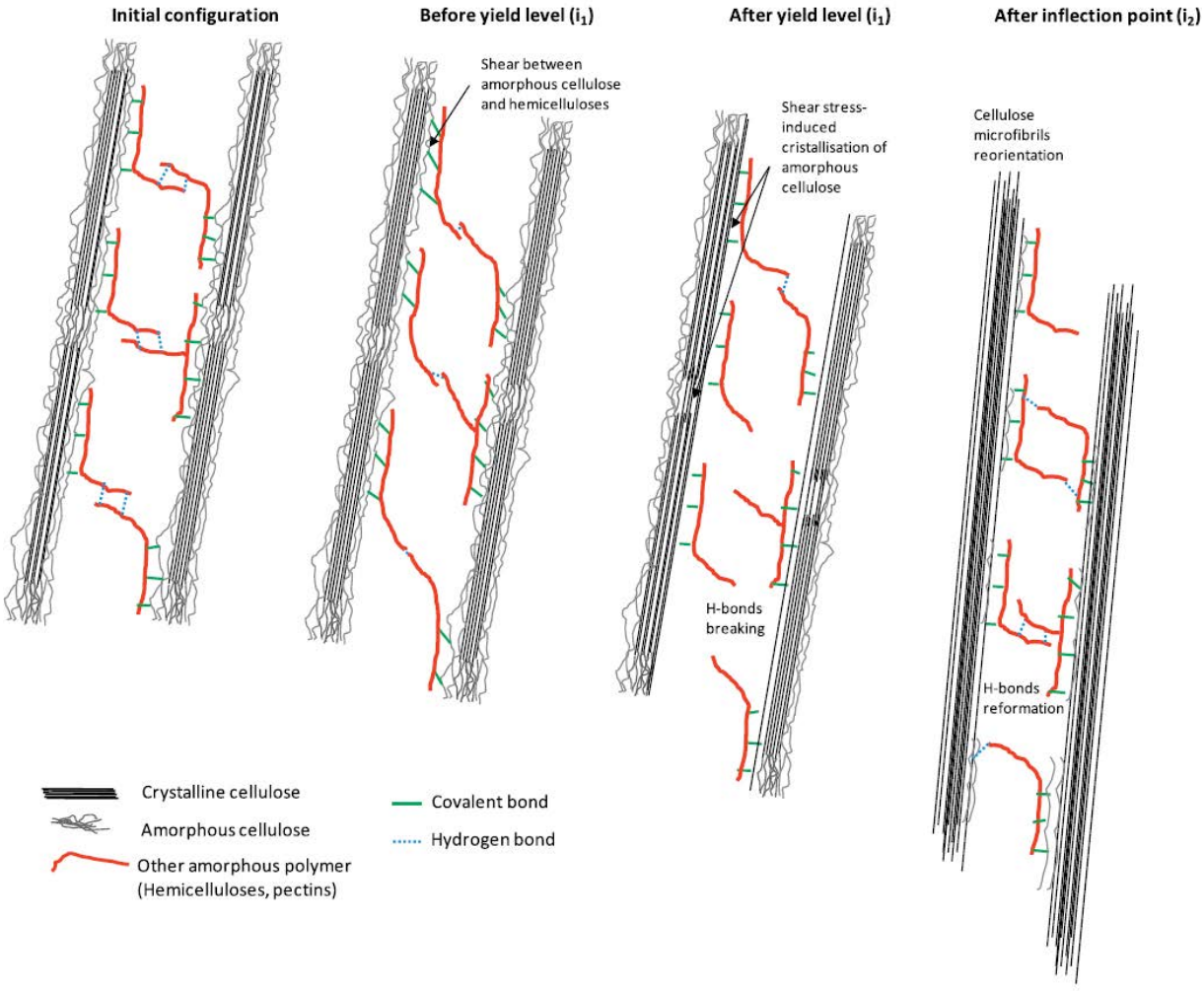

Figure 1-12: explanation of a TIII elementary hemp fibre behaviour (similar to flax) thanks to a scenario suggested in [88], taking into account the "slip and stick" phenomenon, the alignment of microfibrils and the crystallisation of amorphous cellulose.

The first non-linearity observed could be due to the rupture of hydrogen bonds at the micro-fibrils interface due to the local shear stress [89]. This rupture allows micro-fibrils to slide against each other thanks to a viscous flow of the polysaccharide matrix. If the stress is released, hydrogen bonds are created instantly, fixing the micro-fibrils in their new position. This mechanism called “stick and slip” is known for fibres wood [89]. During this slippage, micro-fibrils re-align, locally reducing shear stress and inducing an increase of stiffness observed in the second part of the strain-stress curve. In addition, kink-bands areas, with local MFA values reaching 30-40° [90], realign on the global micro-fibrils orientation, and amorphous cellulose rearranges itself to crystalize [88]. Both phenomena are additional explanations of the stiffness increase.

IV. Interface in flax composites

IV.a. Interface: What are we talking about?

By definition, a composite is an assembly of (at least) two heterogeneous materials. This assembly creates a small zone between materials, where stress transfer occurs between the reinforcement and the matrix [91]. This zone could have a thickness, called interphase, or can be thin enough to be considered an interface. In the specific case of thermoplastic composite, a layer of highly crystallised polymers are present close to the fibre, with properties different from the bulk polymers [92,93]. This polymer layer is considered to be an interphase between the reinforcement and the bulk polymer. On the other hand, the interface englobes phenomena that do not induce a discernable third phase. The adhesion is then created by physicochemical interactions, as presented in Figure 1-13.

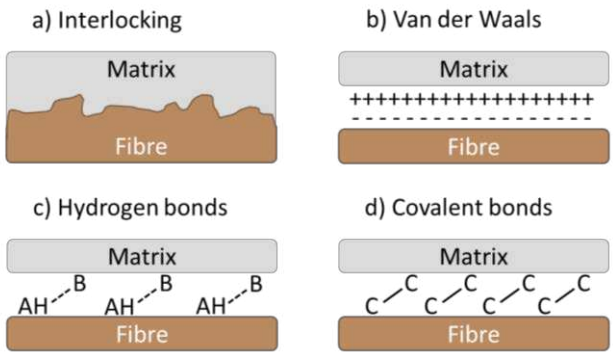

Figure 1-13: Schema of the interfacial mechanism between fibre and matrix, inspired from [94]. Expect from MAPP where d) covalent bonds are present, the interfacial mechanism of a) interlocking and/or b) Van der Waals and/or c) Hydrogen bonds are the predominant interfacial mechanism, especially for PLA, PHAs and PBS.

The physical link mainly refers to interlocking induced by surface roughness, see Figure 1-13.a). During composite processing, a low viscosity matrix can fill holes, crevices, micro-cavities or any surface

irregularity [94]. After matrix solidification, a mechanical anchoring process locks the fibres inside the matrix, lessening the pull-out phenomenon. Additionally, the residual stresses, induced by thermal or hygroscopic expansion or transcrystallinity interphase, increases this interlocking phenomenon due to a local radial compressive pressure between matrix and fibre [91,95], also increasing the static friction between the fibres and the matrix. Thus, the roughness gives rise to an increase of other bonding mechanisms as the contact surface area improves [94]. In the specific case of flax fibres, Baley et al. [96] suggested that the roughness of flax fibres is due to residues adhering poorly to the surface. They can play a role in energy dissipation during interface failure but cannot serve as anchors for interlocking mechanisms.

In addition to physical interaction, chemical interactions have a role in the adhesion between reinforcement and matrix. It can be due to chemical bonds or adsorption through van der Waals reaction or hydrogen bonds. Van der Waals interactions are present as long as two atoms or molecules are close to each other, arising from "*the correlation of fluctuations in the electron distribution of neighbouring molecules*" [97]. This interaction is predominant when at least one of the constituents is chemically inert, which is the case for flax/PP interface due to PP. The surface of elementary flax fibres comprises several agro-polymers, predominantly cellulose, hemicelluloses and pectins [96]. These constituents present hydroxyl groups, allowing flax fibres to be a proton donor, leading to potential hydrogen bonds with the surrounding matrix. As define by Gilli and Gilli [98]: "*Hydrogen bonding occurs between a proton-donor A-H and a proton-acceptor group B, where A is an electronegative atom, O, N, S, X (F, Cl, Br, I) or C and the acceptor group is a lone pair of an electronegative atom or a* π *bond of a multiple bond (unsaturated) system. Generally, a H-bond can be characterized as a proton shared by two lone electron pairs*". As the hydrogen bonds are stiffer than van der Waals interactions [99], the adhesion between flax and a matrix presenting a proton-acceptor group will be higher than with an inert matrix.

Chemical bonding is the strongest chemical interaction potentially present in an interface, where two atoms share electrons. As a result, the surrounding hydroxyl group of flax fibres reacts with the matrix to create a covalent link. As presented in Figure 1-14, this is suggested in the literature that it is the case for flax fibres/MAPP [100].

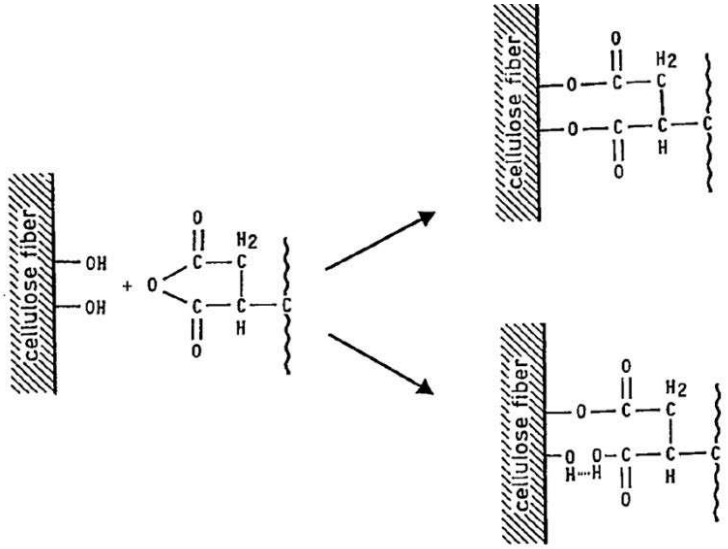

Figure 1-14: The suggested chemical reaction between hydroxyl group present on flax fibres surface and grafted PP with maleic anhydride [100]

Adhesion is a complex phenomenon where all the previously developed phenomena act together. The flax fibres surface corresponds to the primary cell wall (PW) made of celluloses, hemicelluloses and pectins. Each molecule can interact differently with the matrix, inducing adsorption due to a mix of van der Waal interactions and hydrogen bonds, interlocking phenomenon and potential chemical bonds.

IV.b. Several interfaces in a flax composite

Furthermore, as developed in section III.b, flax fibres have a complex structure leading to the presence of multiple types of interfaces and interphases at the composite level [96], as presented in Figure 1-15. An elementary flax fibre/polymer matrix interface is considered the primary stress transfer region between the matrix and the fibre [101], schematised in Figure 1-15.b) and observed for a flax/PBS composite in Figure 1-15.e). Ideally, elementary flax fibres are the only reinforcement arrangement in the composite. However, due to the natural origin of flax fibres and the extraction process, bundles and sometimes shives or cortical parenchyma are also present. The middle lamella appears to be a fibre/fibre interphase linking elementary flax fibres together in bundles, as observed in Figure 1-15.c) and f). The importance of the middle lamella should not be disregarded as it may be a zone of weakness in a composite [102,103]. The cell walls present inside elementary flax fibres can be a critical zone too. Indeed, it was observed by Le Duigou et al. [104] that epoxy resin can impregnate the flax cell walls to a depth of 2 µm. This phenomenon induces that the interface solicited is the cell walls interface rather than the matrix/fibres one. This can lead to a pealing phenomenon [105], observed in Figure 1-15.d).

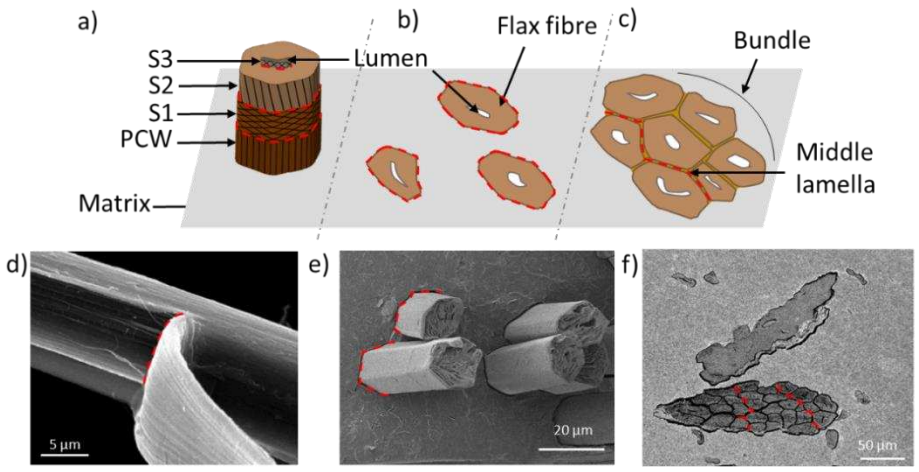

Figure 1-15: Schema and SEM representation of multiple interface and interphase at the composite scale level for flax reinforced composite, a) & d) focus on cell walls interface through pealing phenomena [105], b) & e) focus on the matrix/elementary flax fibres interface, c) & f) deal with the middle lamella as an interphase between elementary flax fibres inside a bundle.

The reliability of making flax composite depends on the affinity between elementary flax fibres. This affinity is physically obtained through the polymer/fibre interface, studied at two scale levels [101]. As many interfaces could be present in a flax composite, the adhesion investigation between elementary flax fibres and polymer is more precise at the micro-scale level, avoiding the influence of the middle-lamella. Using the composite to investigate the interface remains possible. It is more convenient to use, but the mechanical solicitation occurs not only at the flax/matrix interface.

IV.c. Shear characterisation at flax/matrix interface

The micro-scale focus on the interfacial shear strength (IFSS) at the interface fibre/polymer. Many protocols exist with their advantages and disadvantages [101,106]. Among them, the fragmentation test [107–109], pull-out test [110] and micro-droplets test [108,111–113] are the more common and are represented in Figure 1-16.

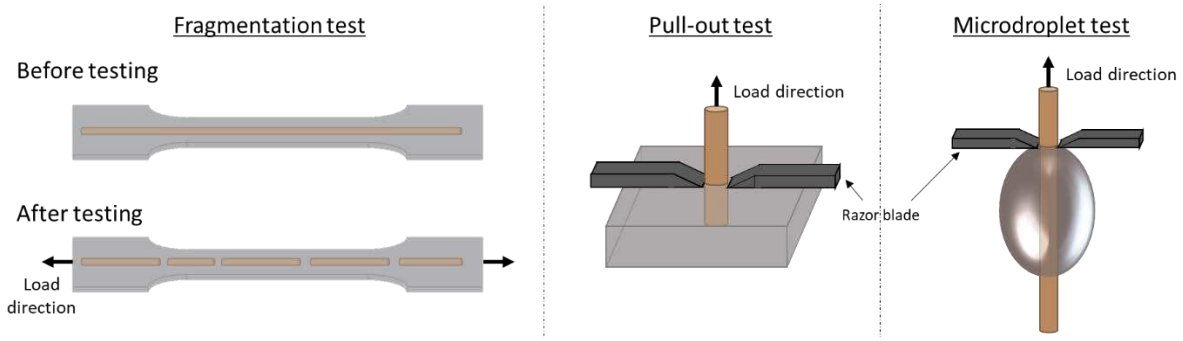

Figure 1-16: Description of the micro-scale investigation protocol for interface strength quantification.

The fragmentation is based on a critical fibre length, leading to fibre debonding rather than fibre breaking [109,114]. The embedded fibre breaks in several pieces during the fragmentation test until these pieces reach the critical length, leading to fibres debonding. The critical length is observed through piece length, and back-calculation leads to IFSS. One limitation is the need for fibre strength value for the back-calculation, which has a non-trivial variance. The variation of the section along the embedded fibres is another limitation for the back-calculation.

The second test is based on the debonding of a fibre inserted in a thin sheet of polymer. The fibre is submitted to a tensile test, with the polymer sheet clamped, leading to a debonding phenomenon. Knowing the debonding force and the embedded fibre area, the IFSS is calculated [101]. The difficulty is to embed only elementary fibre and not bundles. The precise measurements of the length of the embedded fibre is a second issue.

Finally, the micro-droplet test used the same debonding phenomenon; it gives the force obtained by debonding a microdroplet of resin fixed on a single fibre. This last technique has been theoretically described by Miller [111]. A typical micro-droplet load/displacement curve is presented in Figure 1-17. In addition to the interfacial shear stress, this test allows obtaining the friction post debonding, giving clues on the residual strength between fibres and matrix.

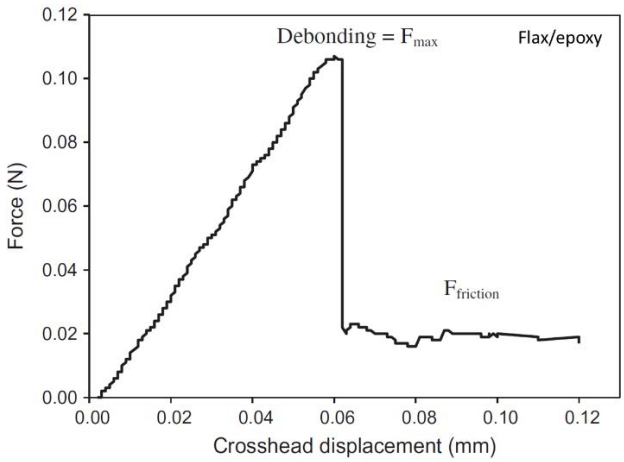

Figure 1-17: Typical debonding curve for a flax/epoxy specimen. Extracted from [115].

As the flax fibre goes through the matrix droplet, this test allows better management of the embedded fibre length than the pull-out test, even if the geometry of a droplet stays complex [116]. All these micro-scale methods assume a uniform shear stress distribution. As these tests induce stress concentrations, the interfacial shear strength obtained is an 'apparent' shear strength. In addition, they require a high number of specimens as a data distribution is present due to some out of control

parameters during sample preparation and testing. Furthermore, differences in IFSS values of up to 80% on the same fibre/matrix couple have been recorded, even when measured by the same operator [108,117]. Indeed, Table 1-4 recaps values obtained by Graupner et al. [114], clearly showing the characterisation methods' influence.

Table 1-4: Difference between the IFSS values (in MPa), obtained from two different methods, between elementary flax fibres and PP, MAPP or PLA matrix. Values are extracted from [117].

	Pull-out test	Fragmentation test	ratio
Flax/PP	17.9 ± 10.5	9.8 ± 6.8	1.8
Flax/MAPP	24.3 ± 11.1	15.8 ± 14.5	1.5
Flax/PLA	28.3 ± 10.9	-	-

Figure 1-18 presents literature data focussing on micro-droplet tests and comparing elementary flax fibres to glass fibres. No difference is observed between the adhesion of flax or glass with poly-(propylene), MAPP and unsaturated polyester. A higher value is reported for PLA/flax than PLA/glass, probably due to a better affinity between the flax fibres than the glass fibres. On the other hand, epoxy/glass presents the highest interfacial shear strength due to coating on the glass fibre specially developed to increase the glass interface with the thermoset matrix [110]. Indeed, as glass is chemically inert, glass fibres for composite application undergo a silane coating to adhere better to the matrix [118]. Thus the Figure 1-18 presents a generic value as the coating between the studies can be different.

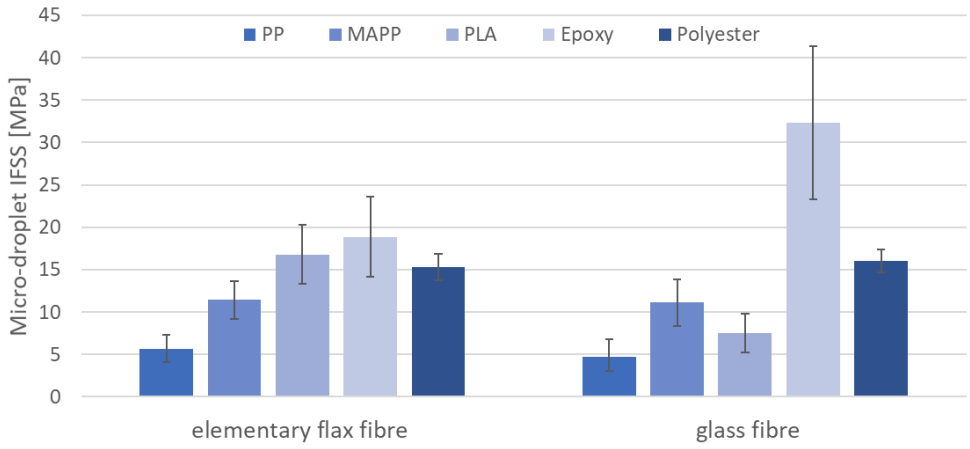

Figure 1-18: Interfacial shear stress (IFSS) measured by micro-droplet test on untreated elementary flax fibres and on glass fibres. Data are extracted from the literature : flax/PP [119–124], flax/MAPP [122–124], flax/PLA [92,105], flax/epoxy [92,104,115,125–128], flax/polyester [92,125,126], glass/PP [129–132], glass/MAPP [129,130], glass/PLA [105], glass/epoxy [111,127,133–136], glass/polyester [92,120,125,133].

IV.d. Macroscopic mechanical properties dependent on the interface

It is possible to obtain information on the interface at the composite scale using the mechanical properties of a laminate composite, such as shear behaviour or transverse tensile behaviour.

The shear behaviour is linked, among other phenomena, to fibres/matrix interfacial solicitation. Even if other phenomena are present, there is a close correlation between the interfacial shear strength obtained at the microscale level and the intralaminar shear strength obtained through composite shear testing [126]. That validates the use of composite-scale tests to obtain interface information conveniently. Several methods exist to measure shear properties in the composite for interface characterisation, presented in Figure 1-19.

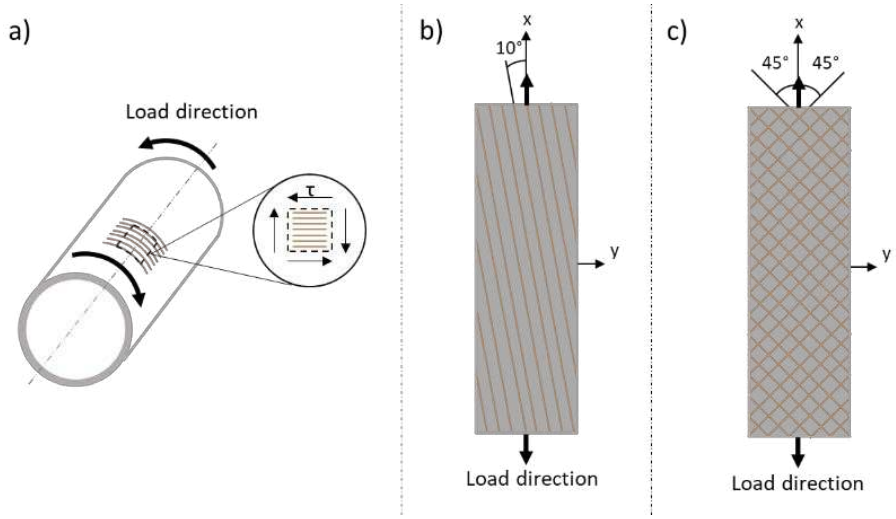

Figure 1-19: Composite shear solicitation methods for interface investigation at macro-scale level, a) thin-walled tube torsion b) 10° off-axis tensile test, c) ± 45° tensile test, based on [137].

Ideally, an in-plane shear solicitation is wanted to obtain intralaminar shear stress. It is experimentally obtained by applying torque to a thin-walled tube [137,138], Figure 1-19.a). This torque induces in-plane shear stress uniformly in the specimen. Other methods exist to obtain intralaminar shear stress where the in-plane shear stress is not the only solicitation. They are much more practical than thin-walled tube torsion, especially in terms of sample manufacturing. Among them, the off-axis test is suggested by Chamis and Sinclair [139] to create a shear strain during a simple axial and transversal tensile test, Figure 1-19.b). Knowing the angle between the fibres and the tensile loading direction, it is possible to back-calculate the shear strain and stress to obtain the shear behaviour using the laminated plate theory. It is considered a relevant test [138,139]; however, it gives shear strength significantly lower (38 %) than in-plane shear stress methods [137]. This difference can be explained by the presence of coupling effects between tensile, torsion and bending due to the asymmetric and

unbalanced assembly of the laminate. One test widely used is the ± 45° tensile test developed by Petit [140] and simplified by Rosen [141], Figure 1-19.c). A $[\pm 45]_s$ laminate is submitted to axial tensile traction. The axial and transversal strain/stress response is measured, which permits the shear stress/strain behaviour calculation. It is simple, cost-efficient and approximates the in-plane shear stress/strain response obtain by a thin-walled tube torsion accurately [137,138]. Other more complex tests exist, such as panel shear or rail shear tests. However, they give similar results to the ± 45° tensile test, which is simpler and more economical to handle [142].

Other composite properties can be used to obtain interface solicitation, such as the transverse tensile strength of a unidirectional composite [143]. On a transverse tensile test, the matrix and the interfaces are suggested to high stress and strain concentration [144]. As a result, the ultimate transverse strength is related to interfacial shear strength but also to matrix properties.

All these macroscopic methods are often easier to handle than microscopic methods. However, the interpretation is more complicated to analyse due to the numerous phenomena occurring simultaneously. Among them, the deformation of the matrix and the shear distribution inside the lamina. In addition, the fibre/fibre interphase is also solicited in these macroscopic tests in the specific case of flax fibres.

V. Manufacturing process

V.a. From plant to preform

It is necessary to describe the flax fibres extraction process briefly before discussing each preform particularity. Flax stems are pulled out at fibres maturity and left on the fields to undergo retting [70]. This natural process consists of partial biodegradation of polysaccharides linking the fibres together, thanks to combined and alternative effects of humidity, temperature, sun and microorganism or enzymes [145,146]. The retting is an essential step as it will help the bundle decohesion later on in the extraction. Furthermore, it influences the elementary flax fibres properties with higher mechanical properties for retted fibres. Indeed, the modulus evolves from 38.6 ± 17.3 GPa for unretted fibres to 55.6 ± 11.8 GPa for retted fibres [147]. Then, the extraction of the fibres is mechanically done thanks to a scutching line, presented in Figure 1-20. Seeds and woody core are removed from the stem to finally collect the scutched technical fibres, made of bundles of single fibres.

During scutching, some elementary flax fibres, and bundles made of a few of them, fall on a second circuit. Shives (fragment of woody core) fall on this second circuit too. The mix between the shives and the short flax becomes a by-product, the tows. At this stage, two qualities of flax fibres are available:

flax scutching tows and flax scutching fibres, the latter being more individualised [148] and assembled in long bundles, allowing their future use in tapes and preform manufacturing.

It has been demonstrated by Martin et al. [148] that both elementary fibres extracted from scutching tows or scutching fibres have similar mechanical properties with respectively a stiffness of 47.0 ± 15.7 GPa against 50.8 ± 15.7 GPa. Flax scutching fibres can be directly hackled to obtain high-quality long flax fibres homogenized into continuous flax ribbons. This process engenders another type of tows. As many shives were already extracted from the flax line production at the scutching step, the hackling tows contain mainly short flax fibres. The main difference between the two tows is the number of shives or parenchyma cortical present. Finally, at the end of the extraction, two tows qualities are obtained (scutching and hackling ones), as well as high-quality long flax fibres under the shape of a continuous ribbon. These different flax fibre qualities are used to make various flax preforms.

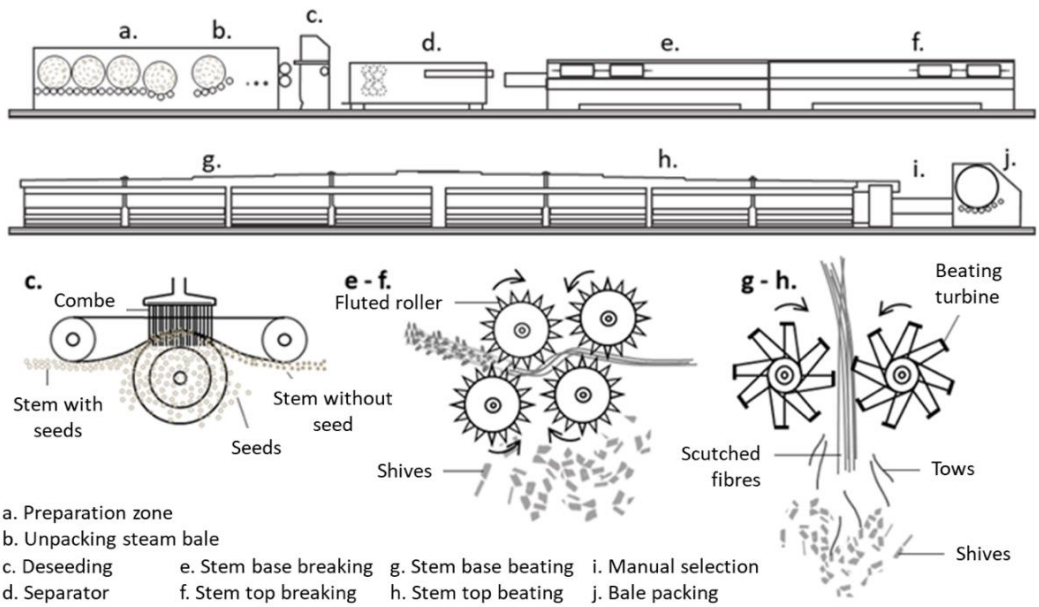

Figure 1-20: Detailed schema of a scutching line extracting flax fibres from flax stem [149]

As ribbons are continuous, they are easily transformed into yarns with the final aim to produce flax fabrics. Yarn strength has to be high enough to not break during the weaving process of manufacturing these fabrics. Without any consolidation, fibre slippage occurs, leading to the early break of the yarn. Several strategies exist to increase the yarn strength [70]. The twist strategies and the use of adhesive agents are discussed here.

Twisting fibres is the common textile approach to obtain yarns. Individual ribbons are pinned together to create friction cohesion, increasing yarn strength [150], presented in Figure 1-21.a). However, there

is an ideal twisting level as a very high twist will induce the breakage of yarns due to the off-axis misorientation of the flax fibres [151], see Figure 1-21.b). Note that the yarn behaviour does not reflect the composite behaviour as the fibres in the yarns are free to reorient, which is not the case once the yarns are embedded in a matrix.

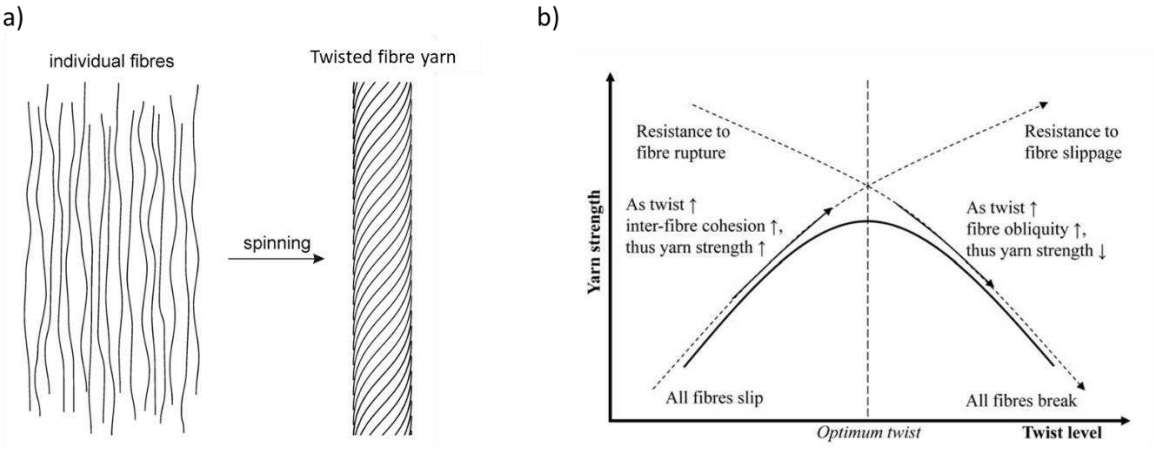

Figure 1-21: a) schema representation of the twist consolidation to obtain yarn, b) relation between the yarn strength and the twist level highlighting an optimum twist. Inspired by [70].

However, twisted yarns are not optimised for composite manufacturing as fibre misorientation decreases the composite's mechanical properties [151–153]. Indeed, Shah et al. [151] developed a modified rule of mixture for longitudinal impregnated yarns, finding a good correlation using a corrective factor of $\cos^2(2\alpha)$, where α corresponds to the twist angle of the yarns. Additionally, the difficulty in impregnation of a twisted yarn induces microporosity in the composite [153–155].

A more convenient process for yarn consolidation for composite application is utilising an adhesive agent to obtain flat yarns, called tape. This tape is made of parallel flax fibres, ideal for impregnation as no twist limits it. Furthermore, flax fibres remain principally oriented in the tape direction. Once impregnated, this flax fibre orientation maximises the composite properties.

Ribbons are directly stretched to manufacture this tape. The required width and area weight is adjusted before being linked by a cohesive agent. Several options are available regarding the cohesive agent. It is suggested by Khalfallah et al. [156] that spraying water will release biochemical components (pectins) from flax. After a drying and calendaring step, the pectins will act as a cohesive agent leading to a flat flax roving. This method is also used to obtain directly a flax preform made of a sizeable unidirectional flax roving [156]. Using water/polyvinyl alcohol (PVA) adhesives mixed is an alternative to obtain higher cohesion [157]. However, the environmental pertinence can be debatable, as well as

the issue of adhesion between such flax coatings and impregnating polymers. Another solution is to pre-impregnate the flax fibres with thermoplastic [158,159].

Once yarns or roving are obtained, the weaving process is used to obtain fabrics. They can be unidirectional or multi-axial, as is the case for glass or carbon fabric. Two techniques exist for holding the yarns together in a fabric shape. The first one is to use stitching yarns to maintain the yarns together. It is used for unidirectional preform as well as uncrimped multidirectional fabrics, as seen in Figure 1-22. A second option suitable for bi-directional fabrics is to crimp the yarns together. Depending on the crimp shape (twill/satin/basket), yarn mobility changes, thereby modifying fabric drapability [160].

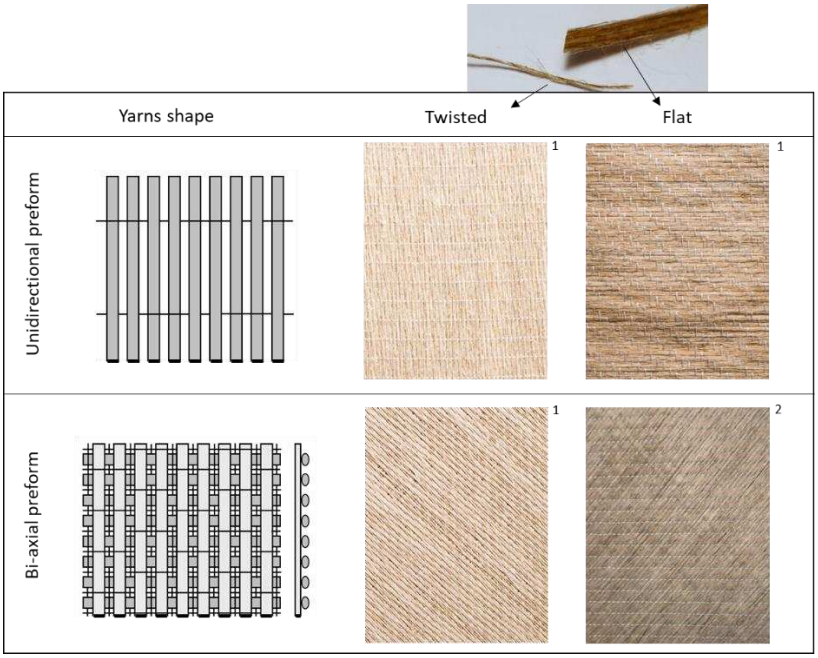

Figure 1-22: Presentation of two types of flax fabrics, unidirectional and uncrimped bi-axial fabrics. Both of them are presented using twisted yarns or flat rovings. Index 1 refers to products from Bcomp, and index 2 is a Depestele product.

Another flax preform is the non-woven, obtained directly from the tows. It is a random 2D preform, which can be made by several processes [161]. The most used are the needle punched and the spinlaced. A focus is done here on the needle punched process as it is used in the thesis scope. This process is presented in Figure 1-23. It is divided into four main steps. First, raw materials are aerated and mixed via a blower to obtain homogenous source material. This step is the opening. Then, the source material is carded, leaving a thin web of fibres. At this step, there is only a slight cohesion between fibres. After the carding, the thin webs are laid one on each other to obtain the area weight targeted for the non-woven.

Finally, these thin webs are assembled thanks to needles hammering them. This leads to a consolidation of the preform, induced by fibres entanglement forced by the needles, see Figure 1-23.c). The density of the needles, the depth of penetration, and the hammering speed influence the deformability and mechanical properties of the non-woven preform [162]. Another method used in this thesis to obtain light non-woven preforms is based on an opening step and a carding step, followed by a hot calendaring step. This last step is used to obtain cohesion in the non-woven by melting the polymer fibres.

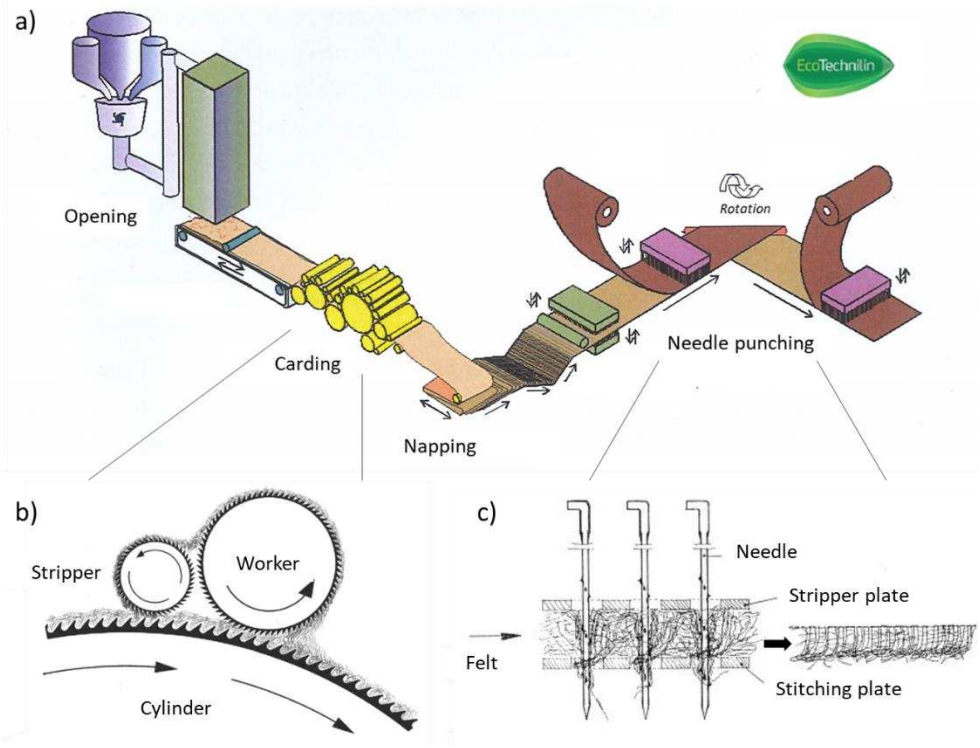

Figure 1-23: a) Needle punching line for non-woven manufacturing with a zoom on b) the carding [163] and c) needle punching [164] operations

This needle-punching process produces non-woven from 300 g/m² to 2500 g/m². Furthermore, it induces a preferential orientation of fibres in the machine direction [165]. Two final products are available using this process. First, a pure flax non-woven preform is obtained using only flax tows as raw materials. Second, it is more relevant for the composite field to make a non-woven using flax tows and polymer fibres as raw materials. That leads to a preform ready for thermo-compression.

V.b. Manufacturing methods for thermoplastic composite

Thermoplastics composite manufacturing needs a preform made of polymers and fibres. It is managed at several scales and thanks to various techniques presented in Figure 1-24. The commingled fibres are the specific case of the non-woven where polymers and reinforced fibre are assembled to obtain the

preform. It is also possible to have this assemblage at the yarn level, by solid polymers under powder form or fibre shape (using twisted yarns) [166] or by impregnating the yarns with melted polymers [158]. The melt impregnation can also be done at the fabric scale [167].

The last solution is the film stacking method. It consists of interlaying dry preforms and thermoplastic films to obtain an adequate amount of raw material. This process is not suitable at the industrial scale as it is time-consuming and difficult to manufacture complex geometries. However, this film stacking compression method is one of the processes chosen for making thermoplastic composite in this thesis. Indeed, it does not require a pre-mixed preform, is currently easier to test with a broader range of polymers (PBS, PHA, PLA) and allows a versatile choice of flax preform selection.

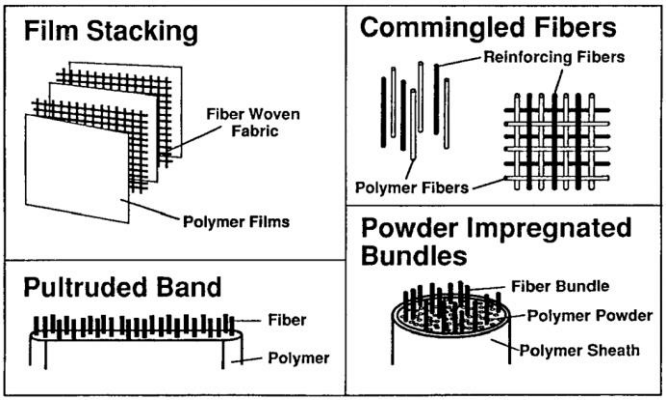

Figure 1-24: Schema of several strategies to bring the thermoplastic polymer close to the reinforcement fibres for a future better impregnation of the reinforcement during the manufacturing step, extracted from [168]

There are several processes to manufacture thermoplastic composites. Extrusion and injection moulding lead to very short fibre composites. Indeed, this process leads to a reduction in fibre length with an average of 1mm flax fibres in the composites [169,170]. However, wood flour is often preferred due to its lower price, several tens cents per kilogramme [171] against several euros per kilo for flax fibres adequate for injection. This manufacturing method enables rapid manufacturing, several pieces by minute, but the tools are costly. That is why it is preferred for big-scale industrial production.

Other manufacturing methods are automatic fibres placement [158] or continuous fibre 3D printing [172]. Using these methods with impregnated continuous flax yarns/rovings is of interest. Indeed these techniques allow precise fibre placement with potential local curvature, the production of complex geometries and the close control of process parameters [173]. However, they are not competitive enough yet to appear in the market. Indeed, these manufacturing processes are usually used for high-performance composite using carbon fibres, having higher specific properties than flax fibres.

A focus is made here on the thermo-compression of flax fibres/thermoplastic preform, see Figure 1-25, as it is the primary manufacturing process used in this thesis. It has the advantage of manufacturing flax fibres composites pieces of several m² in several minutes and to be a one machine process. First, a preform made of reinforcement fibres and thermoplastics is heated in an open mould to melt the polymer. Second, the mould is then closed, the preform takes the mould's shape before the mould is cooling down. Finally, a ready to use composite part is obtained after the cooling step. Using a non-woven preform and playing with the pressure, it is possible to obtain semi-structural composite (low porosity) or composite with acoustic damping properties (high porosity) [174]. As this thermo-compression needs relatively expensive tools (lower than injection tools), a vacuum thermos-compression process can be considered an alternative [175].

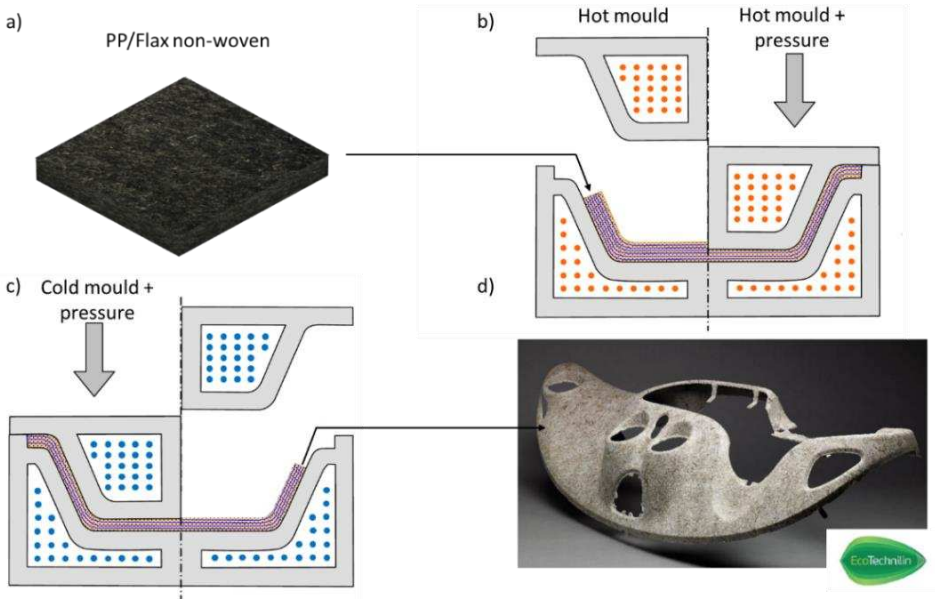

Figure 1-25: Schema of the thermo-compression process of a) a non-woven PP/flax, including b) the heating and compression of the preform in the mould, c) the cooling of the piece under pressure and the demoulding, d) an example of a final part obtain through thermos-compression of a PP/flax non-woven.

V.c. Influence of compaction and permeability

The thermo-compression process is based on the impregnation of dry reinforcement fibres by the melted polymer. However, as observed by Michaud et al. on glass/PP mat [176], melting the thermoplastic is not sufficient to allow the impregnation. Indeed, as the viscosity of the polymer is too high, an applied pressure is required to induce a polymer flow, needed for the reinforcement impregnation [176]. Thus, Ramakrishnan et al. [177] observed a better impregnation by increasing the pressure applied from 2 to 4 MPa, leading to better mechanical properties for their woven 2/2 twill PP/flax fibres composite made by thermo-compression.

Depending on the affinity of the polymers and the fibres, capillary effects can modify the pressure needed [178]. Indeed, a liquid thermoplastic wetting spontaneously the fibres impregnates the reinforcement partially through capillary forces. This wetting potential depends on the surface energy of the thermoplastic and of the fibres. The wettability of a surface can be calculated through static contact angle by the Laplace equation presented in equation (1-1) [179].

$$\gamma_{F1,F2} \cdot \cos(\theta) = \gamma_{S,F1} - \gamma_{S,F2} \quad (1\text{-}1)$$

The static contact angle is designated by θ , the $\gamma_{F1,F2}$ is the surface tension between two fluids where $\gamma_{S,F1}$ and $\gamma_{S,F2}$ referees to the surface tension between a solid and a fluid. In the case of liquid polymers impregnating a porous solid, the second fluid is the air. A contact angle lower than 90° indicates a better affinity between solid and liquid than between liquid and air. Consequently, the liquid wets the surface through capillary pressure, helping the impregnation of the reinforcement. On the contrary, the capillary effect can hinder the impregnation in the case of a non-wetting fluid. As impregnation is a dynamic phenomenon, the dynamic contact angle should be considered, which deviates from the static contact angle depending on the fluid viscosity and velocity [180]. Thus, switching from a wetting behaviour to a non-wetting behaviour is possible as the velocity decreases during the impregnation [180]. However, even if capillary effects reduce the applied pressure needed for impregnation, an external pressure remains necessary to induce the impregnation phenomenon.

Furthermore, the applied pressure compresses the preform, inducing an increase in fibre volume fraction, see in Figure 1-26. This compaction is present at several scales, from yarn deformation and flattening to nesting and packing of fabrics [181].

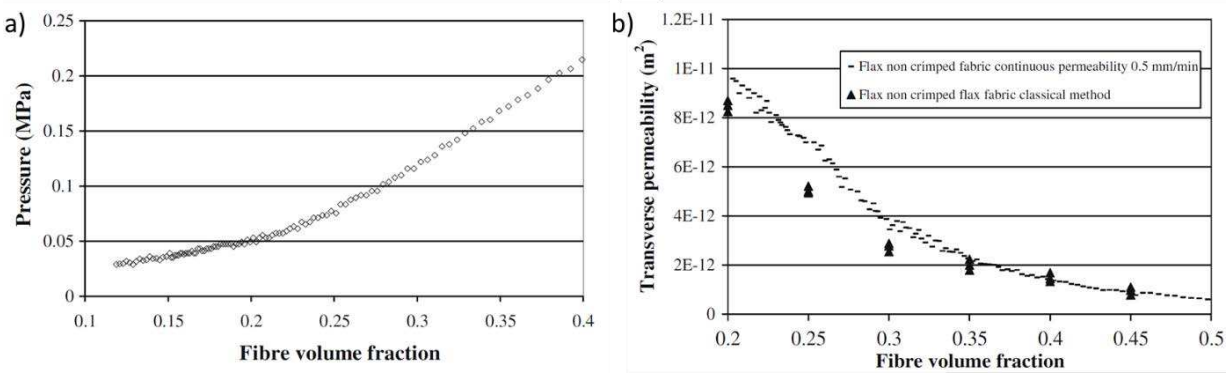

Figure 1-26: a) Pressure evolution during compression of flax mat preform submitted to a constant flow rate, b) continuous and "classical" transverse permeability of flax mat, extracted from [182].

In the specific case of plant fibres, lumens may collapse, inducing additional compaction [183], damaging the fibres irreversibly [178]. These damages are pressure-dependent as Ramakrishnan et al. [177] report an increase in microcracks in flax fibres by increasing the manufacturing pressure from 2 to 4 MPa. Another drawback for high pressure is the decrease of preform permeability due to compaction, as seen in Figure 1-26, which is a crucial parameter for reinforcement impregnation. For flax mats, increasing pressure from 0.05MPa to 0.22MPa leads to a volume fraction increasing from 15% to 40%, thus decreasing transverse permeability from 4.10^{-11} to 4.10^{-12} m² [182], see in Figure 1-26. Therefore, a balance must be found between the volume fraction wanted and the pressure applied to obtain an adequate reinforcement impregnation. This pressure will depend on the architecture of the preform and the proximity between polymers and reinforcement.

Indeed, the impregnation distance (the proximity between polymers and reinforcement), the viscosity of the polymers and the permeability of the preform impact the time needed to complete impregnation. This time could be approximated theoretically from Darcy's law in 1D [184]. Taking into first approximation an isothermal impregnation under a constantly applied pressure and a homogenous incompressible preform, the transverse impregnation time (t_{imp}) can be estimated from equation (1-2),

$$t_{imp} = \frac{\mu . l^2 . (1 - V_f)}{2 . K_t . \Delta P} \quad (1\text{-}2)$$

where μ is the viscosity of the melted thermoplastic, l is the length of impregnation, V_f the fibre volume fraction, K_t the permeability of the preform and ΔP the pressure difference. The pressure difference is the pressure applied less the atmospheric pressure and the potential capillary pressure due to wetting [185]. This equation shows the influencing parameters involving the impregnation phenomenon. As the permeability can vary from 10^{-9} to 10^{-12} m² for natural plant composite preforms [181], it is clear that decreasing it through compaction will have a crucial impact on the impregnation process. Furthermore, as the permeability is not equal in all the preform directions (in-plane or transverse), the resin flow direction chosen can be a strategy to decrease the impregnation time.

The incomprehensible preform hypothesis used for this equation is debatable. Indeed, it was observed that the matrix transfers the applied pressure to the reinforcement during the transverse impregnation. The reinforcement rearranges itself locally due to compaction, creating easier flow ways for the matrix leading to a fingering phenomenon [186]. Even once the impregnation is completed, heterogeneity of the volume fraction inside the composite is observed [176], with a volume fraction lower near the previous solid polymer. This heterogeneity is the result of the compressibility of the

preform during thermo-compression. This phenomenon can vanish thanks to the reinforcement relaxation in the matrix. However, this relaxation depends on matrix viscosity and takes 40min for a glass fibre mat to relax in a melt PP matrix with a viscosity of 18 Pa.s [176].

The homogeneity of the preform is also important. A preform is often made of yarns, and preform impregnation usually involves a dual-scale flow. Resin flow between yarns (inter-yarn) is referred to as macro-flow, while resin flow through the yarns (intra-yarn) is called micro-flow. As resin flows at low Reynolds numbers, inertial forces can be neglected. Macro-flow is dominated by the viscous flow of the resin, while micro-flow is driven by capillary pressure developed within the tows [178,187].

The dual-scale flow is explained as follows because impregnation in composites often leads to non-wetting dynamic angles [184]. The resin impregnated the preform preferentially through inter-yarn flow. When the inter-yarn flow front advances, the resin impregnates transversally in the yarns. As the resin fills the yarn, the inter-yarn flow rate is reduced. This dual-scale impregnation is of interest as it leads to porosity, discussed in section VI.a. In the specific case of flax fibres and low viscous polymers (thermoset), fibres can absorb the resin [188]. This increases the complexity of the dual flow as the absorbed resin is removed from the inter-yarn flow. Additionally, the fibres swell [189] and modify the capillary behaviour of the yarns. These complex phenomena are still investigated in the literature [181], their actual comprehension being represented in Figure 1-27.

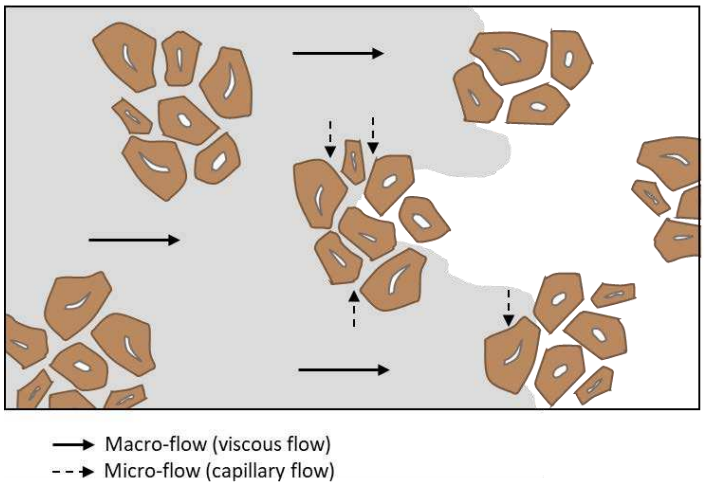

Figure 1-27: Schema explaining the dual scale transverse impregnation for flax fibres.

V.d. Temperature selection for thermoplastic composite manufacturing

As seen previously in equation (1-2) previous, the impregnation of a preform depends on the viscosity of the polymer. The more the polymer is close to the reinforcement, the less way it has to be

impregnated, and the less the viscosity will be critical [190]. In the case of film-stacking, a viscosity between 100 and 500 Pa.s is required [46,190]. The viscosity of a thermoplastic depends on its temperature and the applied shear rate [191]. The typical shear rate of the film-stacking process ranges from 0.1 to 10 s^{-1} [46,190,192].

Regarding the temperature, a thermoplastic heated above its glass transition temperature becomes viscous due to the relaxation of the interactions between amorphous chains. Semi-crystalline polymers must be heated above their melting temperature to dissolve the crystallite and act like a viscous liquid. Once the melting temperature is exceeded, all polymeric chains are mobile. This mobility increases by increasing temperature, leading to a decrease in viscosity [191]. Popineau et al. [175] investigates PP viscosity and found an evolution from 1600 Pa.s at 170°C to 750 Pa.s at 200°C, measured for a shear range of 0.1s^{-1} to 100 s^{-1}. Focussing on PA11, Bourmaud et al. [46] observed a decrease in viscosity from 575 Pa.s at 190°C to 100 Pa.s at 230°C. Therefore, a temperature exists for a given thermoplastic allowing an impregnation with film stacking.

However, this impregnation temperature should not exceed the degradation temperature of the thermoplastic and the flax fibres. It has been reported in the literature that elementary flax fibres submitted to high temperatures become brittle [193–195], and their strength decreases [46,194]. Bourmaud et al. [46] observed a decrease in strength of 32.8% and 64.8% at respectively 210° and 250°C for only 8 min of heat, see in Figure 1-28.a).

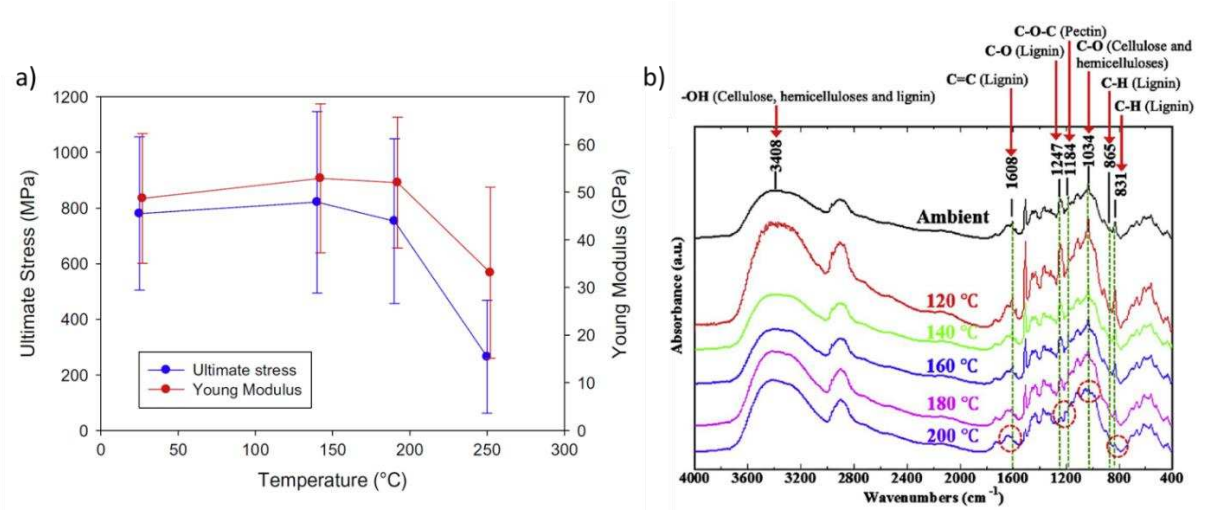

Figure 1-28: a) Temperature influences on the tensile mechanical properties of elementary flax fibres [193], b) Evolution of the biochemical components of elementary flax fibres investigated through FTIR [195].

This brittleness and strength decrease is explained by the biochemical modification of the elementary flax fibres. Velde and Baetens [194] observed that strength decrease starts at 180°C (for 2h of heat),

explaining it by biochemical evolution of the fibres. They did a thermogravimetric analysis (TGA) on flax fibres with various retting degrees (green/underretted/normal retted). As the retting modify the chemical identity of flax fibres, they are able to identify which agro-polymers is degraded during the TGA. It is concluded that at a temperature of 180°C, degradation of pectins occurs, and at 230°C, hemicelluloses and cellulose start to degrades. This is confirmed by Li et al. [195], which observed a decrease in the FTIR peak intensities of pectins and lignin after heating at 200°C for 2h, see in Figure 1-28.b). As pectins are partially responsible for the cohesion of the cellulose microfibrils, their degradation directly impacts the strength of the elementary flax fibres. Furthermore, it appears that temperature impact is time-dependent as a decrease of strength of 45% is observed at 105°C for 14h [196]. The cohesion between micro-fibrils is impacted when water is removed, explaining the strength decrease at low temperature after a long drying time.

Regarding modulus, some authors highlight a decrease of 25% at 250°C (8min) [46] explained by the degradation of microfibril cohesion. However, some others assumed that this biochemical modification is due to the degradation of amorphous biochemical components, leading to the recrystallization of cellulose. This phenomenon explains the 16% increase of flax fibres stiffness observed after heating them 2h at 200°C [195].

This brittleness is reflected at the composite scale level [46,195,196] and confirmed through acoustic emission tensile tests with a drastic change in break signal for samples heated for 2h at 120°C and 200°C [195]. Li et al. [195] report that the rupture appears through multi-failure stages at 120°C (matrix cracking, delamination, interfaces debonding, fibre breaking), against only fibres breaking at 200°C.

VI. Influence of a ply structure on its mechanical properties

After discussing the preform manufacturing and the process to obtain thermoplastic composites, the links between the structure and the mechanical properties of the composite are of interest.

VI.a. Microstructure

Looking at the microstructure and composite constituents, the volume fraction of reinforcement is the parameter mainly impacting the mechanical properties of composites. As presented in Figure 1-29.a), increasing fibre volume fraction increases the flax composite's mechanical performance. Focussing on the longitudinal tensile modulus of flax composite, this increase appears to be linear, see in Figure 1-29.b), which is relevant to the commonly used rule of mixture. On the other hand, the transverse mechanical properties of unidirectional composites are matrix-dominated, less influenced by fibre volume fraction [144]. Furthermore, the influence of volume fraction on the transverse behaviour of

unidirectional composite is complex to predict as the stress field is heterogeneous inside the composite [144]. Hopkins and Chamis [197] developed a theoretical model to characterise this evolution, whereas Halpin-Tsai [198] suggests a semi-empirical law. Both appear to be relevant for flax composite [199]. For other fibres architecture, such as non-woven or multi-axial composites, the mechanical behaviour depends on the reinforcement organisation inside the composite, which is developed in section VI.b.

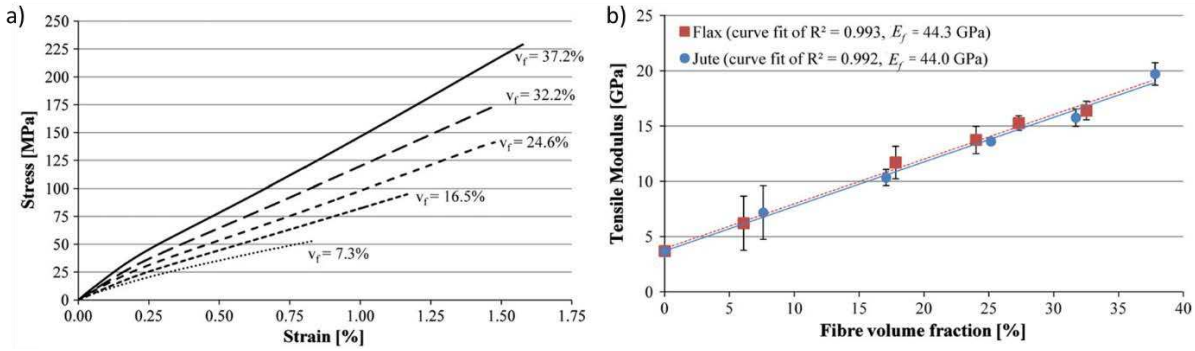

Figure 1-29: Influence of the volume fraction of fibres on a) the mechanical behaviour of a jute/polyester unidirectional composite b) the tensile modulus of a jute/polyester and flax/polyester unidirectional composite, extracted from [200].

The mechanical improvement due to increasing fibre volume fraction has limits. For example, Baley et al. [74] observed fibres packing higher than 95% in the bundles of a green flax stem due to intrusive growth and polygonal fibres section. However, at the composite scale, manufacturing composite with a high fibre volume fraction is challenging. Even if the polygonal section of flax fibres allows better packing than cylindrical glass fibres, the permeability of the preform, the viscosity of the matrix and the process used limit the fibres fraction reachable during composite manufacturing. It is possible to reduce the void content by carefully adapting the process parameters. However, this induces often a higher cost of production [201]. Thus, at a given preform, formulation, and process, a critical volume fraction exists, after which adding more fibres induces porosity rather than a higher volume fraction. Madsen et al. [202] measured this critical volume fraction to be 40.8% for a flax/PP non-woven composite made by film stacking and autoclave consolidation (2.1 MPa), as presented in Figure 1-30.

This void appears due to low compacted fabrics [202], entrapped air during processing [203] or released gases [177], mainly water vapour in the case of flax fibres. Indeed, flax fibres contain 8% of water at 50 RH [204]. This water fully evaporates at 120°C, with a typical decrease observed on a TGA [205]. As the process temperature is often higher than 120°C, water evaporation cannot be avoided. However, a degassing step during the process allows releasing the vapour, reducing the formation of porosity. In addition, it is assumed by Ramakrishnan et al. [177] that pores can appear at high

processing temperatures (240°C) due to fibres degradation releasing volatile substances. Depending on processing parameters, the amount, the localisation and the shape of voids varies.

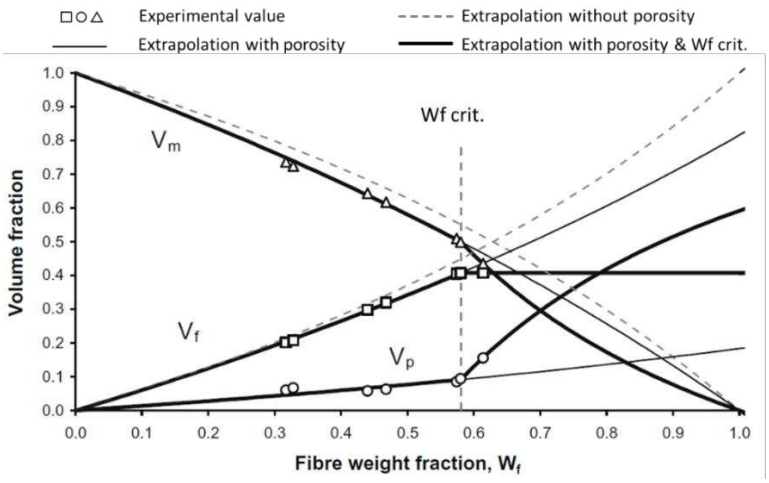

Figure 1-30: Influence of the fibres weight fraction on the volume fraction of matrix (V_m), fibres (V_f) and porosity (V_p) of a flax/PP non-woven composite made by film stacking and auto-clave consolidation (2.1 MPa). A critical fibre weight fraction is highlighted at 58% as the maximum fibre weight before a drastic increase of porosity inside the composite. Extracted from [206]

The typical voids present in flax composites are presented in Figure 1-31. In the case of dual scale impregnation, intern-yarn voids appear for low flow velocities (and high fibre volume fractions), while at high flow velocities (and low fibre volume fractions), viscous flow dominates, leading to intra-yarn voids [207]. The pressure applied during manufacturing reduces the quantity and the size of the void [203]. According to Almeida et al. [208], mechanical properties starts to decrease at 3% of porosity for [0,90] carbon/epoxy composite, with a decrease of flexural strength of 8% at 4% of porosity and 15% at 5% of porosity. Shah et al. [151] obtain a similar value (4%) for a unidirectional flax/polyester composite. The lumen is experimentally characterized as a porosity for flax fibres, but it cannot be assimilated to a composite defect as it is an intrinsic characteristic of flax fibres.

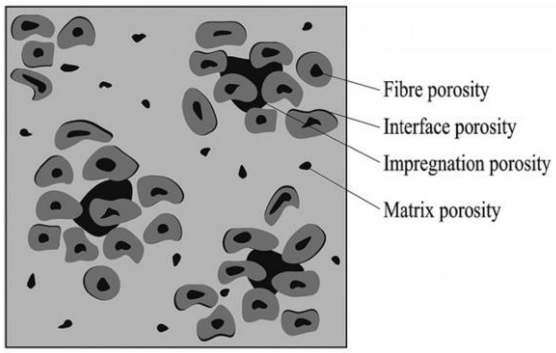

Figure 1-31: Typical porosity which can be observed in a flax composite, extracted from [202].

At higher porosity content, the composites mechanical properties are impacted. The change in properties due to void is well discussed in the literature for hand-made fibre composites and recently reviewed by Mehdikhani et al. [209]. It appears that porosity acts as defects in the composite structure, generating locally high stress/strain concentration and allowing easier crack initiation. This decreases matrix-dominated properties and matrix/fibre interface properties, such as composite strength under inter-laminar shear, compression or transverse tensile solicitation, with a decrease of 10 % by a porosity increment of 1% [209]. This strength reduction appears to be lower for longitudinal tensile solicitation, with a decrease of 1% for a 1% void increase [210]. It is explained by considering the porosity at the fibre/matrix interface, decreasing the local adhesion between fibre and matrix. Studying the tensile stiffness reduction of carbon/epoxy unidirectional composites numerically, Huang and Talreja [201] found a decrease of 5 to 10% in the longitudinal direction, with an increase of 5% of porosity, against a reduction of 12-40% in the transversal direction. This conclusion was validated through experimental comparisons with literature. This low voids sensitivity for longitudinal tensile stiffness is reported experimentally for quasi-UD flax/epoxy composite [203]. In the case of flax composite, Madsen et al. [206] observe a reduction of tensile stiffness for PP/flax fibres mat composites due to the increase of porosity. This can be explained as the stiffness of non-woven composite is sensitive to matrix stiffness, the latter being impacted by porosity. Based on this observation, Madsen et al. [206] used a modified rule of mixture developed by Mackenzie [211] for taking into account the porosity, see in equation (1-3). E_c refers to the composite modulus taking into account the porosity and $E_{c,ROM}$ to the modulus obtained via the role of mixture. V_p is the volume fraction of porosity inside the composite, and the index n is called the porosity efficiency exponent. In the specific case of plant fibres, good fits are obtained with $n = 2$.

$$E_c = E_{c,ROM}.\left(1 - V_p\right)^n \quad (1\text{-}3)$$

However, the void content determined their impact on the mechanical properties, but their shape, size, localisation, and spatial distribution must be considered [209]. The connectivity of the pore with the environment and between them is also important, being the difference between open pore (connected) and closed pore (a close defined volume in the composite). To lead comprehensive models, the deep analysis of voids characteristics and their impact on composite mechanical properties have to be investigated more thoroughly [209].

VI.b. Orientation of the fibres

The angle between the tensile axis and the fibres modifies the mechanical behaviour and properties of the composite. The off-axis mechanical properties of unidirectional composite lay between the

transversal and the longitudinal one, as seen in Figure 1-32.a). A slight in-plane misorientation (deviation from the expected angle) regarding the tensile direction impacts the mechanical properties. Shah et al. [212] measured a decrease of 37% of the tensile modulus of a unidirectional flax/polyester by increasing the angle from 0° to 15°.

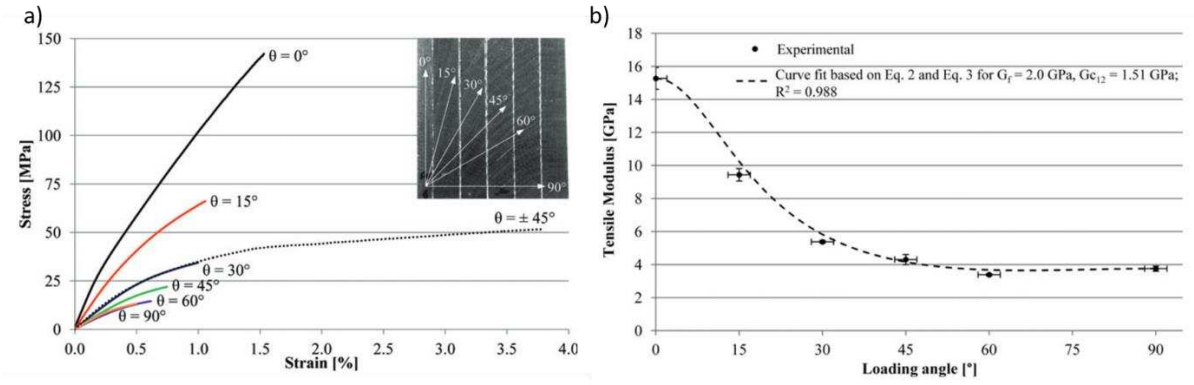

Figure 1-32: Influence of the angle of the off-axis tensile test applied on a flax/polyester unidirectional composite on a) the mechanical behaviour of the composite, b) the tensile modulus of the composite, extracted from [212].

The angle influence on composite tensile stiffness is commonly approached thanks to equation (1-4), being also suitable for flax composite [212]. $E_{c,\theta}$, $E_{c,0}$ and $E_{c,90}$ refers to the tensile modulus of the composite at an angle theta, 0° and 90° respectively, the shear modulus $G_{c,12}$ and $\nu_{c,12}$ refer to shear modulus and Poisson's ratio. Additionally, an out-of-plane misorientation impacts the flexural and the shear strength of the composite [213].

$$E_{c,\theta} = \frac{1}{\frac{\cos(\theta)^4}{E_{c,0}} + \frac{\sin(\theta)^4}{E_{c,90}} + 2\cos(\theta)^2.\sin(\theta)^2\left(\frac{1}{2.G_{c,12}} - \frac{\nu_{c,12}}{E_{c,0}}\right)} \quad (1\text{-}4)$$

Equation (1-4) considers a sharp orientation with only one angle considered. Due to the preform manipulation or the composite manufacturing, the fibres can be misaligned (a repartition of the angle observed). It is especially the case for flax fibres due to their finite length, see in section VI.c. Focussing on the orientation of fibres in an uncrimped and untwisted unidirectional preform, Gager et al. [214] highlight a higher fibres misorientation for flax fibres preform than for glass fibres preform, as presented in Figure 1-33. Furthermore, considering twisted yarns and fibre discontinuity, not all fibre ends are integrated into the yarns. These fibres ends are free to move and lead to additional misorientation of the fibres [215]. This phenomenon is known as yarn "hairiness" [215]. The fibre misalignment influences the mechanical properties. Berthelot et al. [216] used a theoretical approach and found that a misalignment of 10° (considering uniform distribution between -10° and +10°) decreases the longitudinal modulus by 3%.

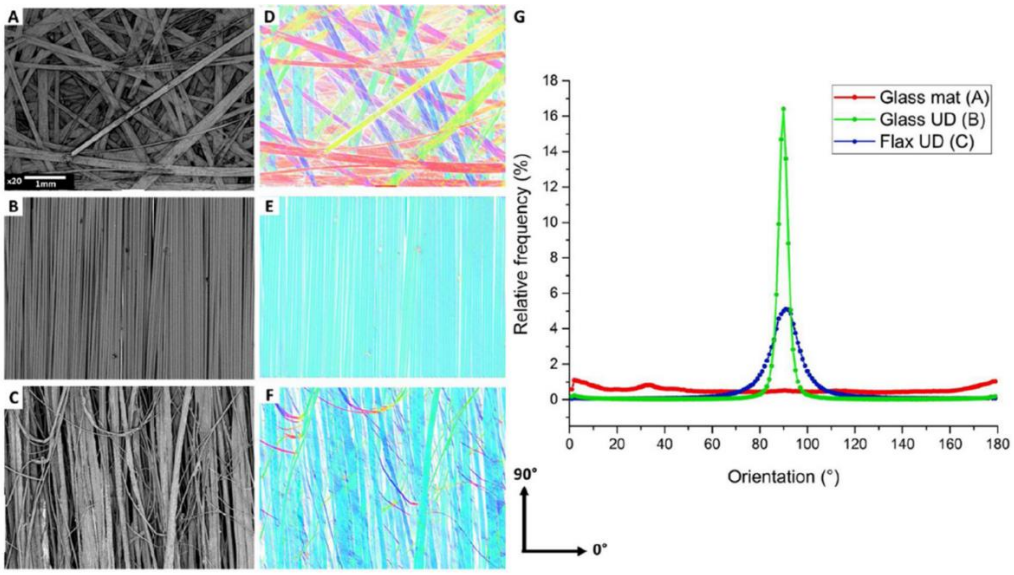

Figure 1-33: Comparison of fibres orientation (G) of glass mat (A & D) and glass unidirectional (B & E) preforms as well as unidirectional flax preform (C & E). The orientation analysis is done through oriented granulometry. Extracted from [214].

Gager et al. [214] also highlight an orientation distribution in random flax mat, as presented in Figure 1-34. Indeed, depending on the manufacturing process, random mats can present a preferential orientation [217]. This preferential orientation induces anisotropy in mechanical properties [165]. In the case of needle-punched non-woven flax composite, this anisotropy induces a difference in composite tensile modulus of 20% (5.4 GPa against 4.4 GPa) depending on the direction of measurement. Of course, this is a problem when an isotropic composite is desired. However, this anisotropy can be seen as an opportunity to obtain highly oriented non-woven preform.

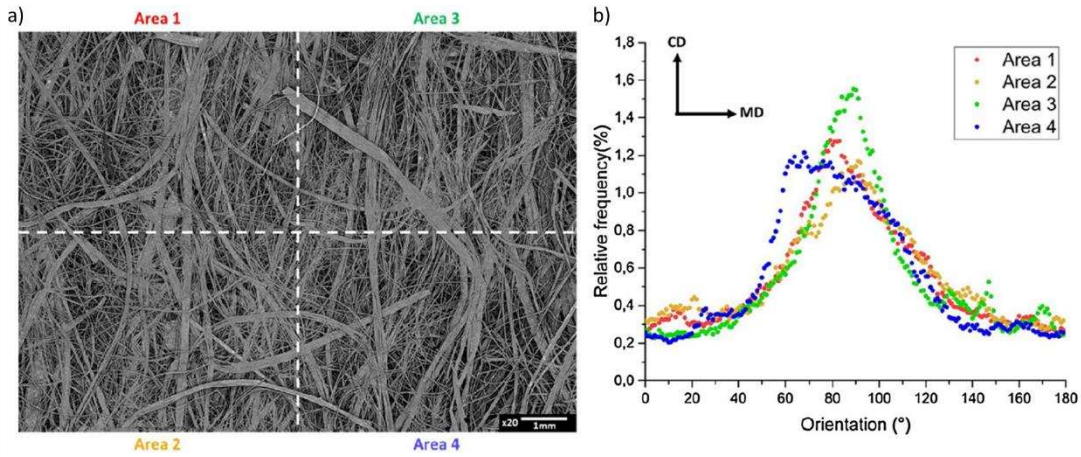

Figure 1-34: Analysis of the orientation of fibres for a flax non-woven preform, a) SEM image used for the analysis, including the separation into for smaller zone, b) The orientation distribution of the fibres inside the non-woven flax preform, CD referees to cross-direction and MD to the machine direction. The orientation analysis is done through oriented granulometry. Extracted from [214].

As the fibre orientation influences the mechanical properties, it is of interest to control it and so to be able to obtain this information experimentally. As the information should be obtained for the whole volume, 3D imaging such as X-ray tomography is an efficient experiment to obtain this information [218]. Furthermore, the 3D characterization of the composite structure can also be obtained thanks to 3D ultrasonic full-waveform scans [219].

VI.c. Specificity of the flax fibres arrangement in the ply

One particularity of flax fibres is their discontinuity. As reported in section III.a, elementary flax fibres have a length of 35 ± 15 mm. The finite length of flax fibres raises the question of the elastic stress transfer between the fibres and the matrix. The axial stress inside an embedded fibre during an axial tensile measurement is derived by Cox [114]. This stress transfer depends on the fibre aspect ratio (length/diameter), fibres volume fraction, stiffness, and matrix shear modulus. Fixing all the parameters except the aspect ratio, a critical value exists before which the fibres' full potential reinforcement is not reached. This could be taken into account by modifying the rule of mixture using a length corrective factor [144]. Madsen et al. [206] implements the Cox model using typical flax input data and calculated this length corrective factor as a function of the aspect ratio. It is represented in Figure 1-35. A fibre aspect ratio of 50 leads to a corrective factor of 0.93. Looking at the morphology of elementary flax fibres, the aspect ratio is approximatively 2,000 [63]. Charlet et al. [73] investigated the geometry of bundles in a stem and observed a maximum surface area of 20,000 µm² along bundles of at least 18 mm. This leads to a minimum aspect ratio of 115, still higher than the critical value. It can be concluded that the discontinuity of the flax fibres is not a drawback regarding the composite stiffness.

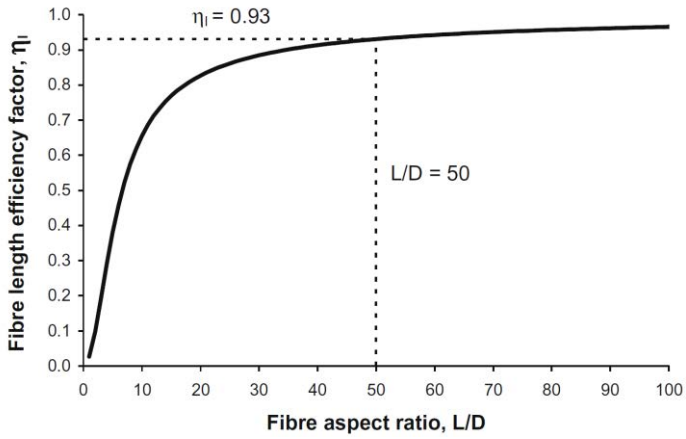

Figure 1-35: Evolution of the fibre length efficiency factor as a function of the aspect ratio of the fibres. It is extracted from [206], which used typical plant fibre composite values to predict this shear lag model.

A potential drawback of the discontinuity of fibres inside the composite is the high shear stress at the fibres extremity. This is observed in injected flax fibres composites by a damaged matrix at the fibres extremity [220], see in Figure 1-36. In addition, the shear stress can lead to premature rupture, lowering the composite strength [144].

Figure 1-36: Micrographs of a PP/Flax injected sample under loading, the red circle highlighting a high shear stress zone due to the presence of a flax fibres extremity, extracted from [220].

However, thanks to the intrusive growth of flax fibres during the plant's development, the flax fibres section decreases at its extremities [70], see in Figure 1-37. This reduction of section moderates the presence of the shear stress and limits the decrease of strength. That is why it is essential to damage as little as possible the flax fibres during extraction and processing to keep the morphological advantages of flax fibres.

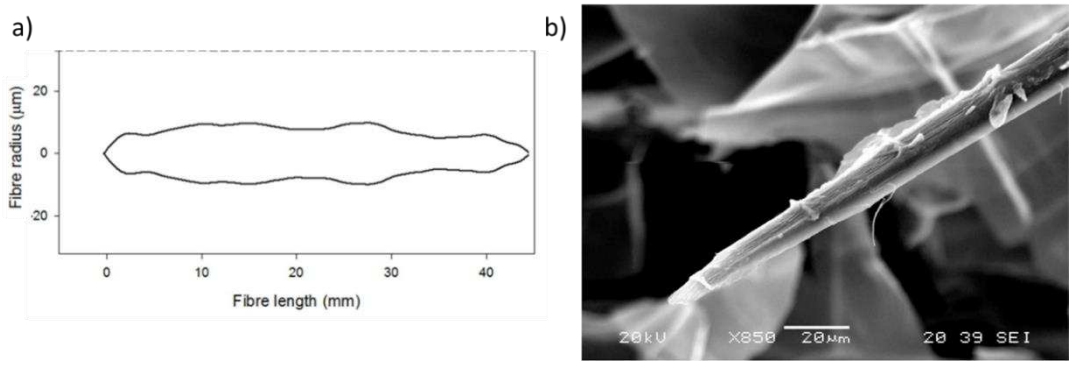

Figure 1-37: Representation of the decrease of the section near the extremities through a) geometry of elementary flax fibres b) SEM observation. Extracted from [74].

Another composite flax fibres characteristic is the heterogeneity of reinforcement distribution inside the composite. Indeed, there are two typical reinforcements (bundles and elementary fibres), and bundles are rich fibre regions by definition. The individualisation of the fibres does not affect the composite stiffness but does affect strength [46,127]. Using an effective coefficient to weight the rule of mixture by taking into account fibre individualisation, Coroller et al. [127] obtain an effective

coefficient of 0.68 for well individualised unidirectional flax/epoxy composite against 0.56 in the case of poor individualisation. It highlights the importance of flax extraction to maximize individualisation and increase composite strength. This individualisation can be increased using harsher extraction. However, mechanical extraction may induce kink bands in flax fibres [221], which act as a fibres defect. That is why a compromise has to be found between well-individualised flax fibre preform and flax fibres with an acceptable amount of defect.

Furthermore, depending on the flax quality used for preform manufacturing, it is possible to find some shives or even some seed holders. These unwanted reinforcements are mainly obtained on flax tows. They increase the heterogeneity of the non-woven composite made from tows. Some shives are still present in unidirectional preform but in much less quantity.

VI.d. Flax composite non-linearity behaviour

As reported in Figure 1-38.a), flax composites present non-linear tensile behaviour. This non-linearity can be partially explained by the non-linearity of flax fibres [222]. Indeed, at early strain, elementary fibres have a decrease of stiffness, reflecting at the composite scale. However, flax fibres stiffness increase at a critical strain stage (0.4 mm/mm), seen in Figure 1-38. b). This increase is not observed in unidirectional flax composite, explained by the appearance of composite damage at critical strain. Thanks to an in-situ X-ray tomography tensile test on a flax/PP unidirectional composite, these damages were observed [223]. Three stages are reported as follows: (i) interface splitting cracks, (ii) matrix shear cracks, (iii) fibres failures. They appear at increasing strain values. However, no specific strains are reported for a transition from a stage to another.

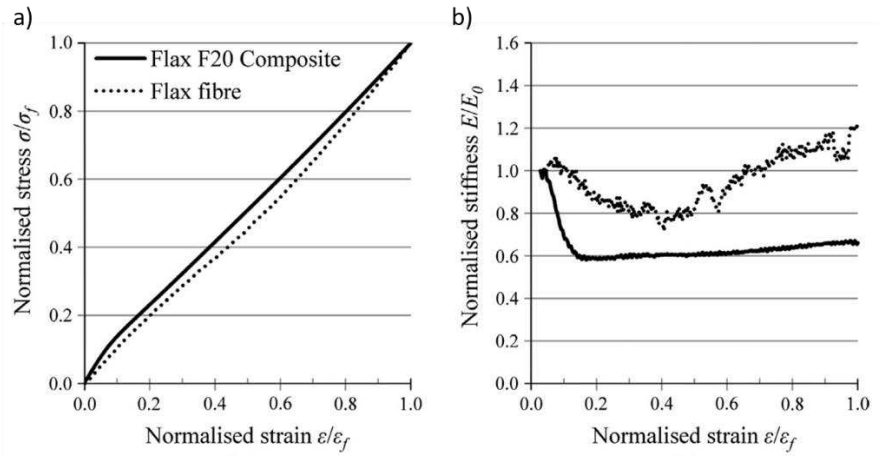

Figure 1-38: Comparison of elementary flax fibre and a flax/polyester unidirectional composite (Vf=20%) regarding a) their tensile behaviour, b) their evolution of stiffness during a tensile test.

During a tensile test, Monti et al. [99] used acoustic emission methods on flax/acrylic resin composite. They couple it with SEM to be able to identify and classify the damage mechanics. They propose a similar sequence of events with the first stage involving matrix cracks (class A) and fibres/matrix debonding (class B), then the presence of friction phenomenon (typically fibre pull-out) (class C) and finally flax fibre failures (class D). The acoustics emission correlated with the tensile behaviour is represented in Figure 1-39. It shows that the matrix cracks and debonding are present during all the tensile tests, with an increase of debonding at a strain of 0.5%. It correlates well with the critical strains previously discussed. Pull-out appears at the final stage, just before the fibres breaking, responsible for the failure of the specimens.

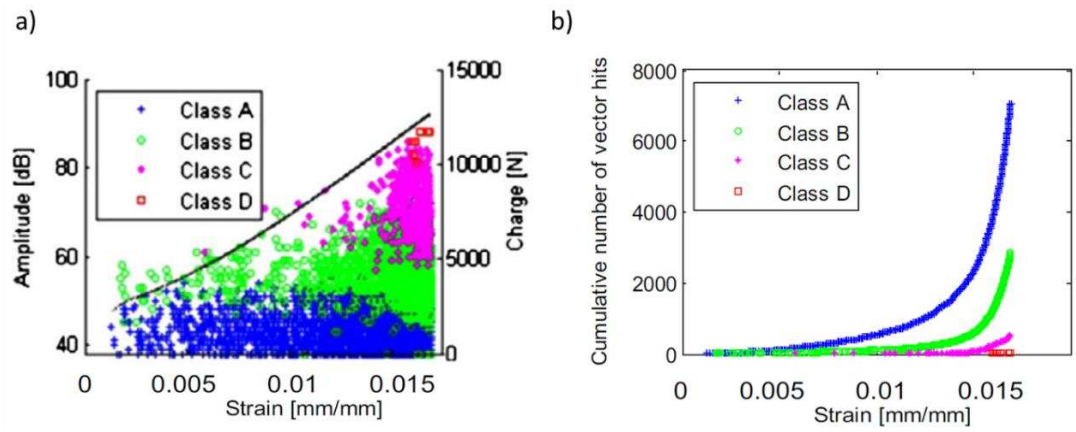

Figure 1-39: Acoustic emission analysis of a UD flax/acrylic composite a)amplitude of the events correlated with the tensile behaviour, b) phenomenon appearance regarding the strain applied. Class A refers to matrix cracks, class B to flax/matrix debounding, class C to pull-out phenomenon and class D to fibres failures. Extracted from [103].

VII. Ageing behaviour of flax composite

The mechanical behaviour and properties of flax fibre composites appear to be environmentally dependent. It is even more true for biodegradable flax composite as biodegradable polymers also appear to be impacted by the environment.

VII.a. Water ageing

Flax fibres are hydrophilic due to their hydrophilic polysaccharides, which are mainly hemicelluloses and pectins. Elementary flax fibres can absorb up to 20% of water in mass [47,204]. The amount of water uptake depends on the relative humidity [204], as observed in Figure 1-40.a). This absorption can be divided into three parts [47]. First, below a relative humidity (RH) of 15%, water molecules are adsorbed, through hydrogen bonds, onto cell walls. Second, between 15% and 70% of RH, water molecules absorb randomly on flax polymers through Van der Waals interaction. Thus, below 70% of

relative humidity, water molecules interacted with the flax fibres, being called bond water. Finally, above 70% of RH, water molecules do not interact with the flax anymore and start to cluster in cavities through capillary condensation. This is free water. This phenomenon induces relaxation of pores and rich water area, inducing the swelling of the fibres. Note that the 70% value is used as an example here. It is not an exact value but it highlights the existence of a critical relative humidity. The swelling of elementary flax fibres was investigated by Le Duigou et al. [224]. They report that fibres mainly swell transversally, with a radial hygroscopic expansion of 1.14 ε/Δm for elementary flax fibres where ε is the elongation induce by the water uptake (Δm), see in Figure 1-40.b). This preferential direction of swelling is due to the low micro-fibrillar angle of elementary flax fibres.

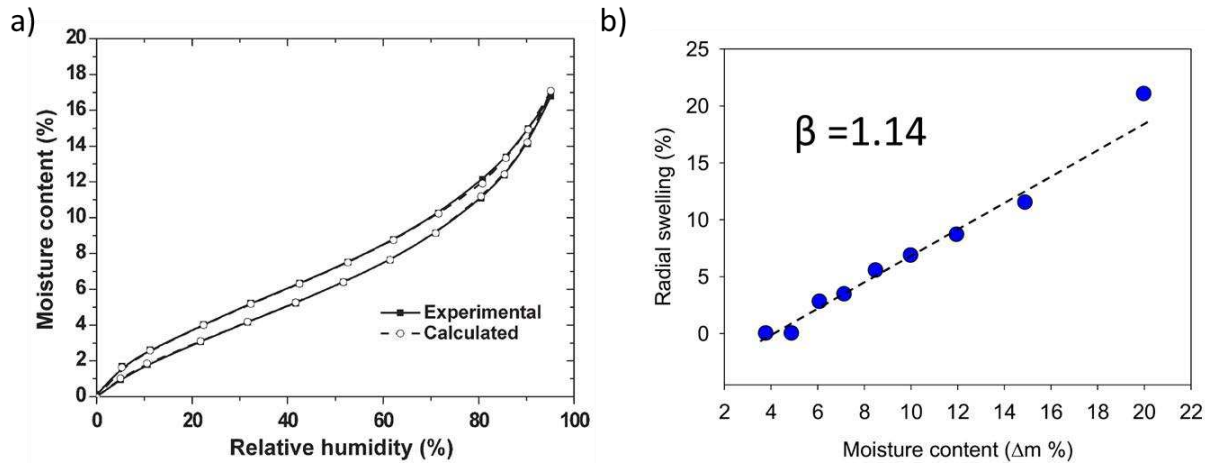

Figure 1-40: a) Evolution of the moisture content of flax fibres as a function of the relative humidity [204]*; b) evolution of the radial swelling of an elementary flax fibre as a function of the moisture content* [224].

This swelling is present also at the bundle scale [225]. Furthermore, bundles' flax composition can be modified by water sorption, especially in the case of immersion. Indeed, the hemicelluloses and the pectins of the middle lamellae are hydrophilic. Therefore, they can be solubilised and removed from flax bundles thanks to water washing [226]. At the flax preform stage, this can be used as a pre-treatment to obtain more individualised fibres without losing the mechanical properties of elementary flax fibres [226].

At the composite scale, water sorption is synonymous with damage in the composite. The composites water uptake is mainly due to flax fibres, even when associated with hydrophilic polymers such as PLA [227]. Focussing on the diffusion behaviour of water in the composite, it follows in most cases Fick's law [47,228]. The saturation of water and the diffusion coefficient depend on the volume fraction of flax fibres [12] and the architecture of the composite [229]. The interface quality can reduce the water uptake, as reported by Arbelaiz et al. [230] comparing PP and MAPP flax composite.

Furthermore, the initial water content of flax fibres impacts the moisture uptake of the composites. Indeed, Lu et al. [231] observed that damp flax fibres make composites less sensitive to moisture cycles. The water uptake in the composite induces fibres swelling, which is limited by the constraining effect of the matrix [232]. Additionally, this swelling can be responsible for crack initiation in the matrix [233]. The steps of impacting the structure of composite are represented in Figure 1-41. In the case of immersion, the impact on the interface is more critical. Indeed, the solubilized polysaccharides can leach-out of interfaces, decreasing the interfacial strength [115]. This leaching phenomenon also impacts fibre properties. Indeed, among the leached polysaccharides, Le Duigou et al. [234] reports that uronic acid leaching is responsible for the nanoindentation modulus decrease of the flax fibres in a flax/epoxy composite.

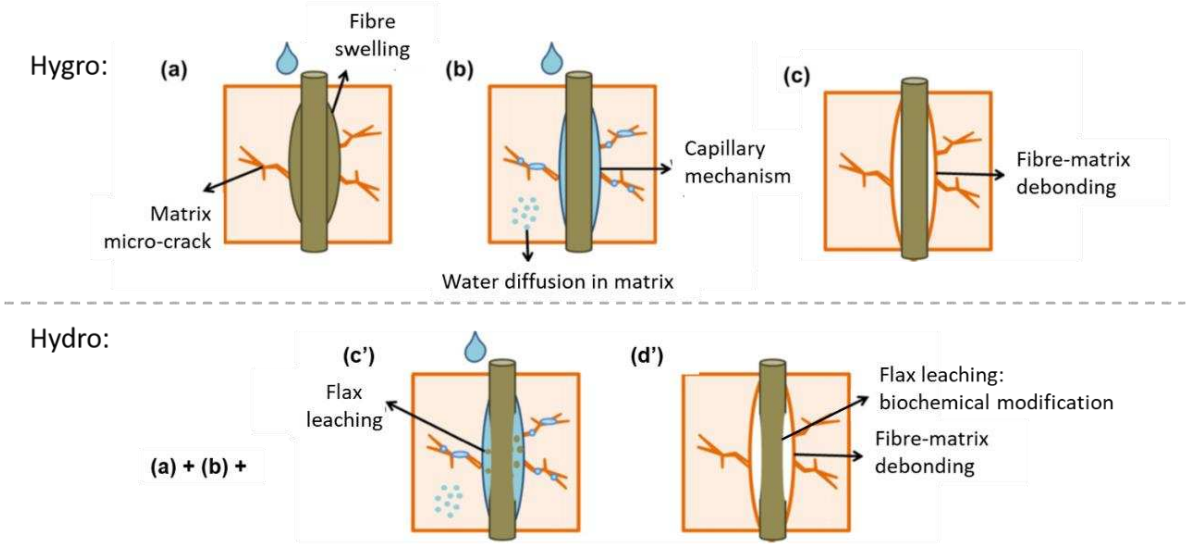

Figure 1-41: Schema of the evolution of microstructure in the case of a) humidity ageing, b) immersion ageing. Rearranged from [235]

All these structural modifications have an impact on the mechanical properties of the composite. Testing under humid conditions, water content inside the composite modifies the behaviour of flax composites [236] and decreases its mechanical properties [237]. Water ageing has a reversible impact (plastification) and an irreversible impact (modification of the structure). These irreversible parts are observed when the composites undergo ageing and are dried before testing. It is reported by Regazzi et al. [227] that immersion at 20°C of an injected flax/PLA composite induces a decrease of elastic modulus of 26% at the wet stage, including 10% of irreversible changes measured after drying. However, it is reported for non-woven flax/PP composite that RH lower than 75% does not impact the mechanical properties of composites [47]. Additionally, Davies et al. [238] suggested that the one-edge immersion process is more realistic regarding naval applications. It is reported that the water uptakes

and then the impact of ageing is less critical, with only a water uptake of 1% after five months for flax/polyester, against 7% in conventional immersion. For hydrophilic matrix, the water can also modify the structure and the mechanical properties of the matrix, resulting in additional modification of the mechanical properties [227].

VII.b. Living environment

As reported in sections II.c and II.d, the flax fibres and biodegradable polymers can be degraded by microorganisms. Consequently, a composite made of both components will age in the presence of these microorganisms, their presence depending on the environment (compost/soil/water). Degradation is commonly highlighted through a decrease in mass [239–241]. Interestingly, flax fibres act as an accelerator for polymer degradation. Indeed, they create channels for water and enzymes in the polymers, increasing the polymer surface subjected to degradation [242]. Depending on the matrix and its capacity to be degraded in the environment, the degradation of composite varies. Teramoto et al. [243] investigate the degradation of several biodegradable polymers reinforced by 10 % in weight of abaca and buried in the soil at 25°C. It appears that abaca/PBS loses 50% of its weight after 60 days, whereas abaca/PLA undergoes only 10% of loss and being stable after that point. In the case where flax fibres are more subjected to degradation than the polymers (flax/PLA at low temperature), increasing the fibre volume fraction increases the maximum weight lost and the degradation rate [242]. The fibre architecture is of interest as it impacts the degradation phenomenon. Under the same condition and with the same formulation, woven or unidirectional lose more weight than non-woven composite [242,244,245]. Indeed, more inner polymers areas are accessible by water and enzymes for the same amount of fibres.

This degradation impacts the mechanical properties of the composite. It is reported that mechanical properties decreased sharply at the early stage [239,241]. However, it is suggested that the humidity, not the microorganism, is responsible for this decrease, assumed to be due to fibre/matrix debonding [241].

The flax/PHBV strength decreases by 30% and the modulus by 45% while the weight of the samples remains stable, see in Figure 1-42. This observation raises the question of the degradation mechanisms of biodegradable composite, especially the role of microorganisms and water.

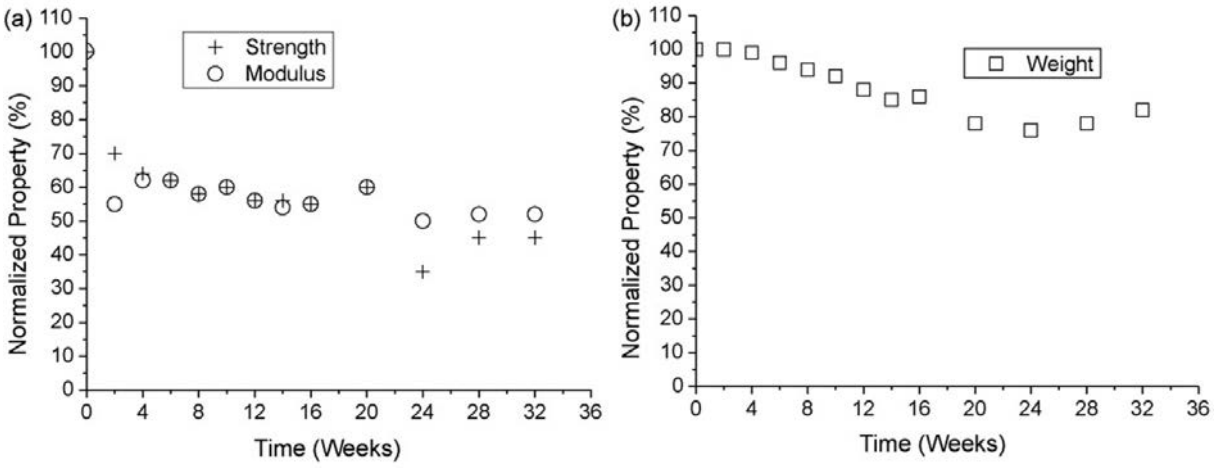

Figure 1-42: Impact of an open soil burial ageing of an injection moulded flax/PHBHV samples (Vf = 20%) on its: a) mechanical properties, b) its weight. Extracted from [241].

VII.c. Temperature influence during ageing

The impact of temperature is already discussed in section V.d., regarding the impact of the manufacturing process. The direct impact of temperature on flax fibres during composite lifetime can be neglected (against moisture). However, the temperature can induce a matrix relaxation for thermoplastics, releasing some internal stresses. Indeed, increasing the temperature increases the mobility of the polymeric chains, allowing structural modification or chemical reactions. For PLA, the impact is drastic as a temperature close to its glass transition temperature (60°C) induces hydrolysis and chain reduction [227], allowing recrystallization when cool it down again. Furthermore, water diffusion in the composite is accelerated by increasing the temperature. This phenomenon can be used in the accelerated ageing protocol [246].

Depending on the temperature and, more generally, the environment (light/oxygen), the microorganism found are not the same. Additionally, the activity of living organisms is temperature dependent [247]. Furthermore, the temperature can fluctuate in a natural environment, increasing the complexity of the degradation phenomena.

Taking compost as an example, the microorganism activity increases at an early stage. Due to the active respiration of these microorganisms, the compost temperature increases [248]. As the temperature increases, the activity of the microorganism also increases, creating a spiralling cycle. The temperature rises until a point that microorganisms cannot survive anymore [249], and a decline of microorganisms is observed before reaching equilibrium, see in Figure 1-43. During this process, the microbial and fungi population evolves, depending on their temperature affinity [247,249]. The temperature difference

during this cycle can rise 40°C [247–250], which is a critical variation speaking about polymeric chains mobility. The impact of temperature in the degradation of biocomposite can be direct via the modification of matrix structure (PLA) but are mainly indirect by increasing the impacts or rate of other phenomena such as water uptake rate, hydrolysis of the matrix or activation of micro-organism.

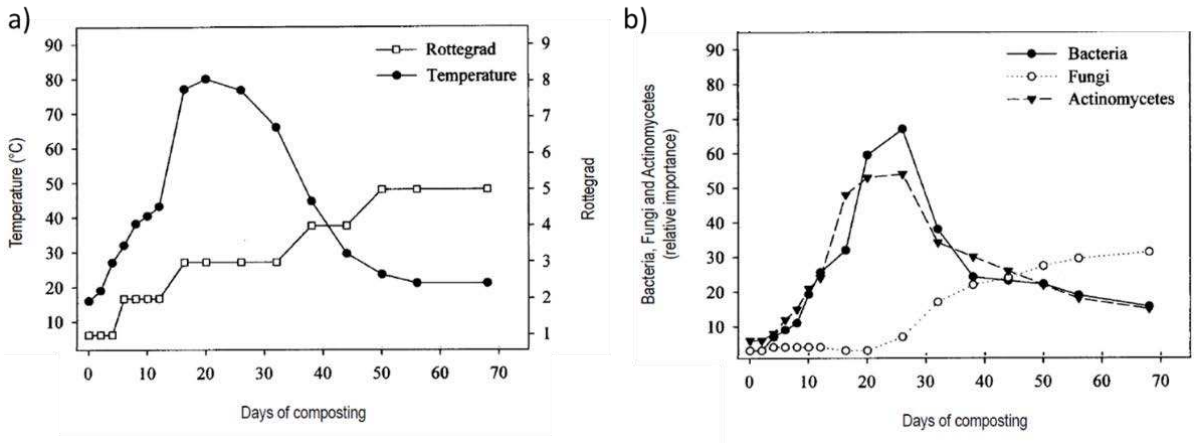

*Figure 1-43: a) Typical temperature evolution and *rottegrad evolution during composting, b) evolution of microbial population during composting. The evolutions presented are extracted from* [247] *and can vary depending on the compost substrate, the outside temperature and humidity or potential aeration and turning effect. *Rottegrad is a scale used in agriculture to discuss the maturity of a compost, going from 1 for an immature to 5 for a mature compost).*

VIII. Environmental impacts of biodegradable composites

It is of importance to separate the potential biodegradation of a material and its added value regarding environments. Indeed, the environmental impacts of material should include its extraction, manufacturing, impacts during utilisation, and end-of-life scenario. The life cycle assessment (LCA) is an efficient method to characterise the environmental (and human health) impacts of a product (and thus materials).

VIII.a. What is a Life Cycle Assessment?

The LCA is based on the ISO 14040 and 14044 [251,252]. It gives detailed results on the environmental impacts of a product. They categorised impacts under several midpoints category such as Abiotic depletion, Acidification, Global warning, Human toxicity, Fossil depletion, Eutrophication, Land use, Photochemical oxidation or Non-renewable energy. Each impact is quantified based on a specific unity. The most known is the global warning unity being the equivalent mass of CO_2 released. The value of a given impact is obtained through value aggregation of input data needed (energy, raw materials) and output data generated (product, emission, waste) at each step of the product's life.

This method should be used carefully as it could easily lead to a skewed conclusion. Indeed, this method aims to compare the impact of several scenarios to fulfil one identical functional unit, which should be quantitative. The investigated scenarios should be delimited with boundaries covering the same functional reality. All the input and output data should be reported to this functional unit. As input values of these boundaries greatly influence the results, metadata explaining their provenance are primordial. As LCA is a comparative method between several scenarios inside a study, the impact values between several studies should be compared carefully as the functional unit, assumption, and methodology could differ. Despite all this precision, it is possible to obtain fruitful information on the literature regarding the environmental impact of biodegradable composite.

VIII.b. Production

As flax fibres are mechanically comparable to glass fibres, it is interesting to compare their environmental impact. First of all, the flax impacts depend on the allocation chosen (mass or price) and the co-products management [253]. As shown in Figure 1-44, it appears that hackled flax fibres present lower environmental impacts than glass fibres regarding many environmental impacts [253]. For example, the depletion of abiotic resources decreases by 90% and human toxicity by 98%. However, an increase is noticed in land use and eutrophication. The latter is explained by fertilizers, which is an important part of the environmental impacts of flax fibres cultivation [253,254]. Gomez-Campos et al. [255] investigate the impact of making some flax weaved textile fabrics and highlight that spinning and weaving are the most impacting step. Furthermore, they compare an all-French production and a partial production in China, concluding that the delocalisation of flax production is an aberration for flax production as it increases drastically many environmental impacts.

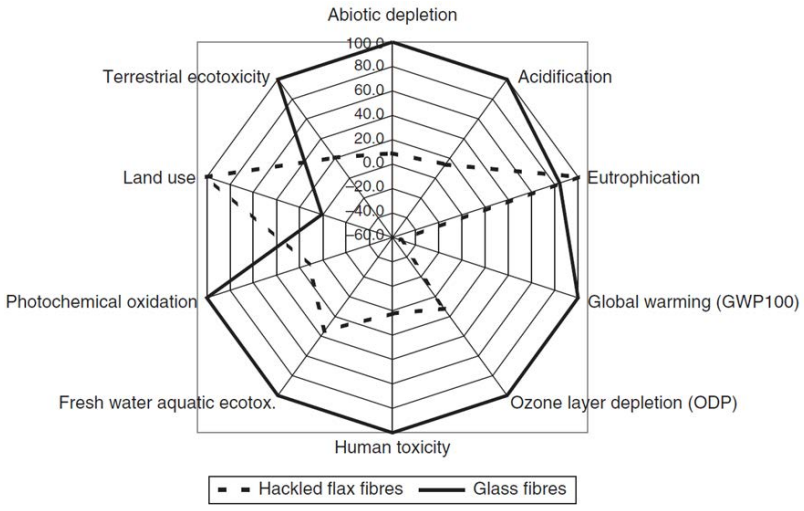

Figure 1-44: Environmental impacts of the production of hackled flax fibres against glass fibres, extracted from [253].

Some investigations focus on the possibility to modify the flax fibres via physical or chemical treatments [256,257]. By modifying the surface of the flax fibres, the compatibility with the matrix and their hydrophobicity can be improved. The alkaline treatment (based on NaOH) is the most studied, leading to the best mechanical improvement for flax composites [258,259]. It removes the non-cellulosic components of flax (hemicelluloses/pectins/lignins), reducing its hydrophilic behaviour and increasing its adhesion with hydrophobic polymers [257]. More specific treatments can have other utilities, such as modifying the fire response of flax composite [257]. Even if treating the flax fibres is of interest to improve flax composite properties, they appear to go against the environmental interest of using flax fibres. To the author's knowledge, there does not exist an LCA dealing with the environmental impact of treating flax fibres. However, the use of chemicals, such as NaOH, should increase flax fibres' environmental impact. In this thesis, no fibre treatment is considered on the preforms used and provided by producers.

Much research exists on the environmental benefits of using biodegradable polymers [260,261]. As there is a wide variation on hypothesis and boundaries considered, life cycle assessment can lead to contradictory results. However, some trends emerged. Two indicators appear to be lower for PLA than for PP: the non-renewable energy use and the global warming potentials [261]. Due to the wide variety of processes and raw materials, it is hard to conclude the environmental benefit for PHA regarding the indicators previously quoted [261,262]. However, both biodegradable polymers appear to have higher acidification potential and eutrophication potential than petrochemical polymers [261]. That can be explained by the bio-mass source, often considering corn for which the cultivation needs fertilizers [263]. Changwichan et al. [264] compared the environmental impact of PLA, PHA and PBS, concluding that PBS presents a lower global warming potential and fossil depletion potential than PLA and PHA. It is explained by less electricity need for PBS production, 0.13kWh/kg against 1.07 and 1.09 for the PLA and the PHAs, respectively. As PBS has a lower melting point than PLA and PHA, the energy needed for composite manufacturing induces fewer environmental impacts. Additionally, it is essential to understand that some improvement is still possible as biodegradable polymer production is a novel value chain with higher environmental impacts than optimized and mature chains of petrochemical polymers [265].

The impacts of flax composite combine the flax preform production (including flax growing and fibres extraction), the polymer production, and the manufacturing step of composite. Increased fibres content decreases the environmental impact of the composite when the matrix is more impacting. It is the case for PP [266,267] or PLA [263]. Comparing flax/PLA and glass/polyester composite by imposing equal tensile mechanical properties, Le Duigou et al. [263] concluded that flax biocomposite

has a lower environmental impact than glass composite (except for land use, eutrophication and aquatic ecotoxicity), as seen in Figure 1-45. The three drawbacks are due to the agricultural production of flax and corns (for the PLA). LCAs have to be based on equal mechanical properties criteria to be accurate, as at equal mass, flax and glass composite present different stiffness. Therefore, elastic responses to an applied charged are commonly chosen. The first method, chosen by Le Duigou et al. [263], balances the mechanical properties by increasing the flax composite needed. The other one is to increase the fibre volume fraction of the flax composite. As discussed previously, increasing the volume fraction of flax in flax composite decreases its environmental impact and increases the environmental impact gap between glass and flax composites [268].

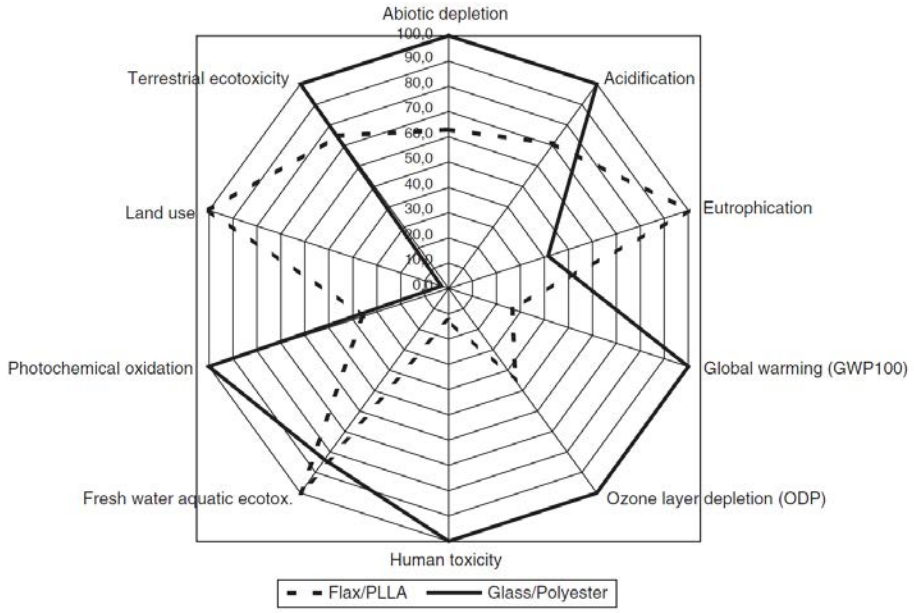

Figure 1-45: Environmental impacts of flax mat/PLA composites against glass mat/polyester. The comparison is based on equal tensile properties, extracted from [263].

VIII.c. Flax composite end-of-life

Despite the production, the end-of-life could be essential on the environmental impact of composite. Waste management is nowadays crucial to limit the human impact on the earth, such as plastic pollution, as presented initially, or global warming. Several end-of-life scenarios exist for biodegradable composite: landfill, incineration and composting. The landfill is the less suitable option as there is no recovery of materials [269], and it induces human toxicity and water pollution [270].

The incineration option releases the CO_2 content in the composite, being a critical drawback for global warming. However, it is preferred to landfill as it recovered energy and heat, which can be subtracted to the one need for manufacturing the composite, decreasing production impacts of the composite. It

is illustrated by Deng et al. [271], comparing landfill and incineration scenarios for flax mat-PP. The incineration of flax composite is much more advantageous than glass fibres composite as, contrary to glass fibres, flax fibres are combustible and have a calorific power [269].

Another potential end-of-life, specific to biodegradable composite, is composting. It appears to be more environmentally attractive than landfill [272] and incineration [270]. Composting is often considered through LCA analysis as another end of life scenario releasing CO_2 without environmental benefit [272]. However, compost has added values for the agriculture area, often not considered on LCA studies due to scarcity of data and difficulty quantifying [273]. Compost is known to supply nutriment, sequester carbon in the soil, suppress disease and pest, increase moisture content, workability and biological properties of soil [273–275]. Thus, replacing fertilizer, disease management and irrigation of fields by using compost should decrease its environmental impacts.

Before thinking about end-of-life scenarios, the best solution is to recycle the composite and reuse it for materials manufacturing. One environmental method is to crush the long fibres composite to obtain flakes [269]. These flakes can be used for making pellets thanks to extrusion or directly used to thermos-compress composite plates. Bensadoun et al. [269] compared the mechanical properties of a raw flax/MAPP non-woven composite with a composite made of flax/MAPP flakes and virgin MAPP to reached several volume fractions. Flakes composites present slightly lower flexural properties but remind comparable to non-woven composites, as presented in Figure 1-46.

Even if the first recycling option (pellets making) induces slightly more environmental impacts due to adding a process [269], the pellets can be stocked and be used by industry easily thanks to injection moulding. The mechanical properties of injected flax composite are lower than long fibres composites, but the materials still present enough mechanical properties for non-structural applications. Additionally, up to (at least) 6 cycles of recycling through the injection can be performed before decreasing the tensile modulus of PP-flax [276]. It is explained by a limited evolution of the aspect ratio of flax fibres through several cycles as injection induces shortening of flax fibres but also bundles individualisation [277]. This modulus stability through injection cycles is also observed for flax/PLA [278]. However, the molecular weight of PLA decreases after three cycles, decreasing the strength and strain at failure of the composite.

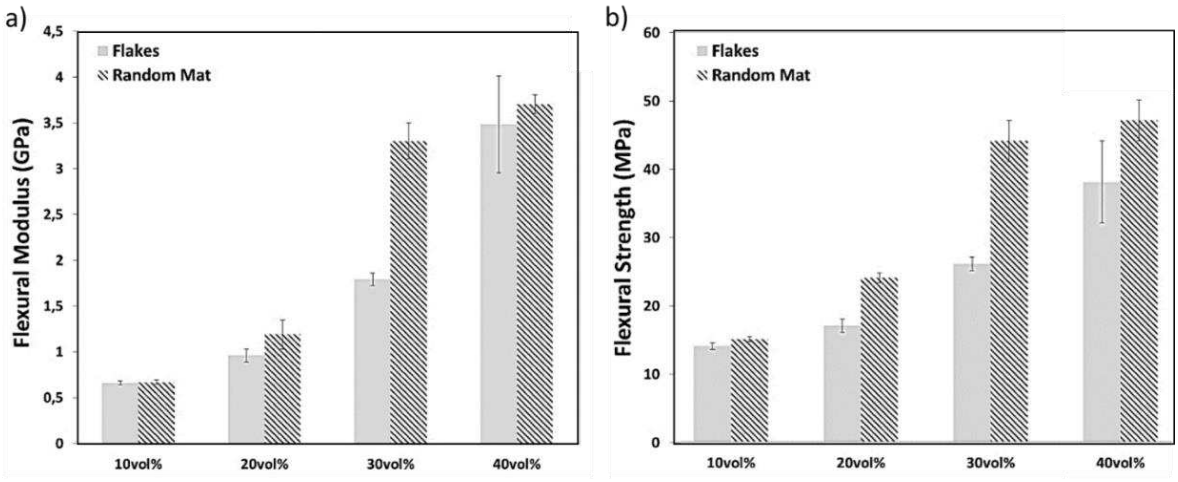

Figure 1-46: Mechanical comparison between a non-woven flax/PP composite and a recycled flax/PP composite made from flakes, obtained through crushing the nonwoven flax/PP. extracted from [269].

Chemical recycling appears to be feasible at the lab scale, being a second recycling way. The matrix is dissolved, and long flax fibres are obtained back [269]. This recycling is more interesting, mechanically speaking, as fibres' mechanical properties and geometry are not impacted. Thus, long fibres composites can be manufacturing using recycled fibres, leading to long fibres composites with equivalent mechanical properties than before recycling. However, this has a much higher environmental burden than mechanical recycling because of the para-xylene solvent used [269].

Due to the potential biodegradation and its recycling opportunities, biodegradable flax composites are perfect for the circular economy. Indeed, the circular economy is a new paradigm based on the regeneration of natural systems, the design out of waste and pollution and keeping products and materials in use. The composting is conformed to the regeneration of natural systems and waste and pollution management. The recycling steps allows maintaining the materials as long as possible in use. The composite can be subject to cascading phenomena during its circular economy process [279]. It can be reused by modifying its structure, lowering its properties but keeping it in service. It is the case when long flax composite is recycled into injected flax composites. Figure 1-47 proposes a circular economy scenario for biodegradable flax composites. The full potential of flax fibres is firstly used to make a structural or semi-structural composite (unidirectional or non-woven). It is then down-cycled through crushing and compounding to be used as raw materials for injection moulding composites. These composites can then be recycled several times as the mechanical properties remain stable during the first cycles. Finally, when the composite is not usable anymore, it can be composted to be used as nutriment for plant growth. The compost could grow flax fibres, closing the circular cycle of the biodegradable flax composite.

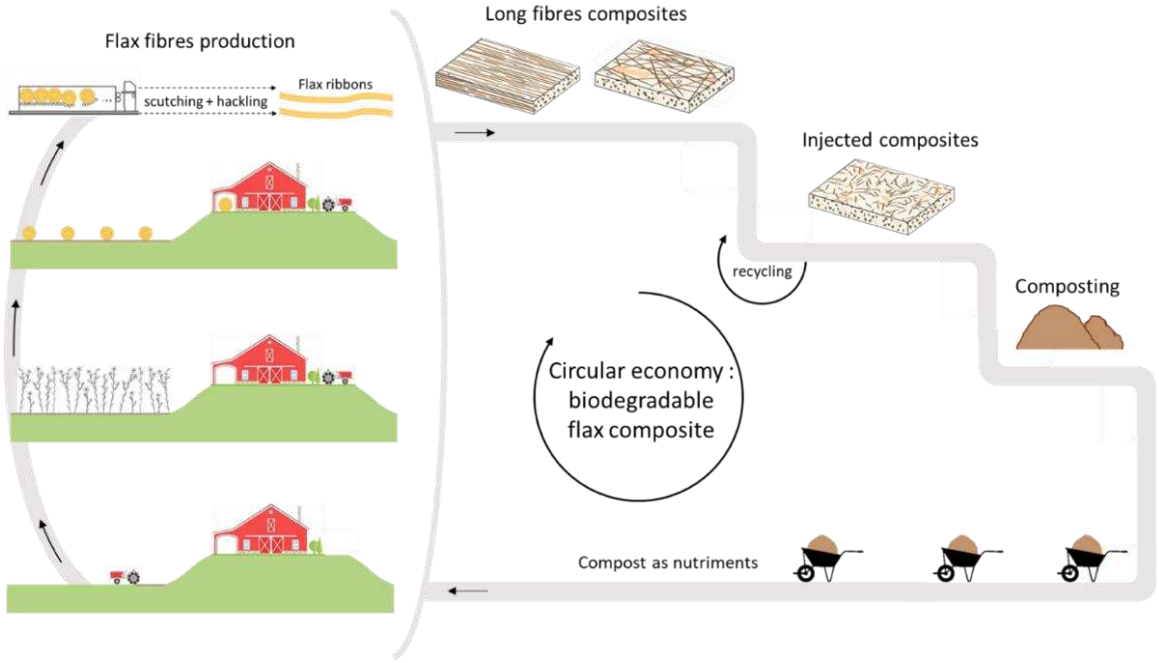

Figure 1-47: Suggestion of the biological cycle of biodegradable flax composite in the scope of a circular economy.

IX. Thesis overview

In this literature review, the feasibility of manufacturing the biodegradable thermoplastic flax composite is presented. PLA, PHA and PBS present a melting temperature lower than the flax degradation, theoretically allowing manufacturing long fibre composite thanks to thermo-compression. However, the viscosity of the melted polymer and the permeability of the flax preform should be adapted to ensure a good impregnation, and thus a low porosity composite. The choice of temperature for an ideal polymer's viscosity is tackled in chapter 2.

Thanks to the LCA review, the environmental interest in biodegradable flax composite is confirmed. However, switching to a more sustainable material does not have to be at the expense of mechanical properties. Understanding the mechanical potential and its evolution during its lifetime is needed to confirm that PLA, PHA or PBS matrix allows sustainable and mechanically performant flax composite. Additionally, it will confirm the opportunity for composite fields to enter the paradigm of the circular economy.

That is why this thesis aims to give clues on the mechanical potential of these biodegradable flax composites. It focuses on structural application as it considered only long flax fibres preforms. As exampled previously, the understanding of the composite's structure is essential to understand mechanical properties. Chapter 3 investigates the structure of a no-isotropic non-woven PLA/flax composite and highlights flax composite particularities.

The structure of a flax composite can evolve during its lifetime through environmental variations, such as moisture. This evolution is of interest in chapter 4, as a biodegradable composite is expected to be more sensitive to moisture than petro-source matrix/flax composite. Indeed, the flax fibres and the matrix appear to be hydrophilic in a biodegradable flax composite. Furthermore, biodegradable polymers mean degradation induced by micro-organisms. Therefore, it should modify the degradation behaviour of biodegradable flax composites. Thanks to garden compost ageing, chapter 5 investigates the degradation mechanisms of the biodegradable flax composites subjected to a harsh environment with a reach micro-organism population.

However, before dealing with the mechanical properties at the composite level, the affinity between the biodegradable polymers and flax fibres has to be investigated. It is tackled in chapter 2, as a good interface is crucial for an efficient stress transfer between flax fibres and matrix. Thus, it allows benefiting for the entire mechanical potential of flax fibres.

Part 1: Multiscale characterisation of biodegradable flax composite: their mechanical properties and their structure

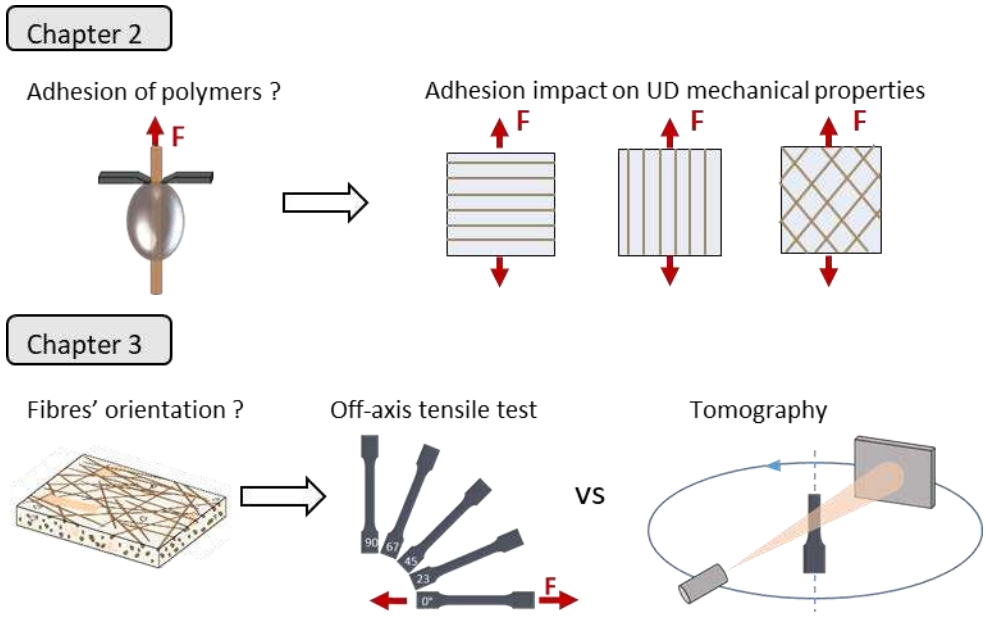

Chapter 2: Interfacial and mechanical characterisation of biodegradable polymer-flax fibre composites

I. Introduction:

Due to their lightweight and high mechanical properties, composites are used in many industrial sectors such as transport and construction. However, they often have a high environmental impact due to the choice of the polymer and the reinforcement, glass and carbon fibres, being the most commonly used. Replacing these synthetic fibres with plant fibres decreases the environmental impact of the composite [268]. Among them, flax fibres are widely chosen as their specific mechanical properties make them competitive against glass fibres [63] and opening the way to structural or semi-structural plant fibre composites.

Using flax fibres as a reinforcement creates a complex material with several mechanical systems and interfacial regions. The main constituents are elementary flax fibres, having a hierarchic structure leading to a complex mechanical behaviour [87] and bundles, aggregating several tens of elementary fibres, and coming from the original arrangement of fibres within a stem. These two main fibrous elements are also present in the composite structure, and the associated interfaces regions need to be taken into account [96]. An elementary flax fibre/polymer matrix interface is considered the primary stress transfer region between the matrix and the fibre [101]. In addition, a fibre/fibre interphase is present in bundles; this is a 50 – 100 nm thick layer of peptic polymers [280] linking fibres together, called the middle lamella. The importance of the middle lamella should not be disregarded as it may be a zone of weakness in a composite material [102].

Polyolefin polymers such as poly-(propylene) (PP) are commonly used with flax fibre reinforcements [63], though these traditional thermoplastics, due to their petrochemical origin and limited end-of-life route (as recycling), have a limited ecological profile. With the emergence of some bio-sourced and biodegradable polymers, examining their potential as alternatives to traditional thermoplastics is relevant. Poly-(lactide) (PLA), poly-(butylene-succinate) (PBS) and poly-(hydroxy alkanoate) (PHA) may replace PP due to their excellent mechanical performance and their relative stability. Interestingly, all three biodegradable polymers (PLA, PHA, PBS) have melting points under 200°C, allowing biocomposites manufacturing without damaging flax fibres [196]. Moreover, biodegradation can be an alternate end-of-life scenario for these polymers, and their flax reinforced biocomposites. However,

it is essential to look at the affinity between flax fibres and these polymers to understand the feasibility of making effective biodegradable biocomposites, as well as appreciate their mechanical properties.

This affinity is physically observed through the polymer/fibre interface, assessed from at least two scales [101]. At the micro-scale, one can measure the interfacial shear strength (IFSS) of the interface between the fibre and polymer. Many protocols exist and have their advantages and disadvantages [101]; the micro-droplet test [111] is employed in this paper. One can also measure the performance of the interface at the composite or macro-scale. In composites science, a widely used test is the ±45° off-axis tensile test developed and simplified by Rosen [281]. As it uses a unidirectional (UD) fibre lay-up, it is more practical to conduct and is employed in this study.

For flax composites, it has been demonstrated at both scales that epoxy resins have good adherence to flax fibres [115]. Regarding thermoplastic polymers, few research studies are available. Nevertheless, it is well-documented that PP presents a poor interface quality with flax, and maleic-anhydride grafted PP (MAPP) is a standard solution to obtain a better interface [282]. Due to its mechanical and ecological potential, the flax/PLA interface was explored and shown to be close to flax/epoxy resin [92]. However, to the authors' knowledge, no articles have studied the interface between PHA or PBS and flax.

This study aims to characterise mechanical properties of the interface at the micro-scale and determine its influence on biocomposite properties, to assess whether heterogeneity of the mesostructure has any role. The micro-droplet method characterises fives thermoplastics (PP, MAPP, PLA, PHA, PBS) and elementary flax fibre adhesion. In addition, $[\pm 45]_s$ in-plane shear tests and tensile tests on unidirectional composites are realised and compared with interfacial shear strength to evaluate the role of the quality of the interface on biocomposite performance.

II. Materials/methods:

II.a. Materials

a.i. Raw materials

Lightweight unidirectional flax preforms (100 gsm), known as Flaxtape® and provided by Ecotechnilin (Yvetot, France), were used to make composites. It is made of untwisted flax fibres linked together by pectin [156]. For consistency, elementary flax fibres used to carry out micro-droplet tests were extracted from this preform. Three biodegradables polymers were used for this study: poly-(lactide) (PLA), poly-(butylene-succinate) (PBS) and poly-(hydroxy alkanoates) (PHA). In addition, Poly-(propylene) (PP) and maleic anhydride grafted poly-(propylene) (MAPP) were used as industry

references. Supplier details and references are provided in Table 2-1. Note that MAPP is considered to behave as PP in the following polymer analysis. Indeed, the MAPP matrix is a mixt with 96% in weight of PP and 4% in weight of the commercial MAPP.

Table 2-1: List of matrix suppliers and reference IDs of the polymers.

Polymer	Provider	reference	Density	MFI
PLA	NatureWorks	PLA3001D	1.24	22 (210°C/2.16kg)
PHA	NaturePlast	PHI002	1.25	15 – 30 (190°C/2.16kg)
PBS	pttMCC	BioPBS™ FZ71PM	1.26	22 (190°C/2.16kg)
MAPP	Arkema	Orevac CA100	0.905	44 (230°C/2.16kg)
PP	Total	PPC10942	1.24	22 (210°C/2.16kg)

a.ii. Polymer thermal analysis

A differential scanning calorimetry (DSC) study was conducted on the different polymers with a DSC3 Mettler Toledo (Mettler Toledo, Greifensee, Switzerland) to determine their thermal behaviour between 25°C and 200°C at a rate of 10°C/min. The melting temperatures were measured to inform processing conditions. Two repetitions were done for each virgin polymer, and mean values were recorded. Figure 2-1 presents the results of a differential scanning calorimetry investigation on virgin polymers. PLA, PHA and PP have a similar melting temperature, 172°C, 177 °C and 168 °C, respectively. PBS presents a lower melting temperature of 119°C. In addition, the glass transition temperature of PLA is not clearly defined here, but relaxation is noticed between 60°C and 70°C. Glass transition temperatures of PHA, PBS and PP are not observed/measured here; they are expected to be below ambient temperature.

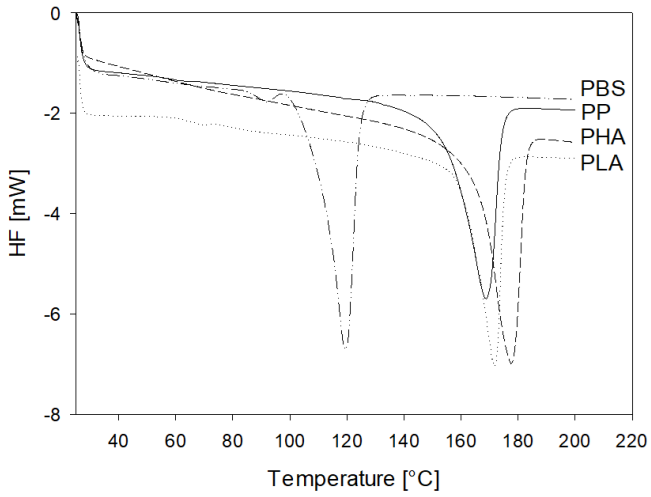

Figure 2-1: Differential scanning calorimetry of the four polymers (PLA, PHA, PBS, PP) used to make flax biocomposites. Tests were done from 25 °C to 200 °C at 10 °C/min in open aluminium pans.

These melting temperatures allow us to consider biocomposite processing cycles below 200°C, which is essential to not thermally degrade the flax fibres and maintain their performance and mechanical behaviour [193].

a.iii. Polymer films manufacturing and characterisation

First, polymer granulates were transformed into films. For this, they were dried at 60°C for 12h under vacuum before undergoing a process of extruding and calendaring using a mono-screw extruder (Labstation Plasticorder Brabender) and a calendaring machine Univex Brabender (Brabender, Duisburg, Germany). The main process parameters are presented in Table 2-2, and Figure 2-2 presents the setup used to manufacture polymer films. After this process step, polymer films were obtained with thicknesses varying from 50 to 100 μm.

Table 2-2: Extrusion and calendaring machine parameters of films.

	Extruding parameters					Calendaring parameters	
Polymer	T die	T zone 3	T zone 2	T zone 1	Screw speed (turns/min)	Roller temperature	Roller speed (turns/min)
PHA	170 °C	190 °C	190 °C	190 °C	40	60 °C	1
PBS	130 °C	140 °C	140 °C	160 °C	40	45 °C	1
PLA	190 °C	190 °C	190 °C	190 °C	50	50 °C	5
PP	200 °C	200 °C	200 °C	200 °C	80	70 °	2

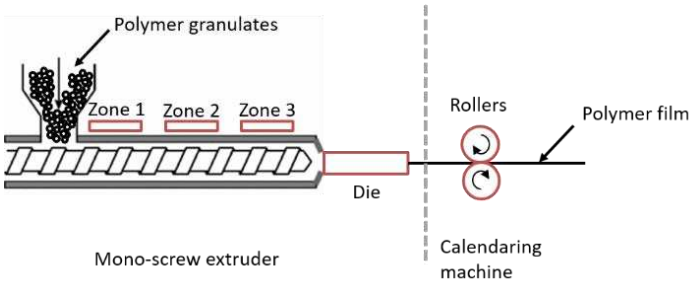

Figure 2-2: Extrusion and calendaring process used to transform polymer granulates into a polymer film.

As the composites are made by film stacking, it is essential to define the appropriate processing temperature to ensure good impregnation of flax preforms with the polymer. During the film stacking process, the shear rate applied is generally between 1 s^{-1} and 10 s^{-1} [46,190,192]. Therefore, a polymer viscosity of 500 ± 50 Pa.s is targeted to ensure good impregnation, considering the light architecture of the flax preform used. Furthermore, processing all composites at the same polymer viscosity is a way to ensure similar impregnation of the flax preforms.

Thus, after calendaring, the viscosity at several temperatures for the virgin polymers has been investigated to find the ideal processing temperature. A rheological study was done using an Anton Paar Physica MCR 301 rheometer (Anton Paar, Graz, Austria). A plate/plate stationary study was performed at a fixed temperature with a shear rate scan from 0.01 s^{-1} to 100 s^{-1} and a gap of 300 µm. Several temperatures were analysed for each polymer depending on their melting temperature, three repetitions at each temperature were realised, and the mean curve was calculated. All the investigation results are presented in Figure 2-3; the black rectangle identifies the film stacking process parameters given above. For all polymers, increasing the temperature induces a decrease in their viscosity. This study leads us to choose the following processing temperature for making composite: 200°C for PLA, 175°C for PHA, 170°C for PBS and 190°C for PP and MAPP.

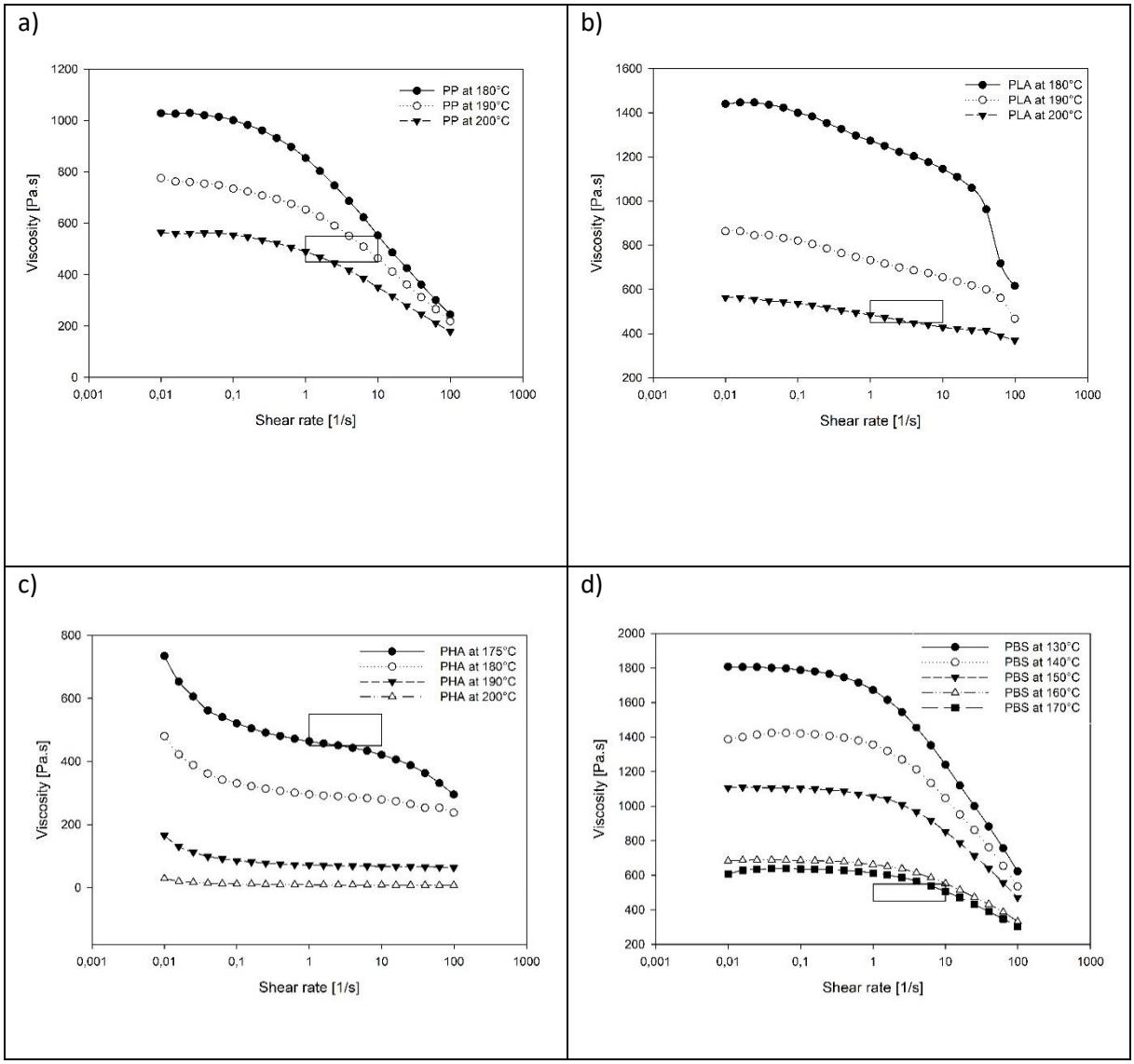

Figure 2-3: Viscosity of virgin polymers at several temperatures close to their melting temperature, a) polypropylene (PP), b) polylactic acid (PLA), c) polyhydroxyalkanoate (PHA), d) polybutylene succinate(PBS). The black rectangle is the valid range for a good film stacking impregnation.

In our case, the process temperatures are a maximum of 200°C, without the risk of self-heating as can be the case in extrusion, and the maximum exposure time was limited to 8 minutes (Figure 2-4). In this time and temperature range, flax fibres retain satisfactory mechanical properties [193,196].

a.iv. Composite manufacturing

As all the polymers investigated are thermoplastics, the film stacking process and thermos-compression were used to manufacture the composite laminates thanks to a hydraulic press LabTech Scientific 50T (Labtech, Samutprakarn, Thailand). Lay-ups were put in an oven at 40°C for 24h under vacuum to dry flax and biopolymer before manufacturing the composite. The thermo-compression cycle, presented in Figure 2-4 for PLA flax composite, had been optimised using thermal and rheological data. The hot plates temperature was fixed during the entire cycle and depend on the polymer: 200°C for PLA, 175°C for PHA, 170°C for PBS and 190°C for PP and MAPP. This temperatures choice aimed to obtain composites with a similar level of impregnation due to a similar polymer viscosity.

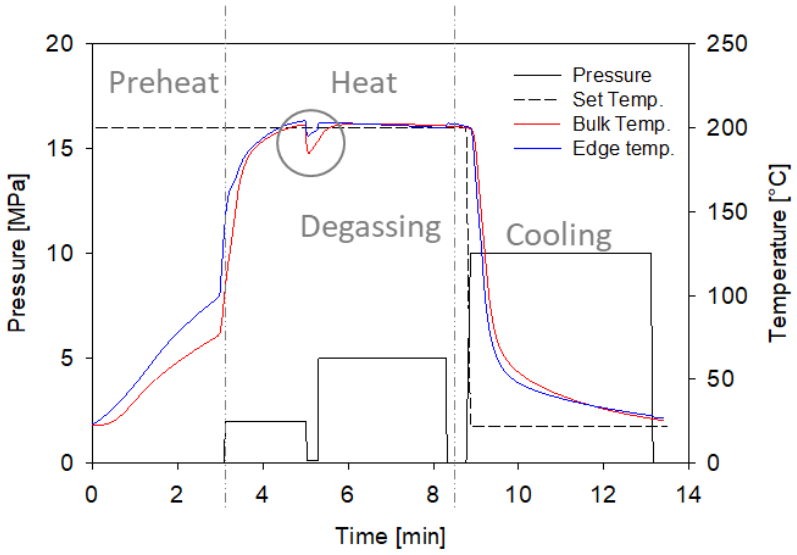

Figure 2-4: Hot-compression cycle used to manufacture the composites. A temperature of 200°C is maintained on the plate, which corresponds to flax/PLA temperature. The temperature of the plate for the PBS, PHA, PP and MAPP are respectively 170°C, 175°C, 190°C and 190°C. The temperature inside the composite is recoded at the middle and the edge using a thermocouple sensor. A degassing step is present to release any water vapour. The quick cooling is managed using a cold plate pressing the composite.

The lay-up was put in the contact of the hot plates for three minutes to melt the polymer. Then, the first compression at 2 MPa was applied for two minutes following by a quick degassing. The last compression at 5 MPa was performed for three minutes. The lay-up was then cooled, placing it

between two cold plates for four minutes under a pressure of 10 MPa. Flax preforms and polymer films were laid sequentially to make unidirectional and bi-axial composites, the orientation of flax fibres depending on the composite: $[0]_{16}$ for UD and $[\pm45]_{8s}$ for bi-axial. A volume fraction of 32 ± 1% was achieved, estimated by a density method, i.e. through the exact weight and dimensions for each sample; then, fibre content was calculated by inverse method, knowing the fibre and matrix density. This manufacturing method yields composites with porosity lower than 2%. Results have been backed up by image analysis. Once these laminates were manufactured, they were cut with a milling machine. Samples with a shape based on ISO 527-4 for the $[\pm45]_{8s}$ and ISO 527-5 for the $[0]_{16}$ were fabricated. Longitudinal 0° and transverse 90° samples were produced from the unidirectional laminates.

As the matrix mechanical properties are of interest to discussed experimental values, pure polymer plates of 110x110x2mm were manufactured by injection moulding with Battenfeld BA800 injection machine (Wittmann Battenfeld, Kottingbrunn, Austria). They are cut by a milling machine based on ISO 527-4.

a.v. Micro-droplet sample manufacturing

Elementary flax fibres were extracted manually from the Flaxtape®. Some polymers wires were obtained by melting and rapidly stretching polymer films. A polymer wire was then manually fixed to an elementary fibre by making a double knot around the fibre (Figure 2-5.a)). Finally, the system was put in an oven for 8 min at 200°C to melt the polymer double knots and transform them into micro-droplets (Figure 2-5.b)). The geometry of every droplet was measured with an optical microscope. The length, diameter, and fibre diameter were obtained for each droplet through an average of two measures. The aspect ratio was extracted from these measures by dividing the length of the droplet by its radius. The pictures used for the aspect ratio characterisation were analysed using software provided by *GBX* to identify the contact angle by a Song's method [116]. For each formulation, contact angle and aspect ratio are mean values from at least 20 valid measurements.

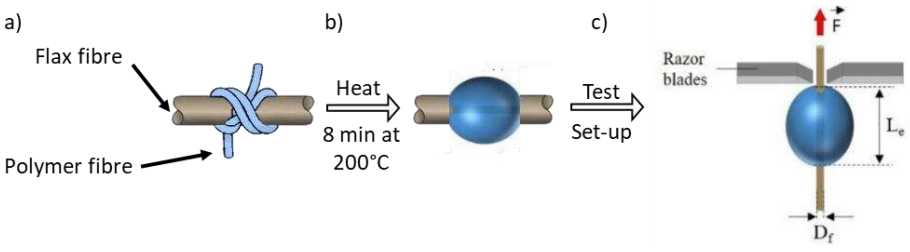

Figure 2-5: Process to manufacture micro-droplet using thermoplastic wires; a) double knot is made manually with the polymer fibre around an elementary flax fibre previously extracted; b) the fibre is heated to melt the polymer and create a micro-droplet; c) micro-droplet is placed in the setup and is ready to be tested (extracted from [113])

II.b. Methods

b.i. Micro-droplet tests

The elementary fibre/micro-droplet system was placed in a tensile machine equipped with a 2 N load cell. The fibre is placed between two razor blades with the droplet just below them. The fibre is pulled at a displacement rate of 0.1 mm/min, starting with the blades locking the droplet and continuing until debonding occurs (Figure 2-5.c)). Load-displacement curves were obtained (Figure 2-6.a)). At least 20 samples were tested for each polymer to calculate the mean interfacial shear strength (IFSS). IFSS is commonly obtained using equation (2-1), where *F* is the debonding force, L_d is the length of the droplet, and D_f is the diameter of the fibre.

$$\text{Interfacial shear strength = IFSS} = \frac{F_{debonding}}{A_{interface}} = \frac{F}{\pi . L_d D_f} \tag{2-1}$$

As recommended by Miller [111], the mean IFSS value in our study is obtained from a linear regression analysis between the debonding load and the interface area (Figure 2-6.b)). In addition, the friction stress ($\tau_{friction}$) is obtained using the same method but using the friction load, which is the load after debounding (Figure 2-6.a)).

b.ii. In-plane shear tests

The $[\pm 45]_{8s}$ samples were tensile tested at a 2 mm/min displacement rate on an Instron machine equipped with a 10 kN load cell. An MTS biaxial extensometer was used to record longitudinal and transverse strain. According to ASTM D 3518, the shear stress (τ_{12}) is given by (2-2) and the shear strain (γ_{12}) by (2-3), where *F* is the force applied, *S* is the sample section, ε_x and ε_y are the axial and transversal strain, respectively.

$$\tau_{12} = \frac{F}{2.S} = \frac{\sigma}{2} \tag{2-2}$$

$$\gamma_{12} = \varepsilon_x - \varepsilon_y \tag{2-3}$$

The shear behaviour was obtained by plotting shear stress versus shear strain. As suggested by the standard, the in-plane shear strength (IPSS) was taken to be equal to the shear stress at a shear strain of 5%. The shear modulus was recorded as supplementary data and calculated between 0.1% and 0.5% shear strain. For each formulation investigated, at least five samples were tested.

b.iii. Tensile tests

Longitudinal 0° samples and transversal 90° samples were placed in an Instron machine and tested at a 1mm/min cross-head speed, using a 10 kN load cell. Tensile tests were carried out following ISO 527, and an Instron extensometer recorded strain in the loading direction. Strength and strain at failure were calculated. A tangent modulus for both orientations was calculated between a strain of 0.02 % and 0.1%. Furthermore, a second tangent modulus was recorded at a 0.6% to 0.8% strain for the longitudinal samples. This threshold is taken when the modulus is stable, whatever the formulation considered on this strain range. Indeed, it is known that UD flax composites have a bi-linear behaviour [222], in part due to the non-linear response of flax fibres induced by its inner structure [283]. For each formulation investigated, at least five samples were tested. The tensile properties of pure polymers are obtained through the same protocol, using a 0.02% to 0.1% range for PHA and 0.1% to 0.5% for PLA, PBS, MAPP and PP, which have a higher elastic zone.

b.iv. Scanning electronic microscopy

A JEOL SEM (JSM-IT500HRSEM) was used to observe the micro-droplet samples after debonding at an acceleration voltage of 3 kV. Transverse sections of UD composites were also observed. Gold sputter coating was carried out using a sputter coater (Scancoat6) from Edward.

III. Results

III.a. Interfacial shear strength at micro-scale

Like other micro-scale interface tests, the micro-droplet test depends on several factors. The first step is to ensure that the studied systems are similar and therefore can be compared. For example, comparing results from studies with different operators, setups, and sample manufacturing processes may be invalid, as these may significantly influence the droplet morphology and test result. However, these parameters stay constant in our systematic study of five different flax/polymer systems. Furthermore, the shape of the droplets has been scrutinised using microscopy to ensure mechanical results can be compared across the different flax/polymer systems. The contact angle of the droplet on the flax fibre and the droplet aspect ratio are presented in Table 2-3 and an example (on the flax-PHA system) of typical debonding load-displacement curve, interfacial shear strength determination by linear regression and SEM images of droplet after debonding, is given in Figure 2-6. As both these parameters are comparable for all polymers, it is concluded that the shape of droplets may be regarded as similar.

*Table 2-3: Mechanical characterisation of flax composites at various scales: micro-droplet test, in-plane shear test, and tensile test on unidirectional composite in both directions. * EI,1 is calculated from a strain of 0.02% to 0.1% and EI,2 from 0.6% to 0.8%.*

		PLA	PHA	PBS	MAPP	PP
Micro-droplet test	Contact angle [°]	69.3 ± 3.5	66.1 ± 7.5	72.3 ± 4.1	64.3 ± 4.6	67.7 ± 5.2
	$L_{droplet}/D_{droplet}$ [-]	1.28 ± 0.08	1.32 ± 0.09	1.24 ± 0.07	1.33 ± 0.14	1.33 ± 0.09
	Interfacial shear strength (IFSS) [MPa]	15.6 ± 2.7	8.3 ± 1.1	8.5 ± 1.5	9.8 ± 1.8	4.6 ± 0.6
	$\tau_{friction}$ [MPa]	4.7 ± 1.6	3.4 ± 0.8	3.2 ± 1.0	2.1 ± 0.4	1.9 ± 0.5
In-plane shear test on $[\pm45]_s$	V_f [%]	32.2 ± 0.4	30.2 ± 0.9	30.4 ± 0.8	30.6 ± 0.4	32.3 ± 0.4
	G_{lt} [MPa]	1756 ± 64	1286 ± 16	572 ± 25	806 ± 18	654 ± 24
	In-plane shear strength (IPSS) MPa]	33.2 ± 1.1	19.4 ± 0.3	13.9 ± 0.3	17.1 ± 0.3	12.0 ± 0.0(4)
	τ_{max}[MPa]	34.2 ± 1.0	-	-	-	-
	γ_{max} [%]	3.1 ± 0.2	-	-	-	-
Tensile test on matrices	E_m [GPa]	3.8 ± 0.1	4.4 ± 0.3	0.75 ± 0.1	1.58 ± 0.05	1.4 ± 0.2
	$\sigma_{rupt,m}$ [MPa]	61.4 ± 0.8	38.6 ± 1.4	39.1 ± 0.5	25.1 ± 0.1	24.4 ± 0.8
	$\varepsilon_{rupt,m}$ [%]	2.0 ± 0.1	1.3 ± 0.1	14.7 ± 5.4	5.3 ± 0.2	4.3 ± 0.7
UD parameter	V_f [%]	33.5 ± 0.2	33.2 ± 0.5	32.9 ± 0.25	33.0 ± 0.8	31.7 ± 0.7
Transversal tensile test on UD	E_t [GPa]	4.2 ± 0.4	3.9 ± 0.9	1.5 ± 0.1	2.5 ± 0.3	2.0 ± 0.2
	$\sigma_{rupt,t}$ [MPa]	25.8 ± 1.0	13.6 ± 0.4	13.4 ± 0.3	15.3 ± 0.5	9.1 ± 0.5
	$\varepsilon_{rupt,t}$ [%]	0.72 ± 0.06	0.60 ± 0.14	2.02 ± 0.30	1.02 ± 0.13	1.39 ± 0.28
Longitudinal tensile test on UD	$E_{l,1}$ [GPa] *	20.1 ± 2.8	20.3 ± 3.1	16.9 ± 2.5	17.8 ± 2.8	17.9 ± 4.3
	$E_{l,2}$ [GPa] *	16.3 ± 0.9	14.8 ± 1.1	13.7 ± 1.3	13.4 ± 2.1	11.9 ± 1.6
	$\sigma_{rupt,l}$ [MPa]	216 ± 17	182 ± 13	184 ± 9	151 ± 9	133 ± 17
	$\varepsilon_{rupt,l}$ [%]	1.30 ± 0.16	1.13 ± 0.10	1.36 ± 0.15	0.99 ± 0.07	1.14 ± 0.19
Back calculation using a ROM	E_{fibre} [GPa] using $E_{l,1}$	59.8 ± 8.3	60.9 ± 9.3	51.6 ± 7.7	53.8 ± 7.4	55.9 ± 13.7
	E_{fibre} [GPa] using $E_{l,2}$	48.5 ± 2.4	44.4 ± 3.0	41.6 ± 4.0	40.4 ± 5.8	29.5 ± 16.1

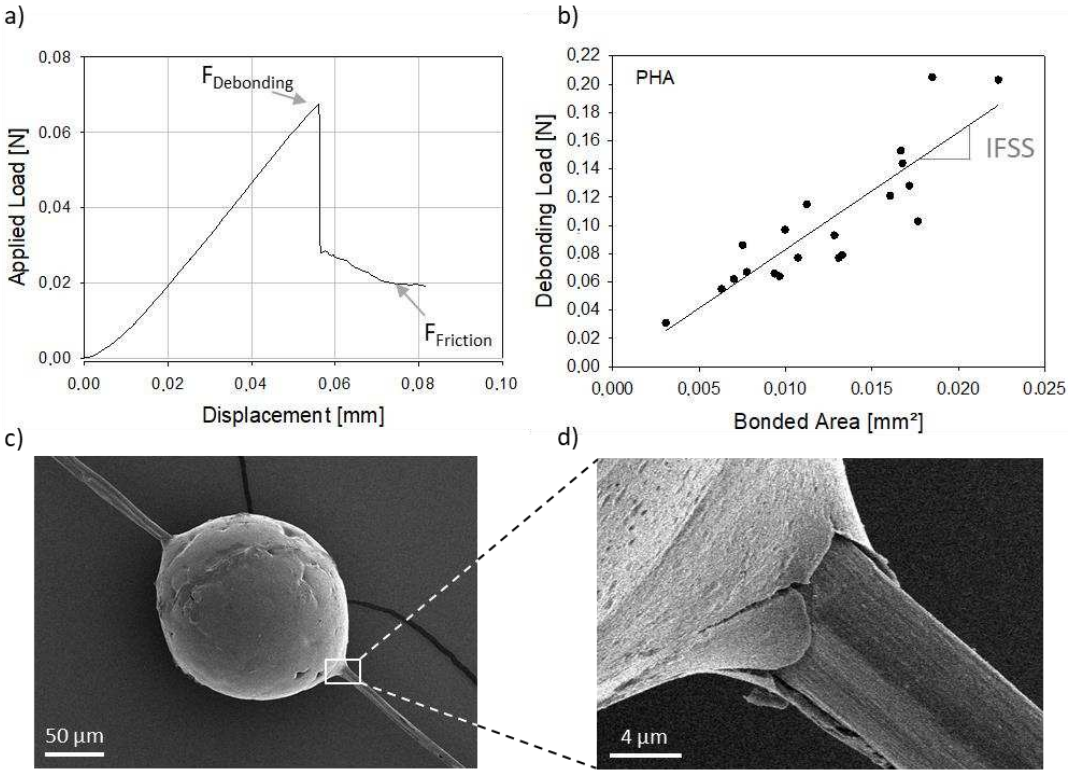

Figure 2-6: a) Typical response of a flax/PHA droplet system undergoing a micro-droplet test; b) Mean interfacial shear strength determination by linear regression of PHA bonded to elementary flax fibre; c)-d) PHA droplet on an elementary flax fibre with a zoomed image showing the interface failing through mode II.

Furthermore, the rupture mechanism of the interfaces was observed by SEM. It was ascribed as interfacial shear failure (Mode II) for all polymers investigated here- see in Figure 2-6.c) and Figure 2-6.d) in the case of PHA. This further ensures that the mechanical polymer/fibre systems investigated can be compared. It is observed that PLA has an interface comparable to a poorly-adhered epoxy, as epoxy has a mean IFSS with flax of 18.6 ± 4.8 (mean value based on [92,115,126,127]) against 15.6 ± 2.7 for PLA/flax (based on our study). PHA, PBS and MAPP present similar IFSS with flax, though lower than PLA (Table 2-3). The effectiveness of maleic anhydride is exemplified by the fact that the IFSS of MAPP/flax is double that for PP/flax. Therefore, all bio-polymers have better or comparable adhesion with flax than MAPP and PP. Higher surface tension explains it for PLA/PHA/PBS than for PP/MAPP, see in Table 2-4, which leads to a better power of adhesion. Furthermore, the surface of flax fibres presents many hydroxyl terminations. The presence of ester groups in these biopolymers allows some hydrogen bonds with flax surfaces, not found with PP. These hydrogen bonds are present with MAPP due to the maleic-anhydride, as well as chemical bonds, explaining more comparable results.

Table 2-4: Surface tension of the polymer extracted for literature.

Polymer	γ [mN/m]	γ_{polar} [mN/m]	$\gamma_{dispersive}$ [mN/m]	references
PLA	38.8 ± 0.2	8.5	30.3 ± 0.2	[284]
PHA	42.6 ± 0.5	6.0 ± 0.8	36.6 ± 0.1	[285]
PBS	43.6 ± 0.4	10.5 ± 0.1	33.1 ± 0.3	[284]
MAPP (4%wt MA)	29.6	8.13	21.47	[286]
PP	21.9	4.58	17.32	[286]

III.b. In-plane shear strength at macro-scale

As fibre volume fraction influences the results from the in-plane ± 45° shear test, we have ensured that samples have the same fibre content (Table 2-3). In-plane shear strength (IPSS) results follow the same trend as the interface at the microscale level; values are given in Table 2-3. PLA presents the best results, followed by PHA and then MAPP. PBS is slightly below MAPP but still higher than the industry reference, PP. Once again, the effectiveness of grafting PP with maleic anhydride to improve the interface with flax is observed. Note that the shear stress of PLA reaches a maximum value of 34.2 ± 1.0 MPa before the shear strain is at 5%, leading to an IPSS of 33.2 ± 1.1 MPa.

The in-plane ± 45° shear test is an efficient and straightforward method to obtain IPSS. However, it is essential to be aware that this test does not apply pure shear stress [137]; some inter-laminar stresses and inhomogeneous stress and strain distributions are present. Nevertheless, this test leads to a good approximation [137], which can be used to affirm that flax and biopolymer interfaces are better or comparable to MAPP and PP at the macro-scale, just like it was observed at the micro-scale.

III.c. Unidirectional composite characterisation

c.i. Transverse tensile behaviour

Unidirectional (UD) composites were characterised through transverse 90° tensile tests to obtain the transverse modulus, strength and ultimate elongation. Focussing on the strength, it appears that flax/PLA presents the best transverse strength of 25.8 ± 1.0 MPa, followed by PHA, PBS and MAPP (Table 2-3). As PP presents a lower strength than MAPP, the interface should have a role in the transverse tensile strength of the composite. It will be discussed in section IV.b.i., where the correlation between micro-scale and macro-scale interfacial and transverse strength is examined. Notice that samples submitted to a transverse tensile test present a significant strain concentration in the matrix and at the interfaces [144]. It creates zones of high internal strains, damaging the material by generating micro-cracks. The eventual failure of the composites is due to the coalescing of these micro-cracks into (a) macro-crack(s). The matrices respond to these high local strains differently. Indeed, the behaviour of the transverse-loaded composites (Figure 2-7.b)) is similar to the response of

the corresponding raw polymer (Figure 2-7.a)). Furthermore, there is a clear relation between the ultimate strain of the matrices and the ultimate strain of the transverse-loaded UD composites (Figure 2-7.c)).

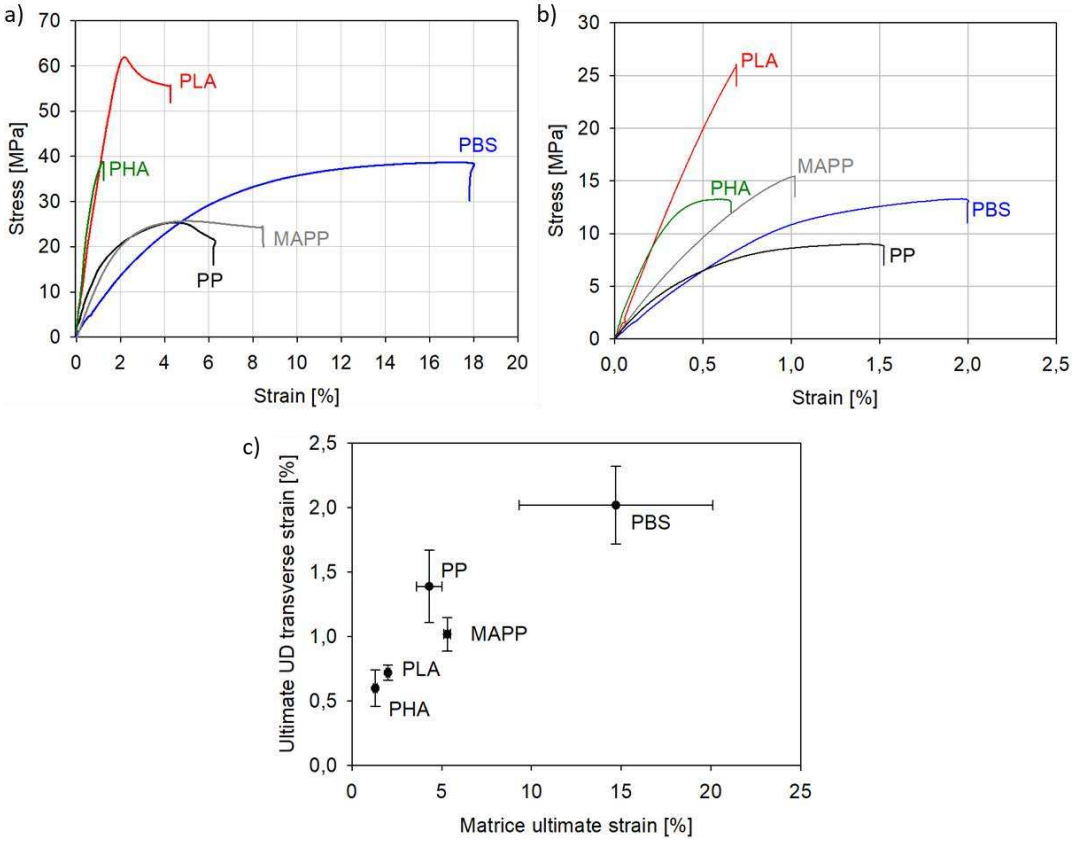

Figure 2-7: a) Virgin polymer behaviour under tensile test, b) Transverse tensile behaviour of UD flax composites at a volume fraction of 32%, c) relation between the ultimate transverse strain of flax composites and the ultimate strain of the corresponding matrices.

The structure of a UD flax composite is more complex than that of a synthetic fibre composite (see Figure 2-8). In the former, the matrix is reinforced by elementary fibres, which are not cylindrical or regular, and larger irregular bundles. It is also possible to find some residual bast tissue due to the natural origin of flax fibres. All these elements generate a different strain concentration and distribution. Furthermore, due to the random dispersion of these fibre elements in the matrix, the high strain distribution in the matrix becomes complex and can be locally high.

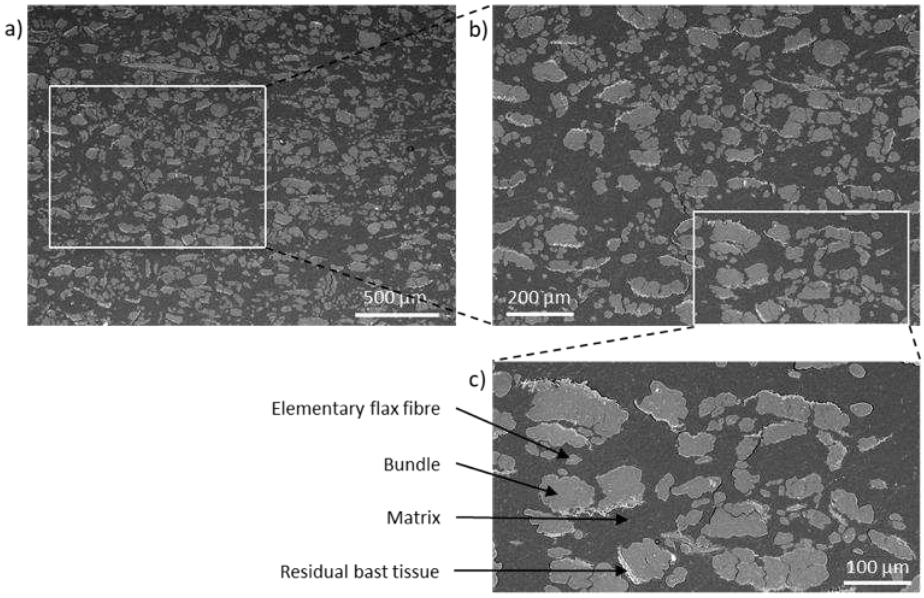

Figure 2-8: Sliced observation of a MAPP/flax composite at several scales.

c.ii. Longitudinal tensile behaviour

It is observed that the tensile behaviour of flax UD composites investigated is generally bilinear (see Figure 2-9). This bilinear behaviour was also observed for flax/unsaturated polyester and flax/epoxy composites [196,212].

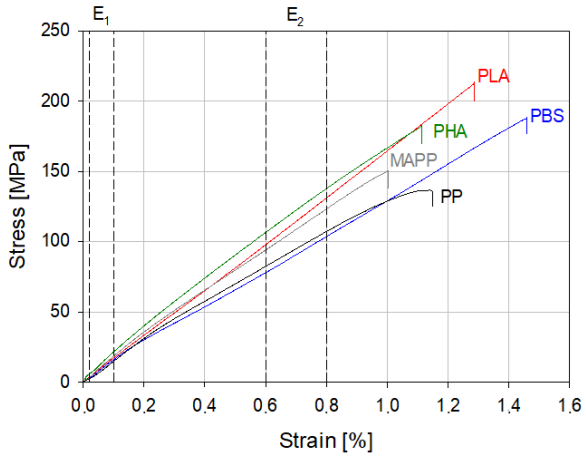

Figure 2-9: Longitudinal tensile behaviour of unidirectional flax composites. The dotted line indicates the strain range for modulus calculation.

Thus, two stiffnesses ($E_{l,1}$ and $E_{l,2}$) were recorded, and for both, bio-polymers present at least comparable values to MAPP. All the results of the longitudinal tensile test are presented in Table 2-3. Regarding strength, PLA is followed by PHA and PBS, and all biopolymers possess composite strength

higher than MAPP. Looking at the change of slope, it seems that the choice of the polymer does not influence the strain where the change in linearity takes place. As this phenomenon is not matrix dependent, it may be due to the behaviour of the fibre [196].

It is possible to back-calculate the fibre modulus using the rule-of-mixtures; results are presented in Table 2-3. Looking at the results from the first composite stiffness ($E_{I,1}$), it appears that the back-calculated flax moduli obtained, see Table 2-3, are close to the literature value of 52.5 ± 8.6 GPa [83] for all considered polymer matrices.

IV. Discussion

IV.a. Influence of interface on composite shear strength

Two scales are of interest to obtain information on the interface(s). The micro-scale examines the adhesion between the polymer and elementary fibres through the IFSS. In contrast, the in-plane shear strength (IPSS) includes effects of the complex mesostructure of a flax composite, such as bundles, heterogeneity in fibre properties, possible remaining cortical components and fibre/fibre interphases. Both experiments show significant differences in the scales investigated, fibre volume fractions used, and stress distribution generated.

Nevertheless, as shown in Figure 2-10, there is a linear correlation between IFSS and IPSS. It indicates that adhesion between elementary flax fibres and the polymer is likely to be a crucial factor affecting in-plane shear strength. The in-plane shear strength IPSS presents a higher value than interfacial shear strength IFSS as the former does not only load interfaces and presumably obtains higher contribution from fibres. Furthermore, this relation depends on the preform's level of individualisation (i.e. ratio of elementary fibres to fibre bundles). It is expected that a preform containing more bundles will deviate from this trend as the micro-droplet test was carried out on elementary fibres, and a bundle's behaviour would be more complex, according to the retting degree and the composition of fibre junctions.

The micro-droplet test focuses directly on the fibre/matrix interface and avoids influence by other factors (present at macro-scale tests). However, the theory is based on a critical assumption of linear stress along the interface [111]. It was demonstrated numerically [101,287] that there is a stress concentration where the razor blades lock the droplet. This stress concentration depends on the shape of the blade [287] and the distance between the blades and the fibre [101,287]. As said previously, the blade shape does not scatter the results in our study as it stays unchanged. Thus, the obtained values can be compared despite the difficulty of validating the assumption of linear stress.

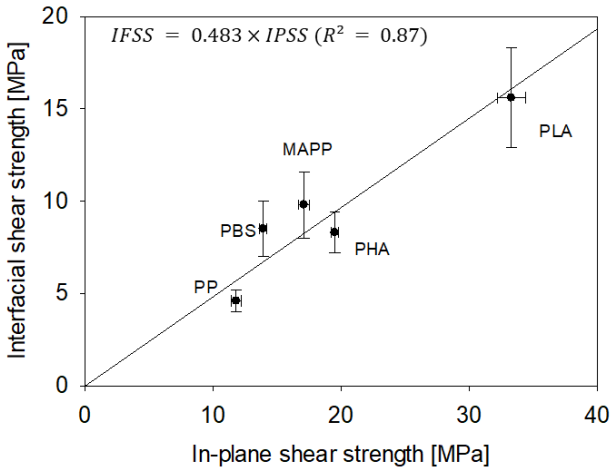

Figure 2-10: Linear correlation between the interfacial shear strength IFSS measured at the micro-scale and the in-plane shear strength IPSS measured at macro-scale for flax/thermoplastic composite systems.

On the other hand, the in-plane shear $[\pm 45]_s$ test gives the in-plane shear strength, considering composites' mesostructure. However, the test does not create pure shear as the matrix is also loaded. Thus, the composite quality has an essential role in the reliability of the results. The heterogeneity of the materials, such as matrix concentration zones and interlaminar zones, may induce unwanted stress concentration. Nevertheless, as all these artefacts are present in a composite, this test reveals the "in-use" interface shear strength, which is more relevant for composite application [137].

IV.b. Influence of interface on UD composite strength

b.i. Transverse strength

Generally speaking, whatever the reinforcement considered, the interface plays an essential role in the behaviour of a UD composite loaded transversally [288]. As shown in Figure 2-11, there is a clear correlation between the transverse strength of a UD composite and the in-plane shear strength characterising the interface. Indeed, the transverse loading of a UD composite induces a high strain concentration at the interfaces [144]. It leads to damage in the composite through the generation of micro-cracks at the interfaces, which coalesce to form (a) macro-crack(s) and eventually fracture the material. The appearance of micro-cracks depends on the ability of the interface to resist applied strain. If a matrix presents a better interface with fibre, the micro-cracks appear at a higher strain level, and higher applied stresses are needed to create some micro-cracks locally, thereby postponing the failure of the composite and leading to a higher ultimate strength.

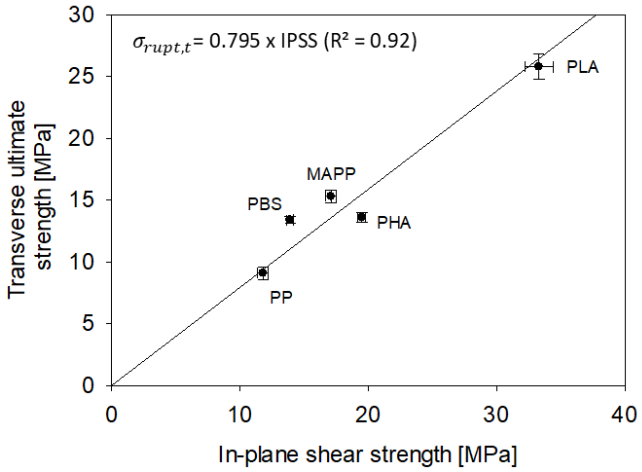

Figure 2-11: Correlation between the in-plane shear strength IPSS and the ultimate transverse strength of unidirectional flax composites.

As mentioned previously, this analysis was done considering a matrix reinforced by elementary fibres, being naturals or synthetics. In a flax composite, bundles also experience this strain concentration. In bundles, fibres are linked together by middle lamellae. It appears that the stiffness of middle lamellae is close to the transverse stiffness of flax fibres [74]. This natural feature found in a stem creates a remarkable cohesion inside bundles when loaded transversely, avoiding its decohesion. During retting, fibre extraction and composite manufacturing, this middle lamella is impacted, damaging this cohesion. In a composite submitted to transverse tensile loading, bundles act as fibres with a more prominent geometry but also as zones of weakness due to the damaged middle lamellae [289].

There is diversity in fibre forms (elementary, bundles) and level of heterogeneity in the UD composite due to the (random) dispersion of these fibre forms (Figure 2-8). The orientation of the bundles emerging from the manufacturing process can reconfigure the distribution of these high strain zones, thereby modifying the composite behaviour (Figure 2-12). Despite considering the complexity of a flax composite, it appears clearly that the transverse strength is interface dependant.

b.ii. Longitudinal strength

Estimating the longitudinal strength of a composite can be challenging, and many models are available. A modified rule of mixture is chosen here, which considers the matrix to be softer than the flax fibres and therefore assumes failure is fibre-dominated. An effective parameter (k_{eff}) is added to match the model and the experiment empirically (2-4). This factor includes all fibre-related phenomena influencing the UD strength, such as the quality of fibre-matrix interface, fibre length distribution, and fibre (mis)orientation [290].

$$\sigma_{UD,l} = k_{eff}.V_f.\sigma_{fibre,l} + (1 - V_f)\sigma_{fiber,l}.\frac{E_m}{E_{fibre,l}} \quad (2\text{-}4)$$

V_f is the volume fraction of fibre, $\sigma_{UD,l}$ and $\sigma_{fibre,l}$ are respectively the longitudinal strength of the UD and the fibres, E_m and $E_{fibre,l}$ are the longitudinal stiffness of respectively the matrix and the fibre. Longitudinal strength and stiffness of flax fibre are taken respectively equal to 1,043 MPa and 53.2 GPa as obtained by Bourmaud et al. with fibres extracted from the same preform [46].

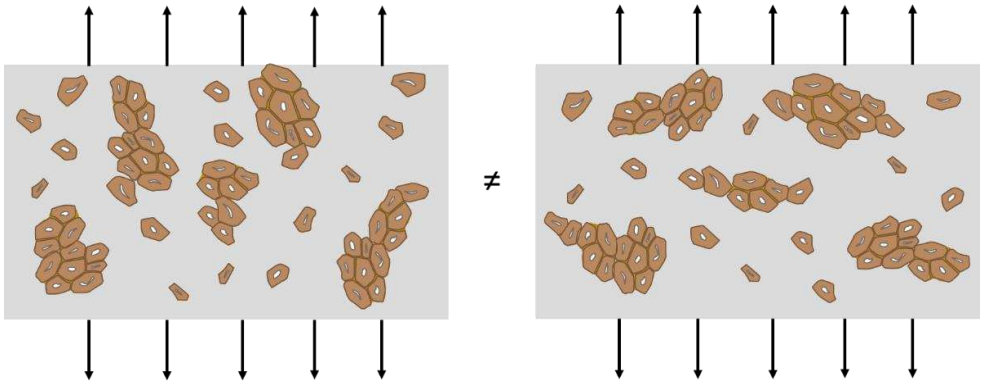

Figure 2-12: Schema of a unidirectional composite loaded in transverse. The behaviour of the two composites will differ due to the orientation of the bundles leading to different zones of high strain concentration.

It appears that the factor k_{eff} is interface dependant (Figure 2-13.a)), but is also influenced by the ultimate strain of the matrix (Figure 2-13.b)). Indeed, even though the interface between PBS and flax is of moderate quality (in comparison to the other polymers), the effective parameter of PBS is high; the moderate interface properties being balanced with the high ultimate strain of the PBS matrix. The reverse is true for PLA, where the effective parameter is principally due to the high quality of the interface (at low ultimate strain of PLA). Several hypotheses are proposed. If a matrix possesses a high ultimate strain, it may spread the applied stress in the composite and avoid high-stress regions responsible for failure. Another explanation is that matrix is more resilient in high strain regions, such as at the ends of fibres. Thus, it avoids the creation of micro-damage inside the material, yielding an increase in apparent strength. Indeed, even if the failure in flax UD composites is due to fibre failure, Monti et al. [103] observed matrix cracking before specimen rupture. In both assumptions, the explanation is related to the local stress and strain concentration inside the composite.

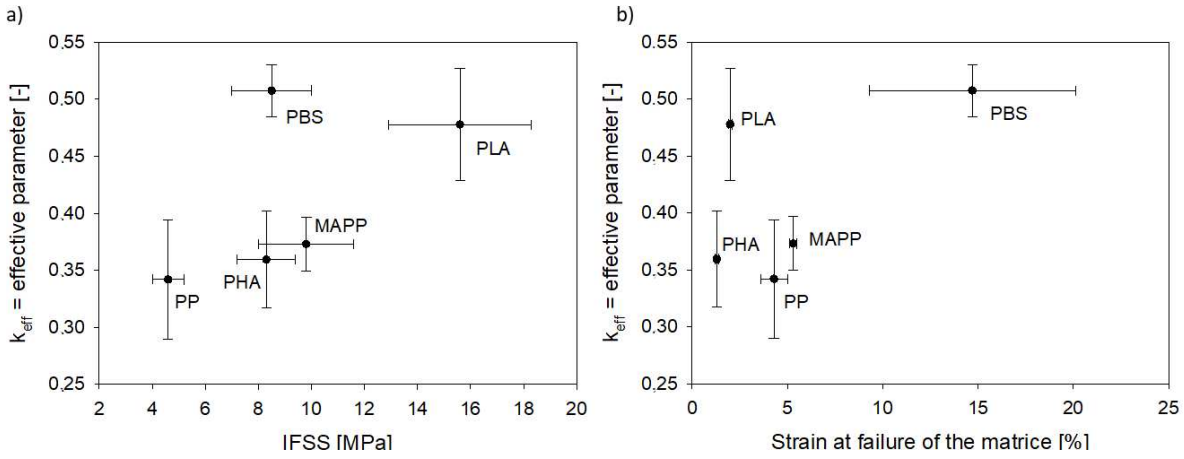

Figure 2-13: Effective parameter (keff) of the fibre contribution at longitudinal strength in function of a) the interfacial shear strength, b) strain at failure of matrices.

Some studies focus on developing the factor k_{eff} to express it clearly [291]. However, these models are not useable on UD flax composites as they are more complex than conventional composite (Figure 2-14).

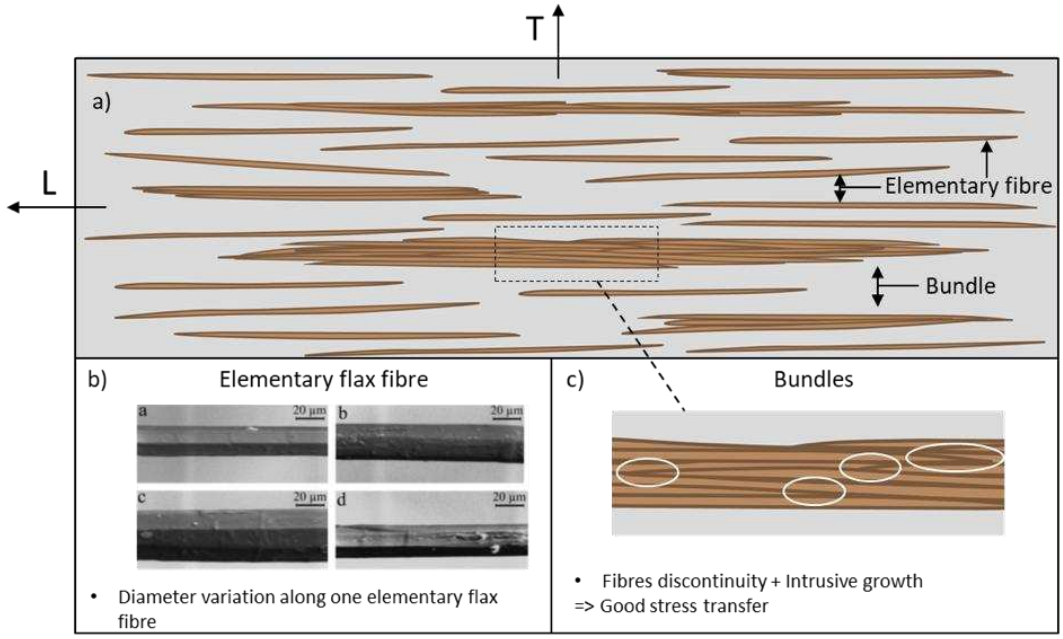

Figure 2-14: a) Schema of a top inner view of a flax UD composite portraying the misorientation, the presence of bundles as well as discontinuous elementary fibres. L and T represent the longitudinal and transversal directions. For clarity, the aspect ratio of the fibre is not to scale. b) SEM images extracted from [292] showing the diameter evolution of elementary flax fibre, c) Schema of a bundle focussing on the fibre discontinuities inside the bundles.

In addition to the heterogeneous fibre distribution and the discontinuity of flax fibres (Figure 2-14.a)), the level of flax fibre individualisation also influences the strength of the composite [127]. More

individualised fibres lead to higher strength, where bundles act as weaknesses inside the composite. It could be due to their lower aspect ratio or the higher stresses generated inside bundles. However, the second hypothesis is debatable due to the arrangement of fibres.

As shown in Figure 2-14.c), flax fibres are discontinuous, but thanks to their intrusive growth in the stem, their diameter tapers and decreases at the ends [74]. These individual fibre ends increase the effectiveness of stress transfer between fibres through the middle lamellae. Besides, Coroller et al. [127] observed that individualisation leads to a more significant increase in strength of a flax UD composite than obtained by selecting and using higher-strength fibres. As hackling is commonly used to extract flax fibres from stems, and it creates defects (*vis.* kink-bands) on fibres, a compromise has to be found between highly individualised fibres and undamaged fibres with higher strength.

Focussing on elementary flax fibres, they present a non-cylindrical section with an apparent diameter evolving along the fibre length [292] (Figure 2-14.b)). In addition to the geometric variability of flax fibres, it appears that fibre strength is dependent on the location in the stem they have been extracted from: fibres of highest strength are extracted from the middle of the stem [74]. A flax preform is typically made with a mix of these flax fibres, leading to dispersion in geometric, structural, and mechanical properties. Examining the same Flaxtape® used in our study, Gager et al. [214] observed a slight fibre misorientation. Fibres are oriented at approximatively 0° ± 15° with only 5% of fibre at 0°. In comparison, a commercial glass UD typically presented an orientation of 0° ± 10° with 13% fibres at 0°. This higher misorientation for flax preforms penalises it against glass preforms and impacts the strength of the final composite.

Despite the complexity of a UD flax composite, interfaces have an essential role in stress transfer and damage development. In addition, the biodegradable polymers present higher interfacial properties with flax and lead to composites with higher mechanical properties than currently industrially used PP and even MAPP.

V. Conclusion

The interface between flax and three biodegradable polymers (PLA, PHA, PBS) was investigated at the micro-scale and compared to PP and MAPP, two industry references. It is demonstrated that the adhesion and interfacial shear strength of biodegradable polymers to flax is at least as good as MAPP and more than twice that of PP. A mechanical investigation at the composite scale is realised through in-plane shear and tensile tests on unidirectional composites. The macro-scale in-plane shear strength, the longitudinal tensile strength and the transversal tensile strength follow the same trend for

fibre/matrix adhesion observed at the micro-scale through micro-droplet tests: flax composites made from biopolymers are at least as good as MAPP/flax composites, with the best values for PLA/flax composites. A comparison is carried out between interfacial properties and composite mechanical properties. It appears that the in-plane shear strength of the composite and the UD transversal strength correlate linearly. In the longitudinal direction, the strength depends on fibre-matrix adhesion but also on the ultimate strain at failure of the matrix. Based on this analysis and due to the good adherence between flax fibres and biodegradable polymers, it is evident that biopolymers should be exploited as alternatives to thermoplastic polyolefins as they present interesting mechanical properties and lead to recyclable and compostable mid-performance materials. In the future, it is imperative to explore the correlation between fibre-matrix adhesion, mechanical behaviour (such as fatigue), composite architecture (such as fibre volume fraction), and durability (including biodegradation).

Chapter 3: Can we predict the microstructure of a non-woven flax/PLA composite through assessment of anisotropy in tensile properties?

I. Introduction:

Due to their lower environmental impact [268] and competitive specific mechanical properties [86], flax fibres have replaced glass fibres in some automotive parts, such as interior panels [48]. These parts, made of non-woven preforms, are thermo-compressed to a near-net shape. Several processes are available to manufacture non-woven preforms, among which spunlacing and needle-punching are common [165]. Thermoplastic polyolefins, such as poly-(propylene) (PP), are currently used as a matrix, leading to potential recyclability of any scraps. However, with the emergence of biodegradable thermoplastics, the automotive industry has started to look at alternatives, such as poly-(lactide), which offer industrial composting as an alternative end-of-life scenario [293].

Furthermore, PLA appears to have the advantage to be stiffer than PP with a tangent modulus of 3.8 GPa against 1.4 GPa and to have a quasi-linear tensile behaviour. As matrix properties influence the mechanical properties of the composite, non-woven flax/PLA composites are observed to have higher stiffness at all volume fractions than non-woven flax/PP composites (Figure 3-1).

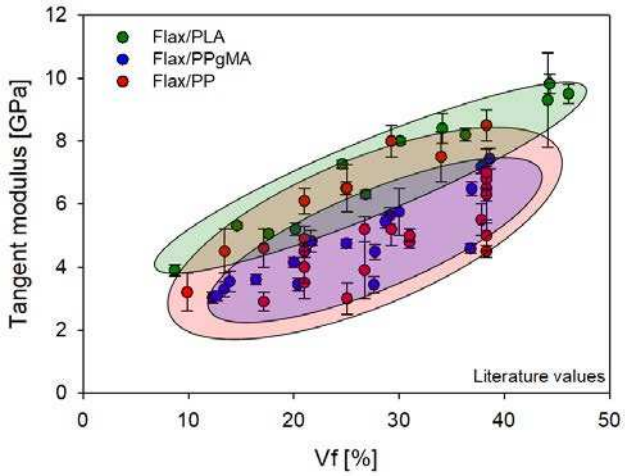

Figure 3-1: Graphical presentation of literature review of the mechanical properties of non-woven flax composites reinforcing PLA [43,240,294–296]; PP [174,206,297–299]; MAPP [43,165].

While matrix properties are relevant, it is mainly the fibres that are responsible for composite mechanical behaviour, with their content directly affecting composite stiffness. The non-woven preform manufacturing process will induce fibre orientation anisotropy resulting in different properties in the machine- and cross- directions of a needle-punching line [165]. Neckar and Das [300] studied the orientation of the fibres in non-woven preforms and derived analytical laws relating to the manufacturing process used. The fibre orientation in the non-woven preforms could be obtained simply by transparency observation or optical microscopy [301]. Such methods are relevant for mono-constituent non-woven preforms. For composites manufacturing, the non-woven preforms may comprise two types of fibres, the reinforcement and the matrix. Other methods have to be used as only the reinforcement fibre orientation needs measurement (as the matrix fibres will melt) to investigate the effect of fibre architecture on composite mechanical properties. Graupner et al. [218] used a synchrotron radiation-based micro-computer tomography approach to obtain cellulose fibre orientation in PLA composites. Another non-destructive method is ultrasound scanning, which leads to the measurement of fibre orientation and plies spacing, fibre volume fraction, and porosity distribution [219]. In both cases, computation is required to extract fibre orientation from the raw data.

Once orientation frequency is known, several theories exist to predict non-woven mechanical properties. The first approach is to modify the rule of mixture (3-1) by including a corrective factor η_o (3-2) [302], where *E* and *V* denote stiffness and volume fraction respectively, and subscripts NW, *f* and *m* denote non-woven composite, fibre constituent and matrix constituent, respectively. The parameter p_n is the appearance frequency of the angle represented by θ_n.

$$E_{NW} = \eta_o . E_f . V_f + E_m . V_m \quad (3\text{-}1)$$

$$\eta_o = \sum_n p_n . cos^4(\theta_n) \quad (3\text{-}2)$$

In the above approach, even though the fibre orientation is considered, the shear contribution is not taken into account, nor are the anisotropic properties of the reinforcement. Halpin and Pagano [22] developed a more precise method to assimilate randomly oriented fibrous composites to a laminate. They showed an excellent mechanical prediction of the experiment by considering symmetric laminate with a thickness weighted with the fibre orientation frequency.

A third constituent important to tackle is the porosity value. The compaction of the non-woven could be controlled to tailor mechanical or acoustic properties [174], leading to low or higher porosity

content. For fully-compressed composites, porosity is still present due to manufacturing and should not be neglected as it influences mechanical properties. Their distribution and shape are also reported to be important [209]. Looking specifically at natural fibres, Madsen et al. discussed the porosity distribution inside flax thermoplastic composites [202] and its influence on composite stiffness [206]. Thus, fibre orientation, fibre anisotropy and porosity appear to be key structural parameters required in precisely describing a non-woven composite, all of them impacting non-woven composite mechanical properties.

In this chapter, the microstructure (porosity/reinforcement content) and the architecture (fibre orientation) of a flax/PLA non-woven are characterised thanks to X-ray microtomographic (XMT) analysis. Off-axis tensile tests are used to characterise the observed anisotropy. Micro-mechanics and laminate theory are used to approximate experimental data. Matching calculated and measured values allow proposing the off-axis mechanical properties as an efficient and straightforward validation tool to address the fibre orientation in a non-woven composite.

II. Materials/methods:

II.a. Reinforcements

Flax/PLA non-woven preform was provided by Ecotechnilin (Yvetot, France). It was made from 50%/50% weight of scutched flax tows and INGEO™ PLA fibres. Due to the utilisation of flax tow, shives were still present in the non-woven preform. Our non-woven presents a more significant proportion of preferential fibres orientations than needle-punched non-wovens due to their manufacturing process: carding and calendaring. The preferential fibres direction is observed on the machine direction (direction of the non-woven preform production). Cross direction refers to the direction perpendicular to the machine direction. Non-wovens with 10% and 30% fibre weight content were also manufactured for comparison. Following, if nothing is indicated, non-woven composite refers to the 50%/50% flax/PLA non-woven.

Additionally, unidirectional (UD) and bi-axial (BX) composites were made of 50 g/m² Flax-tape® (Ecotechnilin) and PLA films using the PLA 3001D (NatureWorks). This difference in PLA grad is justified as the PLA 3001D is not available in fibres shape, where the INGEO™ PLA fibres cannot be transformed easily into films for the film stacking process.

II.b. Composite manufacturing

Non-woven composites were made of several preform plies, UD and BX lay-ups were prepared using film stacking. Pure PLA plates were also prepared to obtain matrix properties. These lay-ups were dried in an oven at 40°C for 24h under vacuum as flax and PLA are moisture-containing. They were then hot compressed at 200°C with a hydraulic press LabTech Scientific 50T (Labtech, Samutprakarn, Thailand), yielding laminate plates of 20 cm x 20 cm x 2mm. The optimised pressure cycle used is presented previously in Chapter 2, section II.a. Milling machine was used to cut samples for tensile property characterisation.

II.c. Tensile tests

An Instron universal testing machine was used to achieve static tensile tests based on ISO 527-4. A displacement rate of 1mm/min was applied, and the elongation was recorded with a unidirectional extensometer, gauge length taken equal to 25mm. For the pure PLA samples (from both grads) as well as for the UD, a bi-axial extensometer was preferred. For each formulation, at least five samples were tested to obtain mean values and standard deviation. The ultimate strength and strain are recorded as well as tangent modulus. The latter was calculated over a strain of 0.02% to 0.1% as recommend for flax composites [212]. The Poisson's ratio is obtained using the NF EN 2561 standard when the bi-axial extensometer is used. The same set-up is employed to perform in-plane shear testing on BX according to ISO 14129, using a bi-axial extensometer and 2mm/min speed. As reported previously in chapter 2, section II.b, the shear modulus is measured between 0.1% and 0.5% shear strain. Pure PLA 3001D, UD and BX characterisation is only performed for back-calculation to obtain flax fibres properties.

II.d. Density

The density of our non-woven composite was obtained through a hydrostatic balance using ethanol as the immersion liquid. This method was chosen as suggested by Kergariou et al. [303] for flax/PLA composite. It was used to obtain the density of the composites. Knowing the apparent density of the composite (ρ_c), the volume fraction of porosity (V_p) of each formulation is obtained using equation (3-3), where W_f is the weight fraction of fibres and ρ_{PLA}, ρ_{flax}, are the density of PLA and flax taken respectively as 1.24 and 1.5 [84]. Porosity results are given as mean values of five samples.

$$V_p = 1 - \left(\frac{1 - W_f}{\rho_{PLA}} + \frac{W_f}{\rho_{flax}} \right) . \rho_c \quad (3\text{-}3)$$

II.e. X-ray microtomography (XMT)

The microstructure of the non-woven composites was investigated with a Brucker© SkyScan 1272 high-resolution scanner. The samples were scanned at a nominal resolution of 4,5 µm. The current (50 eV), the intensity (200 µA) of the X-ray beam, and the nature and thickness of filters were selected to obtain a constant signal transmission of 30%. The X-Ray power source (P=U.I) is kept constant at 10W. A camera pixel binning of 4032×2688 was applied. The scanned orbit was 180 degrees with a rotation step of 0.2° adapted to the magnification. Bruker's NRecon® software was used to reconstruct the scan projections into 2D images using the Feldkamp algorithm. Gaussian smoothing, ring artefact reduction and beam hardening correction were applied. Volume rendered 3D images were generated using an RGBA transfer function in SkyScan CTVox® software.

Image analysis was performed using SkyScan CTAn® software. A specific task list analysis was developed to characterise the porosity and the pore size distribution within composites. In that way, two image segmentations were successively carried out on the original image: the first one to define the sample volume of interest (VOI) and the second one, using an automated Otsu algorithm, to define the object volume within this VOI. After image binarisation, structure separation (=pore size) is preceded by skeletonisation in which the two medial pore axes are identified. Then the "sphere-fitting" local thickness measurement is made for all the voxels lying along this axis.

In order to determine fibre orientation, a sequence of 12 in-plane cuts on face direction on the 3D render is used to generate 2D images. This method is based on granulometry analysis and was the subject of a previous study [214]. Due to the low contrast – a result of the comparable material densities– between flax and PLA, the 2D images had to be pre-treated with Fiji to obtain binary images before orientation analysis. The pre-treatment process is illustrated in Figure 3-2. It is validated by comparing the fibre orientation analysis, with and without pre-treatment, of an optical micrograph, Figure 3-3.

II.a. SEM

Complementary microstructure observations were performed using a JEOL SEM (JSM-IT500HRSEM) at an acceleration voltage of 3 kV. Before the observation step, gold sputter coating was applied to the samples using an Edward sputter coater (Scancoat6).

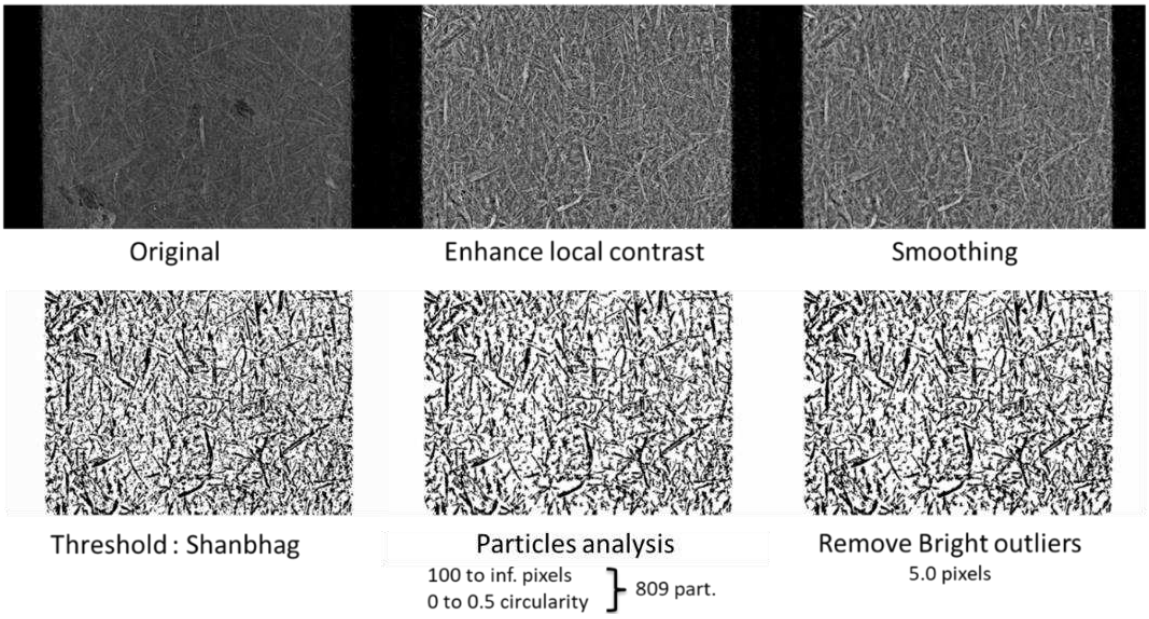

Figure 3-2: Pre-treatment process done on 2D images before orientation analysis.

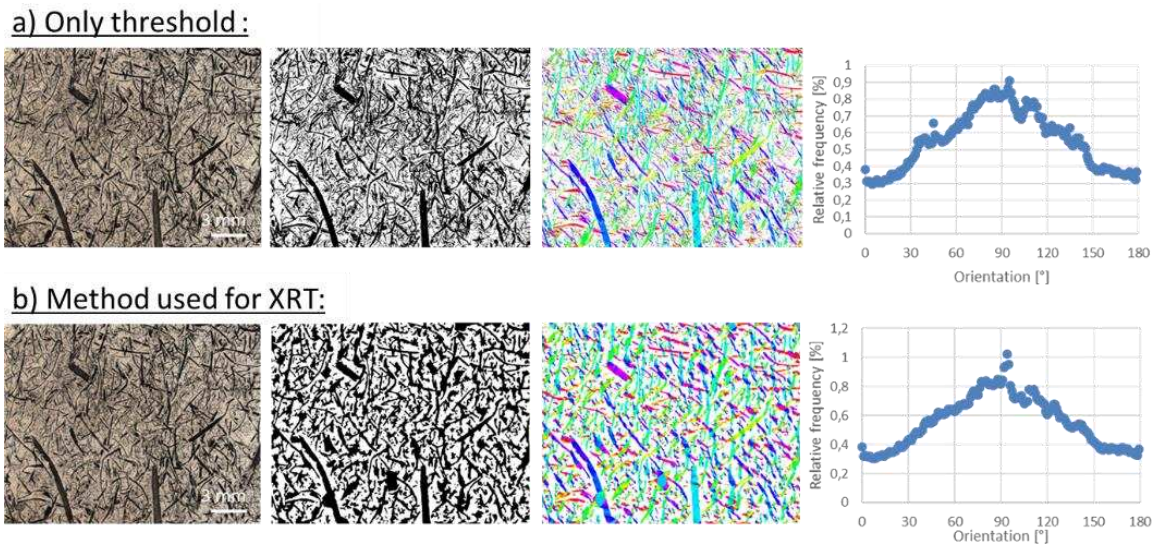

Figure 3-3: Validation of the pre-treatment process by comparing the orientation analysis with (a) and without (b) pre-treatment. These analyses were done on the same optical microscopy picture.

III. Results and discussion

III.a. Fine-scale composite volumetric analysis

The behaviour of a composite is predominantly influenced by the matrix, the reinforcement properties and their content. For flax reinforcements, things are more complex as the matrix is not reinforced by one single type of constituent but by at least two: elementary fibres and fibre bundles. Figure 3-4 presents SEM observations of our non-woven composite. The presence of elementary flax fibres and bundles is confirmed, as well as any preferential orientation. Indeed, non-woven composites are

anisotropic as they present higher properties in one direction than another, depending on the preferential orientation of the fibres [165]. However, the microstructure of this non-woven composite is more complex as it also includes porosity and shives. In addition, quantification of fibre orientation is required to describe the non-woven composite architecture, the aim being to understand better and estimate the composite properties.

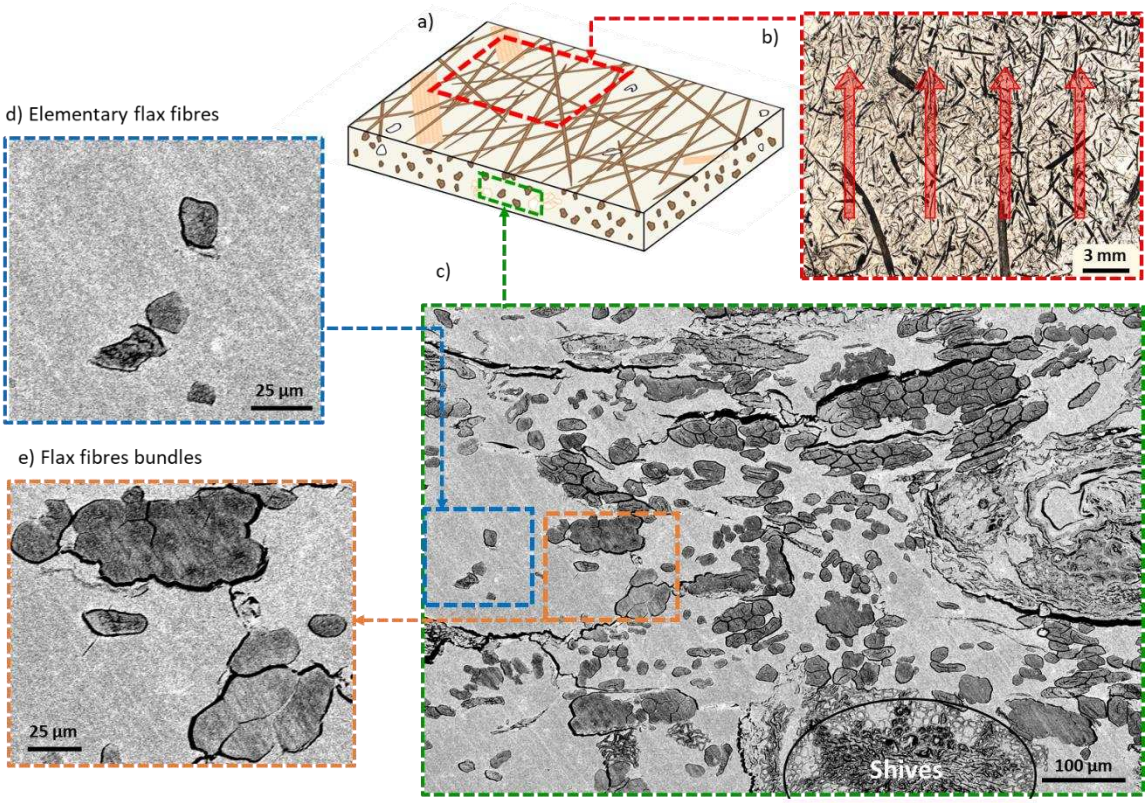

Figure 3-4: SEM observation of the flax/PLA non-woven investigated, a) schema of the analysed sample, b) upper observation, showing preferential fibre orientation (red arrows), c) transverse observation, fissures might be due to water polishing, d) zoom on elementary flax fibres, e) zoom on flax bundles.

a.i. Porosity analysis

Porosity content of 5.6 ± 3.2 % was measured for the non-woven composite thanks to a hydrostatic balance using ethanol as the immersion liquid. A fine-scale analysis was done by XMT to investigate pore localisation and size. A porosity of 4.5 % was obtained, which is comparable to the immersion method value. It could be observed in Figure 3-5.c) thanks to the microtomographic 3D view of porosity. A quantitative analysis presented in Figure 5.b) highlights a few mesoporosities inside the matrix.

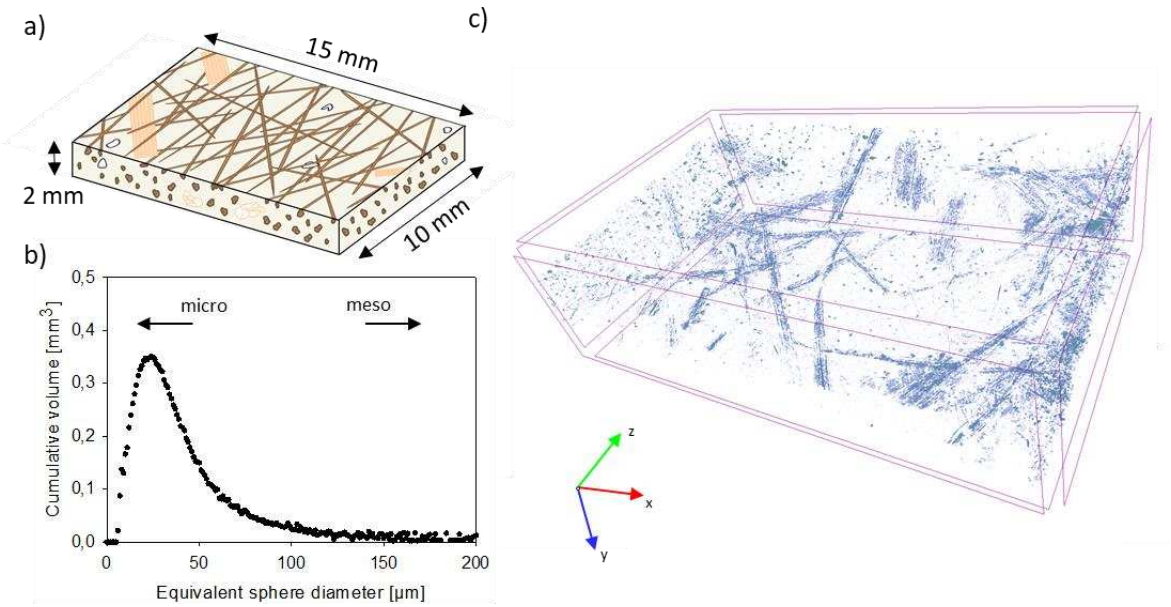

Figure 3-5: Porosity analysis by XMT a) schema of the analysed sample, b) analysis of porosity size, c) the XMT 3D view of porosity.

On the other hand, there is a significant amount of micro-porosity. The latter appears to be mainly located inside bundles and in shives. Indeed, shives come mainly from the xylem tissue, where its primary function is to conduct sap [78]. Thus, inside the stem, these cells exhibit a large lumen of several micrometres, potentially visible through XMT investigations.

a.ii. Shives quantification

Regarding the porosity analysis, it appears that shives are a predominant host of micro-porosity. It is observed in Figure 3-4 and confirmed in Figure 3-6 that shives inside the non-woven composite have collapsed cells, probably due to the compaction pressure applied during the manufacturing process. Indeed, shives contain less cellulose than elementary flax fibres, 45% of dry matter against 80% respectively [304]. As cellulose is responsible for plant fibres' mechanical properties, it is necessary to quantify this third reinforcement type as it should have mechanical behaviour lower than that of the bundles and elementary fibres. Following manual extraction, 5wt% of shives were extracted for the total non-woven reinforcement weight. The volume fraction of shives inside the composite is assessed to be 2.2% by considering a density of 1,430 $kg.m^{-3}$[305], against 43.1% for flax fibres (elementary fibres and fibre bundles). In the following analysis, shives are taking into account by assimilating them into the total flax fibre content at 45.3% by volume.

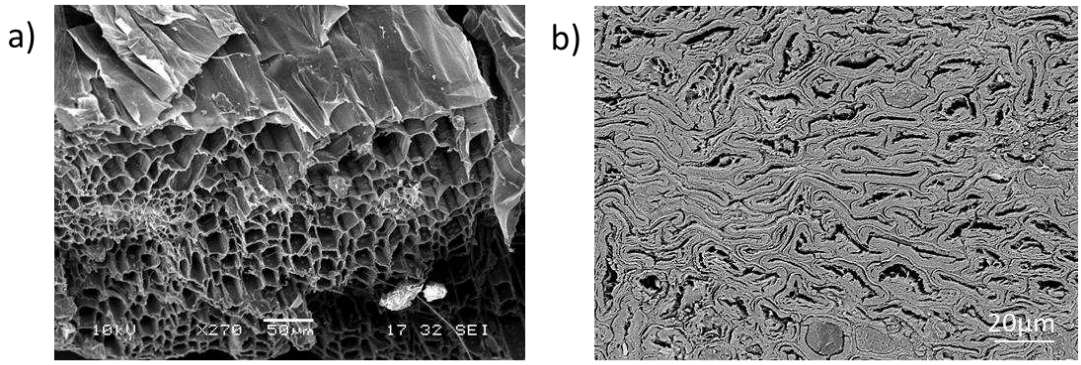

Raw shive extracted from preform | Shive inside the composite

Figure 3-6: SEM observation of a shive a) before the composite manufacturing step with open cells, b) after composite manufacturing, showing collapsed cells.

a.iii. In-plane orientation of fibres

Finally, a fine-scale description of the non-woven composite architecture should include fibre orientation. Thanks to XMT, the orientation was obtained from 12 images, and the mean orientation was calculated. One image's analysis methods are detailed in Figure 3-7 b), c), and d). All results are summarised in Figure 3-7.e). A preferential orientation appears with a maximum relative frequency (calculated degree by degree) of 0.82% and a minimum of 0.38%. It illustrates the expected anisotropy of non-woven materials at the composite scale. This orientation anisotropy appears to be lower than the pure flax fibres non-woven preform analysed with the same technique by Gager et al. [214]. It can be explained by the presence of fine PLA fibres in our non-woven preform, modifying the flax fibre alignment during the calendaring process. Another hypothesis is the modification of the orientation of the fibres during the composite processing with the PLA fibres flowing under heat and pressure. The mean experimental curve is fit using equation (3-4) developed by Neckar and Das [300] (Figure 3-7.e)).

$$f(\theta) = \frac{1}{\pi}\frac{C}{C^2 - (C^2 - 1)cos^2(\theta)} + q \qquad (3\text{-}4)$$

Where f(θ) is the fibre frequency at an angle θ taken between -90° and +90°, *C* is the fitting parameter corresponding to the anisotropy of the non-woven, and the offset is corrected via the parameter *q*. The fit was done by lowering the sum of the difference between experimental and model at each orientation. It gives *C* = 1.84 and *q* = 0.235%. As the trend curve is symmetric, it is preferred over the experimental curve for the micro-mechanical development in section IV.

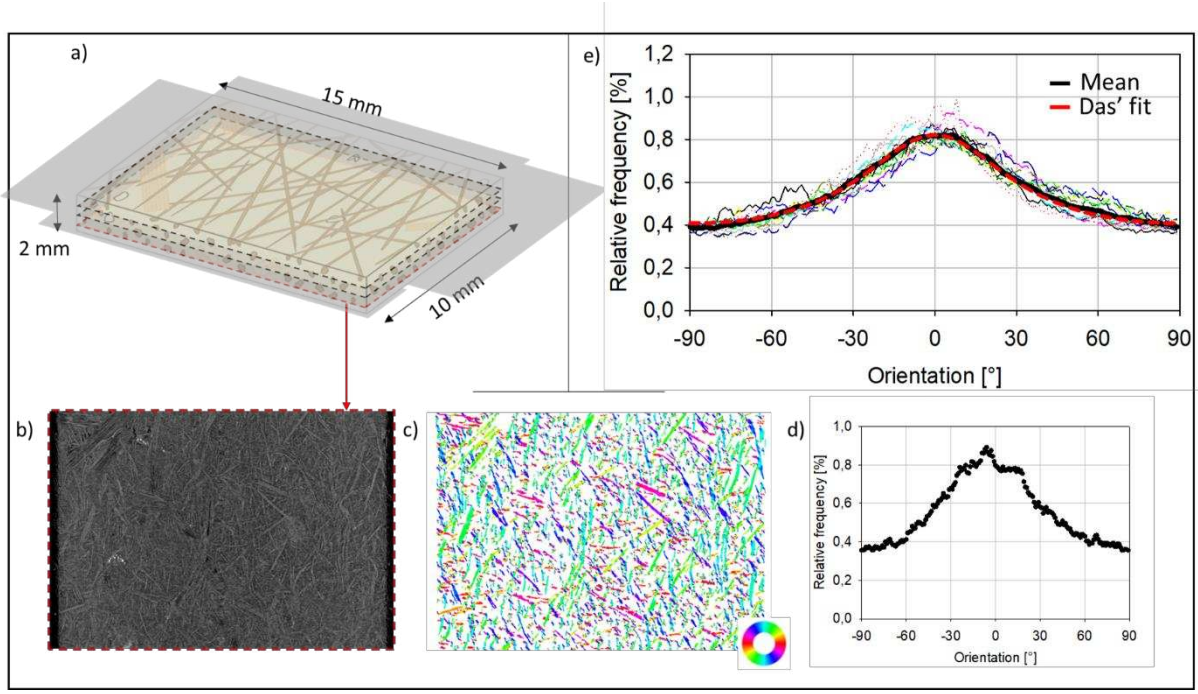

Figure 3-7: Orientation analysis. a) sample schema with slices (marked by dotted line) investigated, b) XMT image analysed for local fibre orientation, c) orientation analysis representation of XMT image (each colour represents an orientation), d) Orientation frequency histogram of one XMT slice, e) global orientation analysis of the composite, based on the mean orientation (black) of twelve XMT slices (dotted coloured lines). An interpolation [300], based on the mean value, is shown in red dotted lines.

IV. Mechanical characterisation and prediction of non-woven composite stiffness

Fibre orientation is a crucial parameter affecting mechanical properties; its direct analysis is possible through expensive and time-consuming 3D investigations such as XMT. In contrast, using mechanical property measurements as an indirect method to ascertain fibre orientation may be faster, easier, and lower-cost. With the aim to check the relevancy of this alternative method, off-axis tensile experiments are compared to a theoretical prediction using laminate theory as described by Halpin and Pagano [306]. The orientation data for the non-woven composites analysed in the preceding sections is matched with a theoretical model used to implement a laminate with 181 distinct laminas (from -90 to +90) with a thickness weighted by the relative orientation frequency. As symmetric lay-up is required, each ply is made of an angle and its symmetric counterpart. The laminate creation is summarised in Figure 3-8.

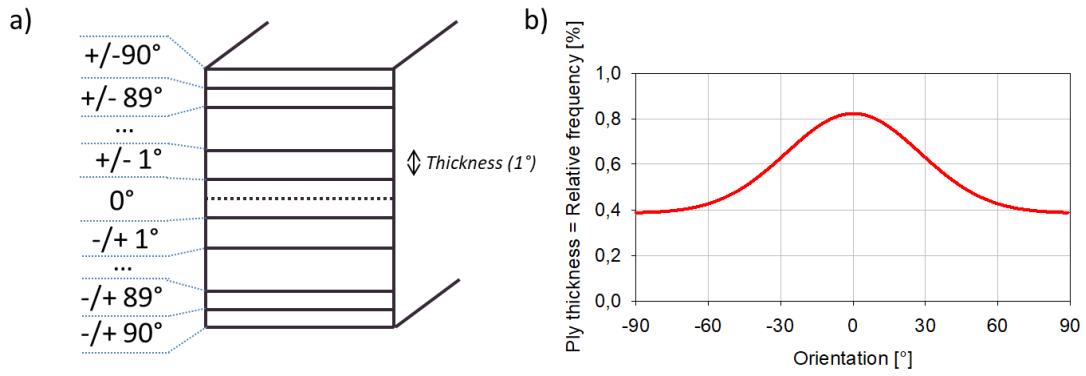

Figure 3-8: Explanation of the laminate building, a) schema of the symmetric laminate with thickness repartition, b) ply thickness used regarding the Gaussian fit of the orientation relative frequency.

IV.a. Angle influence on the tensile response of non-woven composite

Experimental measurements are presented in Table 3-1 and Figure 3-9 to study anisotropy in tensile properties arising from fibre orientation. As expected, the loading angle influences the material's response. A decrease in stiffness and strength of 40.5% and 47.3%, respectively, are observed between the orientations 0° and 90°, see Table 3-1. Thus, it confirms the anisotropy of this material. Furthermore, the mechanical properties of the non-woven composite stay unchanged after a critical angle of 67.5°, being equal to the transverse properties.

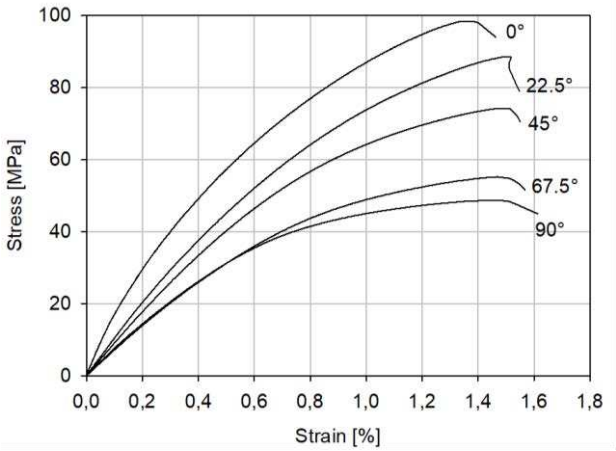

Figure 3-9: Tensile behaviour of non-woven flax/PLA with 50 wt% of fibres at several loading angles. The 0° refer to the machine direction (of the preform manufacturing) and the 90° to the cross direction.

Table 3-1: Experimental values of longitudinal, transversal and off-axis tensile tests on non-woven flax/PLA with 50 wt% of fibres.

Angle [°]	Tangent modulus [GPa]	Strength [MPa]	Strain at rupture [%]
0	12.95 ± 2.09	90.0 ± 6.1	1.44 ± 0.27
22.5	11.21 ± 0.87	84.9 ± 4.3	1.48 ± 0.27
45	9.64 ± 0.67	69.6 ± 6.5	1.30 ± 0.31
67.5	7.82 ± 0.44	53.2 ± 4.1	1.38 ± 0.25
90	7.70 ± 0.85	47.4 ± 4.4	1.25 ± 0.26

IV.b. Flax fibres properties for laminate theory

Input values significantly impact micro-mechanical models, especially for plant fibre whose values have a larger scatter. Indeed, regarding the longitudinal Young's modulus of elementary flax fibres, it is possible to find literature values ranging from 36 GPa to 75 GPa [83,307]. Two sets of values are considered here to take care of this scatter in data. The first one is directly extracted from literature, presented in Table 3-2. The second one is obtained experimentally through back-calculation of UD flax/PLA composite.

Table 3-2 presents the mechanical properties of UD composites used to back-calculate flax fibre properties for each UD composite. The flax fibres properties are obtained through mean values of back-calculate properties calculated at several fibres volume fractions. Comparing this data with the literature, flax fibres longitudinal modulus is similar, whereas its transverse and shear modulus obtained are lower. The thermal history of the fibres and the compaction during the process may have impacted the flax fibres' structure and their mechanical properties. Furthermore, both bundles and shives have been considered as 'fibres' during the back-calculation. They generally have lower transverse and shear properties than elementary flax fibres. The reinforcement distribution inside the composite is also irregular, leading to some regions of higher stress distribution than the theoretical approach. Additionally, as a high volume fraction is achieved, some contact between fibres are present. These contact points will be damaged during processing, damaging the fibres.

The PLA properties used for the model are measured from the pure INGEO^{TM} PLA plates, as it is the PLA used in the non-woven. Its mechanical properties are as following: a stiffness of 3.4 ± 0.1 GPa, a shear modulus of 1.19 ± 0.07 GPa, a Poisson's ratio of 0.38 ± 0.02.

Table 3-2: Flax/PLA UD composite mechanical properties used to obtain mechanical properties of flax via a back-calculation method: rule of mixture for longitudinal modulus (E_l) and Poisson's ratio (ν_{lt}), Halpin Tsaï for shear modulus (G_{lt}) and transverse modulus (E_t).

	V_f [%]	E_l [GPa]	E_t [GPa]	G_{lt} [GPa]	ν_{lt} [-]
Experimental values for Unidirectional Composites	0 (PLA 3001D)	3.73	3.73	1.31	0.41
	30	20.09	4.17	1.76	-
	40	25.98	4.29	1.88	0.39
	50	27.47	4.13	2.04	0.37
Flax fibres properties by back-calculation	30	58.26	5.35	3.76	-
	40	59.34	5.24	3.42	0.35
	50	51.21	4.56	3.33	0.33
Mean back calculated flax fibres value		56.2 ± 3.6	5.05 ± 0.35	3.50 ± 0.18	0.34 ± 0.01
Literature value for flax fibres		52.5 ± 8.6 [83]	8 ± 3 [199]	2.5 ± 0.2 [308]	0.48 [257]

IV.c. Influence of non-woven structure on its mechanical properties

Comparing the laminate theory models with the experimental data will inform us whether off-axis tensile tests can be used to predict the fibre orientation of non-woven flax composite. For each set of values, the mechanical properties of a ply are obtained using the rule of mixture for the longitudinal direction and the Poisson's ratio, and using Halpin-Tsaï [198] for the transverse and shear moduli. Furthermore, as discussed in section III.a.i, porosity is present and has to be taken into account. We use the hydrostatic balance-obtained single porosity value and assume that it is concentrated in the matrix. It induces that the porosity inside shives is assimilated to be matrix porosity. Equation (3-5), developed by Madsen et al. [206], is used to account for the effect of matrix porosity on mechanical properties,

$$P_{m,real} = P_{m,bulk} \cdot \left(1 - V_p\right)^2 \quad (3\text{-}5)$$

With P representing any mechanical property, V_p is the volume fraction of porosity and subscripts $_{m,\ bulk}$ and $_{m,\ real}$ denoting the bulk matrix and the matrix with porosity. Once the ply properties are obtained, the laminate is built as explained previously, and the mechanical properties of the equivalent composite are found. The model generated a curve of the non-woven composite's tangent modulus versus orientation for each value set. The range between both is represented in Figure 3-10 (grey area). The modulus in the machine direction (0°) is well-predicted, falling between both models. A slight deviation appears for 22.5° and 45°, but the models stay close to the experimental value.

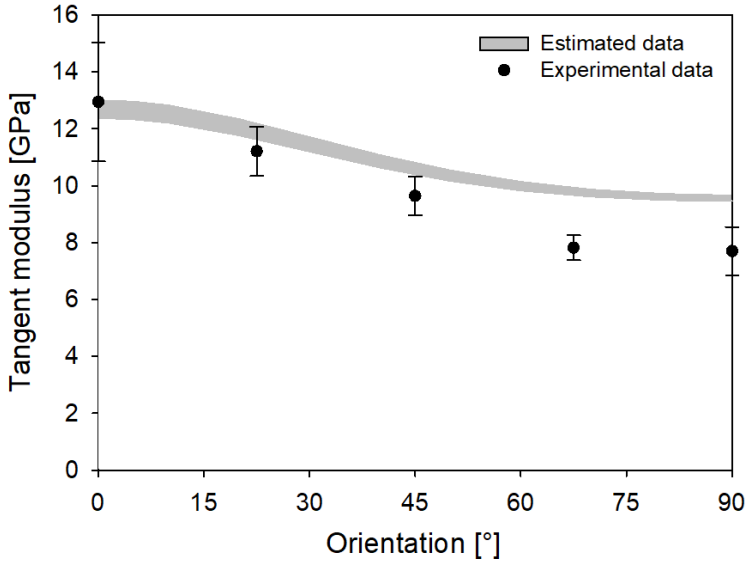

Figure 3-10: Evolution of the tangent modulus with loading orientation for non-woven flax/PLA with 50wt% of fibres tested in tension.

However, increasing the orientation further to 45° leads to an overestimation. This deviation at high orientations is principally due to the assumptions and simplifications used for the model compared to reality. First of all, the model considers an in-plane orientation. It is relevant for machine direction due to a stretching induces by the manufacturing process. However, this stretching is less or not present in other directions. That is why a slight out-of-plane orientation exists, needed for handling the non-woven preform.

Additionally, the model does not consider the reinforcement effect of bundles. A bundle presents a higher diameter than elementary flax fibres and an irregular geometry (fluctuating circularity, section and length), increasing the heterogeneity of the composite structure. Furthermore, bundles behaviour depends on its cohesion, meaning the middle lamella properties. The latter impacts predominantly the composite properties reliant on matrix and interface (such as transverse tensile properties). Furthermore, a small number of shives were detected, adding heterogeneity in the structure too.

What is more, the manufacturing process smashes the shives. This transversal smashing creates damages in this porous structure, decreasing the transverse properties of shives.

Furthermore, the model used here is based on an assumption of linear behaviour. However, it is known that elementary flax fibres do not have a linear longitudinal behaviour [87]. The transverse tensile behaviour of elementary flax fibres is still obscure as it is harsh to make some relevant tests at this micro-scale.

In the non-woven composite, fibres are oriented but are also curved. This curvature is not considered in our orientation analysis, but it is known to have a non-negligible impact on the composite behaviour. Finally, it appears that the anisotropy increases with fibre volume fraction, as observed in Figure 3-11. Thus, this new manufacturing process of non-woven preform allows overtaking in machine direction literature value without decreasing the stiffness significantly in cross-direction.

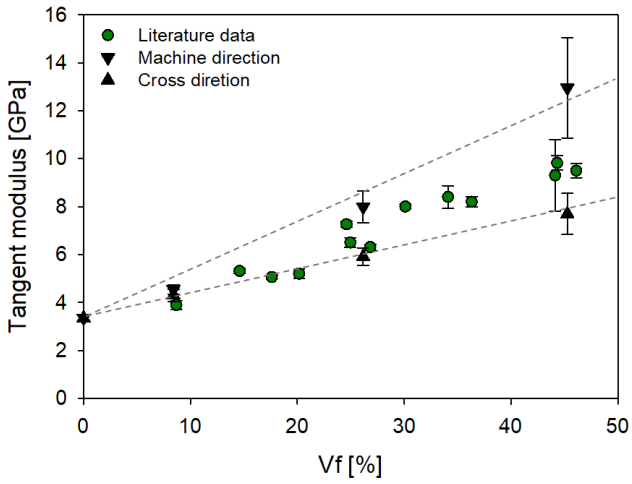

Figure 3-11: Evolution of tangent modulus with fibre volume fraction, with measurements in the orthogonal machine and cross directions presenting anisotropy. A comparison with literature data is also presented.

V. Conclusion

The complex microarchitecture of a non-woven flax/PLA composite with 50%wt of flax fibres was described thanks to X-ray microtomography (XMT) analysis. The microstructural observations show porosity and reveal the preferential orientation of the fibres inside the composite in the machine direction. This anisotropy was also measured through off-axis tensile tests. The mechanical properties highlight an apparent anisotropy where transversal properties are 60% of the longitudinal properties. Both anisotropy characterisations are compared using micro-mechanics and laminate theory to predict the mechanical properties from the XMT orientation analysis.

It is found that off-axis tensile tests could be used to predict the fibre orientation distribution in a non-woven composite indirectly. It is of interest as mechanical tests are much cheaper, faster and convenient to perform than XMT analysis. However, some deviation is apparent between experimental data and micro-mechanical prediction because of the complexity of describing a flax composite due to flax bundles, shives, curved fibres, composite thermal history and potential out-of-plane orientation of fibres.

Part 2: Influences of ageing in the structure and the mechanical properties of biodegradable flax composite

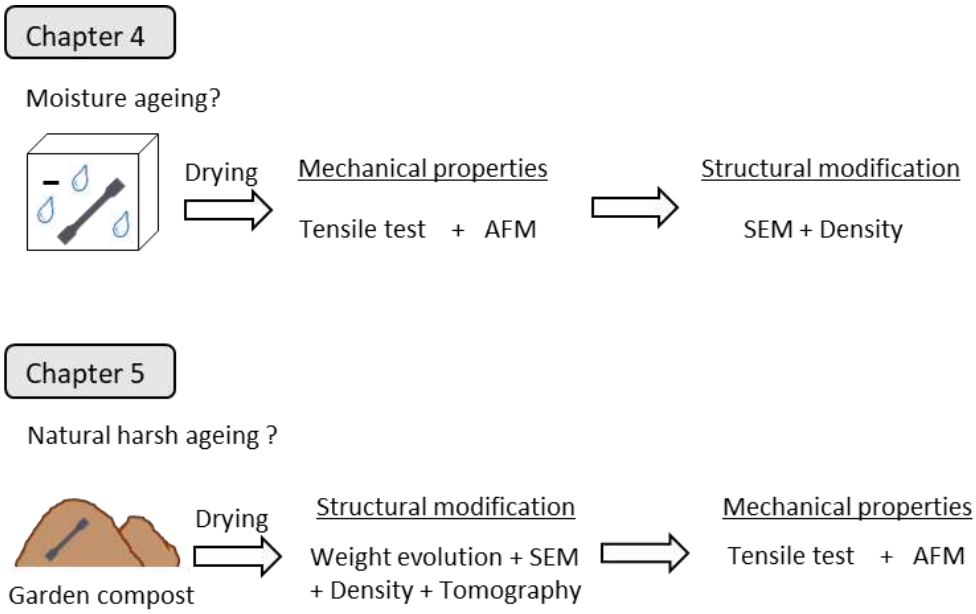

Chapter 4: Influence of the degradation induced by water ageing on mechanical properties of flax/PLA non-woven composite

I. Introduction:

Thanks to their lightweight [84] and their good mechanical properties [86], flax fibres can be drop-in alternatives to glass fibres as composite materials reinforcement in the automotive area [309]. In addition, using thermoplastic as a matrix reduces the composite's environmental impacts, especially thanks to recycling [269], as a potential solution before end-of-life consideration. However, one of the bottlenecks for wider applications is the sorption behaviour of flax composites, especially when considering drastic validation standards of the automotive industry, which imposes the test of materials in a large range of humidity and temperature conditions [47].

An elementary flax fibre, not embedded in a matrix, has a moisture content of 6% at 50% relative humidity (RH) and reaches 18% at 98RH [204]. The flax sorption follows Park's model [310,311], divided into three sorption mechanisms, depending on the relative humidity. The first part follows Langmuir's sorption, where water molecules go on specific sites of interactions. The second is described by Henry's sorption, where water uptake evolves linearly with the relative humidity, and the final stage occurring at high relative humidity is the clustering of water molecules in the remaining free space. Combining these three phenomena leads to a sigmoid relation between the relative humidity and the moisture content in the flax fibres [204]. Interestingly, this phenomenon presents a hysteresis loop meaning that the water content of flax is not the same at a given relative humidity depending on if it is in a sorption or desorption state [204]. Furthermore, this water uptake induces a radial swelling of the flax fibre, correlated linearly with the hygro-expansion coefficient, measured to be 1.14 ε/Δm by Le Duigou et al. [224].

The moisture uptake in a composite is mainly due to flax fibres' water sorption behaviour and the presence of a fibre/matrix interface [227], even for a hydrophilic matrix (PHBV) [312]. The sigmoid sorption/desorption behaviour is also observed at the composite level [47]. For non-woven flax/PP composite (50wt%), Gager et al. [47] report a moisture content of 2.6% at 50RH and 8% at 98RH. The

volume fraction of fibres impacts the moisture sorption of the composites [313]. However, the classical rule of mixture cannot predict the moisture uptake of the composites at high relative humidity. It appears coherent with experimental values for 75RH but over-estimates them at 98RH [313]. This deviation at high relative humidity is explained by El Hachem et al. [313] by the containment effect of the matrix on the flax fibres, limiting their moisture uptake potential. Indeed, flax swelling is observed at the composite scale level with a lower amplitude as the matrix constrains its displacement [232]. For pulpwood, the fibre hygro expansion is reduced by a factor of two considering free to swell fibres or fibres embedded in a PLA matrix [232]. Note that pulpwood is expected to expand less than flax fibres due to higher lignin content [225].

This moisture uptake induces a decrease in stiffness and ultimate strength of the composites [47,227,237]. The origin of this decrease is still discussed in the literature [233,246,314], and several phenomena appear to be involved. It is reported for thermoset flax composite that cracks appear in the matrix [237,314], inducing a debonding at flax/matrix interface [237,246,314] and flax fibres' damages [246,314,315]. All these phenomena are reported to be linked with the swelling of flax fibres inside the composite. However, there is no consensus because the phenomena observed vary depending on the ageing conditions, the experimental methods, or the flax composite mesostructured such as porosity, fibres volume fraction, fibres individualisation or fibre orientation. As an example, Chilali et al. [228] observed that the presence of sealed edges, inducing preferential water diffusion direction, impacts the sorption kinetics and the ageing behaviour. Indeed, they suggest several damaged mechanisms depending on the type of diffusion.

This chapter focuses on the hygroscopic ageing of flax/PLA composite through its mesostructure and mechanical properties evolution. Several hygroscopic conditions are investigated (50 RH / 75 RH / 98 RH) as well as an immersion ageing. The sorption kinetics is followed through weight monitoring, and the mechanical properties are obtained after ageing. The mechanical properties of flax cell walls and matrix after ageing are investigated at microscale thanks to AFM Peakforce measurements in mechanical mode (AFM-PF-QNM). The structure of the composite is managed through density measurement and SEM observation.

II. Materials and methods:

II.a. Materials

a.i. Raw materials

An industrial non-woven flax/PLA preform of 350 g/m², and a flax weight fraction of 40%, was provided by Ecotechnilin (Yvetot, France) from their needle-punched industrial line. The non-woven has a preferred fibre direction. Indeed, the machine direction has slightly more oriented fibres in these industrial non-wovens [165]. The raw materials used are scutched flax tows and INGEO™ PLA fibres. Thanks to the Ecotechnilin needle-punched line process, flax and PLA fibres are commingled together, leading to the non-woven preform.

a.ii. Composite manufacturing

The composites are manufactured using the same process used in chapter 2, section II.a. It consists of an optimised thermo-compression cycle using a hydraulic press LabTech Scientific 50T (Labtech, Samutprakarn, Thailand) press, set at 200°C (for PLA matrix). Eight plies of 200x200 mm are stack together and then dried at 40°C under vacuum for 24h. During the lay-up step, the specific orientation of the preforms is maintained. Therefore, thermo-compression leads to a composite with a preferential orientation of fibres, identical to the preform.

Next, dog-bone samples, according to the ISO 527 standard, are cut from the 2 mm thick composite plates using a milling machine. The centre part of the dog bone has a width of 8 mm, a length of 45 mm and a thickness of 2 mm. The edges of the samples were not sealed to be consistent with industrial applications targeted in the FLOWER project, such as Point of Purchase (POP) panels. Thus, after cutting, flax fibres appear accessible in the edges. Furthermore, the milling process damages the edges by initiating defects, which are likely to influence the ageing response of the composite. Once again, it is chosen to be close to the industrial process, in which edges are not cleaned after cutting.

II.b. Methods

b.i. Ageing protocol

Once manufactured, samples are stored in a controlled humidity chamber at 50RH until weight saturation. Once the weight is stabilised, five samples are dried for 48h in an oven at 105°C and weighted. The initial moisture content of samples is obtained through the mean of the five values. It equals 2.6 ± 0.1 %. The remaining samples are separated into fives batches. One stays in the 50RH chamber until the end of the experiments and is called the 50RH_ref sample. Others undergo humidity

ageing (called also vapour ageing) thanks to controlled humidity chambers (50RH/75RH/98RH) or immersion ageing in distilled water (Immersion). These ageing are conducted during six weeks. The humidity in the chambers is controlled thanks to saturated salt solutions. The salt used and the exact relative humidity condition, controlled thanks to testo 174H captors (Testo Inc., West Chester, USA), are presented in Table 4-1.

Table 4-1: Salt used for conditioning the chambers and the exact relative humidity condition induced by them.

	Temp. [°C]	50 RH [%]	75 RH [%]	98 RH [%]
Mean value	23.3 ± 2.2	55.7 ± 2.9	77.2 ± 1.9	99.7 ± 0.8
Salt used	/	$Mg(NO_3)_2$	NaCl	K_2SO_4

Five samples of each batch are regularly weighted to obtain the weight evolution. After six weeks, once their weight stabilises, the 50RH / 75RH / 98RH / Immersion samples are dried at 40°C until stabilisation. This drying step allows avoiding the hysteresis consideration of flax fibre sorption [204]. Finally, all samples are stabilised again at 50RH. The difference between the 50RH_ref and the 50RH batches remains in the drying and restabilisation step, which is not applied to the 50RH_ref samples. All the ageing protocol is done at room temperature. In the following discussions, wet samples (or wet state) will refer to the samples in saturated state during ageing. The restabilised samples (or restabilised state) will refer to the samples that have undergone ageing, drying and restabilisation at 50RH.

b.ii. Water content

As described before, samples are regularly weighted using a Fisherbrand™ scientific high precision scale having a precision of 10^{-4} g. The sampling depends on the stage of composite sorption, being narrow at the beginning of the sorption phenomenon. The moisture content at a given time ($M_c(t)$) is calculated from the weight evolution using equation (4-1).

$$M_c(t) = \frac{W(t) - W_{dry}}{W_{dry}} \quad (4\text{-}1)$$

Where $W(t)$ is the sample weight at time t and W_{dry} is its dry weight. The dry weight of each sample is calculated equal to 97.4% of the initial mass of the samples. It avoids the drying step for samples before ageing, as it impacts the materials [196].

The sorption kinetics of the samples during ageing is discussed using Fick's law, equation (4-2), where D_{diff} is the diffusion coefficient, and th is the sample thickness. The initial moisture content and the

moisture content at saturation is $M_{c,init}$ and M_∞, respectively. They are extracted from the experimental data for each ageing condition.

$$M_c(t) = (M_\infty - M_{c,init}).\left(1 - \frac{8}{\pi^2}\sum_{n=0}^{\infty}\frac{1}{(2n+1)^2}.exp^{\frac{-\pi^2.(2n+1)^2.D_{diff}.t}{th^2}}\right) + M_{c,init} \quad (4\text{-}2)$$

The diffusion coefficient (D_{diff}) is calculated for all experimental points in the linear part of the experimental curves ($M_c(t) < 0.5M_\infty$) using equation (4-3). The mean diffusion coefficient is used to implement Fick's law, equation (4-2).

$$D_{diff} = \pi.\frac{th^2}{16.t}.\left(\frac{M_c(t) - M_{c,init}}{M_\infty}\right) \quad (4\text{-}3)$$

b.iii. Mechanical characterisation through tensile test

A universal Instron tensile machine is used with a 10kN load cell. The tensile test is based on the ISO 527-4 standard, using a cross-head speed of 1mm/min. The elongation of the samples is measured with an Instron extensometer having a gauge length of 25 mm. The stiffness is calculated between 0.02% and 0.1%. At least nine samples are tested, and the mean value is extracted. Standard deviations are used as errors. The tensile tests are only done on restabilised samples.

b.iv. Density measurement

The density was obtained through a hydrostatic balance using ethanol as immersion liquid, leading to the density of the composites. Density samples are extracted from the centre part of the dog bone samples (2 x 8 x 45 mm) as it is the part loaded in the measurement of mechanical properties. This extraction is done on restabilised samples. Density results are given as mean values of at least five samples.

Thanks to the apparent density of the composite (ρ_c), the volume fraction of porosity (V_p) of each batch is obtained using equation (4-4). The weight fraction of fibres W_f are 40% here. The density of PLA (ρ_{PLA}) and flax (ρ_{flax}) are taken respectively as 1.24 and 1.5 [84]. This flax density value was measured at room temperature and 50RH. The flax fibres were extracted from unidirectional preforms made for composite applications.

$$V_p = 1 - \left(\frac{1 - W_f}{\rho_{PLA}} + \frac{W_f}{\rho_{flax}}\right).\rho_c \quad (4\text{-}4)$$

The assumption of an unchanged fibres density during ageing is taken. The porosity induced by manufacturing will be designed as matrix pores, and the porosity due to ageing will be called defects, or specifically matrix micro-cracks or interface decohesion.

b.v. SEM

Samples are observed thanks to a JEOL SEM (JSM-IT500HRSEM) at an acceleration voltage of 3 kV. For transverse section observation, sample preparation consists of embedding them into an epoxy matrix, polishing and gold-coating thanks to a sputter coating (Scancoat6) from Edward. For flax/PLA interface observation, samples underwent a brittle fracture under nitrogen before being sputter coated. The surface erosion was observed, skipping the embedding step as no polishing is wanted.

b.vi. Biochemical analysis

Biochemical analysis is done on the immersion leachate to quantify the polysaccharides realised by the composite. Before undergoing the biochemical analysis, the leachate was centrifuged (3min at 800 rpm). Three samples of supernatants (500µL) were collected. First, the 2-déoxy-D-ribose is added before samples are hydrolysed (2h at 120°C). Then, the uronic acid (UA) concentration was determined by an automated m-hydroxybiphenyl method [316]. Additionally, the neutral sugar concentration was analysed as their alditol acetate derivatives [317] by GC gas chromatography (PerkinElmer, Clarus 580, Shelton, CT, USA) equipped with a DB 225 capillary column (J&W Scientific, Folsorn, CA, USA) at 205°C, with H_2 as the carrier gas.

b.vii. AFM

A Multimode 8 AFM instrument (Bruker, Billerica, Massachusetts, USA) was used in PF-QNM imaging mode. This mode is based on the recording of force-distance curves at a high rate (2 kHz) for a limited maximum load (200 nN here), and thus limited indentation depth (of the order of a nanometre here), while the tip scans the surface of the sample thus allowing to make maps. The indentation modulus is obtained from the unloading part of the force-distance curve using an appropriate contact model. We used a DMT model here, which corresponds to the Hertz contact model (small indentation depth compared to the tip apex radius) modified to take into account the adhesion force (mainly due to water capillarity in our case) between the tip and the sample surface [318]. The indentation modulus obtained is similar to that obtained by nanoindentation measurements but with the required resolution to study mechanical gradient within cell wall layers [71]. RTESPA-525 (Bruker) silicon probe with a spherical tip apex was used here. Its spring constant (between 136 and 177 N/m) was calibrated using the Sader method (https://sadermethod.org/), and the tip radius adjusted between 20 and 80

nm on an aramid sample having a similar indentation modulus than flax fibre cell wall. The image resolution of 384×384 pixels was achieved, and a peak force amplitude between 50 and 100 nm was set for indentation modulus measurements. This variety of amplitude depends on the rigidity of the region investigated.

Only the reference, the 98 RH and the immersion batches were investigated in regards to the mechanical properties, the density results and the SEM observation. AFM samples of 2 mm^3 are extracted from the middle of the centre part of the dog bones. It avoids edge influence. They are embedded into agar resin (Agar Scientific, Stansted, UK) and cut thanks to an ultramicrotome (Leica Ultracut R). Four images, including flax fibres and PLA, were used for each reference to obtain the mean indentation modulus of the reinforcement and the matrix. The samples were analysed in a perpendicular plane of the direction with the predominant orientation of fibres (machine direction of the preform). For flax fibres, which are highly anisotropic, elliptical fibres were not selected to avoid the risk of fibre misorientation.

III. Results

III.a. Moisture content evolution

First, the moisture content at saturation of the composite stored at 50 RH is 2.6 ± 0.1 %. As expected for flax composite, the moisture sorption at room temperature follows Fick's law [315,319], as presented in Figure 4-1. The parameters used for Fick's law are extracted from the experimental curves and are given in Table 4-2.

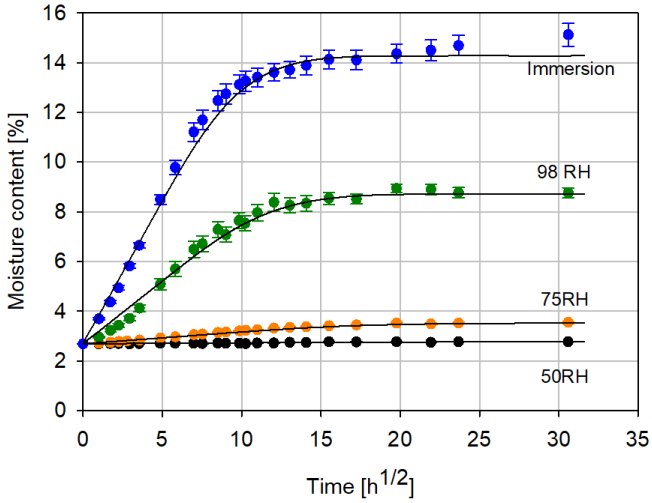

Figure 4-1: Moisture content evolution of a non-woven flax/PLA composite (Wf=40%) under several ageing conditions. The dark lines correspond to Fick's laws extrapolation. The experimental curves are used to obtain the diffusion coefficients and the moisture content at saturation.

Table 4-2: Parameters used to calculate Fick's law, depending on the ageing condition.

	50 RH	75 RH	98 RH	Immersion
$D_{diff}.10^{-6}$ [mm²/s]	0.56	0.72	1.53	2.15
M_∞ [%]	2.77	3.52	8.72	14.275

The moisture contents at saturation after each ageing step can be observed in Figure 4-1. Before discussing the results, note that the stabilised moisture sorption of virgin PLA was measured by Deroiné et al. [320] to be 0.59 ± 0.03% under immersion at 25°C. This low moisture sorption is explained by the high glass transition temperature of the PLA (60°C) [13]. As our flax/PLA composite uptakes 15.12 ± 0.46% of moisture under immersion at room temperature, it can be concluded that flax fibres and/or composites architecture (matrix pores/defects induced by ageing) are principally responsible for moisture uptake. As a consequence, PLA moisture sorption is not considered in any further detail in this chapter.

Besides a slightly higher moisture content at saturation, the moisture uptake behaviour at 50RH and 75RH are similar, as observed in Table 4-3. The moisture uptake appears to be more critical for the 98RH ageing and immersion. The sorption behaviour of flax fibres can explain this. It has been reported by Gouanvé et al. [311] that the mechanism of sorption of flax fibres evolves after a relative humidity close to 80%. Water molecules are absorbed on specific interaction sites or randomly adsorbed by flax, and thereafter, the water molecules cluster in the interstice and porosity of flax fibres, such as lumen or cell wall micropores [311]. Such micropores have been observed by Melelli et al. [90] on flax kink bands, where the flax structure is more heterogeneous and presents significant cavities compared to intact cell walls. This phenomenon is also observed for composite [47], where the matrix pores and the interfaces (matrix/fibres or fibres/fibres) are other places for potential water clustering.

Table 4-3: Moisture content in non-woven flax/PLA composite (Wf=40%) at each ageing step for all the ageing conditions,

		50 RH	75 RH	98 RH	Immersion
Water content at saturation [-]	ageing	2.77 ± 0.01 %	3.55 ± 0.04 %	8.76 ± 0.21 %	15.12 ± 0.46 %
	drying	1.46 ± 0.04 %	1.59 ± 0.05 %	1.17 ± 0.11 %	0.24 ± 0.07 %
	restabilisation	2.72 ± 0.02 %	2.88 ± 0.03 %	2.86 ± 0.09 %	1.94 ± 0.05 %

Regarding the drying and restabilisation step, all batches return close to their initial moisture content of 2.6%, except the immersion one. Interestingly, the 98RH samples lose more water during the drying step, meaning it has potentially a higher free/bonded water ratio than the 75RH and 50RH batches. The difference between their close mean water content at restabilisation is checked thanks to t-tests. It appears that 50RH have a different mean value than 75RH and immersed samples, where 75 RH and 98RH have an identical mean value statistically. In the case of immersion, the moisture content after

ageing and restabilisation is lower than the initial moisture content. It is mainly due to a decrease in the sample weight, distorting the moisture content value. Considering that the moisture content of the immerged samples after stabilisation should be similar to other ageing conditions (2.8%), this weight loss equals 0.9%.

This decrease can be induced by a leaching phenomenon already reported in the literature [234]. It is confirmed by a change in the colour of the leachate during immersion ageing. Polysaccharides of the flax are dissolved and released in the surrounding water, inducing a modification of the flax fibre composition. The total mass of samples immersed is 40 g in one litre of distilled water. Thus, the weight loss should induce a sugar concentration of 360 µg/mL, considering leaching as the only origin of the mass evolution. However, thanks to biochemical analysis of the leachate, the total sugar concentration only equals 25.7 µg/mL. This concentration includes 18.9 µg/mL of neutral sugars and 6.8 µg/mL of uronic acids. The detailed biochemical analysis of the leachate is given in Table 4-4.

Table 4-4: Biochemical analysis of the leachate obtained after flax/PLA non-woven composite immersion ageing. N/A refers to undetected sugar.

	Rhamnose	Fucose	Arabinose	Xylose	Mannose	Galactose	Glucose	Uronic acids
Concentration [µg/mL]	4.6 ± 1.6	N/A	N/A	N/A	N/A	5.2 ± 1.7	9.1 ± 4.4	6.8 ± 0.3

As dissolved polysaccharides alone cannot explain all the weight lost, PLA surface erosion due to fibre swelling at the surface is assumed to have a role [242]. The surface erosion is observed through SEM in Figure 4-2. Interestingly, the composite manufacturing process exposes flax fibres on the surface (face and edge) of unaged composites, see Figure 4-2. These fibres are a preferential path for water molecules, influencing the sorption kinetics observed in Figure 4-1.

Additionally, an increase in erosion is observed qualitatively from the reference to immersion samples (see Figure 4-2.a), .b)). Indeed, the surface roughness and the quantity of exposed flax fibres increases. At a lower scale, the impact of ageing on surface erosion is more evident. The reference sample presents few exposed fibres at the composite face/edge, which are still surrounded by PLA (see Figure 4-2.c)). The number of exposed flax fibres in the immersion samples appear higher, and they are locally detached from the PLA as gaps are present (see Figure 4-2.d)). They can even be uncoupled from PLA in some cases. It highlights the surface erosion and liberation of PLA micro-particles, explaining the weight loss.

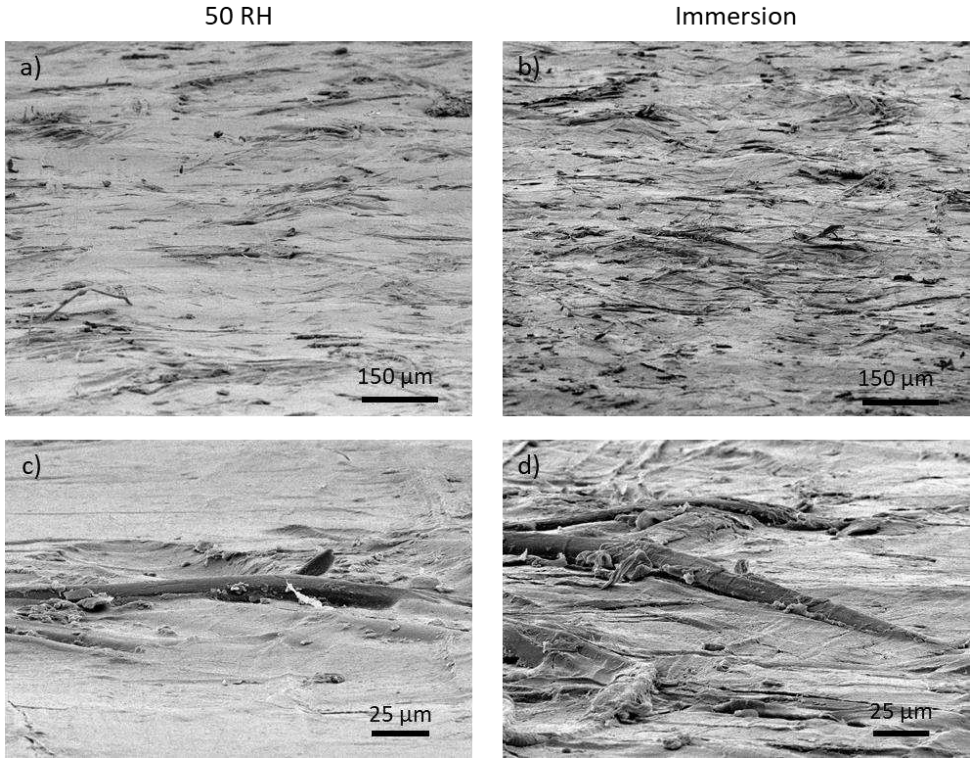

Figure 4-2: Tilt SEM observation of surface erosion after 50RH (a&c) and immersion (b&d) ageing. a) & b) are global views of the surface aspect, c) & d) focus on the aspect of exposed flax fibres.

The role of swelling in this erosion is observed in Figure 4-3. Where a flat surface is observed for reference, the topography surface of the immersed sample highlights the swelling of the fibres. Additionally, cracks are reported close to the fibres, confirming the PLA erosion induced by the flax swelling.

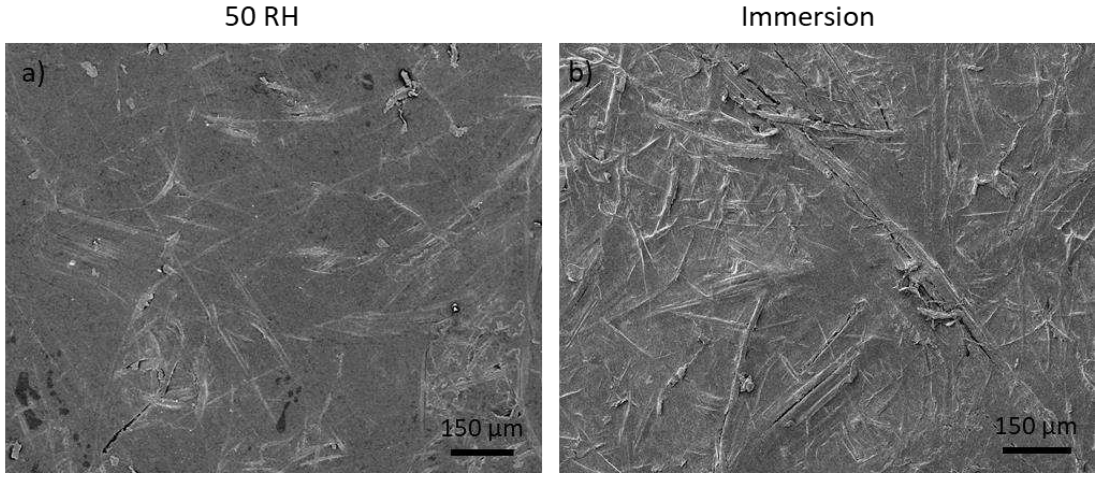

Figure 4-3: Perpendicular SEM observation of the surface erosion after 50RH (a) ant immersion (b) ageing, focussing on the role of flax fibres swelling.

III.b. Tensile properties

By testing the mechanical properties of restabilised samples, their irreversible alteration induced by the water sorption is characterised. The tensile behaviours are represented in Figure 4-4.a) and the mechanical properties are summarised in Table 4-5. The 50RH and 75RH samples do not present significant differences with the 50RH_ref batch, as they present similar tensile behaviour (Figure 4-4.a)). That means the drying step (40°C until stabilisation) does not impact the reference composite, and ageing at 75RH does not induce irreversible change in the flax/PLA composite. However, a decrease in stiffness and strength are observed for the 98RH and immersion batches (Figure 4-4. b)), with a stiffness decrease of 20.3% for 98RH and 33.4% for immersion. It agrees with the moisture uptakes of wet samples, which is much higher for 98RH and immersion than for the three undamaged batches.

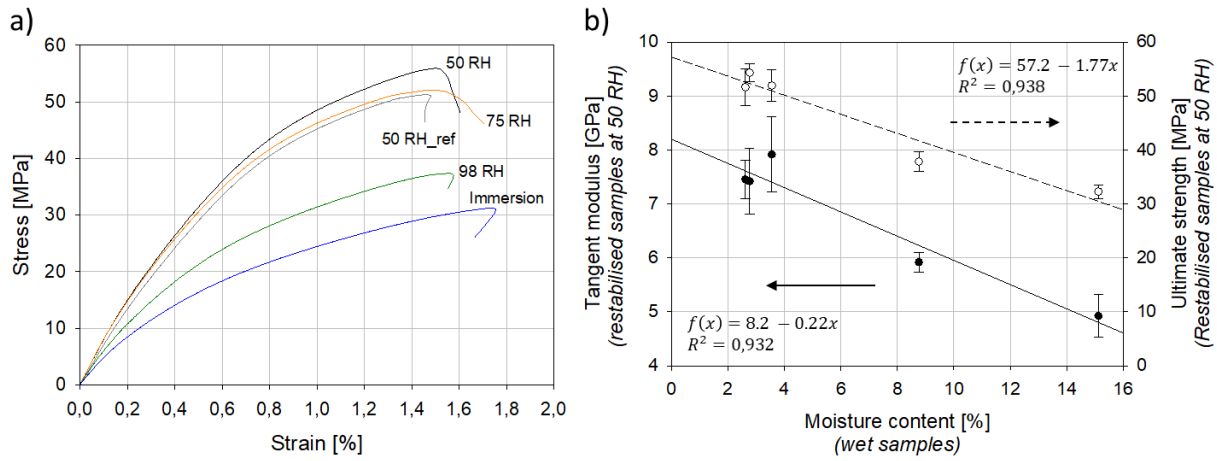

Figure 4-4: a) Tensile behaviour of flax/PLA composite (Wf=40%) after ageing under several conditions, drying and restabilisation at 50 RH (restabilised state), b) Influence of moisture content at saturation (wet state) on the tensile properties of the flax/PLA composite after ageing, drying and restabilisation at 50 RH (restabilised state).

Interestingly, the decrease in mechanical properties of restabilised samples appears to directly depend on the moisture content at the wet state, as reported in Figure 4-4.b). These correlations approach a linear behaviour, with a decrease factor of 1.77 MPa/% for the strength and 0.22GPa/% for the modulus. This linearity might be due to the progressive increase of defect inside the composite induced by the moisture content. These linear decreases were observed for an injected PLA/flax immersed in seawater [11], and an increase in defects in the composite is assumed.

Interestingly, the strain of the composite remains around 1.6 – 1.8% even for 98RH and immersed samples, which is the failure of the fibre. Thus, composite behaviour is still fibre dominated even after ageing.

It highlights the existence of a critical relative humidity between 75RH and 98RH, where flax composites present irreversible damage. As the moisture content of flax composites is described by a sigmoid [47,311], a relative humidity close to 80RH induces a drastic increase of the water content inside the composite. This relative humidity is probably the limit to not reach to avoid irreversible damage in the composite. This critical relative humidity can be observed using more relative humidity ageing between 75 RH and 98 RH. Additionally, it will help to identify more precisely the nature of the trend. The dry states (lower than 2.6%) can result in different damage mechanisms, leading to another modification of mechanical properties not highlighted by the presented trend Figure 4-4.b).

Interestingly, the water molecules change from the gas phase to the liquid phase when the saturation pressure of water is reached. It occurs at the physical limits of relative humidity of 99,9%. For the flax/PLA non-woven composite, the moisture content jumps from 9% to 15% by switching from a 98RH to an immersion ageing. Therefore, the moisture content range of 9% to 15% is not reachable. However, the immersion impact on tensile properties appears to align with the vapour ageing impact, as observed in Figure 4-4.b). The shortcut of immersion as accelerated vapour ageing should be used carefully as the water molecules are not in the same state. Thus, ageing mechanisms could be different between vapour and immersion conditions. The latter is expected harsher.

Table 4-5: Tensile properties of flax/PLA composite (Wf=40%) after ageing under several conditions, drying and reconditioning at 50 RH (restabilised state). The pure PLA values are extracted from chapter 3, measured on unaged INGEO™ PLA samples.

	50 RH_ref	50 RH	75 RH	98 RH	Immersion	Pure PLA (unaged)
Tangent modulus [GPa]	7.4 ± 0.3	7.4 ± 0.6	7.9 ± 0.7	5.9 ± 0.2	4.9 ± 0.4	3.4 ± 0.1
Ultimate strength [MPa]	51.6 ± 3.3	54.3 ± 1.6	51.9 ± 3.0	37.8 ± 1.8	32.3 ± 1.3	37.6 ± 0.8
Strain at failure [%]	1.5 ± 0.2	1.5 ± 0.1	1.4 ± 0.1	1.6 ± 0.1	1.8 ± 0.3	2.6 ± 0.4

The amount of water uptake is the origin of the composite degradation. Two hypotheses have to be verified. First, contact with water can decrease the mechanical properties of the flax fibres [321] and the matrix [320]. Indeed, the mechanical properties of elementary flax fibres depend on the surrounding relative humidity [321], with a decrease in strength of ca. 15% and an increase of ca. 25% of strain at high relative humidity.

Second, the composite structure can deteriorate through decohesion of the flax and matrix or by creating matrix micro-cracks induced by flax swelling [235]. The combination of both phenomena will induce connected defects. For example, the decohesion at the interface creates a gap between the

flax and the matrix. These gaps could be linked together by the micro-cracks present in the matrix. The reduction in composite density can be used to quantify the volume of these structural defects.

IV. Discussion

IV.a. Evolution of flax and matrix stiffness in the composite

As expressed previously, one hypothesis is that ageing impacts the properties of flax or the matrix. Therefore, their mechanical properties are assessed through AFM measurement on the reference and the two impacted batches. Table 4-6 presents the averaged indentation modulus for flax and PLA matrix, whereas Figure 4-5 presents the indentation modulus mapping used for one measurement.

Table 4-6: Impact of the ageing condition on the mechanical properties of the flax fibres cell walls and PLA in the composite. It is investigated at the micro-scale level through AFM-QNM measurements.

	50 RH ref	98 RH	Immersion
Flax fibre indentation modulus [GPa]	15.3 ± 1.0	13.4 ± 1.8	13.9 ± 0.9
PLA indentation modulus [GPa]	5.5 ± 0.1	5.4 ± 0.3	5.4 ± 0.2

First, the mechanical properties of PLA do not evolve during ageing, with a constant indentation modulus value of ca. 5.5 GPa. Thus, there is no local recrystallisation of the PLA. This is expected as the PLA is relatively insensitive to immersion ageing at 25°C [320]. Indeed, Deroiné et al. [320] reported, for virgin PLA aged six months in distilled water at 25°C, no decrease in mechanical properties at the macro-scale and only a tiny chemical evolution with a moderate decrease of number-average molecular weight from 75 000 g/mol (unaged) to 66 300 g/mol.

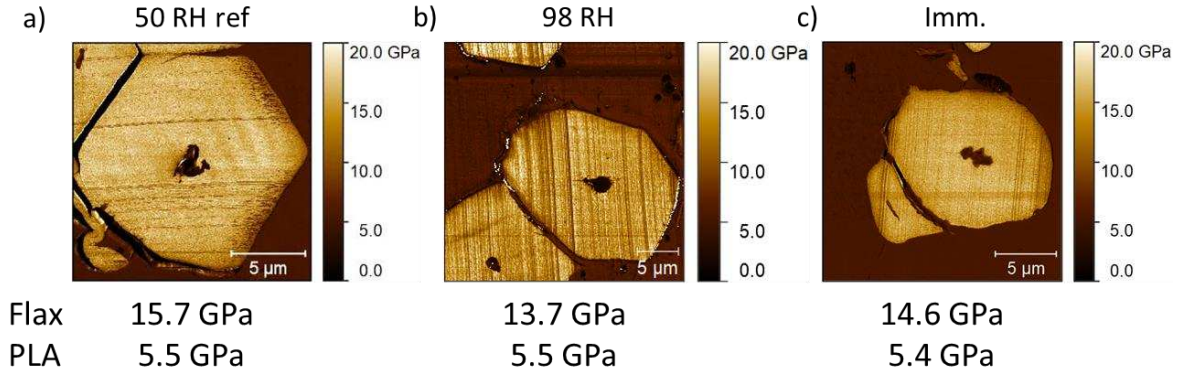

Figure 4-5: AFM indentation stiffness map for one fibre of flax/PLA composite after a) no ageing (50RH ref), b) moisture ageing at 98 RH, c) immersion ageing with distilled water.

For the flax fibres, a slight decrease appears between the reference and the impacted samples. The impacted samples (98RH and immersion) are considered statistically identic, as a t-test give a

probability of similarity equals to 63%. However, due to the close value between the reference and the impacted samples, their standard deviation and the operator influence on the selection of the fibres, it can be concluded that flax cell walls present similar mechanical properties whatever the ageing condition used. Note that these values are slightly lower than the indentation modulus usually obtained in the literature using AFM, being between 17-22 GPa [322].

Interestingly, this stable indentation modulus does not agree with Le Duigou et al.'s [234] results from nanoindentation measurements on immerged unidirectional flax/PLA composite. Indeed, they observed a 40% decrease in nanoindentation modulus after four weeks, compared to a 10% decrease (without considering the standard deviation) after six weeks in this study. They explain the decrease of the mechanical properties by the solubilisation of uronic acids, playing a role in transferring loads in the second wall (S2) of the flax fibres [234]. They observed a ratio of 2.5 between the uronic acids released and the neutral sugars. Thanks to the biochemical analysis, this ratio is calculated to be 0.36 in our leachate, supporting the unchanged mechanical properties of the flax fibres in the immersed samples.

The difference between both experiments can be explained by the difference in flax preform and manufacturing process. Le Duigou et al. [234] used a vacuum film stacking method to manufacture flax/PLA unidirectional composite at a fibres weight fraction of 50%. This manufacturing method leads to lower compaction than the thermo-compression due to low pressure (≈ 0.95 bar) [175] and potentially modify flax fibres composition as it requires the severe manufacturing condition of 180°C for 1 hour. In addition, the unidirectional orientation of fibres leads to easier leaching than random orientation as the fibres percolation in the composite is higher for unidirectional. Finally, they used a magnetic stirrer, which may increase the leaching phenomenon.

Thus, the evolution of flax cell walls and PLA's mechanical properties cannot explain the decrease in stiffness observed at the composite scale. Therefore, the second hypothesis relating to the evolution in composite structure (and density) should be investigated as it may be responsible for the mechanical properties evolution.

IV.b. Composite density evolution

The structural modification of the composite through ageing is potentially due to the decohesion phenomenon or micro-cracks generation in the matrix, both being related to flax fibre swelling [235]. These mechanisms are directly linked to the composite density, as they modify its structure by creating a gap at the interfaces for the first one and matrix micro-cracks for the second. The density

measurement is presented in Figure 4-6.a). The porosity calculated is presented in Figure 4-6.b), considering constant flax and matrix density. However, the assumption of a constant flax density is debatable as the moisture uptake and swelling phenomena can modify flax fibre structure, where the leaching phenomenon (immersed samples only) modifies its biochemical composition.

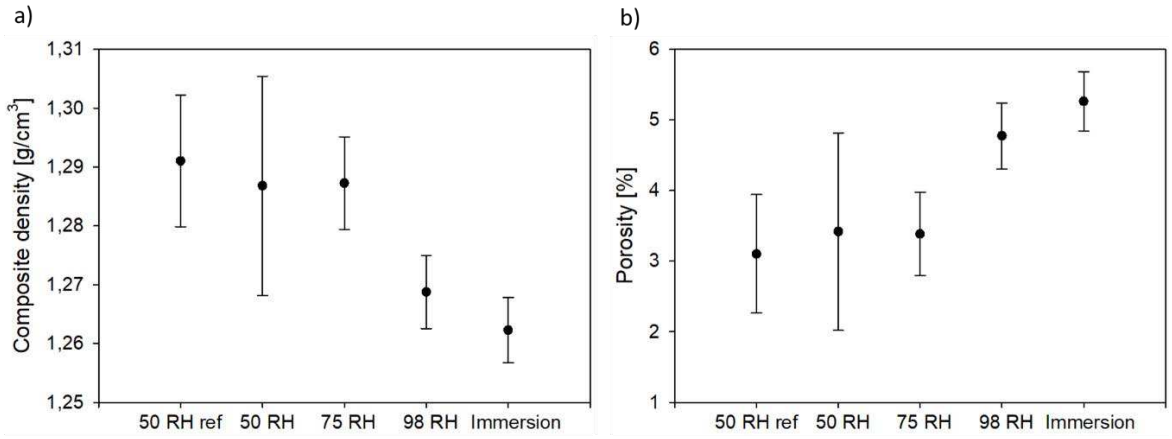

Figure 4-6: Evolution of the a) composite density and b) porosity of restabilised samples after different ageing conditions. The porosity is calculated assuming ageing does not modify the PLA nor flax density.

Nevertheless, the results fall in line with the mechanical properties evolution. Indeed, the porosity appears similar for the 50RH_ref / 50RH / 75RH samples, increasing from 98RH to Immersion samples (see Figure 4-6.b). Thus, ageing induces a modification of the inner structure of the composite. The origin of the structural modification needs further investigations to understand its influence on mechanical properties.

IV.c. Interface decohesion

First, interface cohesion is checked through SEM observation on cryo-fractured samples. The obtained pictures are presented in Figure 4-7. If a gap is observed, a physical decohesion can be identified. The embedded length should not be considered here as these samples are observed before any tensile test.

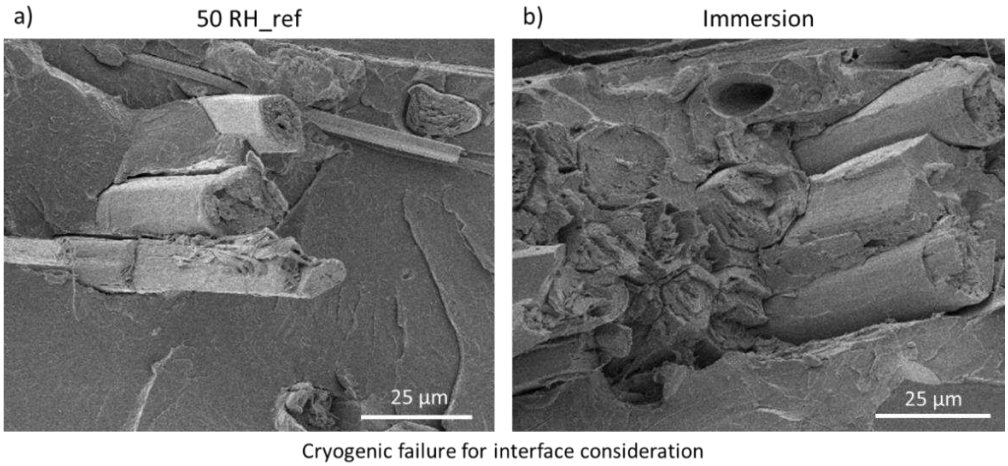

Figure 4-7: Interface observation by SEM of flax/PLA composite after a failure of the sample under cryogenic condition, a) observation of the reference and b) observation of the most damaged batches, being the immersion one. No decohesion is observed after an immersion ageing as no gap is present.

No significant decohesion at the flax/matrix or the flax/flax interfaces could be observed for reference or aged flax/PLA composite. There are two explanations, the first being that the interface is not damaged during ageing. One possibility is that fibres embedded within the PLA in the core of the sample are not subjected to water uptake nor swelling. However, this is unrealistic as the randomness of the preform induces interconnectivity of the flax fibres, percolating the open edges in contact with the environment.

The second more realistic explanation is a damaged interface, but it could not be observed. This damage can be due to chemical modification (leaching [234]) or hidden physical decohesion. During the thermo-compression process, the flax fibres have a low water content due to the high temperature. Thus, the flax fibres in the 50RH_ref composite are already constrained. In addition to the hygroscopic stress, some residual stresses due to the thermal history of the polymer and flax fibres are present. Nevertheless, residual thermal stresses are negligible against the hygroscopic stress [224]. In addition, flax fibres act as nucleating agents for the PLA, creating a transcrystalline layer around the fibres [93].

During the ageing, the flax fibres swell enough to overcome the matrix's yield point locally and irreversibly deform the matrix. The drying step allows the flax fibres to retract as their water content decrease, creating a gap at the interface and releasing the internal residual stresses. Through the restabilisation at 50RH, the flax fibres are now free to swell, as the matrix did not constrain it, and fill the gap previously created, hiding the decohesion. This phenomenon, schematised in Figure 4-8, should not significantly modify the composite's density (nor the porosity).

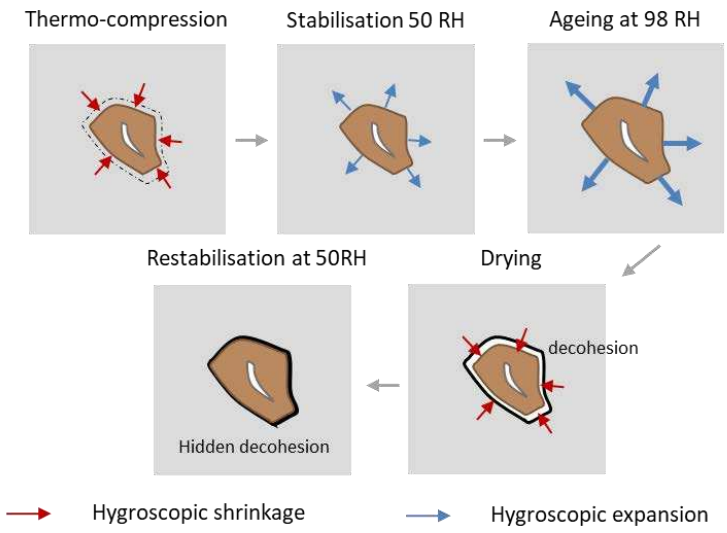

Figure 4-8: Schematic explanation of the formation of hidden decohesion due to the alternation of shrinkage and expansion of flax fibres inside the composite. Inspired from [224].

This potential damages at the interface can explain the decrease of the mechanical properties of flax/PLA composite as the stress transfer between reinforcement and matrix. Consequently, the reinforcement of flax fibres is less efficient, inducing a decrease in the modulus and the ultimate strength of the composite without any increase in its ultimate strain.

IV.d. Micro-cracks generation in the matrix

The swelling of the fibres during ageing has another consequence in the composite structure. As observed in Figure 4-9, the aged composite presents micro-cracks inside the matrix, initiated at the matrix/fibre interfaces. It suggests that the stresses applied by the swelled flax fibres to the matrix are higher than its ultimate strength. Therefore, the presence of these micro-cracks decreases the mechanical properties of the composites. Indeed, they act as defects, lowering the ultimate strength of the composite but also reducing the apparent stiffness of the matrix.

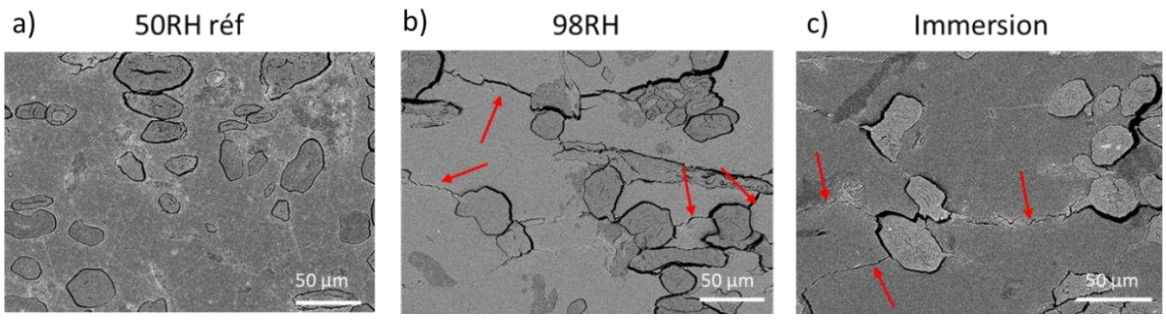

Figure 4-9: SEM observation of flax/PLA composite after a) no ageing, b) ageing at 98 RH, c) an immersion ageing. The observations are perpendicular to the direction of the sample. The red arrows focus on the presence of matrix micro-cracks.

As a first approach, the stiffness of a random non-woven composite (E_{NW}) is estimated thanks to $E_{NW} = \frac{3}{8}.E_{UD,longi} + \frac{5}{8}.E_{UD,transv}$, where $E_{UD,longi}$ and $E_{UD,transv}$ are the longitudinal and transversal stiffness of an equivalent unidirectional composite, respectively. The matrix stiffness is the predominant parameter of the unidirectional transversal stiffness. Thus, the apparent matrix stiffness reduction due to micro-cracks directly decreases the transversal stiffness of an equivalent unidirectional composite, and so does the non-woven composite stiffness. In addition, a higher number of matrix micro-cracks might induce a lower apparent matrix stiffness. It has been observed in Figure 4-4.b) that the tensile stiffness of a dry sample depends on its moisture uptake in the wet state. As the number of micro-cracks should increase with higher moisture uptake (due to higher flax swelling), the generation of matrix micro-cracks is responsible for the decrease in the tensile stiffness of aged non-woven flax/PLA composites. Thus, these matrix micro-cracks decrease the composite strength but also its stiffness.

The fact that immersion ageing influences mechanical properties in line with vapour ageing indicates that the main damage mechanisms are mutual to immersion and vapour ageing. It can be the matrix micro-cracks or the hidden decohesion. The leaching phenomenon is discarded as it is specific to immersed samples.

An analytic calculation is made at the micro-scale level to confirm the assumption of local stress induced by flax swelling. It is based on a model developed by Nairn [323], see Appendix 1. This model calculated the residual thermal stresses in a unidirectional composite due to the difference in thermal expansion of the composite's constituents. The model focussed on one cylindrical fibre embedded in a cylindrical matrix pipe. It assumes a linearly elastic and isotropic matrix, a linearly elastic and transversely isotropic fibre, and a perfect bond between constituents. These assumptions are debatable for flax/PLA composites. Nevertheless, as a first approach, this model can lead to a fruitful discussion.

Here, an analogy between thermal expansion and hygro-expansion is considered. A moisture content variation of 6.2% is used as it is the experimental variation obtained between the composite's initial moisture content and the moisture content during the 98 RH ageing. A transversely isotropic cylindrical flax fibre is embedded in an isotropic cylindrical PLA pipe, both subjected to expansion. Radii are selected to be consistent with a weight fraction of 40 %. All the input values used are summarised in Table 4-7. The highest stresses in the matrix are at the fibres' contact. Radial compressive stress of 88 MPa and tangent tensile stress of 187 MPa are calculated. Even considering volume effects (local transcrystalline layer close to the fibres) which can justify a local higher ultimate strength for PLA

(being 60 MPa for a macro-sample), the local stresses induced by flax swelling appears critical. That confirms that the local stress generated can damage the matrix locally. Therefore, it is highlighted here that fibre's swelling can be responsible for the appearance of matrix micro-cracks. Additionally, the matrix yield stress is overcome, validating the possibility of hidden decohesion between flax and matrix.

These results are coherent with a numerical study of Chilali et al. [324], founding von Mises mean stress higher than 200 MPa in a flax/epoxy system. Djellouli et al. [325] reported that the local stresses increase up to 110%, switching from a regular to a random distribution of flax fibres inside a unidirectional composite. This increase is expected even higher for non-woven composite as the random distribution occurs in three directions. Furthermore, the analogy assumption between thermal and hygro expansion underestimates these local stresses, as the moisture content is not homogenous, higher in the flax fibres than in the matrix.

This model can also be used backwards to identify the critical moisture content inducing tensile stress higher than the PLA strength (60MPa). This moisture content is the limit to generate matrix micro-cracks. It appears that composite moisture content of 4.6 % induces tensile stress in the matrix of 60.2 MPa and compressive stress of 28 MPa. This moisture content value corresponds to a critical relative humidity, expected to impact the composite irreversibly. Once again, this value should be used by keeping in mind the previous assumption discussed.

*Table 4-7: data used for the calculation of the local radial stress, *the transverse Poisson's ratio is calculated using* $\frac{E_L}{\vartheta_{LT}} = \frac{E_T}{\vartheta_{TL}}$.

	Stiffness [GPa]	Poisson's coefficient [-]	hygro-expansion coefficient [ε/Δm]
PLA	3.4 [chap. 3]	0.38 [chap. 3]	0.001 [232]
Flax fibres (longitudinal)	52.5 [83]	0.34 [chap. 3]	0 [224]
Flax fibres (transverse)	8 [199]	0.05*	1.14 [224]

Because of a lack of raw non-woven materials, only flax/PLA composite has been investigated experimentally. However, it can be interesting to have some clues about the potential ageing of flax/PHA or flax/PBS composite. As the PHA and the PLA have similar modulus, they are attended to act similarly. The focus is on the PBS as it appears to be softer than the two other biodegradable matrices. Using the same model (same hygro-expansion coefficient) but considering the PBS stiffness of 0.7 GPa, it appears that the radial and tangent stress reduce to 20 MPa and 43 MPa, with is much closer to the ultimate strength of the PBS, being equals to 39 MPa. Using a less stiff matrix appears to be a potential solution to reduce the ageing impacts of flax composites, considering a matrix with a

similar water sorption behaviour to PLA. A matrix with a higher hygro-expansion coefficient will modify the residual stress concentration.

Note that these micro-cracks were observed on epoxy embedded and polished samples (with water). The friction induced by polishing and water sorption at the surface could have been responsible for these cracks. However, the reference samples did not present micro-cracks. This gives confidence these micro-cracks are created during ageing and not during the samples preparation. A CT-scan analysis could avoid this damaging effect and confirm the presence of the micro-cracks due to ageing. Such analysis could give additional information such as the number of matrix micro-cracks, their connectivity and their geometry. Furthermore, it can confirm the link between the number of matrix micro-cracks, the water uptakes at the wet state and the tensile mechanical properties of the dry sample. However, that needs a high resolution as such micro-cracks have a thickness of no more than a few micrometres.

V. Conclusion

The evolution of the microstructure and the mechanical properties of a flax non-woven composite subjected to water ageing (at 50% RH / 75% RH / 98% RH / immersion) is investigated. The ageing conditions selected aim to understand the first degradation step of a flax/PLA non-woven composite. The ageing process is monitored by following the composite's moisture content over six weeks and waiting for stabilisation in their weight before being dried and restabilised at 50% RH. Interestingly, ageing at 75% RH does not impact the mechanical properties nor the composite structure. On the other hand, ageing at 98% RH or immersion for six weeks presents a significant uptake of water, decreasing the strength and stiffness of the composites significantly. A deeper analysis was conducted to better understand the ageing mechanisms. Thanks to an AFM investigation using the peak-force mode, the flax fibres cell walls and the PLA appear to keep their initial mechanical properties. Thus, the composite softening is due to an evolution of the composite’s structure, confirmed by increased porosity for the two impacted batches. The interface is observed thanks to the cryogenic failure of aged samples. No gap was observed, indicating that decohesion of matrix and PLA could not be observed, probably due to the restabilisation step and the free swelling of fibres, closing (‘hiding’) the gap created by ageing. It appears that the porosity increase is due to the creation of transverse micro-cracks induced by flax-fibres swelling. The generation of micro-cracks is discussed using an analytical model. It appears that the local stress induced in the matrix due to the fibre swelling is higher than its yield and ultimate strength. That confirmed that the swelling of the fibres is responsible for the structural evolution of the composite, hidden decohesion or matrix micro-crack generation. These

structural evolutions impact the tensile properties of the flax/PLA non-woven composite by decreasing its ultimate strength and stiffness.

On the one hand, investigating more relative humidity conditions in the range of 75RH and 98RH can help identify the presence of a critical relative humidity at which mechanical properties and structure start to get significantly affected. Additionally, extending these experimental investigations of flax/PLA non-woven composites with various fibres volume fractions could lead to additional clues on the degradation mechanisms. Furthermore, using cycling tensile loading cycles could give information on the role of interfacial defects on the composite mechanical behaviour. Finally, the effect of protecting the edges and the surface by a thin PLA layer could be investigated as it is expected to reduce the sorption kinetics. On the other hand, using the same model but considering a softer matrix, the local stress generated decreases, showing the potential of a softer polymer to be used as a matrix for more ageing-resilient flax composites. This needs to be examined experimentally.

Chapter 5: Monitoring of mechanical performances of flax non-woven biocomposites during a home compost degradation

I. Introduction

I.a. Benefits of non-woven flax fabrics

Thanks to their low density [84], competitive specific mechanical properties [85,86], and environmental profile [268], plant fibres such as flax are replacing glass fibres in industrial components like interior car parts [48,326]. Both injected and thermo-compressed non-woven parts can be found, though the latter represents a more significant share of the global biocomposite market. Various processes exist to manufacture non-woven reinforcement preforms, the most common of which are the needle-punching and the spun-lacing methods, yielding similar composite mechanical properties [165]. These non-woven composites possess mechanical properties that fall between a unidirectional composite and an injection-moulded composite [64]. Nevertheless, non-woven fabrics are substantially more economical in price than aligned unidirectional composites [64]. Furthermore, non-woven preforms are more compliant than unidirectional preforms, thereby enabling the processing of complex-shaped products.

Non-woven biocomposites are usually embedded in a polyolefin thermoplastic matrix, typically poly-(propylene) (PP) for the automotive sector due to its technical advantages, which include temperature stability (during service), low melting (processing) temperature, good mechanical properties, as well as its low price. However, mixing biomass plant fibres with a petroleum-derivative polyolefin polymer tarnishes the eco-profile of the biocomposite - even if the use of recycled PP as a matrix can be an attractive compromise [327]. Of course, the environmental impact of the plant fibre/PP non-woven biocomposite can be reduced by recycling the material at its end-of-life [328–331]. Hence, it is a relevant solution in a circular recycling context for the non-woven sector where such wastes represent 25%wt of the production. However, most commonly, incineration (with or without energy recovery) is the selected option.

Arguably, replacing the petrochemical polymer with a biodegradable polymer unlocks alternate end-of-life scenarios, namely (bio-)degradation through composting. This scenario may be desirable when

sustainability policies and regulations are based on solid waste generation (vis. plastic challenge) rather than energy use or carbon emission over the product life cycle.

I.b. Compost-based degradation of bioplastics

Indeed, the scale of our ocean plastic pollution challenge [332] has drawn rapidly surging interest in biodegradable polymers. To better understand the degradation behaviour of flax-reinforced bioplastics, here, we focus on the degradation of poly-(lactide) (PLA), poly-(butylene-succinate) (PBS) and poly-(hydroxy alkanoates) (PHA). The degradation of these biopolymers is well studied [7,8,10,333] and is described to be a complex phenomenon. Degradation depends on the chemical nature of the polymer, the environment the degradation is occurring in, and the degradation period. For instance, the temperature has an essential effect on the degradation of PLA [49,334] mainly because of its transition to a rubbery state above its glass transition temperature T_g. Indeed, in a simulated compost held at 58°C, PLA (T_g = 61.2 °C) [335] exhibits rapid erosion in its molecular weight, which decreases from $225 \cdot 10^3$ to 500 Daltons over 30 days [336], while it needs more than 150 days to fragment in the soil at a temperature between 15°C and 25°C [337]. However, in this same soil condition, PHA can be fragmented enough not to find any macroscopic residue within 60 days [337]. In contrast, Luo et al. [24] show that PHA loses 80% of its weight after 50 days in manure-based compost. On the other hand, PBS degrades in a soil compost of 30°C at a slower rate, losing only 13.5% of its weight after 80 days [338].

Degradation relates to the erosion of the material over time [7,8], and for a polymer-based material, degradation includes polymer chain scission and potential macro- and micro-fragmentation. This erosion phenomenon is induced by water and/or microorganisms and is dependent on several parameters such as sample geometry (e.g. thickness) and temperature. At the end of the degradation process, the polymer is reduced to oligomers and/or monomers. This degradation, however, should not be confused with biodegradation, which is the bio-assimilation of the oligomers and monomers by microorganisms. This bio-assimilation leads to their conversion to mainly CO_2, H_2O and living matter. Biodegradation (therefore) follows after degradation.

I.c. Compost-based degradation of plant fibre/biopolymer composites

As plant fibres are biodegradable, their incorporation in composites can modify the degradation behaviour of the polymer matrix. Indeed, plant fibres are highly hydrophilic and often degrade faster than biodegradable polymers. Furthermore, embedding plant fibres in polymers induce two interfaces: one between the polymer and the fibres and a second between the fibres inside a fibre bundle. Both interfaces are likely to influence both mechanical properties and the degradation behaviour of

composites. Several authors have already shown interest in mechanical property evolution and biodegradability of biocomposites [339–341].

PLA is the leading biopolymer used in studies on flax fibre biodegradable composites, and it is reported to have mechanical properties better than that of glass fibre/PP [44] and glass fibre/polyester [43]. The melting temperature of PLA is around 170°C, which avoids thermal degradation of plant fibres during composite processing typically seen above 200°C [46]. It has been shown that in compost at 25°C, non-woven flax/PLA degrades more (and faster) with increasing fibre content [342]. Furthermore, the architecture of the flax preform - unidirectional or non-woven - influences the composite degradation behaviour as flax fibres act as a porous media drawing in water [240,242] and potentially microorganisms. As PLA's rapid degradation occurs close to 60°C [334], it is relevant to look at other less-used biodegradable polymers, such as PHA and PBS, as matrices for non-woven flax composites. However, limited investigations have examined their mechanical properties [43] or the degradation of their flax reinforced composites. Furthermore, it is hard to compare all these literature studies as the degradation behaviour directly depends on many factors, including the polymer used as a matrix (including molecular weight), the fibre volume fraction [242,342], the preform architecture [240,242], the sample geometry [57], the composite and interface quality, as well as the compost environment. See Table 5-1 for a detailed literature recap.

A systematic study exploring the potential of these various biodegradable polymers to be used in non-woven flax composites and monitoring their degradation under the same environment, with sample geometry representative of current industrial parts, will give fascinating insights. Furthermore, it will inform industrial materials choices that resolve the 'biodegradation paradox', achieving adequate mechanical properties and the desired degradation kinetics.

This study focuses on the degradation of three biocomposite materials made of flax non-woven preforms embedded in a PLA, PBS or PHA matrix. As PP is industrially used nowadays, its reinforced composite will set the benchmark. First, the tensile mechanical properties of the four as-produced formulations are assessed and compared to inform their potential in industrial components. Then, their ageing (degradation) behaviour in a garden compost over six months is investigated, periodically monitoring the evolution in weight, mechanical properties, as well as microstructure. Mechanisms and kinetics of degradation are then discussed, and the 'design service life' of the biocomposite materials is determined.

Table 5-1: Summary of literature study results on the degradation of non-woven biocomposites in compost.

Materials	Environment	Wf [%]	Thickness [mm]	weight loss [%] (time)	Residual strength [%]	reference
Non-woven thermos-compressed						
Flax/PLA	Compost (25°C)	40	2.00	6 (120 days)	30 (flexural)	[342]
	Compost (-°C)	50	2.30	27 (120 days)	20 (flexural)	[240]
	Compost (40 ± 7°C)	30	3.00	4 (56 days)	/	[242]
	Farmland soil (25 ± 5 °C)	20	0.65	25 (90 days)	/	[244]
Jute/PBS	Compost 30 ± 2°C	30	/	30 (120 days)	/	[245]
Injection-Moulded						
Abaca/PLA	Soil (25-30 °C)	10	0.50	10 (60 days)	/	[243]
Flax/PHA	Soil (-°C)	20	2.00	15 (112 days)	55 (tensile)	[241]
Abaca /PHBV	Soil (25-30 °C)	10	0.50	50 (90 days)	/	[243]
Abaca/PBS	Soil (25-30 °C)	10	0.50	45 (60 days)	/	[243]

II. Materials and Methods

II.a. Materials

Flax non-woven preform (100 ± 15 g/m²) was provided by Ecotechnilin (Yvetot, France). The non-woven is extracted from a needle-punching line making flax non-woven preforms, but the material extraction takes place just before the napping step, before the consolidation step. This induces an anisotropic non-woven preform. The main characteristics of polymers selected for this study are indicated in Table 5-2.

Table 5-2: Main characteristics of the thermoplastic polymers used in this study (from datasheets).

Polymer	Provider	reference	Density	MFI
PLA	NatureWorks	PLA3001D	1.24	22 (210°C/2.16kg)
PHA	NaturePlast	PHI002	1.25	15 – 30 (190°C/2.16kg)
PBS	pttMCC	BioPBS™ FZ71PM	1.26	22 (190°C/2.16kg)
PP	Total	PPC10942	1.24	22 (210°C/2.16kg)

II.b. Composite manufacturing

A lay-up made of ten plies of flax preform and several plies of polymer films were assembled. The number of polymer plies varied according to polymer density and the thickness of the film. The orientation of the preform is conserved during the lay-up process, leading to an anisotropic flax

composite. A constant fibre volume fraction of 30 ± 1% was maintained for all the composites. The lay-up was then hot compression moulded with a hydraulic press LabTech Scientific 50T (Labtech, Samutprakarn, Thailand), yielding laminate plates of 20 cm x 20 cm x 2mm. The thermo-compression cycle is the same as the one presented in chapter 2, section II.a.

As references, pure polymer plates of 11x11 cm with a thickness of 2mm were made from injection moulding with a Battenfeld BA800 injection machine (Wittmann Battenfeld, Kottingbrunn, Austria). Once the composite and pure polymer plates were made, these were cut with a milling machine into dog-bone shaped samples based on the ISO 527-4.

II.c. Compost degradation

A 900-litre wooden compost bin was filled with the compost mix, comprising green and brown plant waste, see Figure 5-1. Two EL-USB-2-LCD Lascar electronics recorders monitored the compost's temperature at a depth of 30 cm. Samples were buried into the compost at a depth between 20 and 40 cm. This compost mix was used as a harsh environment for ageing the composites. No intervention was done to the compost during experiments, and the compost was not covered. Weather data (mean temperature and daily rainfall) was obtained from the University of Cambridge Botanic Garden weather station located 2m from the compost bin.

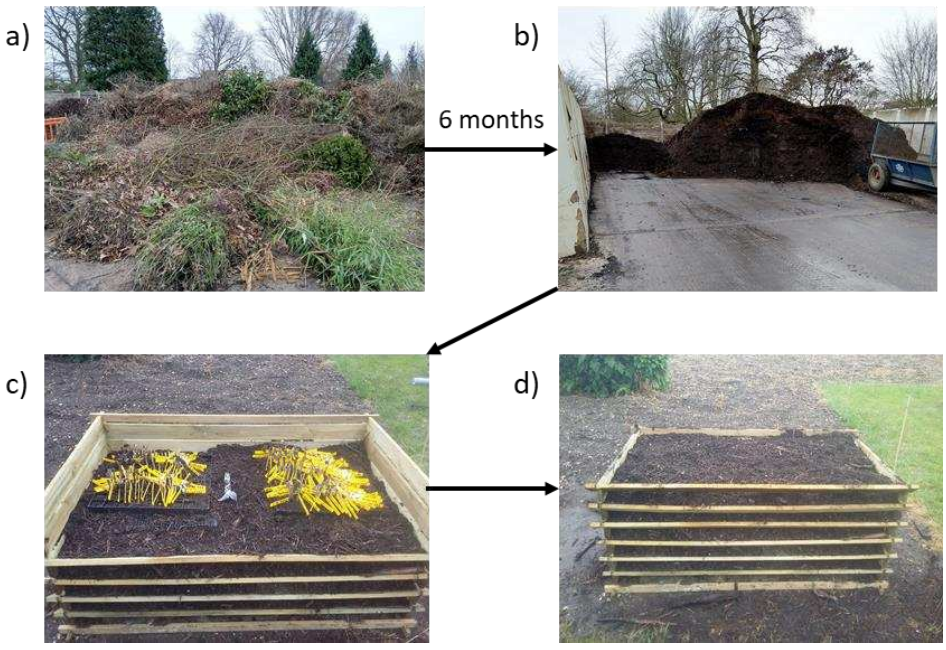

Figure 5-1: Garden compost set-up used as harsh ageing, a) green and brown plant waste b) inoculum obtained after four months c) samples dig in the compost, each one identified through its yellow labels, d) the wooden compost bin including garden compost and composite samples.

For each biocomposite and their virgin polymer, ten sampling phases were planned. For the industry reference PP and flax/PP, four sampling phases were planned, as they were not expected to degrade as much or degrade much more slowly. Samples were dried (for 32h at 40°C) before being buried in the compost (to determine initial dry mass) and then again before mechanical testing (to determine aged dry mass and mechanical properties) to avoid moisture effects overshadowing the degradation effects. Sample batches were extracted after 0, 6, 14, 20, 38, 55,70, 104, 125 and 190 days.

II.d. Weight evolution

The weight loss evolution was calculated according to (1) and expressed as a percentage. w_i is the initial weight before any degradation and w_t corresponds to the weight of the composite at *t* time.

$$\Delta w = \frac{w_i - w_t}{w_i} \times 100 \quad (1)$$

II.e. Composite tensile test

Static tensile tests were performed on an Instron 5500R machine (Instron, Norwood, MA, USA), where an EIR LE-05 laser extensometer recorded displacement and strain. The gauge length was 25mm, and the displacement speed was 1mm/min. Eight samples were tested for each formulation at each sampling phase, and at least five data points were kept (e.g. ignoring grip failures). The tensile test occurs in the preferential direction of fibre direction inside the composite. The tangent modulus was calculated over a strain of 0.02% to 0.1% for all the flax reinforced biocomposites [212] and neat PHA bioplastic. The tangent modulus was calculated from 0.1% to 0.5% applied strain for neat PLA, PBS, and PP, which have a higher elastic zone. Normalized strength is used to compare the strength evolution of biocomposites. It is defined as following (2), where σ_i is the initial tensile strength and σ_t the strength of the composite after a time *t* of degradation.

$$\Delta\sigma = \frac{\sigma_i - \sigma_t}{\sigma_i} \quad (2)$$

II.f. Microtomography

A microtomography study was performed on a lab-based Nikon XT H225 ST X-ray micro-tomography system to observe the microstructure of the samples and their evolution upon compost degradation. The middle section of the dog-bone samples was imaged. An X-ray tube voltage of 65kV and a tube current of 100 µA were used, with an exposure time of 1000 ms, a total of 3141 projections, and an optimal voxel (3D pixel) size of 7.00 µm. One sample by formulation was observed via micro-tomography before composting, after 70 days and 190 days. Images were extracted and analyzed using

the software VGStudio Max 2.2 to obtain a porosity analysis by a greyscale threshold in a volume of 9x7x1.5mm on each analyzed sample. This volume was selected in the middle of the analyzed 3D picture, at an equal distance of edges in all directions.

II.g. SEM

Sample observation was also done using a JEOL SEM (JSM-IT500HRSEM) at an acceleration voltage of 3 kV, and a gold sputter coating was performed for preparing samples using a sputter coating (Scancoat6) from Edward. For interface analyses, samples underwent a brittle fracture under nitrogen before being sputter coated.

II.h. AFM investigation

A Multimode 8 AFM instrument (Bruker, Billerica, Massachusetts, USA) was used in PF-QNM imaging mode. The method is described precisely in chap 4, section II.b. It allows local topography and rigidity measurement and can highlight evolution in the multi-layer structure of flax fibres. RTESPA-525 (Bruker, https://www.brukerafmprobes.com/p-3915-rtespa-525.aspx) silicon probe with a spherical tip apex was used here.

Its spring constant was calibrated using the Sader method, and the tip radius was adjusted between 20 and 80 nm on an aramid sample. The image resolution was 512×512, 384×384 or 256×256 pixels depending on the aim of the image captured. The peak force amplitude was set between 50 and 100 nm for fibres measurement, depending on the region investigated and its rigidity.

III. Results and Discussion

III.a. Mechanical characterization of composite

Figure 5-2 illustrates the tensile stress-strain behaviours of the four neat polymers (Figure 5-2.a)), alongside their non-woven flax reinforced composite (Figure 5-2.b)); measured tensile properties are presented in Table 5-3. The three biopolymers present a higher ultimate tensile strength than PP, the industry reference. With a tangent modulus close to 4.0 GPa, PLA and PHA have similar stiffness and significantly higher than PP (1.4 ± 0.2 GPa). On the other hand, PBS is less stiff than the others with Young's modulus of only 0.8 ± 0.1 GPa, but it exhibits a strain at failure three times higher than PP.

Interestingly, at the biocomposite scale (Figure 5-2.b)), differences in mechanical properties are much less pronounced than for the virgin polymers, highlighting that the fibre substantially modulates the mechanical properties. Indeed, all composites exhibit tensile strengths and Young's moduli at the same order of magnitude. Flax/PLA is the stiffest formulation (13.2 ± 1.3 GPa), followed by flax/PHA (10.3 ±

1.5 GPa). Flax/PP and flax/PBS present a similar modulus of 8.2 ± 0.7 MPa and 7.3 ± 1.2 GPa, respectively. Thus, even though virgin PBS has a different mechanical behaviour (e.g. lower stiffness, higher failure strain) than the other polymers, the stiffness of flax/PBS is comparable in magnitude to the other formulations.

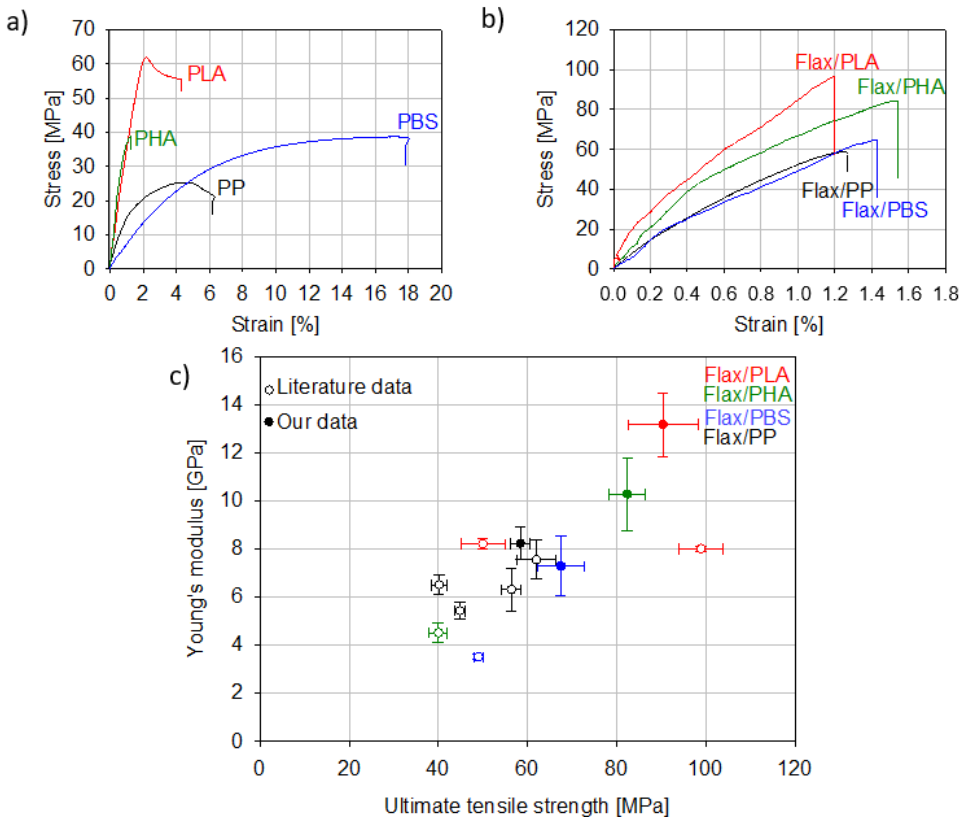

Figure 5-2: Mechanical behaviour of a) virgin polymers used in the biocomposites manufacturing, and b) flax non-woven composites at a fibre volume fraction of 30%. The axes scales are different in a) and b). c) A comparison with literature data (unfilled circles) is presented. References for literature values are available in Table 5-4.

It indicates that the increase in stiffness of the polymer upon flax fibre incorporation, at the same fibre volume fraction, is more pronounced for flax/PBS than for flax/PLA with a modulus change of +867% and +250%, respectively. This substantial stiffness 'leap' between virgin and fibre reinforced PBS has been shown in injected parts [42]. In the present work, all biocomposites have the same fibre volume fraction (30 ± 1%), void volume fraction (< 2%) and are made from the same flax non-woven preform architecture. However, in addition to fibre morphology, the quality of the interface between fibre and matrix is preponderant to ensure efficient stress transfer. Non-polar PP is known to have poor interfacial compatibility with polar plant fibres [124], which penalizes the mechanical properties of the non-woven flax/PP composite. The ultimate tensile strength ranking is similar to the stiffness, with the strength of flax/PBS (67.5 ± 5.3 MPa) being slightly better than flax/PP (58.4 ± 2.1 MPa).

Table 5-3: Mechanical properties of polymers and non-woven composites before any degradation. 'Change' refers to the improvement between raw polymer and non-woven flax composite with a fibre volume fraction of 30%.

Materials	Tangent Modulus [GPa]	Maximum Strength [MPa]	Strain at Maximum strength [%]
PLA	3.79 ± 0.14	61.4 ± 0.8	2.0 ± 0.1
PLA/Flax	13.16 ± 1.32	90.4 ± 7.8	1.0 ± 0.1
Change	+ 250 %	+ 47 %	- 49 %
PHA	4.39 ± 0.34	38.6 ± 1.4	1.3 ± 0.1
PHA/Flax	10.27 ± 1.52	82.4 ± 4.1	1.5 ± 0.2
Change	+ 134 %	+ 113 %	+ 12 %
PBS	0.75 ± 0.09	39.1 ± 0.5	14.7 ± 5.4
PBS/Flax	7.27 ± 1.23	67.5 ± 5.3	1.4 ± 0.3
Change	+ 867 %	+ 73%	- 91 %
PP	1.42 ± 0.24	24.4 ± 0.8	4.3 ± 0.7
PP/Flax	8.22 ± 0.67	58.4 ± 2.1	1.2 ± 0.1
Change	+ 480 %	+ 58%	- 73 %

Mechanical data obtained are similar to the ones found in the literature for PP, Figure 5-2.c), which confirms the conformity of our manufacturing process and the resulting composites [47,174,343]. Regarding the mechanical properties of our biocomposites, they are higher than the composites produced in literature studies [43,294] (Table 5-4). It is due to the quality of the preform, and the optimized manufacturing process used, yielding porosity lower than 2% - determined via microtomography. Here, we emphasize that the three flax/bioplastics investigated are, mechanically speaking, credible and promising alternatives to flax/PP composites.

Table 5-4: Comparison with literature study results on mechanical properties of biocomposite made with non-woven flax fibres

Materials	Fibre volume fraction [%]	Tangent Modulus [GPa]	Maximum Strength [MPa]	Reference
PLA/Flax	30	13.2 ± 1.3	90.4 ± 7.8	This study
	30	8.0 ± 0.1	99.0 ± 5.0	[43]
	36	8.2 ± 0.2	50.0 ± 5.0	[294]
PHA/Flax	30	10.3 ± 1.5	82.4 ± 4.1	This study
	30	4.5 ± 0.4	40.0 ± 2.0	[43]
PBS/Flax	30	7.3 ± 1.2	67.5 ± 5.3	This study
	30	3.5 ± 0.1	49.0 ± 1.0	[43]
PP/Flax	30	8.2 ± 0.7	58.4 ± 2.1	This study
	34	7.6 ± 0.8	62.0 ± 4.3	[47]
	36	5.4 ± 0.3	44.9 ± 1.1	[174]
	38	6.5 ± 0.4	40.2 ± 1.7	[297]
	38	6.3 ± 0.9	56.4 ± 2.2	[297]

III.b. Ageing analysis

b.i. Surface erosion

In this study, garden compost is chosen as a harsh environment for the ageing and degradation study. Figure 5-3 shows the evolution in weight loss for each composite, compared to their virgin polymer. SEM micrographs further depict the degree of surface erosion of the composite during ageing. It is evident that at any given time and for any considered polymer, flax composites degrade more (i.e. more weight loss) than the virgin polymer. It is mainly due to flax degradation inside the composite and the surface erosion induced by flax. Indeed, flax/PP shows a weight loss of 5.75 ± 0.50% after 190 days, even though virgin PP does not measurably degrade in this time scale.

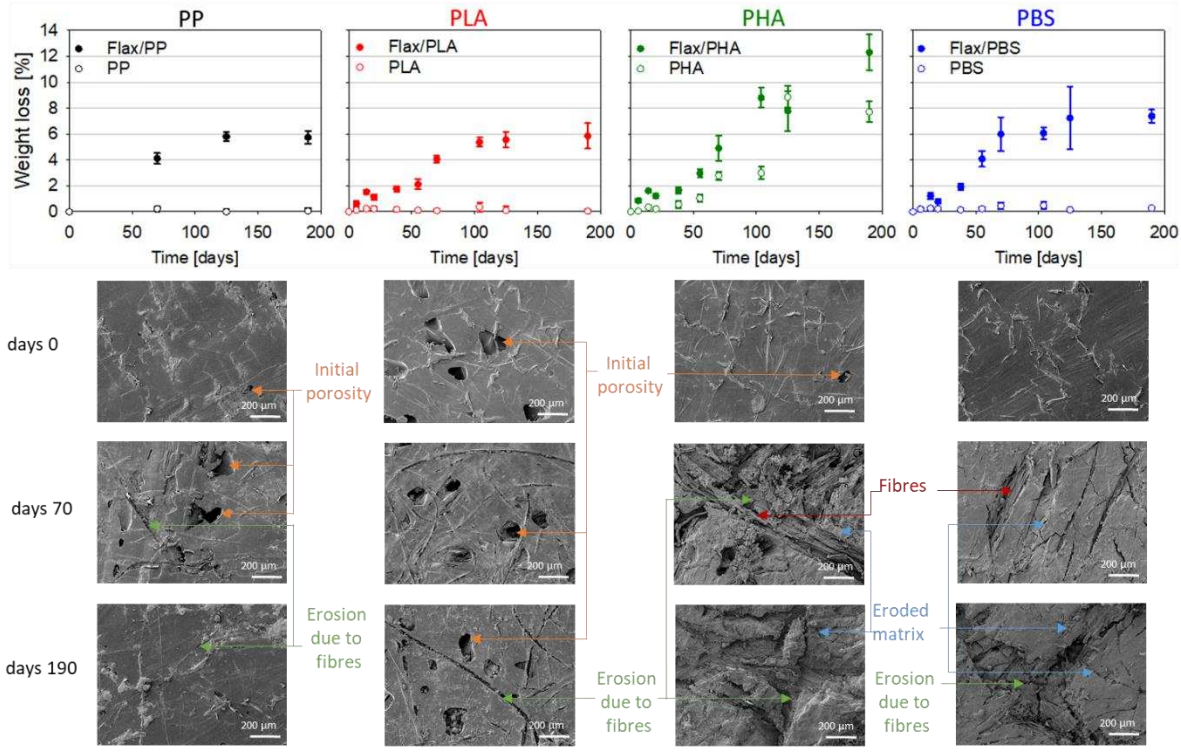

Figure 5-3: Comparison of weight loss for each composite and associated virgin polymer. SEM pictures are presented for key periods to depict surface degradation of the biocomposites.

As observed in Figure 5-3, flax/PLA and flax/PP have similar weight loss evolution. For both formulations, SEM observations at 70 and 190 days (Figure 5-3) reveal no matrix erosion and only slight surface erosion due to the degradation of flax. As the compost temperature remains below 37.5°C after ten days, PLA is handicapped at the lower compost temperature.

Indeed, PLA has to be close to its glass transition temperature for speeded degradation [49]. In an in-vessel compost maintained at 80 ± 5°C, the loss of weight of unidirectional kenaf/PLA reached 40% in

only 28 days [344], whereas our flax/PLA biocomposite buried in garden compost, with fluctuating temperatures between 8°C and 37.5°C after ten days, loses 6% of its weight after 190 days. This temperature influence is lower for the PHA and the PBS as they have low glass transition temperatures of 0°C and -30°C, respectively. With the emergence of porosity, degradation of fibres and increased roughness, flax/PHA and flax/PBS both undergo surface erosion and polymer degradation (Figure 5-3). Furthermore, their weight decreased more than flax/PP; 12.3 ± 1.4% for flax/PHA and 7.4 ± 0.5% for flax/PBS, compared to 5.75 ± 0.5% for flax/PP after 190 days. While virgin PBS's degradation is very low, flax/PBS degradation is higher than flax/PP.

Two potential explanations are easier degradation of flax in PBS than in PP and the presence of flax promoting PBS to degrade, for example, by increasing the surface contact area between water and PBS. The second explanation has been used to explain flax/PLA degradation in an elevated temperature compost [242]. On the other hand, the high value for flax/PHA is mainly explained by the degradation of virgin PHA, which is significant: 7.7 ± 0.8% after 190 days. Consequently, flax/PHA shows a substantially eroded surface than the other biocomposites [345].

What are the main mechanisms in biopolymer degradation? Hydrolysis needs to take place to reduce polymer chain size and degrade a polymer [7]. On the other hand, PLA undergoes bulk erosion as hydrolysis occurs in the volume after the water diffuses throughout the specimen [14]. Regarding PBS, some studies have noted surface erosion [346], while others have observed the same behaviour as for PLA [55]. For example, Wu et al. [51] observed a decrease in molecular weight during PBS degradation in compost at 30°C, indicating that it undergoes bulk degradation. However, these mechanisms compete, and many factors can influence which one is dominant [14,56], including the thickness of the sample [57].

b.ii. Flax fibres and matrix decohesion

This difference in polymer degradation behaviour could influence the way degradation occurs in the biocomposites. Thus, it is interesting to compare the biocomposites' surface erosion, which is the main contributor to weight evolution, with the evolution in porosity measured by microtomography (Figure 5-4). We observe that flax/PBS and flax/PHA do not show an apparent increase in porosity even though they present eroded surfaces. Interestingly, flax/PLA does not show notable surface erosion but does undergo a substantial increase in porosity, starting at 2.1% and reaching 5.2% after 190 days. This phenomenon is also observed on the industry reference, flax/PP, increasing from 1.5% to 2.8% in 190 days. It implies internal degradation, which was not expected based on the weight loss measurements.

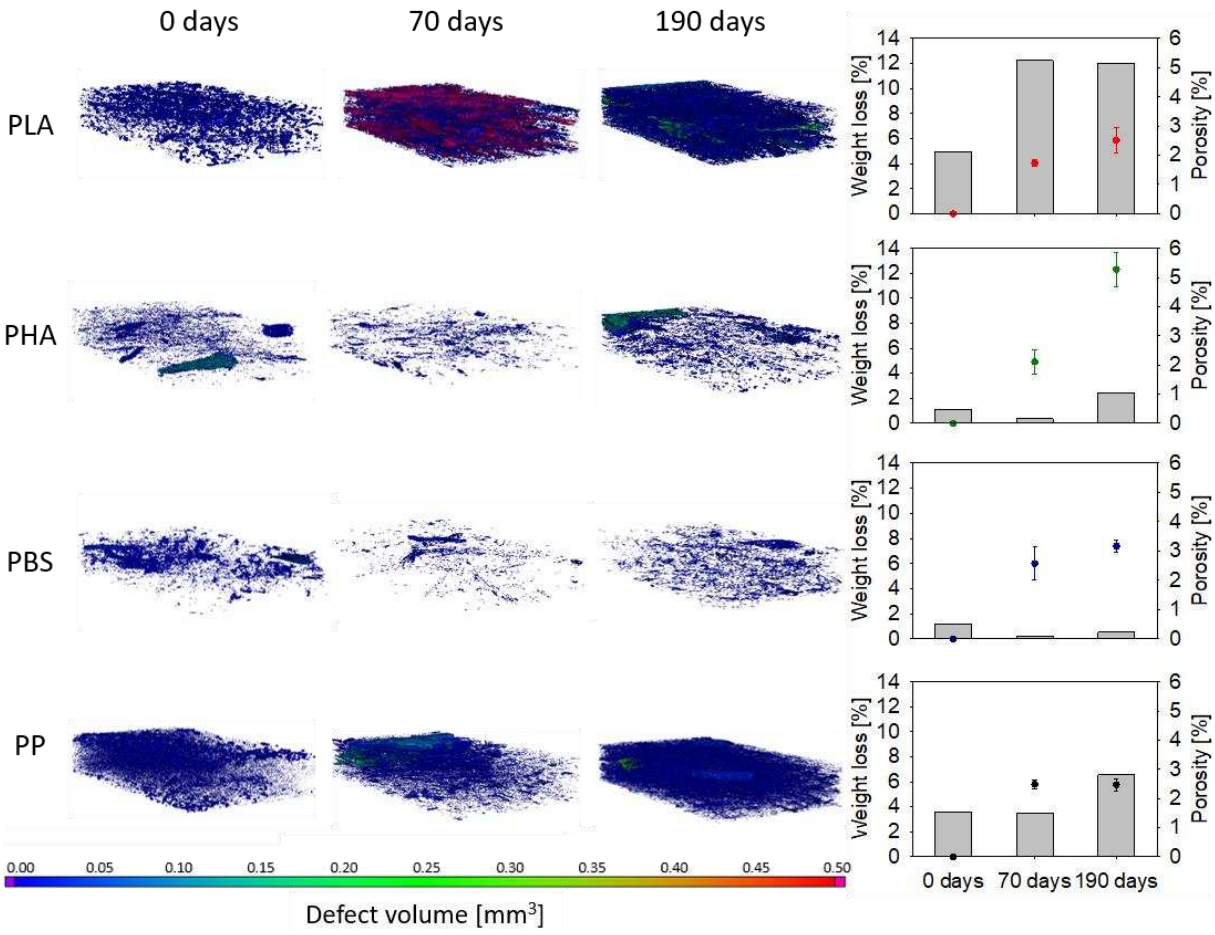

Figure 5-4: Evolution in microporosity. Observation and measurement with microtomography analysis in a sample's volume of 9x7x1.5 mm, taken in the middle of the sample. To the right, for each biocomposite, evolution in internal porosity (bars) is compared to evolution in weight loss (dots).

Looking at the shape of the pores (Figure 5-4), porosity appears to be mainly present at the interface between the matrix and flax fibres. The phenomenon responsible for this interface degradation could be the swelling of flax fibres in the composite, which is an anisotropic hygroscopic expansion [347,348], coupled with the plasticizing (deformation) of the matrix. As the polymer undergoes a lower hygroscopic expansion, internal stress is generated at the interface. This stress could be large enough to damage the interface permanently with micro-cracks or debonding [227,235,349]. Interestingly, this phenomenon is mainly present for flax/PLA. It is probably due to its glass transition temperature, which is higher than the compost temperature. This is not the case for the other polymers investigated. PLA is damaged because of the stress applied by the swelling, whereas other biopolymers only undergo a reversible deformation with no impact on the interface. It is known that the interface between flax fibre and PP is poor [124]. Thus, the swelling effect impacts this interface even though PP has a lower glass transition temperature than the compost. Another explanation is the enzymatic degradation of

residual pectic components at fibre's surface induced by microorganisms in the compost, which deteriorates the fibre/polymer interface [234].

b.iii. Impact on composite mechanical properties

In composite science, it is well known that the interface is a critical zone for stress transfer between the polymer and the fibres. Thus, the presence of porosity at the interface will significantly impact the mechanical properties of a composite. Figure 5-5 presents the evolution of the normalized ultimate strength during the ageing of the composites, and SEM micrographs illustrate changes in the flax/polymer interface; see Table 5-5 for all mechanical data during ageing. The compost temperature and external weather (mean temperature and rainfall) are plotted to inform our discussion of the results. Note that the temperature evolution of our compost is typical for this kind of compost [247–249].

Table 5-5: Evolution in ultimate strength and normalized ultimate strength for composite during ageing.

Days in compost	PLA/Flax	PHA/Flax	PBS/Flax	PP/Flax
Initial tensile strength [MPa]				
0 days	90.4 ± 7.8	82.4 ± 4.1	67.5 ± 5.3	58.4 ± 2.1
Normalized strength [-]				
0 days	1	1	1	1
6 days	0.63 ± 0.03	0.76 ± 0.04	0.93 ± 0.03	/
14 days	0.61 ± 0.05	0.74 ± 0.02	0.84 ± 0.04	/
20 days	0.64 ± 0.05	0.78 ± 0.04	0.89 ± 0.05	/
38 days	0.68 ± 0.03	0.78 ± 0.04	0.81 ± 0.05	/
55 days	0.69 ± 0.04	0.67 ± 0.04	0.71 ± 0.05	/
70 days	0.38 ± 0.03	0.60 ± 0.03	0.71 ± 0.03	0.61 ± 0.03
104 days	0.39 ± 0.04	0.55 ± 0.03	0.68 ± 0.04	/
125 days	0.49 ± 0.04	0.55 ± 0.05	0.58 ± 0.09	0.57 ± 0.03
190 days	0.52 ± 0.03	0.53 ± 0.05	0.56 ± 0.05	0.59 ± 0.03

First of all, a significant drop in ultimate strength from 90.4 ± 7.8 MPa to 56.6 ± 2.5 MPa is observed for flax/PLA. This drop of 37% could be directly related to interface deterioration, where porosity between flax fibres and PLA matrix appears after only six days. A drop of 24% is also observed for the flax/PHA during that time period, whereas a slight reduction in strength is evident for flax/PBS.

As discussed before, this observation may have several explanations and especially the high compost temperature of 58.5°C (Figure 5-5) at the beginning of the experiments, approaching the PLA's glass transition temperature of 61.2°C [335]. It increases chain mobility inducing higher deformation due to flaw swelling. That could also lead to recrystallization, inducing a shrinking of PLA and generate porosity.

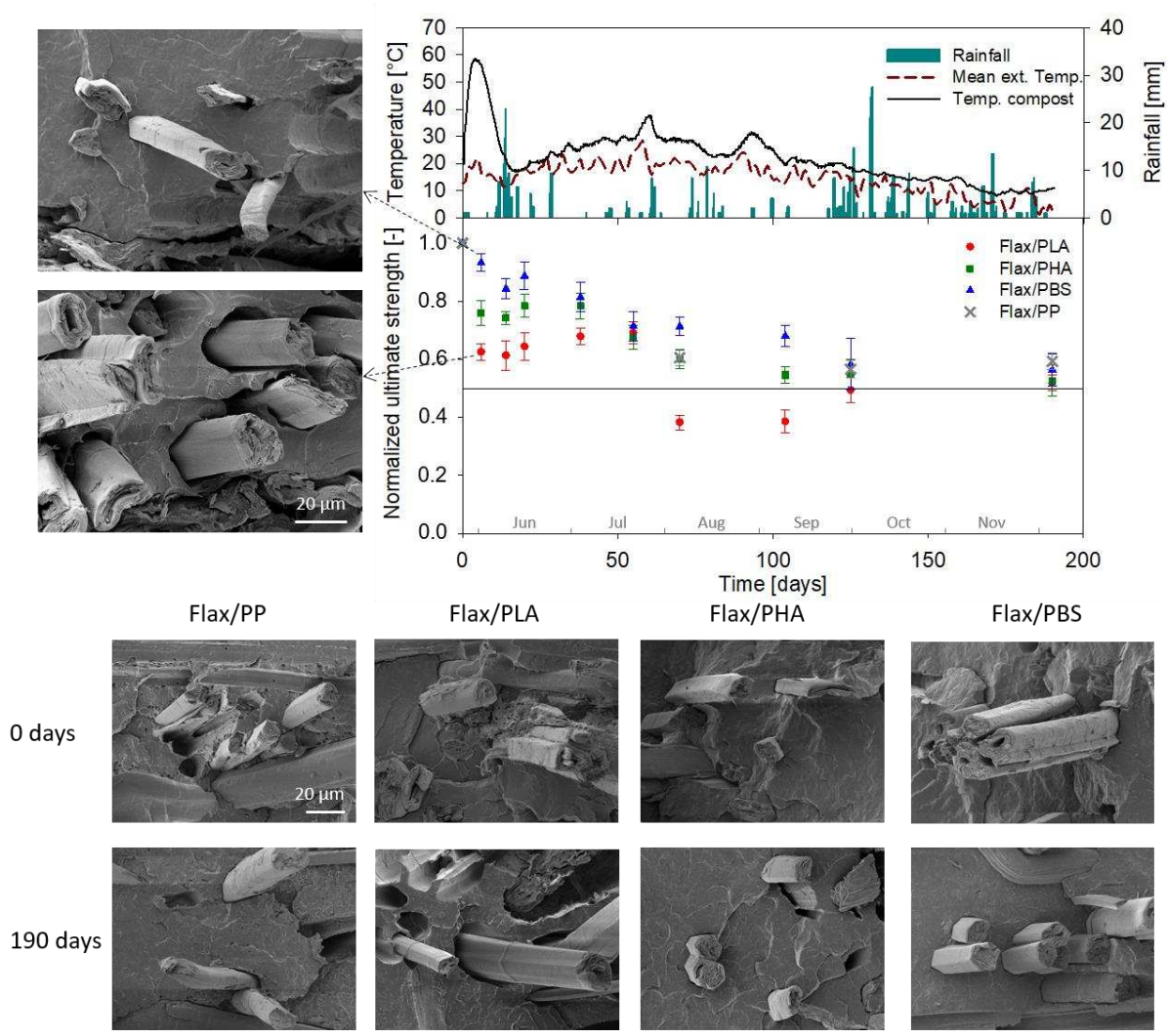

Figure 5-5: Normalized ultimate strength evolution for the three biocomposites and the industry reference. The horizontal line depicts the design service strength limit of 50%. At the top right: Compost temperature, average outdoor temperature and rainfall are plotted on a graph to discuss the results. After 20 days, the compost's temperature follows the external temperature. Top left: Cryo-SEM observation of the interface after six days of composting for flax/PBS (top) for which slight debonding is observed and for flax/PLA (bottom), which undergoes significant debonding. Bottom: Cryo-SEM observations of the evolution (from 0 days to 190 days) of the flax/polymer interface for each composite, focusing on the debonding zone.

As this strength drop occurs after only six days, the hypothesis of polymer degradation at the interface seems quite doubtful. In contrast, the creation of porosity has been observed in flax/PLA aged in seawater, meaning the swelling and/or shrinking scenario is more probable [234]. After this initial drop, flax/PLA's and flax/PHA's ultimate strength stays constant until 55 days, corresponding to our increased weight loss rate observations. Then, flax/PLA undergoes a further drop, retaining only 38% of its initial strength and falling below the 50% initial strength, which can be considered the acceptable service limit stress. On the other hand, flax/PHA undergoes a constant decrease after this point.

Remarkably, the ultimate strength of flax/PBS decreases constantly. Composite mechanical properties are mainly influenced by fibre properties and interface quality in this case. As the flax/PBS interface is only slightly impacted by ageing, and considering that the virgin PBS's mechanical properties stay unchanged during ageing (Table 5-6), the decrease in ultimate strength is principally due to degradation of the fibre. In the compost, fibres are exposed to moisture, which decreases fibres' mechanical properties [234,315]. This moisture could also impact bundles as it has been shown that immersion in clear water for only 72h at 23°C degrades the middle lamella of bundles (flax/flax interface) [226]. Thus, this phenomenon leads to a poor interface between the fibres leading to decreased stress transfer capacity inside a bundle.

Table 5-6: Evolution in ultimate strength and normalized ultimate strength for virgin polymer during ageing

Days in compost	PLA	PHA	PBS	PP
Initial tensile strength [MPa]				
0 days	61.4 ± 0.8	38.6 ± 1.4	39.1 ± 0.5	24.4 ± 0.8
Normalized strength [-]				
0 days	1	1	1	1
6 days	1.00 ± 0.03	0.89 ± 0.05	0.97 ± 0.01	/
14 days	1.06 ± 0.03	0.94 ± 0.01	1.02 ± 0.02	/
20 days	1.00 ± 0.03	0.89 ± 0.02	1.01 ± 0.01	/
38 days	0.99 ± 0.02	0.89 ± 0.01	1.01 ± 0.02	/
55 days	0.94 ± 0.02	0.86 ± 0.02	0.95 ± 0.02	/
70 days	0.89 ± 0.03	0.74 ± 0.02	0.95 ± 0.03	0.94 ± 0.01
104 days	0.92 ± 0.07	0.71 ± 0.03	0.97 ± 0.03	/
125 days	0.70 ± 0.14	0.65 ± 0.03	0.99 ± 0.02	0.97 ± 0.05
190 days	0.87 ± 0.08	0.64 ± 0.05	1.00 ± 0.02	1.02 ± 0.01

After 190 days, all composites - flax/biodegradable polymer composites and the industry reference, flax/PP - have similar normalized ultimate strength close to 55%. Thus, the formulations investigated here are not only comparable in the context of unaged mechanical properties, but also the impact of ageing is comparable. What is more, even if the initial strength of flax/PLA (90.4 ± 7.7MPa) is higher than flax/PBS (68.6 ± 5.0MPa), flax/PLA falls (temporarily) below the design limit of 50% after 70 days, where flax/PBS undergoes more predictable and gradual ageing which could be preferable for long term applications. Note that all strength data presented here are slightly underestimated as the cross-section area is overestimated due to the surface modification and the roughness of degraded samples such as flax/PHA and flax/PBS.

b.iv. Impact on flax fibres in the composite

It is also possible that microorganisms present in the compost play a role in degrading the fibre. It is assessed through an AFM investigation of a flax/PLA sample after 125 days spent in compost. Three stages of fibre degradation are identified, for which results are shown in Figure 5-6.

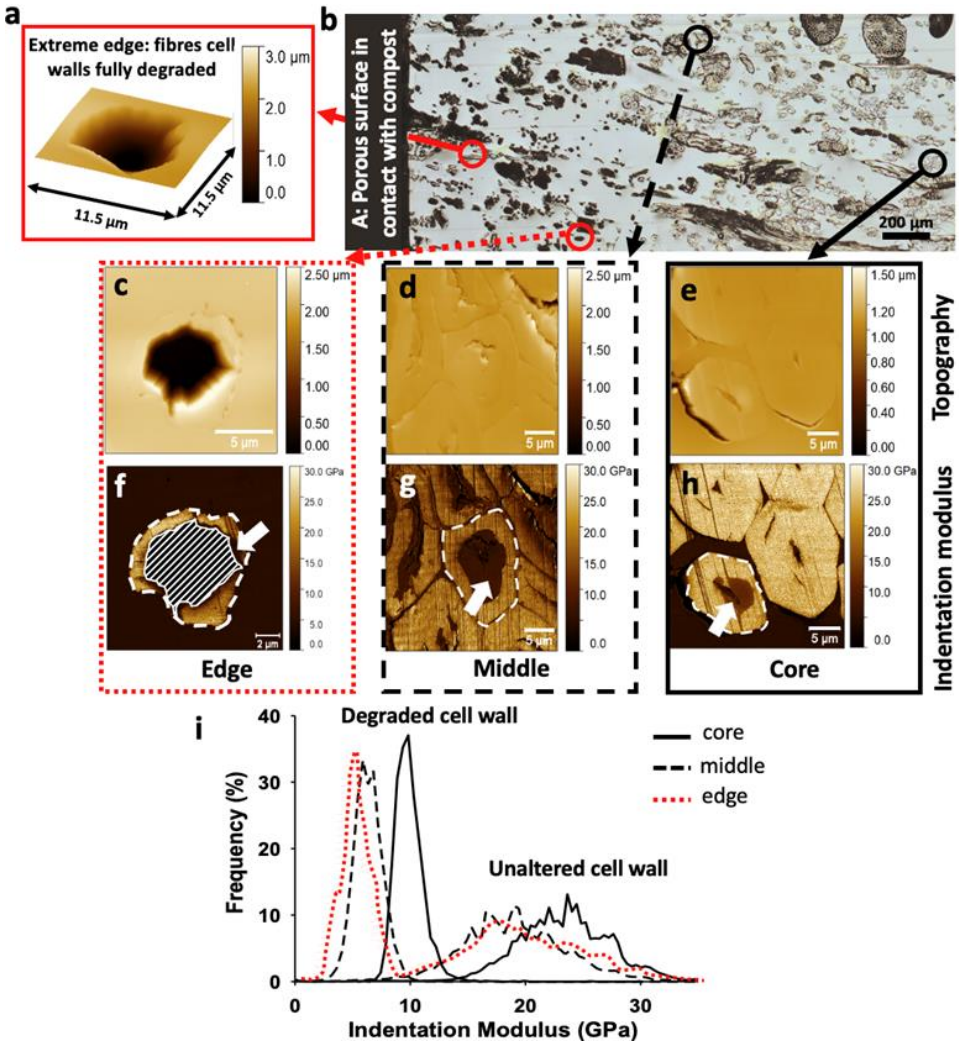

Figure 5-6: AFM investigation of flax/PLA composite after 125 days in compost, a) 3D AFM topographic image of a fully degraded fibre, located at the extreme edge of the sample; b) Face C investigated through AFM-PF-QNM; black and red circles indicate the fibres selected for AFM measurements; (c), (d) and (e) are AFM topographic images of edge, middle and core areas, respectively and (f), (g) and (h) the corresponding indentation modulus maps. (i) shows the indentation modulus distribution for each investigated region, indicated in white dot lines in (f), (g) and (h); In (f), no data was recorded in the hatched area.

After 125 days in compost, some fibres were found to be still intact (Figure 5-6.b), .e) and .h)) and with an indentation modulus around 18-23 GPa, in line with indentation moduli generally found for flax fibres recorded in other papers by AFM or nanoindentation [322]. Nevertheless, one can notice a

beginning of degradation in these fibres located in the core of the sample, with low indentation modulus area around the lumen (Figure 5-6. H)), inducing a bimodal distribution of indentation modulus (Figure 5-6.i)) with two prominent peaks around 23 and 10 GPa. A progressive degradation, with first an attack of more labile polymers, such as hemicelluloses and pectins, can be hypothesized. It should be considered that the section investigated in this work represents only a slice of the whole sample. Fibres and fibre bundles at different planes can be more or less degraded than the one investigated, as was demonstrated by Björdal et al. [350] thanks to tomographic analysis.

Fibres investigated in the middle region of the sample show more pronounced decay than those in the core, with an increase of the degraded area from the lumen region. More precisely, the mechanical properties of the second wall decreased considerably (around 5-7 GPa) in the degraded regions (Figure 5-6.g) and Figure 5-6.i)). However, a part of the secondary wall still appeared intact with stiffness around 18 GPa (Figure 5-6.i)). The third step of fibre decay, mainly observed for fibres located at the edge of the biocomposite sample, consists of the complete degradation of the cell wall fragments until only one cavity remains. Despite the advanced state of degradation of the whole cell, S1 and the last parts of the second cell wall seemed to be partially preserved (Figure 5-6.f)) at the periphery of the fibre. However, cell walls are fully degraded when fibre located at the extreme edge of the sample is considered (Figure 5-6.a)).

The progressive decrease in indentation modulus observed here, from the lumen to fibre periphery, is linked to the severity of the biological attack. In Figure 5-6.g), one can note that fibres investigated in the middle of the biocomposite lose their mechanical properties following the fibre shape, confirming that the second cell wall of flax is easily degraded; in the present case, cell wall degradation is probably initiated by structural hemicelluloses, less recalcitrant than crystalline cellulose. Reducing efficient fibres proportion due to microorganism degradation adds another degrading phenomenon that plays an essential role in decreasing composite properties.

IV. Conclusion

The mechanical performance and compost ageing behaviour of three biocomposites made of non-woven flax fabrics and biodegradable polymers (flax/PLA, flax/PHA, flax/PBS) were investigated and compared to flax/PP, an industry reference. We showed that all flax/biodegradable polymer composites had better strength and stiffness than flax/PP. Our ageing investigations reveal that flax composites degrade predominantly through one of two possible routes, depending on the composite formulation (i.e. polymer selected): surface erosion or porosity generation at fibre/matrix interfaces. While surface erosion diminishes composite mass, interfacial porosity substantially reduces composite

ultimate tensile strength, making the ageing behaviour less predictable. We observe that flax/PLA primarily degrades at the interface, with localized porosity forming and reducing its strength by 37% after just six days of burial in garden compost. In contrast, due to surface degradation of fibres and polymer, flax/PHA losses 12.3 ± 1.4% mass after 190 days. We find that all the flax/biodegradable polymer biocomposites have lost 50% of their initial strength after 190 days in the garden compost, comparable to the industry reference flax/PP. These flax/biodegradable polymer biocomposites have the potential to resolve the 'biodegradation paradox': they can be designed to have adequate mechanical performance for industrial products, even after ageing in harsh conditions, and yet offer biodegradation as an alternative end-of-life disposal route to incineration.

General conclusions and perspectives

I. Conclusions and perspectives

This thesis aimed to explore the potential of three biodegradable thermoplastics to be reinforced by flax fibres: poly-(lactide) (PLA), poly-(butylene-succinate) (PBS) and poly-(hydroxy alkanoates) (PHA). The potential use of the resulting composites for various applications can be investigated through various material properties. This study first focused on relating composite architecture and static mechanical properties. Second, understanding the ageing behaviour of biodegradable composites was explored, and specifically how composite architectures (and dominating ageing mechanisms) influence mechanical property over time. The work was split into two parts; the first one (chapters 2 and 3) characterised the mechanical properties and the structure of biodegradable flax composites. The second one (chapters 4 and 5) is dedicated to the composite's structural and mechanical property evolution due to ageing.

Before presenting experimental results, **chapter 1** dealt with literature to highlight some crucial notions for the understanding of this thesis work, going from the biodegradation notion to the environmental impact of flax thermoplastic composite; a bibliographic assessment of methods of interface characterisation, manufacturing processes of flax thermoplastic composites and the link between interface and mechanical properties of a laminate composite was addressed.

In **chapter 2**, the interface between elementary flax fibres and biodegradable polymers was investigated through micro-droplet tests. It appears that PLA presents the highest affinity with flax, followed by PHA and PBS having a similar adherence with flax as MAPP. All the biodegradable thermoplastics present higher mechanical properties than PP, chosen with MAPP as an industrial reference. This demonstrates the ability of these biodegradable polymers to be reinforced by flax fibres to produce performing transport materials.

Complementary to this, the mechanical properties of unidirectional composites are investigated and correlated to interface properties. Composite properties (in-plane shear strength/longitudinal tensile strength/transversal tensile strength) follow the same trends with comparable properties between PHA, PBS or MAPP composite, and higher performance for PLA and lower for PP. The composite properties correlate linearly with the flax/matrix adherence (measured through in-plane shear strength and transversal tensile strength). The introduction of an effective coefficient in the rule of

mixtures took account of the influence of interface shear strength on longitudinal tensile strength. This coefficient increases monotonously with interfacial-shear strength of the flax/matrix interface, except for PBS. This exception is explained by the high strain at failure of the PBS, spreading the applied stress in the composite and avoiding high-stress concentration. Thanks to their good adherence to flax, which is reflected at the composite level, the biodegradable polymers appear suitable for flax composite application.

To complete the interface study, observing the decohesion of a polymer micro-droplet in-situ (through a camera) could be interesting. It will give more information on the decohesion process, possibly shining more light on the stress concentration (e.g. through DIC) induced by this test. Additionally, some loading and unloading micro-droplet tests can be interesting to investigate the damage progression of the interface during the test. That will lead to a better understanding of the adherence between the flax and polymers.

Another finding requiring more investigation is the general potential of PBS in spreading the stress applied in the composite, leading to efficient flax unidirectional composites. Some fatigue behaviour should give clues on this phenomenon, as well-distributed stress should create less internal damage. Micro X-ray tomography, using synchrotron, should allow observing the influence of tensile behaviour on the structural evolution of the composite, such as the initiation and growing of micro cracks. Comparing PLA and PHA flax composites will add values to the investigations, confirming that PBS flax composite presents better resilience than PLA and PHA flax composite.

In **chapter 3**, the flax/PLA non-woven composite structure is better understood by analysing porosity, shive content, and fibre orientation. The porosity content was measured at 5.5 %. Thanks to a deeper porosity analysis done by X-ray micro-tomography, the size distribution and the localisation of the pores were observed. Mesoporosity is present in the matrix, induced by the manufacturing process. The second class of pore is microporosity, which is principally present in bundles area or inside shives. The presence of such microporosity in shives raises the question of this third component in the fibre-matrix composite. However, shives represent a volume fraction of 2.2% in the composite against 43.1% for flax fibres. Therefore, it was chosen to neglect their effects on mechanical properties. The last structural parameter investigated was fibre orientation. Thanks to X-ray micro-tomographic analysis, a preferential fibre orientation was observed in the machine direction of the non-woven composite. This method is efficient but does not fit industrial criteria in terms of speed and cost. Parallel to this, off-axis tensile tests were conducted and highlight mechanical anisotropy. This anisotropy appears to match the fibre orientation observed by tomography. The structure of a non-woven composite is

complex with the presence of porosity, shives and fibres orientations. However, porosity can be managed through the immersion test, shives can be ignored if present in small proportion, and fibre orientations could be approximate thanks to off-axis tensile tests, allowing a first structural description of a non-woven composite in relation to its mechanical behaviour.

In this study, the presence of shives was considered negligible as they were found in a relatively small fraction. However, it could be attractive to understand better their influence on the mechanical properties of the composite. Introducing shives deliberately to obtain a range of non-woven composites can be a way to obtain the critical shives fraction not to overcome to keep the mechanical properties of the composite well-predicted and reliable. That can be of industry interest as shives are cheaper than flax but present some reinforcing potential. During this test, it would be essential to keep the proportion of reinforcement constant (flax fibres + shives) to obtain comparable results.

Another industrial perspective is to control the fibre orientation to develop non-wovens with more aligned fibres orientations. Thanks to the suggested off-axis tensile test as a rapid fibre orientation analysis tool, the quality assessment of developed products can be faster and cheaper. A machine parameter investigation is now required to optimise the fibre orientation. Various highly oriented non-woven preforms will close the market gap between non-woven and unidirectional flax preform in terms of mechanical properties and price.

Thanks to these first chapters, the mechanical and structural properties of flax/biodegradable polymers were investigated and carefully addressed. The other chapters deal with the ageing of such composites and the evolution in structure and mechanical properties. In **chapter 4**, flax/PLA non-woven composites were submitted to hygroscopic (50RH/75RH/98RH/immersion) ageing for six weeks. By following their mass evolution, the moisture content of the composites was measured. For the 50RH and 75RH samples, the maximum water content measured is closed, being 2.7% and 2.9%. As a reference, the initial water content of the samples is 2.6%. The 98RH and immersion conditions induce a critical moisture content of 8.8% and 15.1%, respectively. These later samples undergo irreversible structural and mechanical modification, not observed for the 50RH and 75RH ageing. It highlights a critical relative humidity condition below which the composite is not impacted by ageing. The ageing mechanism of the composite was further studied through microscale investigation. The flax fibres and the matrix appears to present unchanged mechanical properties, highlighting the role of composite's structure modification on the decrease of its mechanical properties. For both impacted samples, the interface could be impacted due to flax swelling and chemical modification. However, no physical decohesion was observed. Nevertheless, transverse microcracks appear in the matrix,

initiated at flax fibres location. An analytical model was used to confirm the ability of flax fibres to induced these microcracks. Their swelling can generate local stresses three times higher than the strength of PLA. Additionally, this fibre swelling appears to be responsible for surface erosion.

Using shorter sampling intervals for the humidity ageing study (e.g. tests at 90%,80%, 70%RH) will help determine the critical relative humidity below which irreversible changes in composite properties occur. Furthermore, more fibre volume fractions should be investigated, giving additional clues on the degradation mechanism. A quantification and localisation analysis of the porosity through X-ray micro-tomography can quantify the impact of ageing and confirm the hypothesis of a swelling originated phenomenon. Additionally, observing in-situ water immersion under micro-tomography can help understand the path water took inside the composite.

Furthermore, investigating the hygroscopic ageing of PHA and PBS flax composites is of interest. Especially in the case of PBS to confirm the hypothesis that its low stiffness allows a better ageing resistance as the flax fibres' swelling will induce smaller critical stress. Furthermore, the geometry evolution analysis of the matrix and the flax composite through various moisture ageing can lead to a hygro-expansion investigation, another clue of the damage mechanism for flax fibres composites. Finally, the thesis studied the irreversible impact of one sorption/desorption cycle. It could be interesting to do several cycles, as it is a more realistic solicitation, to highlight irreversible changes induced and comparing them to one cycle damages.

The last investigation of this thesis (**chapter 5**) aims to understand the ageing of biodegradable flax composite on garden compost. This harsh ageing environment was chosen arbitrarily. Thus, non-woven flax composites made of PLA, PHA, PBS or PP were buried in garden compost for six months. Before the ageing step, their mechanical properties were compared, ensuring the biodegradable non-woven composites are an alternative to the industry reference. Thanks to this harsh ageing, two degradation behaviours were highlighted, depending on the matrix. For the PLA and PP, bulk degradation was observed through an increase in inner porosity, mainly at the flax/matrix interface. It induces a sudden drop in composite strength at an early stage due to interface degradation. For PBS, the degradation appeared on the surface, inducing a higher loss of weight than the bulk degradation but no increase in inner porosity. Interestingly, it leads to a more predictable mechanical evolution as the interface is less impacted. In addition, AFM Peafkforce investigation evidenced a decrease in flax cell wall mechanical properties, contributing to the drop in composite strength. These two behaviours are models and compete in natural degradation. For PHA, surface erosion is predominant, but a slight decohesion at the interface is present, inducing a slight strength drop at the early ageing stage.

Remarkably, ageing damages the biodegradable composite as much as the industrial reference, showing the former's potential even in harsh ageing.

In complement to this study, the flax fibre degradation mechanism in a composite buried in compost should be deeply investigated to understand how microorganisms are responsible for this degradation. That can help to develop scientific strategies to control or anticipate the degradation of the composite. Additionally, this thesis focuses on the degradation mechanism, which is of interest regarding the in-service lifetime. However, biodegradable tests in several environments will bring complementary information on these biodegradable composites. Ecotoxicity tests must be carried out to ensure the viability of the biodegradable composite solution suggested in this thesis. Furthermore, reliable LCA will be useful to compare the environmental benefit of biodegradable flax composite. Thus, it will give clues to develop the adapted disposal scenario for biodegradable flax composites in the future.

II. General discussion

Thanks to all these investigations, PLA, PHA and PBS appear suitable to be reinforced by flax fibres to obtain biodegradable composites. They present mechanical properties adequate for structural application, and these properties remain acceptable even under harsh environments. Thus, these materials fulfil the challenging paradox of maintaining good mechanical properties over their service lifetime until biodegradation upon disposal.

Focussing on the work presented, the flax/PLA appears to have the highest mechanical properties, close to flax/thermoset composites. However, an important notion to come back to is biodegradation. PLA, and so its flax composite, is only biodegradable in industrial compost, where PBS can be bioassimiled in home compost and PHA in seawater (according to standard). It highlights the presence of a compromise between the virgin composite mechanical properties and its biodegradation potential. Therefore, flax/PLA is not necessarily the best solution to obtain a biodegradable flax composite. Attention must be paid to its end of life and communication towards customers and consumers.

Furthermore, the kinetics of biodegradation of polymers is faster (in an adequate environment) than flax fibres. Indeed, flax fibres (and generally plants) did not match the biodegradation standards developed for biodegradable polymers. Thus, the development of new polymer formulations, with the kinetics of biodegradation equals to the flax fibres, could be a way to optimise the time in service of biodegradable flax composites.

However, focussing only on the mechanical properties, the ageing of samples and its biodegradation potential is not enough to validate such materials for industry.

First, there is the question of the size effects. How could the ageing mechanism predict the lifetime of industrial pieces, taking into account the sealed or open edges, the kinetics of diffusion, or the geometry of the piece? A deep understanding of all the mechanisms involved and their coupling effects should allow the development of complex but acquired models, helpful for industries.

Another critical point is the cost disadvantage of biodegradable flax composites. In industry, and especially in the transportation sector, PP composites are ubiquitous. This polymer has a price of 1€/kg, against 3-4 €/kg for PLA or PBS and 10 €/kg for PHA. It appears to be the principal limit for the use of biodegradable flax composite nowadays, especially for automotive applications where the price of each part tends to be reduced. This price difference could decrease in the future due to the conjugated increasing demand for biodegradable polymer associated with the increasing maturity of industrial production and the decrease in fossil resources.

Appendices

Appendix 1: Nairn's model

This is a rewriting of the model developed by Nairn in 1985 [323], considering only the part used in the thesis.

Thermoelastic Analysis of Residual Stresses in *Unidirectional, High-Performance Composites*

JOHN A. NAIRN
Central Research and Development Department
E. I. DuPont de Nemours & Company
Experimental Station
***Wilmington, Delaware** 19898*

COMPOSITE CYLINDER MODEL:

In this section, the method of solving for thermal stresses in the composite cylinder model is outlined. The composite cylinder model, illustrated in Figure A.1, includes a matrix and a fibre. We assume that the matrix is linearly elastic and isotropic and that the fibre is linearly elastic and transversely isotropic. The bonds between the components are assumed to be perfect.

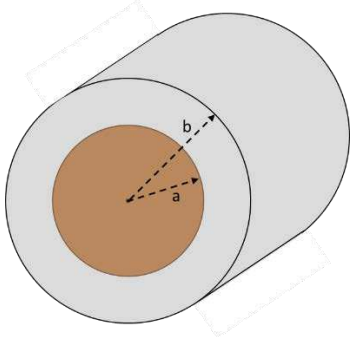

Figure A.1: Cross-section of composite cylinder model for a unidirectional composite.

We begin by writing down the form of the stresses in each component. The stresses in the matrix are taken from the general solution for an isotropic, hollow cylinder under internal pressure, external pressure, and uniform axial stress. The results are:

$$\begin{aligned} \sigma_{rm} &= A_1 + \frac{A_2}{r^2} \\ \sigma_{\theta m} &= A_1 - \frac{A_2}{r^2} \\ \sigma_{zm} &= A_3 \end{aligned} \tag{1}$$

Here r, θ, and z indicate radial, hoop, and longitudinal stresses, subscript m is for matrix, and A_1 to A_3 are constants. The stresses in the transversely isotropic fibre have the form

$$\begin{aligned} \sigma_{rf} &= A_7 \\ \sigma_{\theta f} &= A_7 \\ \sigma_{zf} &= A_8 \end{aligned} \tag{2}$$

where A_7 and A_8 are constants. The shear stresses in all three components are zero. […] The solution of the composite cylinder problem is now reduced to determining the constants A_i (i= 1,2,3,7 or 8) by using the boundary conditions. The boundary conditions for the stresses are

$$\begin{aligned} \sigma_{rm} &= 0 \ \ at\, r = b \\ \sigma_{rm} &= \sigma_{rf}\ at\, r = a \\ \sigma_{zf} &= A_8 \\ \sigma_{zm}.(b^2 - a^2) + \sigma_{zf}.a^2 &= A_8 \end{aligned} \tag{3}$$

The last condition is force balance in the z-direction. From these conditions, the problem reduces to

$$A_2 = -b^2.A_1$$
$$A_7 = A_1.\left(1 - \frac{b^2}{a^2}\right) \quad (4)$$
$$A_8 = A_3.\left(\frac{a^2 - b^2}{a^2}\right)$$

There are now two unknowns, A_1 and A_3. They are found by using the following two displacement restrictions:

$$\varepsilon_{zm} = \varepsilon_{zf} \ \ at\ r = a$$
$$u_{rm} = u_{rf} \ \ at\ r = a \quad (5)$$

where ε_z is longitudinal strain and u_r is radial displacement. With the radial symmetry in the cylinder model $u_r = r.\varepsilon_\theta$. Using the conditions in Eq (5) and the stress-strain relations for transversely isotropic and isotropic materials, the problem reduces to two equations in two unknowns:

$$A^{NI}.\begin{pmatrix} A_1 \\ A_3 \end{pmatrix} = \begin{pmatrix} (\alpha_m - \alpha_{f,L}).\Delta T \\ (\alpha_m - \alpha_{f,T}).\Delta T \end{pmatrix} \quad (6)$$

where the elements of A^{NI} are in Table A.1, Here, α is the thermal expension and ΔT is the temperature change. The latter is negative for cooling. In Table A.1, ϑ refers to the Poisson's ratio, V the volume fraction and E the modulus.

Table A.1: Elements of matrix A^{NI} in Eq (6)

Matrix Element	Expression
A_{11}^{NI}	$2.\left(\frac{\vartheta_m}{E_m} + \frac{\vartheta_{f,LT}.V_m}{E_{f,L}.V_f}\right)$
A_{12}^{NI}	$-\left(\frac{V_m}{E_{f,L}.V_f} + \frac{1}{E_m}\right)$
A_{21}^{NI}	$-\left(\frac{(1-\vartheta_{f,TL})V_m}{E_T V_f} + \frac{(1-\vartheta_m)}{E_m} + \frac{(1+\vartheta_m)}{E_m.V_f}\right)$
A_{22}^{NI}	$\left(\frac{\vartheta_m}{E_m} + \frac{\vartheta_{f,LT}.V_m}{E_{f,L}.V_f}\right)$

The rewriting of the model stops here. Some comments are following:

1) Solving the two equations in Eq (6) using $r = a$ gives the stresses generated at the fibre/matrix interface.

2) In the thesis, an analogy between thermal and hygroscopic solicitation is made by replacing the thermal-expansion coefficient and the temperature variation with the hygro-expansion coefficients and the moisture content variation, respectively.

References

[1] UN-Treaty.pdf, (n.d.). https://www.newplasticseconomy.org/assets/doc/UN-Treaty.pdf (accessed April 8, 2021).

[2] E. MacArthur, Beyond plastic waste, Science. 358 (2017) 843–843. https://doi.org/10.1126/science.aao6749.

[3] E. Elhacham, L. Ben-Uri, J. Grozovski, Y.M. Bar-On, R. Milo, Global human-made mass exceeds all living biomass, Nature. 588 (2020) 442–444. https://doi.org/10.1038/s41586-020-3010-5.

[4] EuBP_FS_What_are_bioplastics.pdf, (n.d.). https://docs.european-bioplastics.org/publications/fs/EuBP_FS_What_are_bioplastics.pdf (accessed April 8, 2021).

[5] D20 Committee, Test Methods for Determining the Biobased Content of Solid, Liquid, and Gaseous Samples Using Radiocarbon Analysis, ASTM International, n.d. https://doi.org/10.1520/D6866-20.

[6] Y. Dommergues, F. Mangenot, Ecologie microbienne du sol, Masson, 1970.

[7] N. Lucas, C. Bienaime, C. Belloy, M. Queneudec, F. Silvestre, J.-E. Nava-Saucedo, Polymer biodegradation: Mechanisms and estimation techniques – A review, Chemosphere. 73 (2008) 429–442. https://doi.org/10.1016/j.chemosphere.2008.06.064.

[8] B. Laycock, M. Nikolić, J.M. Colwell, E. Gauthier, P. Halley, S. Bottle, G. George, Lifetime prediction of biodegradable polymers, Progress in Polymer Science. 71 (2017) 144–189. https://doi.org/10.1016/j.progpolymsci.2017.02.004.

[9] A.A. Shah, F. Hasan, A. Hameed, S. Ahmed, Biological degradation of plastics: A comprehensive review, Biotechnology Advances. 26 (2008) 246–265. https://doi.org/10.1016/j.biotechadv.2007.12.005.

[10] Y. Tokiwa, B.P. Calabia, Biodegradability and Biodegradation of Polyesters, J Polym Environ. 15 (2007) 259–267. https://doi.org/10.1007/s10924-007-0066-3.

[11] A. Le Duigou, P. Davies, C. Baley, Seawater ageing of flax/poly(lactic acid) biocomposites, Polymer Degradation and Stability. 94 (2009) 1151–1162. https://doi.org/10.1016/j.polymdegradstab.2009.03.025.

[12] A. Regazzi, R. Léger, S. Corn, P. Ienny, Modeling of hydrothermal aging of short flax fiber reinforced composites, Composites Part A: Applied Science and Manufacturing. 90 (2016) 559–566. https://doi.org/10.1016/j.compositesa.2016.08.011.

[13] G. Francois, B. Stéphane, D. Guillaume, F. Pascale, C. Emmanuelle, G. Jeff, G. Régis, G. Matthieu, H. Arnaud, L. Fabienne, others, Pollution des océans par les plastiques et les microplastiques Pollution of oceans by plastics and microplastics, Techniques de l'Ingenieur. (2020) BIO9300. https://archimer.ifremer.fr/doc/00663/77471/.

[14] F. von Burkersroda, L. Schedl, A. Göpferich, Why degradable polymers undergo surface erosion or bulk erosion, Biomaterials. 23 (2002) 4221–4231. https://doi.org/10.1016/S0142-9612(02)00170-9.

[15] M.T. Zumstein, A. Schintlmeister, T.F. Nelson, R. Baumgartner, D. Woebken, M. Wagner, H.-P.E. Kohler, K. McNeill, M. Sander, Biodegradation of synthetic polymers in soils: Tracking carbon into CO_2 and microbial biomass, Sci. Adv. 4 (2018) eaas9024. https://doi.org/10.1126/sciadv.aas9024.

[16] A. Dutt Tripathi, V. Paul, A. Agarwal, R. Sharma, F. Hashempour-Baltork, L. Rashidi, K. Khosravi Darani, Production of polyhydroxyalkanoates using dairy processing waste – A review, Bioresource Technology. 326 (2021) 124735. https://doi.org/10.1016/j.biortech.2021.124735.

[17] S. Chardron, S. Bruzaud, B. Lignot, A. Elain, O. Sire, Characterization of bionanocomposites based on medium chain length polyhydroxyalkanoates synthesized by Pseudomonas oleovorans, Polymer Testing. 29 (2010) 966–971. https://doi.org/10.1016/j.polymertesting.2010.08.009.

[18] R.W. Lenz, R.H. Marchessault, Bacterial polyesters: biosynthesis, biodegradable plastics and biotechnology, Biomacromolecules. 6 (2005) 1–8. https://doi.org/10.1021/bm049700c.

[19] T.V. Ojumu, J. Yu, B.O. Solomon, Production of Polyhydroxyalkanoates, a bacterial biodegradable polymers, African Journal of Biotechnology. 3 (2004) 18–24. https://doi.org/10.4314/ajb.v3i1.14910.

[20] D. Garlotta, A Literature Review of Poly(Lactic Acid), Journal of Polymers and the Environment. 9 (2001) 63–84. https://doi.org/10.1023/A:1020200822435.

[21] J. Lunt, Large-scale production, properties and commercial applications of polylactic acid polymers, Polymer Degradation and Stability. 59 (1998) 145–152. https://doi.org/10.1016/S0141-3910(97)00148-1.

[22] R. Auras, B. Harte, S. Selke, An Overview of Polylactides as Packaging Materials, Macromolecular Bioscience. 4 (2004) 835–864. https://doi.org/10.1002/mabi.200400043.

[23] L. Avérous, Chapter 21 - Polylactic Acid: Synthesis, Properties and Applications, in: M.N. Belgacem, A. Gandini (Eds.), Monomers, Polymers and Composites from Renewable Resources, Elsevier, Amsterdam, 2008: pp. 433–450. https://doi.org/10.1016/B978-0-08-045316-3.00021-1.

[24] J. Xu, B.-H. Guo, Poly(butylene succinate) and its copolymers: Research, development and industrialization, Biotechnology Journal. 5 (2010) 1149–1163. https://doi.org/10.1002/biot.201000136.

[25] L. Sisti, G. Totaro, P. Marchese, PBS makes its entrance into the family of biobased plastics, Biodegradable and Biobased Polymers for Environmental and Biomedical Applications. 7 (2016) 225–285. https://doi.org/10.1002/9781119117360.ch7.

[26] J.S. Cooper, B.W. Vigon, Life cycle engineering guidelines, US Environmental Protection Agency, Office of Research and Development, 2001. Report 600/R-01/101.

[27] T. Keshavarz, I. Roy, Polyhydroxyalkanoates: bioplastics with a green agenda, Current Opinion in Microbiology. 13 (2010) 321–326. https://doi.org/10.1016/j.mib.2010.02.006.

[28] P.J. Barham, A. Keller, E.L. Otun, P.A. Holmes, Crystallization and morphology of a bacterial thermoplastic: poly-3-hydroxybutyrate, J Mater Sci. 19 (1984) 2781–2794. https://doi.org/10.1007/BF01026954.

[29] V. Jost, M. Schwarz, H.-C. Langowski, Investigation of the 3-hydroxyvalerate content and degree of crystallinity of P3HB-co-3HV cast films using Raman spectroscopy, Polymer. 133 (2017) 160–170. https://doi.org/10.1016/j.polymer.2017.11.026.

[30] P. Lemechko, M. Le Fellic, S. Bruzaud, Production of poly(3-hydroxybutyrate-co-3-hydroxyvalerate) using agro-industrial effluents with tunable proportion of 3-hydroxyvalerate monomer units, International Journal of Biological Macromolecules. 128 (2019) 429–434. https://doi.org/10.1016/j.ijbiomac.2019.01.170.

[31] P. Gatenholm, J. Kubát, A. Mathiasson, Biodegradable natural composites. I. Processing and properties, J. Appl. Polym. Sci. 45 (1992) 1667–1677. https://doi.org/10.1002/app.1992.070450918.

[32] M. Avella, E. Martuscelli, M. Raimo, Review Properties of blends and composites based on poly(3-hydroxy)butyrate (PHB) and poly(3-hydroxybutyrate-hydroxyvalerate) (PHBV) copolymers, Journal of Materials Science. 35 (2000) 523–545. https://doi.org/10.1023/A:1004740522751.

[33] M. Ferri, M. Vannini, M. Ehrnell, L. Eliasson, E. Xanthakis, S. Monari, L. Sisti, P. Marchese, A. Celli, A. Tassoni, From winery waste to bioactive compounds and new polymeric biocomposites: A contribution to the circular economy concept, Journal of Advanced Research. 24 (2020) 1–11. https://doi.org/10.1016/j.jare.2020.02.015.

[34] G. Perego, G.D. Cella, C. Bastioli, Effect of molecular weight and crystallinity on poly(lactic acid) mechanical properties, Journal of Applied Polymer Science. 59 (1996) 37–43. https://doi.org/10.1002/(SICI)1097-4628(19960103)59:1<37::AID-APP6>3.0.CO;2-N.

[35] A.P. Gupta, V. Kumar, New emerging trends in synthetic biodegradable polymers – Polylactide: A critique, European Polymer Journal. 43 (2007) 4053–4074. https://doi.org/10.1016/j.eurpolymj.2007.06.045.

[36] E. Llorens, L.J. del Valle, J. Puiggalí, Electrospun scaffolds of polylactide with a different enantiomeric content and loaded with anti-inflammatory and antibacterial drugs, Macromol. Res. 23 (2015) 636–648. https://doi.org/10.1007/s13233-015-3082-5.

[37] T. Tábi, A.F. Wacha, S. Hajba, Effect of D-lactide content of annealed poly(lactic acid) on its thermal, mechanical, heat deflection temperature, and creep properties, Journal of Applied Polymer Science. 136 (2019) 47103. https://doi.org/10.1002/app.47103.

[38] T. Fujimaki, Processability and properties of aliphatic polyesters, 'BIONOLLE', synthesized by polycondensation reaction, Polymer Degradation and Stability. 59 (1998) 209–214. https://doi.org/10.1016/S0141-3910(97)00220-6.

[39] S. Mizuno, T. Maeda, C. Kanemura, A. Hotta, Biodegradability, reprocessability, and mechanical properties of polybutylene succinate (PBS) photografted by hydrophilic or hydrophobic membranes, Polymer Degradation and Stability. 117 (2015) 58–65. https://doi.org/10.1016/j.polymdegradstab.2015.03.015.

[40] J. Xu, B.-H. Guo, Microbial Succinic Acid, Its Polymer Poly(butylene succinate), and Applications, in: G.G.-Q. Chen (Ed.), Plastics from Bacteria, Springer Berlin Heidelberg, Berlin, Heidelberg, 2010: pp. 347–388. https://doi.org/10.1007/978-3-642-03287-5_14.

[41] G.-Q. Chen, M.K. Patel, Plastics derived from biological sources: present and future: a technical and environmental review, Chemical Reviews. 112 (2012) 2082–2099.

[42] A. Bourmaud, Y.-M. Corre, C. Baley, Fully biodegradable composites: Use of poly-(butylene-succinate) as a matrix and to plasticize l-poly-(lactide)-flax blends, Industrial Crops and Products. 64 (2015) 251–257. https://doi.org/10.1016/j.indcrop.2014.09.033.

[43] E. Bodros, I. Pillin, N. Montrelay, C. Baley, Could biopolymers reinforced by randomly scattered flax fibre be used in structural applications?, Composites Science and Technology. 67 (2007) 462–470. https://doi.org/10.1016/j.compscitech.2006.08.024.

[44] A.K. Bledzki, A. Jaszkiewicz, Mechanical performance of biocomposites based on PLA and PHBV reinforced with natural fibres – A comparative study to PP, Composites Science and Technology. 70 (2010) 1687–1696. https://doi.org/10.1016/j.compscitech.2010.06.005.

[45] N.C. Loureiro, J.L. Esteves, Green composites in automotive interior parts, in: Green Composites for Automotive Applications, Elsevier, 2019: pp. 81–97. https://doi.org/10.1016/B978-0-08-102177-4.00004-5.

[46] A. Bourmaud, A. Le Duigou, C. Gourier, C. Baley, Influence of processing temperature on mechanical performance of unidirectional polyamide 11–flax fibre composites, Industrial Crops and Products. 84 (2016) 151–165. https://doi.org/10.1016/j.indcrop.2016.02.007.

[47] V. Gager, A. Le Duigou, A. Bourmaud, F. Pierre, K. Behlouli, C. Baley, Understanding the effect of moisture variation on the hygromechanical properties of porosity-controlled nonwoven biocomposites, Polymer Testing. 78 (2019). https://doi.org/10.1016/j.polymertesting.2019.105944.

[48] A.K. Bledzki, O. Faruk, V.E. Sperber, Cars from Bio-Fibres, Macromolecular Materials and Engineering. 291 (2006) 449–457. https://doi.org/10.1002/mame.200600113.

[49] M. Itävaara, S. Karjomaa, J.-F. Selin, Biodegradation of polylactide in aerobic and anaerobic thermophilic conditions, Chemosphere. 46 (2002) 879–885. https://doi.org/10.1016/S0045-6535(01)00163-1.

[50] T. Suyama, Y. Tokiwa, P. Ouichanpagdee, T. Kanagawa, Y. Kamagata, Phylogenetic Affiliation of Soil Bacteria That Degrade Aliphatic Polyesters Available Commercially as Biodegradable Plastics, Appl. Environ. Microbiol. 64 (1998) 5008–5011. https://doi.org/10.1128/AEM.64.12.5008-5011.1998.

[51] Y. Wu, W. Xiong, H. Zhou, H. Li, G. Xu, J. Zhao, Biodegradation of poly(butylene succinate) film by compost microorganisms and water soluble product impact on mung beans germination, Polymer Degradation and Stability. 126 (2016) 22–30. https://doi.org/10.1016/j.polymdegradstab.2016.01.009.

[52] J.-H. Zhao, X.-Q. Wang, J. Zeng, G. Yang, F.-H. Shi, Q. Yan, Biodegradation of poly(butylene succinate) in compost, Journal of Applied Polymer Science. 97 (2005) 2273–2278. https://doi.org/10.1002/app.22009.

[53] Y.-X. Weng, Y. Wang, X.-L. Wang, Y.-Z. Wang, Biodegradation behavior of PHBV films in a pilot-scale composting condition, Polymer Testing. 29 (2010) 579–587. https://doi.org/10.1016/j.polymertesting.2010.04.002.

[54] M. Deroiné, A. Le Duigou, Y.-M. Corre, P.-Y. Le Gac, P. Davies, G. César, S. Bruzaud, Seawater accelerated ageing of poly(3-hydroxybutyrate-co-3-hydroxyvalerate), Polymer Degradation and Stability. 105 (2014) 237–247. https://doi.org/10.1016/j.polymdegradstab.2014.04.026.

[55] H. Li, J. Chang, A. Cao, J. Wang, in vitro Evaluation of Biodegradable Poly(butylene succinate) as a Novel Biomaterial, Macromol. Biosci. 5 (2005) 433–440. https://doi.org/10.1002/mabi.200400183.

[56] K. Shi, T. Su, Z. Wang, Comparison of poly(butylene succinate) biodegradation by Fusarium solani cutinase and Candida antarctica lipase, Polymer Degradation and Stability. 164 (2019) 55–60. https://doi.org/10.1016/j.polymdegradstab.2019.04.005.

[57] S. Lyu, D. Untereker, Degradability of Polymers for Implantable Biomedical Devices, International Journal of Molecular Sciences. 10 (2009) 4033–4065. https://doi.org/10.3390/ijms10094033.

[58] R. Berlemont, Distribution and diversity of enzymes for polysaccharide degradation in fungi, Sci Rep. 7 (2017) 222. https://doi.org/10.1038/s41598-017-00258-w.

[59] D. Fernando, A. Thygesen, A.S. Meyer, G. Daniel, Elucidating field retting mechanisms of hemp fibres for biocomposites: effects of microbial actions and interactions on the cellular micro-morphology and ultrastructure of hemp stems and bast fibres, BioResources. 14 (2019) 4047–4084. https://doi.org/10.15376/biores.14.2.4047-4084.

[60] Z. Jankauskienė, B. Butkutė, E. Gruzdevienė, J. Cesevičienė, A.L. Fernando, Chemical composition and physical properties of dew- and water-retted hemp fibers, Industrial Crops and Products. 75 (2015) 206–211. https://doi.org/10.1016/j.indcrop.2015.06.044.

[61] J. van den Brink, R.P. de Vries, Fungal enzyme sets for plant polysaccharide degradation, Appl Microbiol Biotechnol. 91 (2011) 1477–1492. https://doi.org/10.1007/s00253-011-3473-2.

[62] A. Chesson, C.W. Forsberg, Polysaccharide degradation by rumen microorganisms, in: P.N. Hobson, C.S. Stewart (Eds.), The Rumen Microbial Ecosystem, Springer Netherlands, Dordrecht, 1997: pp. 329–381. https://doi.org/10.1007/978-94-009-1453-7_8.

[63] A. Bourmaud, J. Beaugrand, D.U. Shah, V. Placet, C. Baley, Towards the design of high-performance plant fibre composites, Progress in Materials Science. 97 (2018) 347–408. https://doi.org/10.1016/j.pmatsci.2018.05.005.

[64] D.U. Shah, Natural fibre composites: Comprehensive Ashby-type materials selection charts, Materials & Design (1980-2015). 62 (2014) 21–31. https://doi.org/10.1016/j.matdes.2014.05.002.

[65] S. Réquilé, C. Goudenhooft, A. Bourmaud, A. Le Duigou, C. Baley, Exploring the link between flexural behaviour of hemp and flax stems and fibre stiffness, Industrial Crops and Products. 113 (2018) 179–186. https://doi.org/10.1016/j.indcrop.2018.01.035.

[66] A. Melelli, F. Jamme, D. Legland, J. Beaugrand, A. Bourmaud, Microfibril angle of elementary flax fibres investigated with polarised second harmonic generation microscopy, Industrial Crops and Products. 156 (2020) 112847. https://doi.org/10.1016/j.indcrop.2020.112847.

[67] A. Bourmaud, C. Morvan, A. Bouali, V. Placet, P. Perré, C. Baley, Relationships between micro-fibrillar angle, mechanical properties and biochemical composition of flax fibers, Industrial Crops and Products. 44 (2013) 343–351. https://doi.org/10.1016/j.indcrop.2012.11.031.

[68] CIPALIN, Le C.I.P.A.LIN -l'interprofession Française du lin -dresse un état des lieux objectif de sa filière suite aux effets du COVID19., (2020). https://www.agpl-lin.fr/wp-content/uploads/2020/06/CIPALIN-COM-INFO-FILIERE-LIN-N-1_2020_04_02.pdf.

[69] Greenboat, GREENBOATS. (n.d.). https://green-boats.de/ (accessed May 25, 2021).

[70] C. Baley, M. Gomina, J. Breard, A. Bourmaud, S. Drapier, M. Ferreira, A. Le Duigou, P.J. Liotier, P. Ouagne, D. Soulat, P. Davies, Specific features of flax fibres used to manufacture composite materials, Int J Mater Form. 12 (2019) 1023–1052. https://doi.org/10.1007/s12289-018-1455-y.

[71] A. Melelli, O. Arnould, J. Beaugrand, A. Bourmaud, The Middle Lamella of Plant Fibers Used as Composite Reinforcement: Investigation by Atomic Force Microscopy, Molecules. 25 (2020) 632. https://doi.org/10.3390/molecules25030632.

[72] C. Morvan, C. Andème-Onzighi, R. Girault, D.S. Himmelsbach, A. Driouich, D.E. Akin, Building flax fibres: more than one brick in the walls, Plant Physiology and Biochemistry. 41 (2003) 935–944. https://doi.org/10.1016/j.plaphy.2003.07.001.

[73] K. Charlet, J.P. Jernot, S. Eve, M. Gomina, J. Bréard, Multi-scale morphological characterisation of flax: From the stem to the fibrils, Carbohydrate Polymers. 82 (2010) 54–61. https://doi.org/10.1016/j.carbpol.2010.04.022.

[74] C. Baley, C. Goudenhooft, M. Gibaud, A. Bourmaud, Flax stems: from a specific architecture to an instructive model for bioinspired composite structures, Bioinspir. Biomim. 13 (2018) 026007. https://doi.org/10.1088/1748-3190/aaa6b7.

[75] C. Goudenhooft, A. Bourmaud, C. Baley, Varietal selection of flax over time: Evolution of plant architecture related to influence on the mechanical properties of fibers, Industrial Crops and Products. 97 (2017) 56–64. https://doi.org/10.1016/j.indcrop.2016.11.062.

[76] I.H. Isenberg, Pulp and paper microscopy, Georgia Institute of Technology, 1967.

[77] K. Charlet, J.-P. Jernot, J. Breard, M. Gomina, Scattering of morphological and mechanical properties of flax fibres, Industrial Crops and Products. 32 (2010) 220–224. https://doi.org/10.1016/j.indcrop.2010.04.015.

[78] C. Goudenhooft, A. Bourmaud, C. Baley, Flax (Linum usitatissimum L.) Fibers for Composite Reinforcement: Exploring the Link Between Plant Growth, Cell Walls Development, and Fiber Properties, Front. Plant Sci. 10 (2019). https://doi.org/10.3389/fpls.2019.00411.

[79] E. Richely, S. Durand, A. Melelli, A. Kao, A. Magueresse, H. Dhakal, T. Gorshkova, F. Callebert, A. Bourmaud, J. Beaugrand, S. Guessasma, Novel Insight into the Intricate Shape of Flax Fibre Lumen, Fibers. 9 (2021) 24. https://doi.org/10.3390/fib9040024.

[80] T. Gorshkova, T. Chernova, N. Mokshina, M. Ageeva, P. Mikshina, Plant 'muscles': fibers with a tertiary cell wall, New Phytologist. 218 (2018) 66–72. https://doi.org/10.1111/nph.14997.

[81] M. Eder, O. Arnould, J.W.C. Dunlop, J. Hornatowska, L. Salmén, Experimental micromechanical characterisation of wood cell walls, Wood Sci Technol. 47 (2013) 163–182. https://doi.org/10.1007/s00226-012-0515-6.

[82] Y. Nishiyama, Structure and properties of the cellulose microfibril, J Wood Sci. 55 (2009) 241–249. https://doi.org/10.1007/s10086-009-1029-1.

[83] C. Baley, A. Bourmaud, Average tensile properties of French elementary flax fibers, Materials Letters. 122 (2014) 159–161. https://doi.org/10.1016/j.matlet.2014.02.030.

[84] M. Le Gall, P. Davies, N. Martin, C. Baley, Recommended flax fibre density values for composite property predictions, Industrial Crops and Products. 114 (2018) 52–58. https://doi.org/10.1016/j.indcrop.2018.01.065.

[85] P. Wambua, J. Ivens, I. Verpoest, Natural fibres: can they replace glass in fibre reinforced plastics?, Composites Science and Technology. 63 (2003) 1259–1264. https://doi.org/10.1016/S0266-3538(03)00096-4.

[86] A. Lefeuvre, A. Bourmaud, C. Morvan, C. Baley, Tensile properties of elementary fibres of flax and glass: Analysis of reproducibility and scattering, Materials Letters. 130 (2014) 289–291. https://doi.org/10.1016/j.matlet.2014.05.115.

[87] A. Lefeuvre, A. Bourmaud, C. Morvan, C. Baley, Elementary flax fibre tensile properties: Correlation between stress–strain behaviour and fibre composition, Industrial Crops and Products. 52 (2014) 762–769. https://doi.org/10.1016/j.indcrop.2013.11.043.

[88] V. Placet, O. Cissé, M. Lamine Boubakar, Nonlinear tensile behaviour of elementary hemp fibres. Part I: Investigation of the possible origins using repeated progressive loading with in situ microscopic observations, Composites Part A: Applied Science and Manufacturing. 56 (2014) 319–327. https://doi.org/10.1016/j.compositesa.2012.11.019.

[89] P. Fratzl, I. Burgert, H.S. Gupta, On the role of interface polymers for the mechanics of natural polymeric composites, Phys. Chem. Chem. Phys. 6 (2004) 5575–5579. https://doi.org/10.1039/B411986J.

[90] A. Melelli, S. Durand, O. Arnould, E. Richely, S. Guessasma, F. Jamme, J. Beaugrand, A. Bourmaud, Extensive investigation of the ultrastructure of kink-bands in flax fibres, Industrial Crops and Products. 164 (2021) 113368. https://doi.org/10.1016/j.indcrop.2021.113368.

[91] L. Di Landro, M. Pegoraro, Evaluation of residual stresses and adhesion in polymer composites, Composites Part A: Applied Science and Manufacturing. 27 (1996) 847–853. https://doi.org/10.1016/1359-835X(96)00046-2.

[92] A. Le Duigou, P. Davies, C. Baley, Interfacial bonding of Flax fibre/Poly(l-lactide) bio-composites, Composites Science and Technology. 70 (2010) 231–239. https://doi.org/10.1016/j.compscitech.2009.10.009.

[93] S. Garkhail, B. Wieland, J. George, N. Soykeabkaew, T. Peijs, Transcrystallisation in PP/flax composites and its effect on interfacial and mechanical properties, J Mater Sci. 44 (2009) 510–519. https://doi.org/10.1007/s10853-008-3089-9.

[94] Y. Zhou, M. Fan, L. Chen, Interface and bonding mechanisms of plant fibre composites: An overview, Composites Part B: Engineering. 101 (2016) 31–45. https://doi.org/10.1016/j.compositesb.2016.06.055.

[95] P.P. Parlevliet, H.E.N. Bersee, A. Beukers, Residual stresses in thermoplastic composites—A study of the literature—Part I: Formation of residual stresses, Composites Part A: Applied Science and Manufacturing. 37 (2006) 1847–1857. https://doi.org/10.1016/j.compositesa.2005.12.025.

[96] C. Baley, A. Le Duigou, A. Bourmaud, P. Davies, Reinforcement of polymers by flax fibres: The role of interfaces. Chapitre de l'ouvrage: Bio-based Composites for High-Performance Materials: From Strategy to Industrial application. Editors: W. Smitthipong, R. Chollakup, M. Nardin, 2014, Taylor and Francis, 2014.

[97] L.-H. Lee, Roles of molecular interactions in adhesion, adsorption, contact angle and wettability, Journal of Adhesion Science and Technology. 7 (1993) 583–634. https://doi.org/10.1163/156856193X00871.

[98] G. Gilli, P. Gilli, The nature of the hydrogen bond: outline of a comprehensive hydrogen bond theory, 1. ed in paperback, Oxford Univ. Press, Oxford, 2013.

[99] M. Nardin, J. Schultz, Relationship between Work of Adhesion and Equilibrium Interatomic Distance at the Interface, Langmuir. 12 (1996) 4238–4242. https://doi.org/10.1021/la9602168.

[100] J.M. Felix, P. Gatenholm, The nature of adhesion in composites of modified cellulose fibers and polypropylene, Journal of Applied Polymer Science. 42 (1991) 609–620. https://doi.org/10.1002/app.1991.070420307.

[101] P.J. Herrera-Franco, L.T. Drzal, Comparison of methods for the measurement of fibre/matrix adhesion in composites, Composites. 23 (1992) 2–27. https://doi.org/10.1016/0010-4361(92)90282-Y.

[102] K. Charlet, A. Béakou, Mechanical properties of interfaces within a flax bundle – Part I: Experimental analysis, International Journal of Adhesion and Adhesives. 31 (2011) 875–881. https://doi.org/10.1016/j.ijadhadh.2011.08.008.

[103] A. Monti, A. El Mahi, Z. Jendli, L. Guillaumat, Mechanical behaviour and damage mechanisms analysis of a flax-fibre reinforced composite by acoustic emission, Composites Part A: Applied Science and Manufacturing. 90 (2016) 100–110. https://doi.org/10.1016/j.compositesa.2016.07.002.

[104] A. Le Duigou, A. Kervoelen, A. Le Grand, M. Nardin, C. Baley, Interfacial properties of flax fibre–epoxy resin systems: Existence of a complex interphase, Composites Science and Technology. 100 (2014) 152–157. https://doi.org/10.1016/j.compscitech.2014.06.009.

[105] A. le Duigou, A. Bourmaud, E. Balnois, P. Davies, C. Baley, Improving the interfacial properties between flax fibres and PLLA by a water fibre treatment and drying cycle, Industrial Crops and Products. 39 (2012) 31–39. https://doi.org/10.1016/j.indcrop.2012.02.001.

[106] J. Müssig, N. Graupner, Test Methods for Fibre/Matrix Adhesion in Cellulose Fibre-Reinforced Thermoplastic Composite Materials: A Critical Review, in: Progress in Adhesion and Adhesives, John Wiley & Sons, Ltd, 2021: pp. 69–130. https://doi.org/10.1002/9781119846703.ch4.

[107] J.R. Wood, G. Marom, Determining the interfacial shear strength in the presence of transcrystallinity in composites by the 'single-fibre microcomposite compressive fragmentation test,' Appl Compos Mater. 4 (1997) 197–207. https://doi.org/10.1007/BF02481389.

[108] V. Rao, P. Herrera-franco, A.D. Ozzello, L.T. Drzal, A Direct Comparison of the Fragmentation Test and the Microbond Pull-out Test for Determining the Interfacial Shear Strength, The Journal of Adhesion. 34 (1991) 65–77. https://doi.org/10.1080/00218469108026506.

[109] D. Tripathi, F.R. Jones, Single fibre fragmentation test for assessing adhesion in fibre reinforced composites, Journal of Materials Science. 33 (1998) 1–16. https://doi.org/10.1023/A:1004351606897.

[110] E. Pisanova, E. Mäder, Acid–base interactions and covalent bonding at a fiber–matrix interface: contribution to the work of adhesion and measured adhesion strength, Journal of Adhesion Science and Technology. 14 (2000) 415–436. https://doi.org/10.1163/156856100742681.

[111] B. Miller, P. Muri, L. Rebenfeld, A microbond method for determination of the shear strength of a fiber/resin interface, Composites Science and Technology. 28 (1987) 17–32. https://doi.org/10.1016/0266-3538(87)90059-5.

[112] M.Q. Tran, K.K.C. Ho, G. Kalinka, M.S.P. Shaffer, A. Bismarck, Carbon fibre reinforced poly(vinylidene fluoride): Impact of matrix modification on fibre/polymer adhesion, Composites Science and Technology. 68 (2008) 1766–1776. https://doi.org/10.1016/j.compscitech.2008.02.021.

[113] S. Réquilé, A. Le Duigou, A. Bourmaud, C. Baley, Interfacial properties of hemp fiber/epoxy system measured by microdroplet test: Effect of relative humidity, Composites Science and Technology. 181 (2019) 107694. https://doi.org/10.1016/j.compscitech.2019.107694.

[114] H.L. Cox, The elasticity and strength of paper and other fibrous materials, Br. J. Appl. Phys. 3 (1952) 72. https://doi.org/10.1088/0508-3443/3/3/302.

[115] A. Le Duigou, P. Davies, C. Baley, Exploring durability of interfaces in flax fibre/epoxy micro-composites, Composites Part A: Applied Science and Manufacturing. 48 (2013) 121–128. https://doi.org/10.1016/j.compositesa.2013.01.010.

[116] B. Song, A. Bismarck, R. Tahhan, J. Springer, A Generalized Drop Length–Height Method for Determination of Contact Angle in Drop-on-Fiber Systems, Journal of Colloid and Interface Science. 197 (1998) 68–77. https://doi.org/10.1006/jcis.1997.5218.

[117] N. Graupner, J. Rößler, G. Ziegmann, J. Müssig, Fibre/matrix adhesion of cellulose fibres in PLA, PP and MAPP: A critical review of pull-out test, microbond test and single fibre fragmentation test results, Composites Part A: Applied Science and Manufacturing. 63 (2014) 133–148. https://doi.org/10.1016/j.compositesa.2014.04.011.

[118] S.P. Reilly, J.L. Thomason, Effects of silane coating on the properties of glass fibre and glass fibre reinforced epoxy resin, in: 14th European Conference on Composite Materials, ECCM14, Budapest, Hungary, 2010: p. Paper 009. https://strathprints.strath.ac.uk/20626/.

[119] J. Borsa, K. László, L. Boguslavsky, E. Takács, I. Rácz, T. Tóth, D. Szabó, Effect of mild alkali/ultrasound treatment on flax and hemp fibres: the different responses of the two substrates, Cellulose. 23 (2016) 2117–2128. https://doi.org/10.1007/s10570-016-0909-y.

[120] R. Joffe, J. Andersons, L. Wallström, Strength and adhesion characteristics of elementary flax fibres with different surface treatments, Composites Part A: Applied Science and Manufacturing. 34 (2003) 603–612. https://doi.org/10.1016/S1359-835X(03)00099-X.

[121] T. Czigány, B. Morlin, Z. Mezey, Interfacial adhesion in fully and partially biodegradable polymer composites examined with microdroplet test and acoustic emission, Composite Interfaces. 14 (2007) 869–878. https://doi.org/10.1163/156855407782106447.

[122] H.L. Bos, The potential of flax fibres as reinforcement for composite materials, University Press, Eindhoven, 2004. https://doi.org/10.6100/IR575360.

[123] T. Yu, C.-M. Wu, C.-J. Wang, S.-P. Rwei, Effects of surface modifications on the interfacial bonding of flax/β-polypropylene composites, Composite Interfaces. 20 (2013) 483–496. https://doi.org/10.1080/15685543.2013.807168.

[124] J. Merotte, A. Le Duigou, A. Kervoelen, A. Bourmaud, K. Behlouli, O. Sire, C. Baley, Flax and hemp nonwoven composites: The contribution of interfacial bonding to improving tensile properties, Polymer Testing. 66 (2018) 303–311. https://doi.org/10.1016/j.polymertesting.2018.01.019.

[125] C. Baley, F. Busnel, Y. Grohens, O. Sire, Influence of chemical treatments on surface properties and adhesion of flax fibre–polyester resin, Composites Part A: Applied Science and Manufacturing. 37 (2006) 1626–1637. https://doi.org/10.1016/j.compositesa.2005.10.014.

[126] L. Marrot, A. Bourmaud, P. Bono, C. Baley, Multi-scale study of the adhesion between flax fibers and biobased thermoset matrices, Materials & Design (1980-2015). 62 (2014) 47–56. https://doi.org/10.1016/j.matdes.2014.04.087.

[127] G. Coroller, A. Lefeuvre, A. Le Duigou, A. Bourmaud, G. Ausias, T. Gaudry, C. Baley, Effect of flax fibres individualisation on tensile failure of flax/epoxy unidirectional composite, Composites Part A: Applied Science and Manufacturing. 51 (2013) 62–70. https://doi.org/10.1016/j.compositesa.2013.03.018.

[128] A. Lefeuvre, A.L. Duigou, A. Bourmaud, A. Kervoelen, C. Morvan, C. Baley, Analysis of the role of the main constitutive polysaccharides in the flax fibre mechanical behaviour, Industrial Crops and Products. 76 (2015) 1039–1048. https://doi.org/10.1016/j.indcrop.2015.07.062.

[129] Z. Zhai, Z. Liu, L. Feng, S. Liu, Interfacial adhesion of glass fibre reinforced polypropylene–maleic anhydride modified polypropylene copolymer composites, Journal of Reinforced Plastics and Composites. 33 (2014) 785–793. https://doi.org/10.1177/0731684413519006.

[130] E. Mäder, E. Pisanova, Characterization and design of interphases in glass fiber reinforced polyproplyene: Characterization and Design of Interphases, Polym Compos. 21 (2000) 361–368. https://doi.org/10.1002/pc.10194.

[131] L. Yang, J.L. Thomason, Interface strength in glass fibre–polypropylene measured using the fibre pull-out and microbond methods, Composites Part A: Applied Science and Manufacturing. 41 (2010) 1077–1083. https://doi.org/10.1016/j.compositesa.2009.10.005.

[132] J.L. Thomason, L. Yang, Temperature dependence of the interfacial shear strength in glass–fibre polypropylene composites, Composites Science and Technology. 71 (2011) 1600–1605. https://doi.org/10.1016/j.compscitech.2011.07.006.

[133] C. Baley, Y. Grohens, F. Busnel, P. Davies, Application of Interlaminar Tests to Marine Composites. Relation between Glass Fibre/Polymer Interfaces and Interlaminar Properties of Marine Composites, Applied Composite Materials. 11 (2004) 77–98. https://doi.org/10.1023/B:ACMA.0000012884.02847.65.

[134] Q. Charlier, F. Lortie, J.-F. Gérard, Interfacial adhesion in glass-fiber thermoplastic composites processed from acrylic reactive systems, a multi-scale experimental analysis, International Journal of Adhesion and Adhesives. 98 (2020) 102536. https://doi.org/10.1016/j.ijadhadh.2019.102536.

[135] U. Gaur, B. Miller, Microbond method for determination of the shear strength of a fiber/resin interface: Evaluation of experimental parameters, Composites Science and Technology. 34 (1989) 35–51. https://doi.org/10.1016/0266-3538(89)90076-6.

[136] C.K. Moon, J.-O. Lee, H.H. Cho, K.S. Kim, Effect of diameter and surface treatment of fiber on interfacial shear strength in glass fiber/epoxy and HDPE, J. Appl. Polym. Sci. 45 (1992) 443–450. https://doi.org/10.1002/app.1992.070450309.

[137] C.C. Chiao, R.L. Moore, T.T. Chiao, Measurement of shear properties of fibre composites: Part 1. Evaluation of test methods, Composites. 8 (1977) 161–169. https://doi.org/10.1016/0010-4361(77)90011-8.

[138] S. Lee, M. Munro, Evaluation of in-plane shear test methods for advanced composite materials by the decision analysis technique, Composites. 17 (1986) 13–22. https://doi.org/10.1016/0010-4361(86)90729-9.

[139] C.C. Chamis, J.H. Sinclair, Ten-deg off-axis test for shear properties in fiber composites: It is demonstrated that the 10-deg off-axis tensile test is an accurate and convenient test method for the intralaminar-shear characterization of unidirectional fiber composites, Experimental Mechanics. 17 (1977) 339–346. https://doi.org/10.1007/BF02326320.

[140] P. Petit, A simplified method of determining the inplane shear stress-strain response of unidirectional composites, in: Composite Materials: Testing and Design, ASTM International, 1969.

[141] B.W. Rosen, A Simple Procedure for Experimental Determination of the Longitudinal Shear Modulus of Unidirectional Composites, (n.d.) 3.

[142] G. Terry, A comparative investigation of some methods of unidirectional, in-plane shear characterization of composite materials, Composites. 10 (1979) 233–237. https://doi.org/10.1016/0010-4361(79)90025-9.

[143] I. Verpoest, M. Desaeger, J. Ivens, M. Wevers, Interfaces in polymer matrix composites from micromechanical tests to macromechanical properties, Makromolekulare Chemie. Macromolecular Symposia. 75 (1993) 85–98. https://doi.org/10.1002/masy.19930750109.

[144] I.M. Daniel, O. Ishai, Engineering mechanics of composite materials, 2nd ed, Oxford University Press, New York, 2006.

[145] C. Djemiel, S. Grec, S. Hawkins, Characterization of Bacterial and Fungal Community Dynamics by High-Throughput Sequencing (HTS) Metabarcoding during Flax Dew-Retting, Front. Microbiol. 8 (2017). https://doi.org/10.3389/fmicb.2017.02052.

[146] D.E. Akin, J.A. Foulk, R.B. Dodd, D.D. McAlister, Enzyme-retting of flax and characterization of processed fibers, Journal of Biotechnology. 89 (2001) 193–203. https://doi.org/10.1016/S0168-1656(01)00298-X.

[147] N. Martin, N. Mouret, P. Davies, C. Baley, Influence of the degree of retting of flax fibers on the tensile properties of single fibers and short fiber/polypropylene composites, Industrial Crops and Products. 49 (2013) 755–767. https://doi.org/10.1016/j.indcrop.2013.06.012.

[148] N. Martin, P. Davies, C. Baley, Comparison of the properties of scutched flax and flax tow for composite material reinforcement, Industrial Crops and Products. 61 (2014) 284–292. https://doi.org/10.1016/j.indcrop.2014.07.015.

[149] L. Nuez, Contribution à l'étude multi-échelle des fibres élémentaires de lin et du xylème pour un usage comme renfort de matériaux composites, PhD Thesis, Lorient, 2021.

[150] M. Rask, B. Madsen, Twisting of fibres in yarns for natural fibre composites, in: Korea, Republic of, 2011. http://www.iccm18.org/.

[151] D.U. Shah, Determining the minimum, critical and maximum fibre content for twisted yarn reinforced plant fibre composites, Compos. Sci. Technol. 72 (2012) 1909–1917.

[152] F. Omrani, P. Wang, D. Soulat, M. Ferreira, Mechanical properties of flax-fibre-reinforced preforms and composites: Influence of the type of yarns on multi-scale characterisations, Composites Part A: Applied Science and Manufacturing. 93 (2017) 72–81. https://doi.org/10.1016/j.compositesa.2016.11.013.

[153] S. Goutianos, T. Peijs, B. Nystrom, M. Skrifvars, Development of Flax Fibre based Textile Reinforcements for Composite Applications, Appl Compos Mater. 13 (2006) 199–215. https://doi.org/10.1007/s10443-006-9010-2.

[154] M. Rask, B. Madsen, TWISTING OF FIBRES IN YARNS FOR NATURAL FIBRE COMPOSITES, (n.d.) 6.

[155] D. Shah, P.J. Schubel, M.J. Clifford, P. Licence, Mechanical characterization of vacuum infused thermoset matrix composites reinforced with aligned hydroxyethylcellulose sized plant bast fibre yarns, in: 4th International Conference on Sustainable Materials, Polymers and Composites, 2011: pp. 6–7.

[156] M. Khalfallah, B. Abbès, F. Abbès, Y.Q. Guo, V. Marcel, A. Duval, F. Vanfleteren, F. Rousseau, Innovative flax tapes reinforced Acrodur biocomposites: A new alternative for automotive applications, Materials & Design. 64 (2014) 116–126. https://doi.org/10.1016/j.matdes.2014.07.029.

[157] J. DECORME, A. Duval, E. Vanfleteren, F. Vanfleteren, Method for producing a continuous web of fibers comprising long natural fibers, and associated apparatus and web, US20140287216A1, 2014. https://patents.google.com/patent/US20140287216A1/en (accessed June 4, 2021).

[158] C. Baley, A. Kervoëlen, M. Lan, D. Cartié, A. Le Duigou, A. Bourmaud, P. Davies, Flax/PP manufacture by automated fibre placement (AFP), Materials & Design. 94 (2016) 207–213. https://doi.org/10.1016/j.matdes.2016.01.011.

[159] O.P.L. McGregor, M. Duhovic, A.A. Somashekar, D. Bhattacharyya, Pre-impregnated natural fibre-thermoplastic composite tape manufacture using a novel process, Composites Part A: Applied Science and Manufacturing. 101 (2017) 59–71. https://doi.org/10.1016/j.compositesa.2017.05.025.

[160] P. Ouagne, D. Soulat, C. Tephany, D. Duriatti, S. Allaoui, G. Hivet, Mechanical characterisation of flax-based woven fabrics and in situ measurements of tow tensile strain during the shape forming, Journal of Composite Materials. 47 (2013) 3501–3515. https://doi.org/10.1177/0021998312467217.

[161] S. Maity, D.P. Gon, P. Paul, A Review of Flax Nonwovens: Manufacturing, Properties, and Applications, Journal of Natural Fibers. 11 (2014) 365–390. https://doi.org/10.1080/15440478.2013.861781.

[162] S. Ghosh, L. Chapman, Effects of Fiber Blends and Needling Parameters on Needlepunched Moldable Nonwoven Fabric, Journal of the Textile Institute. 93 (2002) 75–87. https://doi.org/10.1080/00405000208630553.

[163] S.J. Russell, Handbook of Nonwovens, Woodhead Publishing, 2006.

[164] W. Albrecht, H. Fuchs, W. Kittelmann, eds., Nonwoven Fabrics: Raw Materials, Manufacture, Applications, Characteristics, Testing Processes, 1st ed., Wiley, 2002. https://doi.org/10.1002/3527603344.

[165] N. Martin, P. Davies, C. Baley, Evaluation of the potential of three non-woven flax fiber reinforcements: Spunlaced, needlepunched and paper process mats, Industrial Crops and Products. 83 (2016) 194–205. https://doi.org/10.1016/j.indcrop.2015.10.008.

[166] U.K. Vaidya, K.K. Chawla, Processing of fibre reinforced thermoplastic composites, International Materials Reviews. 53 (2008) 185–218. https://doi.org/10.1179/174328008X325223.

[167] O. Ishida, J. Kitada, K. Nunotani, K. Uzawa, Impregnation and resin flow analysis during compression process for thermoplastic composite production, Advanced Composite Materials. 30 (2021) 39–58. https://doi.org/10.1080/09243046.2020.1752964.

[168] L. Ye, V. Klinkmuller, K. Friedrich, Impregnation and Consolidation in Composites Made of GF/PP Powder Impregnated Bundles, Journal of Thermoplastic Composite Materials. 5 (1992) 32–48. https://doi.org/10.1177/089270579200500103.

[169] N.M. Barkoula, S.K. Garkhail, T. Peijs, Effect of Compounding and Injection Molding on the Mechanical Properties of Flax Fiber Polypropylene Composites, Journal of Reinforced Plastics and Composites. 29 (2010) 1366–1385. https://doi.org/10.1177/0731684409104465.

[170] A. Bourmaud, D. Åkesson, J. Beaugrand, A. Le Duigou, M. Skrifvars, C. Baley, Recycling of L-Poly-(lactide)-Poly-(butylene-succinate)-flax biocomposite, Polymer Degradation and Stability. 128 (2016) 77–88. https://doi.org/10.1016/j.polymdegradstab.2016.03.018.

[171] C.M. Clemons, D.F. Caufield, Wood flour, Functional Fillers for Plastics. Weinheim : Wiley-VCH, 2005: Pages [249]-270. (2005). https://www.fs.usda.gov/treesearch/pubs/23122 (accessed June 24, 2021).

[172] A. Le Duigou, A. Barbé, E. Guillou, M. Castro, 3D printing of continuous flax fibre reinforced biocomposites for structural applications, Materials & Design. 180 (2019) 107884. https://doi.org/10.1016/j.matdes.2019.107884.

[173] D.H.-J.A. Lukaszewicz, C. Ward, K.D. Potter, The engineering aspects of automated prepreg layup: History, present and future, Composites Part B: Engineering. 43 (2012) 997–1009. https://doi.org/10.1016/j.compositesb.2011.12.003.

[174] J. Merotte, A. Le Duigou, A. Bourmaud, K. Behlouli, C. Baley, Mechanical and acoustic behaviour of porosity controlled randomly dispersed flax/PP biocomposite, Polymer Testing. 51 (2016) 174–180. https://doi.org/10.1016/j.polymertesting.2016.03.002.

[175] V. Popineau, A. Célino, M. Le Gall, L. Martineau, C. Baley, A. Le Duigou, Vacuum-Bag-Only (VBO) Molding of Flax Fiber-reinforced Thermoplastic Composites for Naval Shipyards, Appl Compos Mater. (2021). https://doi.org/10.1007/s10443-021-09890-2.

[176] V. Michaud, R. Törnqvist, J.-A.E. Månson, Impregnation of Compressible Fiber Mats with a Thermoplastic Resin. Part II: Experiments, Journal of Composite Materials. 35 (2001) 1174–1200. https://doi.org/10.1177/002199801772662280.

[177] K.R. Ramakrishnan, N. Le Moigne, O. De Almeida, A. Regazzi, S. Corn, Optimized manufacturing of thermoplastic biocomposites by fast induction-heated compression moulding: Influence of processing parameters on microstructure development and mechanical behaviour, Composites Part A: Applied Science and Manufacturing. 124 (2019) 105493. https://doi.org/10.1016/j.compositesa.2019.105493.

[178] D. Salvatori, B. Caglar, H. Teixidó, V. Michaud, Permeability and capillary effects in a channel-wise non-crimp fabric, Composites Part A: Applied Science and Manufacturing. 108 (2018) 41–52. https://doi.org/10.1016/j.compositesa.2018.02.015.

[179] P.A. Thompson, W.B. Brinckerhoff, M.O. Robbins, Microscopic studies of static and dynamic contact angles, Journal of Adhesion Science and Technology. 7 (1993) 535–554. https://doi.org/10.1163/156856193X00844.

[180] J. Verrey, V. Michaud, J.-A.E. Månson, Dynamic capillary effects in liquid composite moulding with non-crimp fabrics, Composites Part A: Applied Science and Manufacturing. 37 (2006) 92–102. https://doi.org/10.1016/j.compositesa.2005.04.011.

[181] D. Pantaloni, A. Bourmaud, C. Baley, M.J. Clifford, M.H. Ramage, D.U. Shah, A Review of Permeability and Flow Simulation for Liquid Composite Moulding of Plant Fibre Composites, Materials. 13 (2020) 4811. https://doi.org/10.3390/ma13214811.

[182] P. Ouagne, J. Bréard, Continuous transverse permeability of fibrous media, Composites Part A: Applied Science and Manufacturing. 41 (2010) 22–28. https://doi.org/10.1016/j.compositesa.2009.07.008.

[183] G. Francucci, A. Vázquez, E.S. Rodríguez, Key differences on the compaction response of natural and glass fiber preforms in liquid composite molding, Textile Research Journal. 82 (2012) 1774–1785. https://doi.org/10.1177/0040517511424533.

[184] H. Darcy, Les fontaines publiques de la ville de Dijon: exposition et application ..., Victor Dalmont, 1856.

[185] W. Woigk, C.A. Fuentes, J. Rion, D. Hegemann, A.W. van Vuure, E. Kramer, C. Dransfeld, K. Masania, Fabrication of flax fibre-reinforced cellulose propionate thermoplastic composites, Composites Science and Technology. 183 (2019) 107791. https://doi.org/10.1016/j.compscitech.2019.107791.

[186] A.G. Gibson, J.-A. Månson, Impregnation technology for thermoplastic matrix composites, Composites Manufacturing. 3 (1992) 223–233. https://doi.org/10.1016/0956-7143(92)90110-G.

[187] R. Gennaro, A. Greco, A. Maffezzoli, Micro- and macro-impregnation of fabrics using thermoplastic matrices, Journal of Thermoplastic Composite Materials. 26 (2013) 527–543. https://doi.org/10.1177/0892705711425849.

[188] G. Francucci, E.S. Rodríguez, A. Vázquez, Study of saturated and unsaturated permeability in natural fiber fabrics, Composites Part A: Applied Science and Manufacturing. 41 (2010) 16–21. https://doi.org/10.1016/j.compositesa.2009.07.012.

[189] G.A. Testoni, S. Kim, A. Pisupati, C.H. Park, Modeling of the capillary wicking of flax fibers by considering the effects of fiber swelling and liquid absorption, Journal of Colloid and Interface Science. 525 (2018) 166–176. https://doi.org/10.1016/j.jcis.2018.04.064.

[190] S.T. Jespersen, M.D. Wakeman, V. Michaud, D. Cramer, J.-A.E. Månson, Film stacking impregnation model for a novel net shape thermoplastic composite preforming process, Composites Science and Technology. 68 (2008) 1822–1830. https://doi.org/10.1016/j.compscitech.2008.01.019.

[191] J.Z. Liang, W. Peng, Melt viscosity of PP and FEP/PP blends at low shear rates, Polymer Testing. 28 (2009) 386–391. https://doi.org/10.1016/j.polymertesting.2009.02.002.

[192] G. Agarwal, G. Reyes, P. Mallick, Study of compressibility and resin flow in the development of thermoplstic matrix composite laminates by film stacking technique, Manufacturing of Composites. DEStech Publications. (2013) 215–227.

[193] C. Gourier, A. Le Duigou, A. Bourmaud, C. Baley, Mechanical analysis of elementary flax fibre tensile properties after different thermal cycles, Composites Part A: Applied Science and Manufacturing. 64 (2014) 159–166. https://doi.org/10.1016/j.compositesa.2014.05.006.

[194] K.V. de Velde, E. Baetens, Thermal and Mechanical Properties of Flax Fibres as Potential Composite Reinforcement, Macromolecular Materials and Engineering. 286 (2001) 342–349. https://doi.org/10.1002/1439-2054(20010601)286:6<342::AID-MAME342>3.0.CO;2-P.

[195] Q. Li, Y. Li, H. Ma, S. Cai, X. Huang, Effect of processing temperature on the static and dynamic mechanical properties and failure mechanisms of flax fiber reinforced composites, Composites Communications. 20 (2020) 100343. https://doi.org/10.1016/j.coco.2020.04.009.

[196] C. Baley, A. Le Duigou, A. Bourmaud, P. Davies, Influence of drying on the mechanical behaviour of flax fibres and their unidirectional composites, Composites Part A: Applied Science and Manufacturing. 43 (2012) 1226–1233. https://doi.org/10.1016/j.compositesa.2012.03.005.

[197] D. Hopkins, C. Chamis, A Unique Set of Micromechanics Equations for High-Temperature Metal Matrix Composites, in: N. Adsit, P. DiGiovanni (Eds.), Testing Technology of Metal Matrix Composites, ASTM International, 100 Barr Harbor Drive, PO Box C700, West Conshohocken, PA 19428-2959, 1988: pp. 159-159–17. https://doi.org/10.1520/STP25950S.

[198] J.C.H. Affdl, J.L. Kardos, The Halpin-Tsai equations: A review, Polymer Engineering & Science. 16 (1976) 344–352. https://doi.org/10.1002/pen.760160512.

[199] C. Baley, Y. Perrot, F. Busnel, H. Guezenoc, P. Davies, Transverse tensile behaviour of unidirectional plies reinforced with flax fibres, Materials Letters. 60 (2006) 2984–2987. https://doi.org/10.1016/j.matlet.2006.02.028.

[200] D.U. Shah, P.J. Schubel, P. Licence, M.J. Clifford, Determining the minimum, critical and maximum fibre content for twisted yarn reinforced plant fibre composites, Composites Science and Technology. 72 (2012) 1909–1917. https://doi.org/10.1016/j.compscitech.2012.08.005.

[201] H. Huang, R. Talreja, Effects of void geometry on elastic properties of unidirectional fiber reinforced composites, Composites Science and Technology. 65 (2005) 1964–1981. https://doi.org/10.1016/j.compscitech.2005.02.019.

[202] B. Madsen, A. Thygesen, H. Lilholt, Plant fibre composites – porosity and volumetric interaction, Composites Science and Technology. 67 (2007) 1584–1600. https://doi.org/10.1016/j.compscitech.2006.07.009.

[203] Y. Li, Q. Li, H. Ma, The voids formation mechanisms and their effects on the mechanical properties of flax fiber reinforced epoxy composites, Composites Part A: Applied Science and Manufacturing. 72 (2015) 40–48. https://doi.org/10.1016/j.compositesa.2015.01.029.

[204] C.A.S. Hill, A. Norton, G. Newman, The water vapor sorption behavior of flax fibers—Analysis using the parallel exponential kinetics model and determination of the activation energies of sorption, Journal of Applied Polymer Science. 116 (2010) 2166–2173. https://doi.org/10.1002/app.31819.

[205] K. Van de Velde, P. Kiekens, Thermoplastic polymers: overview of several properties and their consequences in flax fibre reinforced composites, Polymer Testing. 20 (2001) 885–893. https://doi.org/10.1016/S0142-9418(01)00017-4.

[206] B. Madsen, A. Thygesen, H. Lilholt, Plant fibre composites – porosity and stiffness, Composites Science and Technology. 69 (2009) 1057–1069. https://doi.org/10.1016/j.compscitech.2009.01.016.

[207] V. Michaud, A Review of Non-saturated Resin Flow in Liquid Composite Moulding processes, Transp Porous Med. 115 (2016) 581–601. https://doi.org/10.1007/s11242-016-0629-7.

[208] S.F.M. de Almeida, Z. dos S.N. Neto, Effect of void content on the strength of composite laminates, Composite Structures. 28 (1994) 139–148. https://doi.org/10.1016/0263-8223(94)90044-2.

[209] M. Mehdikhani, L. Gorbatikh, I. Verpoest, S.V. Lomov, Voids in fiber-reinforced polymer composites: A review on their formation, characteristics, and effects on mechanical performance, Journal of Composite Materials. 53 (2019) 1579–1669. https://doi.org/10.1177/0021998318772152.

[210] P. Olivier, J.P. Cottu, B. Ferret, Effects of cure cycle pressure and voids on some mechanical properties of carbon/epoxy laminates, Composites. 26 (1995) 509–515. https://doi.org/10.1016/0010-4361(95)96808-J.

[211] J.K. Mackenzie, The Elastic Constants of a Solid containing Spherical Holes, Proc. Phys. Soc. B. 63 (1950) 2–11. https://doi.org/10.1088/0370-1301/63/1/302.

[212] D.U. Shah, P.J. Schubel, M.J. Clifford, P. Licence, The tensile behavior of off-axis loaded plant fiber composites: An insight on the nonlinear stress-strain response, Polymer Composites. 33 (2012) 1494–1504. https://doi.org/10.1002/pc.22279.

[213] M.R. Piggott, The effect of fibre waviness on the mechanical properties of unidirectional fibre composites: A review, Composites Science and Technology. 53 (1995) 201–205. https://doi.org/10.1016/0266-3538(95)00019-4.

[214] V. Gager, D. Legland, A. Bourmaud, A. Le Duigou, F. Pierre, K. Behlouli, C. Baley, Oriented granulometry to quantify fibre orientation distributions in synthetic and plant fibre composite preforms, Industrial Crops and Products. 152 (2020) 112548. https://doi.org/10.1016/j.indcrop.2020.112548.

[215] D.U. Shah, M.J. Clifford, Compaction, Permeability and Flow Simulation for Liquid Composite Moulding of Natural Fibre Composites, in: M.S. Salit, M. Jawaid, N.B. Yusoff, M.E. Hoque (Eds.), Manufacturing of Natural Fibre Reinforced Polymer Composites, Springer International Publishing, Cham, 2015: pp. 65–99. https://doi.org/10.1007/978-3-319-07944-8_4.

[216] J.M. Berthelot, Effect of fibre misalignment on the elastic properties of oriented discontinuous fibre composites, Fibre Science and Technology. 17 (1982) 25–39. https://doi.org/10.1016/0015-0568(82)90059-8.

[217] D. Das, B. Neckář, 3 - Structure of composite nonwovens, in: D. Das, B. Pourdeyhimi (Eds.), Composite Non-Woven Materials, Woodhead Publishing, 2014: pp. 30–57. https://doi.org/10.1533/9780857097750.30.

[218] N. Graupner, F. Beckmann, F. Wilde, J. Müssig, Using synchroton radiation-based micro-computer tomography (SR μ-CT) for the measurement of fibre orientations in cellulose fibre-reinforced polylactide (PLA) composites, J Mater Sci. 49 (2014) 450–460. https://doi.org/10.1007/s10853-013-7724-8.

[219] R.A. Smith, L.J. Nelson, N. Xie, C. Fraij, S.R. Hallett, Progress in 3D characterisation and modelling of monolithic carbon-fibre composites, Insight. 57 (2015) 131–139. https://doi.org/10.1784/insi.2014.57.3.131.

[220] A. Bourmaud, G. Ausias, G. Lebrun, M.-L. Tachon, C. Baley, Observation of the structure of a composite polypropylene/flax and damage mechanisms under stress, Industrial Crops and Products. 43 (2013) 225–236. https://doi.org/10.1016/j.indcrop.2012.07.030.

[221] L.G. Thygesen, The effects of growth conditions and of processing into yarn on dislocations in hemp fibres, J Mater Sci. 46 (2011) 2135–2139. https://doi.org/10.1007/s10853-010-5049-4.

[222] D.U. Shah, Damage in biocomposites: Stiffness evolution of aligned plant fibre composites during monotonic and cyclic fatigue loading, Composites Part A: Applied Science and Manufacturing. 83 (2016) 160–168. https://doi.org/10.1016/j.compositesa.2015.09.008.

[223] M. Rask, B. Madsen, B.F. Sørensen, J.L. Fife, K. Martyniuk, E.M. Lauridsen, In situ observations of microscale damage evolution in unidirectional natural fibre composites, Composites Part A: Applied Science and Manufacturing. 43 (2012) 1639–1649. https://doi.org/10.1016/j.compositesa.2012.02.007.

[224] A. le Duigou, J. Merotte, A. Bourmaud, P. Davies, K. Belhouli, C. Baley, Hygroscopic expansion: A key point to describe natural fibre/polymer matrix interface bond strength, Composites Science and Technology. 151 (2017) 228–233. https://doi.org/10.1016/j.compscitech.2017.08.028.

[225] W. Garat, N. Le Moigne, S. Corn, J. Beaugrand, A. Bergeret, Swelling of natural fibre bundles under hygro- and hydrothermal conditions: Determination of hydric expansion coefficients by automated laser scanning, Composites Part A: Applied Science and Manufacturing. 131 (2020) 105803. https://doi.org/10.1016/j.compositesa.2020.105803.

[226] A. Bourmaud, C. Morvan, C. Baley, Importance of fiber preparation to optimize the surface and mechanical properties of unitary flax fiber, Industrial Crops and Products. 32 (2010) 662–667. https://doi.org/10.1016/j.indcrop.2010.08.002.

[227] A. Regazzi, S. Corn, P. Ienny, J.-C. Bénézet, A. Bergeret, Reversible and irreversible changes in physical and mechanical properties of biocomposites during hydrothermal aging, Industrial Crops and Products. 84 (2016) 358–365. https://doi.org/10.1016/j.indcrop.2016.01.052.

[228] A. Chilali, M. Assarar, W. Zouari, H. Kebir, R. Ayad, Effect of geometric dimensions and fibre orientation on 3D moisture diffusion in flax fibre reinforced thermoplastic and thermosetting composites, Composites Part A: Applied Science and Manufacturing. 95 (2017) 75–86. https://doi.org/10.1016/j.compositesa.2016.12.020.

[229] E.H. Saidane, D. Scida, M. Assarar, R. Ayad, Assessment of 3D moisture diffusion parameters on flax/epoxy composites, Composites Part A: Applied Science and Manufacturing. 80 (2016) 53–60. https://doi.org/10.1016/j.compositesa.2015.10.008.

[230] A. Arbelaiz, B. Fernández, J.A. Ramos, A. Retegi, R. Llano-Ponte, I. Mondragon, Mechanical properties of short flax fibre bundle/polypropylene composites: Influence of matrix/fibre modification, fibre content, water uptake and recycling, Composites Science and Technology. 65 (2005) 1582–1592. https://doi.org/10.1016/j.compscitech.2005.01.008.

[231] M.M. Lu, A.W. Van Vuure, Improving moisture durability of flax fibre composites by using non-dry fibres, Composites Part A: Applied Science and Manufacturing. 123 (2019) 301–309. https://doi.org/10.1016/j.compositesa.2019.05.029.

[232] T. Joffre, E.L.G. Wernersson, A. Miettinen, C.L. Luengo Hendriks, E.K. Gamstedt, Swelling of cellulose fibres in composite materials: Constraint effects of the surrounding matrix, Composites Science and Technology. 74 (2013) 52–59. https://doi.org/10.1016/j.compscitech.2012.10.006.

[233] T. Cadu, L. Van Schoors, O. Sicot, S. Moscardelli, L. Divet, S. Fontaine, Cyclic hygrothermal ageing of flax fibers' bundles and unidirectional flax/epoxy composite. Are bio-based reinforced composites so sensitive?, Industrial Crops and Products. 141 (2019) 111730. https://doi.org/10.1016/j.indcrop.2019.111730.

[234] A. Le Duigou, A. Bourmaud, C. Baley, In-situ evaluation of flax fibre degradation during water ageing, Industrial Crops and Products. 70 (2015) 204–210. https://doi.org/10.1016/j.indcrop.2015.03.049.

[235] Z.N. Azwa, B.F. Yousif, A.C. Manalo, W. Karunasena, A review on the degradability of polymeric composites based on natural fibres, Materials & Design. 47 (2013) 424–442. https://doi.org/10.1016/j.matdes.2012.11.025.

[236] M. Abida, F. Gehring, J. Mars, A. Vivet, F. Dammak, M. Haddar, Hygro-mechanical coupling and multiscale swelling coefficients assessment of flax yarns and flax / epoxy composites, Composites Part A: Applied Science and Manufacturing. 136 (2020) 105914. https://doi.org/10.1016/j.compositesa.2020.105914.

[237] M. Assarar, D. Scida, A. El Mahi, C. Poilâne, R. Ayad, Influence of water ageing on mechanical properties and damage events of two reinforced composite materials: Flax–fibres and glass–fibres, Materials & Design. 32 (2011) 788–795. https://doi.org/10.1016/j.matdes.2010.07.024.

[238] P. Davies, Environmental degradation of composites for marine structures: new materials and new applications, Phil. Trans. R. Soc. A. 374 (2016) 20150272. https://doi.org/10.1098/rsta.2015.0272.

[239] S. Alimuzzaman, R.H. Gong, M. Akonda, Biodegradability of nonwoven flax fiber reinforced polylactic acid biocomposites, Polymer Composites. 35 (2014) 2094–2102. https://doi.org/10.1002/pc.22871.

[240] M. Akonda, S. Alimuzzaman, D.U. Shah, A.N.M.M. Rahman, Physico-Mechanical, Thermal and Biodegradation Performance of Random Flax/Polylactic Acid and Unidirectional Flax/Polylactic Acid Biocomposites, Fibers. 6 (2018) 98. https://doi.org/10.3390/fib6040098.

[241] N.M. Barkoula, S.K. Garkhail, T. Peijs, Biodegradable composites based on flax/polyhydroxybutyrate and its copolymer with hydroxyvalerate, Industrial Crops and Products. 31 (2010) 34–42. https://doi.org/10.1016/j.indcrop.2009.08.005.

[242] T. Bayerl, M. Geith, A.A. Somashekar, D. Bhattacharyya, Influence of fibre architecture on the biodegradability of FLAX/PLA composites, International Biodeterioration & Biodegradation. 96 (2014) 18–25. https://doi.org/10.1016/j.ibiod.2014.08.005.

[243] N. Teramoto, K. Urata, K. Ozawa, M. Shibata, Biodegradation of aliphatic polyester composites reinforced by abaca fiber, Polymer Degradation and Stability. 86 (2004) 401–409. https://doi.org/10.1016/j.polymdegradstab.2004.04.026.

[244] R. Kumar, M.K. Yakubu, R.D. Anandjiwala, Biodegradation of flax fiber reinforced poly lactic acid, Express Polym. Lett. 4 (2010) 423–430. https://doi.org/10.3144/expresspolymlett.2010.53.

[245] L. Liu, J. Yu, L. Cheng, X. Yang, Biodegradability of poly(butylene succinate) (PBS) composite reinforced with jute fibre, Polymer Degradation and Stability. 94 (2009) 90–94. https://doi.org/10.1016/j.polymdegradstab.2008.10.013.

[246] G. Koolen, J. Soete, A.W. van Vuure, Interface modification and the influence on damage development of flax fibre – Epoxy composites when subjected to hygroscopic cycling, Materials Today: Proceedings. 31 (2020) S273–S279. https://doi.org/10.1016/j.matpr.2020.01.183.

[247] J. Ryckeboer, J. Mergaert, K. Vaes, S. Klammer, D.D. Clercq, J. Coosemans, H. Insam, J. Swings, A survey of bacteria and fungi occurring during composting and self-heating processes, Annals of Microbiology. 53 (2003) 349–410.

[248] A.M. Fogarty, O.H. Tuovinen, Microbiological degradation of pesticides in yard waste composting, Microbiological Reviews. 55 (1991) 225–233. https://doi.org/10.1128/mr.55.2.225-233.1991.

[249] J. Ryckeboer, J. Mergaert, J. Coosemans, K. Deprins, J. Swings, Microbiological aspects of biowaste during composting in a monitored compost bin, Journal of Applied Microbiology. 94 (2003) 127–137. https://doi.org/10.1046/j.1365-2672.2003.01800.x.

[250] S.M. Tiquia, H.C. Wan, N.F.Y. Tam, Microbial Population Dynamics and Enzyme Activities During Composting, Compost Science & Utilization. 10 (2002) 150–161. https://doi.org/10.1080/1065657X.2002.10702075.

[251] 14:00-17:00, ISO 14040:2006, ISO. (n.d.). https://www.iso.org/cms/render/live/fr/sites/isoorg/contents/data/standard/03/74/37456.html (accessed July 15, 2021).

[252] 14:00-17:00, ISO 14044:2006, ISO. (n.d.). https://www.iso.org/cms/render/live/fr/sites/isoorg/contents/data/standard/03/84/38498.html (accessed July 15, 2021).

[253] A. Le Duigou, P. Davies, C. Baley, Environmental Impact Analysis of the Production of Flax Fibres to be Used as Composite Material Reinforcement, J Biobased Mat Bioenergy. 5 (2011) 153–165. https://doi.org/10.1166/jbmb.2011.1116.

[254] N. De Beus, M. Carus, M. Barth, Carbon footprint and sustainability of different natural fibres for biocomposites and insulation material, Technical Report: Nova Institute. (2019).

[255] A. Gomez-Campos, C. Vialle, A. Rouilly, C. Sablayrolles, L. Hamelin, Flax fiber for technical textile: A life cycle inventory, Journal of Cleaner Production. 281 (2021) 125177. https://doi.org/10.1016/j.jclepro.2020.125177.

[256] A.K. Bledzki, J. Gassan, Composites reinforced with cellulose based fibres, Progress in Polymer Science. 24 (1999) 221–274. https://doi.org/10.1016/S0079-6700(98)00018-5.

[257] C. Baley, Fibres naturelles de renfort pour matériaux composites. sl: Techniques de l'ingénieur, Ref. AM. 5 (2014) 130.

[258] G. Lazorenko, A. Kasprzhitskii, V. Yavna, V. Mischinenko, A. Kukharskii, A. Kruglikov, A. Kolodina, G. Yalovega, Effect of pre-treatment of flax tows on mechanical properties and microstructure of natural fiber reinforced geopolymer composites, Environmental Technology & Innovation. 20 (2020) 101105. https://doi.org/10.1016/j.eti.2020.101105.

[259] I. Van de Weyenberg, J. Ivens, A. De Coster, B. Kino, E. Baetens, I. Verpoest, Influence of processing and chemical treatment of flax fibres on their composites, Composites Science and Technology. 63 (2003) 1241–1246. https://doi.org/10.1016/S0266-3538(03)00093-9.

[260] P. Ramesh, S. Vinodh, State of art review on Life Cycle Assessment of polymers, International Journal of Sustainable Engineering. 13 (2020) 411–422. https://doi.org/10.1080/19397038.2020.1802623.

[261] M.R. Yates, C.Y. Barlow, Life cycle assessments of biodegradable, commercial biopolymers—A critical review, Resources, Conservation and Recycling. 78 (2013) 54–66. https://doi.org/10.1016/j.resconrec.2013.06.010.

[262] M. Patel, C. Bastioli, L. Marini, E. Würdinger, Environmental assessment of bio-based polymers and natural fibres, Netherlands: Utrecht University. (2002).

[263] A.L. Duigou, P. Davies, C. Baley, Replacement of Glass/Unsaturated Polyester Composites by Flax/PLLA Biocomposites: Is It Justified?, Journal of Biobased Materials and Bioenergy. 5 (2011) 466–482. https://doi.org/10.1166/jbmb.2011.1178.

[264] K. Changwichan, T. Silalertruksa, S.H. Gheewala, Eco-Efficiency Assessment of Bioplastics Production Systems and End-of-Life Options, Sustainability. 10 (2018) 952. https://doi.org/10.3390/su10040952.

[265] M. Smidt, J. den Hollander, H. Bosch, Y. Xiang, M. van der Graaf, A. Lambin, J.-P. Duda, Life Cycle Assessment of Biobased and Fossil-Based Succinic Acid, in: J. Dewulf, S. De Meester, R.A.F. Alvarenga (Eds.), Sustainability Assessment of Renewables-Based Products, John Wiley & Sons, Ltd, Chichester, UK, 2015: pp. 307–321. https://doi.org/10.1002/9781118933916.ch20.

[266] L. Shen, M.K. Patel, Life Cycle Assessment of Polysaccharide Materials: A Review, J Polym Environ. 16 (2008) 154. https://doi.org/10.1007/s10924-008-0092-9.

[267] A. Le Duigou, C. Baley, Coupled micromechanical analysis and life cycle assessment as an integrated tool for natural fibre composites development, Journal of Cleaner Production. 83 (2014) 61–69. https://doi.org/10.1016/j.jclepro.2014.07.027.

[268] S.V. Joshi, L.T. Drzal, A.K. Mohanty, S. Arora, Are natural fiber composites environmentally superior to glass fiber reinforced composites?, Composites Part A: Applied Science and Manufacturing. 35 (2004) 371–376. https://doi.org/10.1016/j.compositesa.2003.09.016.

[269] F. Bensadoun, B. Vanderfeesten, I. Verpoest, A.W. Van Vuure, K. Van Acker, Environmental impact assessment of end of life options for flax-MAPP composites, Industrial Crops and Products. 94 (2016) 327–341. https://doi.org/10.1016/j.indcrop.2016.09.006.

[270] J. Beigbeder, L. Soccalingame, D. Perrin, J.-C. Bénézet, A. Bergeret, How to manage biocomposites wastes end of life? A life cycle assessment approach (LCA) focused on polypropylene (PP)/wood flour and polylactic acid (PLA)/flax fibres biocomposites, Waste Management. 83 (2019) 184–193. https://doi.org/10.1016/j.wasman.2018.11.012.

[271] Y. Deng, Y. Guo, P. Wu, G. Ingarao, Optimal design of flax fiber reinforced polymer composite as a lightweight component for automobiles from a life cycle assessment perspective, Journal of Industrial Ecology. (2019). https://doi.org/10.1111/jiec.12836.

[272] S. Kim, B.E. Dale, L.T. Drzal, M. Misra, Life Cycle Assessment of Kenaf Fiber Reinforced Biocomposite, J Biobased Mat Bioenergy. 2 (2008) 85–93. https://doi.org/10.1166/jbmb.2008.207.

[273] J. Martínez-Blanco, C. Lazcano, T.H. Christensen, P. Muñoz, J. Rieradevall, J. Møller, A. Antón, A. Boldrin, Compost benefits for agriculture evaluated by life cycle assessment. A review, Agron. Sustain. Dev. 33 (2013) 721–732. https://doi.org/10.1007/s13593-013-0148-7.

[274] G. Adugna, A review on impact of compost on soil properties, water use and crop productivity, Academic Research Journal of Agricultural Science and Research. 4 (2016) 93–104. https://doi.org/10.14662/ARJASR2016.010.

[275] T. Sayara, R. Basheer-Salimia, F. Hawamde, A. Sánchez, Recycling of Organic Wastes through Composting: Process Performance and Compost Application in Agriculture, Agronomy. 10 (2020) 1838. https://doi.org/10.3390/agronomy10111838.

[276] C. Gourier, A. Bourmaud, A. Le Duigou, C. Baley, Influence of PA11 and PP thermoplastic polymers on recycling stability of unidirectional flax fibre reinforced biocomposites, Polymer Degradation and Stability. 136 (2017) 1–9. https://doi.org/10.1016/j.polymdegradstab.2016.12.003.

[277] G. Ausias, A. Bourmaud, G. Coroller, C. Baley, Study of the fibre morphology stability in polypropylene-flax composites, Polymer Degradation and Stability. 98 (2013) 1216–1224. https://doi.org/10.1016/j.polymdegradstab.2013.03.006.

[278] A. Le Duigou, I. Pillin, A. Bourmaud, P. Davies, C. Baley, Effect of recycling on mechanical behaviour of biocompostable flax/poly(l-lactide) composites, Composites Part A: Applied Science and Manufacturing. 39 (2008) 1471–1478. https://doi.org/10.1016/j.compositesa.2008.05.008.

[279] K. Navare, B. Muys, K.C. Vrancken, K. Van Acker, Circular economy monitoring – How to make it apt for biological cycles?, Resources, Conservation and Recycling. 170 (2021) 105563. https://doi.org/10.1016/j.resconrec.2021.105563.

[280] M.S. Zamil, A. Geitmann, The middle lamella—more than a glue, Phys. Biol. 14 (2017) 015004. https://doi.org/10.1088/1478-3975/aa5ba5.

[281] B.W. Rosen, A simple procedure for experimental determination of the longitudinal shear modulus of unidirectional composites, Journal of Composite Materials. 6 (1972) 552–554.

[282] M.H. Akonda, H.M. El-Dessouky, Effect of Maleic-Anhydride Grafting on the Properties of Flax Reinforced Polypropylene Textile Composites, Journal of Textile Science and Technology. 05 (2019) 69. https://doi.org/10.4236/jtst.2019.54007.

[283] I. Burgert, P. Fratzl, Plants control the properties and actuation of their organs through the orientation of cellulose fibrils in their cell walls, Integr Comp Biol. 49 (2009) 69–79. https://doi.org/10.1093/icb/icp026.

[284] S. Ravati, B.D. Favis, Tunable morphologies for ternary blends with poly(butylene succinate): Partial and complete wetting phenomena, Polymer. 54 (2013) 3271–3281. https://doi.org/10.1016/j.polymer.2013.04.005.

[285] S.I. Zubairi, A. Bismarck, A. Mantalaris, The effect of surface heterogeneity on wettability of porous three dimensional (3-D) scaffolds of poly(3-hydroxybutyric acid) (PHB) and poly(3-hydroxybutyric-co-3-hydroxyvaleric acid) (PHBV), Jurnal Teknologi. 75 (2015). https://doi.org/10.11113/jt.v75.3960.

[286] J.-M. Park, S.T. Quang, B.-S. Hwang, K.L. DeVries, Interfacial evaluation of modified Jute and Hemp fibers/polypropylene (PP)-maleic anhydride polypropylene copolymers (PP-MAPP) composites using micromechanical technique and nondestructive acoustic emission, Composites Science and Technology. 66 (2006) 2686–2699. https://doi.org/10.1016/j.compscitech.2006.03.014.

[287] G. Pandey, C.H. Kareliya, R.P. Singh, A study of the effect of experimental test parameters on data scatter in microbond testing, Journal of Composite Materials. 46 (2012) 275–284. https://doi.org/10.1177/0021998311410508.

[288] K. Benzarti, L. Cangemi, F. Dal Maso, Transverse properties of unidirectional glass/epoxy composites: influence of fibre surface treatments, Composites Part A: Applied Science and Manufacturing. 32 (2001) 197–206. https://doi.org/10.1016/S1359-835X(00)00136-6.

[289] V. Mazzanti, R. Pariante, A. Bonanno, O. Ruiz de Ballesteros, F. Mollica, G. Filippone, Reinforcing mechanisms of natural fibers in green composites: Role of fibers morphology in a PLA/hemp model system, Composites Science and Technology. 180 (2019) 51–59. https://doi.org/10.1016/j.compscitech.2019.05.015.

[290] J. Gironès, J.P. Lopez, F. Vilaseca, J. Bayer R., P.J. Herrera-Franco, P. Mutjé, Biocomposites from Musa textilis and polypropylene: Evaluation of flexural properties and impact strength, Composites Science and Technology. 71 (2011) 122–128. https://doi.org/10.1016/j.compscitech.2010.10.012.

[291] M.R. Piggott, M. Ko, H.Y. Chuang, Aligned short-fibre reinforced thermosets: Experiments and analysis lend little support for established theory, Composites Science and Technology. 48 (1993) 291–299. https://doi.org/10.1016/0266-3538(93)90146-8.

[292] K. Charlet, C. Baley, C. Morvan, J.P. Jernot, M. Gomina, J. Bréard, Characteristics of Hermès flax fibres as a function of their location in the stem and properties of the derived unidirectional composites, Composites Part A: Applied Science and Manufacturing. 38 (2007) 1912–1921. https://doi.org/10.1016/j.compositesa.2007.03.006.

[293] V.M. Ghorpade, A. Gennadios, M.A. Hanna, Laboratory composting of extruded poly(lactic acid) sheets, Bioresource Technology. 76 (2001) 57–61. https://doi.org/10.1016/S0960-8524(00)00077-8.

[294] S. Alimuzzaman, R.H. Gong, M. Akonda, Nonwoven polylactic acid and flax biocomposites, Polymer Composites. 34 (2013) 1611–1619. https://doi.org/10.1002/pc.22561.

[295] B. Bax, J. Müssig, Impact and tensile properties of PLA/Cordenka and PLA/flax composites, Composites Science and Technology. 68 (2008) 1601–1607. https://doi.org/10.1016/j.compscitech.2008.01.004.

[296] F. Roussière, C. Baley, G. Godard, D. Burr, Compressive and Tensile Behaviours of PLLA Matrix Composites Reinforced with Randomly Dispersed Flax Fibres, Appl Compos Mater. 19 (2012) 171–188. https://doi.org/10.1007/s10443-011-9189-8.

[297] K. Oksman, Mechanical Properties of Natural Fibre Mat Reinforced Thermoplastic, Applied Composite Materials. 7 (2000) 403–414. https://doi.org/10.1023/A:1026546426764.

[298] J. Andersons, E. Spārniņš, R. Joffe, Stiffness and strength of flax fiber/polymer matrix composites, Polymer Composites. 27 (2006) 221–229. https://doi.org/10.1002/pc.20184.

[299] K.-P. Mieck, R. Lützkendorf, T. Reussmann, Needle-Punched hybrid nonwovens of flax and ppfibers—textile semiproducts for manufacturing of fiber composites, Polymer Composites. 17 (1996) 873–878. https://doi.org/10.1002/pc.10680.

[300] B. Neckář, D. Das, Modelling of fibre orientation in fibrous materials, The Journal of The Textile Institute. 103 (2012) 330–340. https://doi.org/10.1080/00405000.2011.578357.

[301] M. Miao, M. Shan, Highly aligned flax/polypropylene nonwoven preforms for thermoplastic composites, Composites Science and Technology. 71 (2011) 1713–1718. https://doi.org/10.1016/j.compscitech.2011.08.001.

[302] H. Krenchel, Fibre reinforcement; theoretical and practical investigations of the elasticity and strength of fibre-reinforced materials, (1964).

[303] C. Kergariou, A.L. Duigou, V. Popineau, V. Gager, A. Kervoelen, A. Perriman, H. Saidani-Scott, G. Allegri, T.H. Panzera, F. Scarpa, Measure of porosity in flax fibres reinforced polylactic acid biocomposites, Composites Part A: Applied Science and Manufacturing. (2020) 106183. https://doi.org/10.1016/j.compositesa.2020.106183.

[304] P. Evon, B. Barthod-Malat, M. Grégoire, G. Vaca-Medina, L. Labonne, S. Ballas, T. Véronèse, P. Ouagne, Production of fiberboards from shives collected after continuous fiber mechanical extraction

from oleaginous flax, Journal of Natural Fibers. 16 (2019) 453–469. https://doi.org/10.1080/15440478.2017.1423264.

[305] L. Nuez, J. Beaugrand, D.U. Shah, C. Mayer-Laigle, A. Bourmaud, P. D'Arras, C. Baley, The potential of flax shives as reinforcements for injection moulded polypropylene composites, Industrial Crops and Products. 148 (2020) 112324. https://doi.org/10.1016/j.indcrop.2020.112324.

[306] J.C. Halpin, N.J. Pagano, The Laminate Approximation for Randomly Oriented Fibrous Composites, Journal of Composite Materials. 3 (1969) 720–724. https://doi.org/10.1177/002199836900300416.

[307] C. Baley, A. Le Duigou, C. Morvan, A. Bourmaud, Tensile properties of flax fibers, in: Handbook of Properties of Textile and Technical Fibres, Elsevier, 2018: pp. 275–300. https://doi.org/10.1016/B978-0-08-101272-7.00008-0.

[308] C. Baley, A. Kervoëlen, A. Le Duigou, C. Goudenhooft, A. Bourmaud, Is the low shear modulus of flax fibres an advantage for polymer reinforcement?, Materials Letters. 185 (2016) 534–536. https://doi.org/10.1016/j.matlet.2016.09.067.

[309] J. Holbery, D. Houston, Natural-fiber-reinforced polymer composites in automotive applications, JOM. 58 (2006) 80–86. https://doi.org/10.1007/s11837-006-0234-2.

[310] S. Alix, E. Philippe, A. Bessadok, L. Lebrun, C. Morvan, S. Marais, Effect of chemical treatments on water sorption and mechanical properties of flax fibres, Bioresource Technology. 100 (2009) 4742–4749. https://doi.org/10.1016/j.biortech.2009.04.067.

[311] F. Gouanvé, S. Marais, A. Bessadok, D. Langevin, M. Métayer, Kinetics of water sorption in flax and PET fibers, European Polymer Journal. 43 (2007) 586–598. https://doi.org/10.1016/j.eurpolymj.2006.10.023.

[312] W.V. Srubar, C.W. Frank, S.L. Billington, Modeling the kinetics of water transport and hydroexpansion in a lignocellulose-reinforced bacterial copolyester, Polymer. 53 (2012) 2152–2161. https://doi.org/10.1016/j.polymer.2012.03.036.

[313] Z. El Hachem, A. Célino, G. Challita, M.-J. Moya, S. Fréour, Hygroscopic multi-scale behavior of polypropylene matrix reinforced with flax fibers, Industrial Crops and Products. 140 (2019) 111634. https://doi.org/10.1016/j.indcrop.2019.111634.

[314] L. Van Schoors, T. Cadu, S. Moscardelli, L. Divet, S. Fontaine, O. Sicot, Why cyclic hygrothermal ageing modifies the transverse mechanical properties of a unidirectional epoxy-flax fibres composite?, Industrial Crops and Products. 164 (2021) 113341. https://doi.org/10.1016/j.indcrop.2021.113341.

[315] A. Le Duigou, A. Bourmaud, P. Davies, C. Baley, Long term immersion in natural seawater of Flax/PLA biocomposite, Ocean Engineering. 90 (2014) 140–148. https://doi.org/10.1016/j.oceaneng.2014.07.021.

[316] J. THIBAULT, AUTOMATISATION DU DOSAGE DES SUBSTANCES PECTIQUES PAR LA METHODE AU METAHYDROXYDIPHENYL, AUTOMATISATION DU DOSAGE DES SUBSTANCES PECTIQUES PAR LA METHODE AU METAHYDROXYDIPHENYL. (1979).

[317] A.B. Blakeney, P.J. Harris, R.J. Henry, B.A. Stone, A simple and rapid preparation of alditol acetates for monosaccharide analysis, Carbohydrate Research. 113 (1983) 291–299. https://doi.org/10.1016/0008-6215(83)88244-5.

[318] K.L. Johnson, J.A. Greenwood, An Adhesion Map for the Contact of Elastic Spheres, Journal of Colloid and Interface Science. 192 (1997) 326–333. https://doi.org/10.1006/jcis.1997.4984.

[319] W. Wang, M. Sain, P.A. Cooper, Study of moisture absorption in natural fiber plastic composites, Composites Science and Technology. 66 (2006) 379–386. https://doi.org/10.1016/j.compscitech.2005.07.027.

[320] M. Deroiné, A. Le Duigou, Y.-M. Corre, P.-Y. Le Gac, P. Davies, G. César, S. Bruzaud, Accelerated ageing of polylactide in aqueous environments: Comparative study between distilled water and seawater, Polymer Degradation and Stability. 108 (2014) 319–329. https://doi.org/10.1016/j.polymdegradstab.2014.01.020.

[321] A. Thuault, S. Eve, D. Blond, J. Bréard, M. Gomina, Effects of the hygrothermal environment on the mechanical properties of flax fibres, Journal of Composite Materials. 48 (2014) 1699–1707. https://doi.org/10.1177/0021998313490217.

[322] O. Arnould, D. Siniscalco, A. Bourmaud, A. Le Duigou, C. Baley, Better insight into the nano-mechanical properties of flax fibre cell walls, Industrial Crops and Products. 97 (2017) 224–228. https://doi.org/10.1016/j.indcrop.2016.12.020.

[323] J.A. Nairn, Thermoelastic analysis of residual stresses in unidirectional, high-performance composites, Polym. Compos. 6 (1985) 123–130. https://doi.org/10.1002/pc.750060211.

[324] A. Chilali, M. Assarar, W. Zouari, H. Kebir, R. Ayad, Analysis of the hydro-mechanical behaviour of flax fibre-reinforced composites: Assessment of hygroscopic expansion and its impact on internal stress, Composite Structures. 206 (2018) 177–184. https://doi.org/10.1016/j.compstruct.2018.08.037.

[325] B. Djellouli, W. Zouari, M. Assarar, R. Ayad, Analysis of the hygroscopic and hygroelastic behaviours of water aged flax-epoxy composite, Composite Structures. 265 (2021) 113692. https://doi.org/10.1016/j.compstruct.2021.113692.

[326] A. Magurno, Vegetable fibres in automotive interior components, Die Angewandte Makromolekulare Chemie. 272 (1999) 99–107. https://doi.org/10.1002/(SICI)1522-9505(19991201)272:1<99::AID-APMC99>3.0.CO;2-C.

[327] A. Bourmaud, A. Le Duigou, C. Baley, What is the technical and environmental interest in reusing a recycled polypropylene–hemp fibre composite?, Polymer Degradation and Stability. 96 (2011) 1732–1739. https://doi.org/10.1016/j.polymdegradstab.2011.08.003.

[328] A. Bourmaud, C. Baley, Investigations on the recycling of hemp and sisal fibre reinforced polypropylene composites, Polymer Degradation and Stability. 92 (2007) 1034–1045. https://doi.org/10.1016/j.polymdegradstab.2007.02.018.

[329] A.R. Dickson, D. Even, J.M. Warnes, A. Fernyhough, The effect of reprocessing on the mechanical properties of polypropylene reinforced with wood pulp, flax or glass fibre, Composites Part A: Applied Science and Manufacturing. 61 (2014) 258–267. https://doi.org/10.1016/j.compositesa.2014.03.010.

[330] N. Renouard, J. Mérotte, A. Kervoëlen, K. Behlouli, C. Baley, A. Bourmaud, Exploring two innovative recycling ways for poly-(propylene)-flax non wovens wastes, Polymer Degradation and Stability. 142 (2017) 89–101. https://doi.org/10.1016/j.polymdegradstab.2017.05.031.

[331] A. Bourmaud, M. Fazzini, N. Renouard, K. Behlouli, P. Ouagne, Innovating routes for the reused of PP-flax and PP-glass non woven composites: A comparative study, Polymer Degradation and Stability. 152 (2018) 259–271. https://doi.org/10.1016/j.polymdegradstab.2018.05.006.

[332] M. Eriksen, L.C.M. Lebreton, H.S. Carson, M. Thiel, C.J. Moore, J.C. Borerro, F. Galgani, P.G. Ryan, J. Reisser, Plastic Pollution in the World's Oceans: More than 5 Trillion Plastic Pieces Weighing over 250,000 Tons Afloat at Sea, PLoS ONE. 9 (2014) e111913. https://doi.org/10.1371/journal.pone.0111913.

[333] G. Kale, T. Kijchavengkul, R. Auras, M. Rubino, S.E. Selke, S.P. Singh, Compostability of Bioplastic Packaging Materials: An Overview, Macromolecular Bioscience. 7 (2007) 255–277. https://doi.org/10.1002/mabi.200600168.

[334] M. Agarwal, K.W. Koelling, J.J. Chalmers, Characterization of the Degradation of Polylactic Acid Polymer in a Solid Substrate Environment, Biotechnol. Prog. 14 (1998) 517–526. https://doi.org/10.1021/bp980015p.

[335] S. Yang, Z.-H. Wu, W. Yang, M.-B. Yang, Thermal and mechanical properties of chemical crosslinked polylactide (PLA), Polymer Testing. 27 (2008) 957–963. https://doi.org/10.1016/j.polymertesting.2008.08.009.

[336] G. Kale, R. Auras, S.P. Singh, R. Narayan, Biodegradability of polylactide bottles in real and simulated composting conditions, Polymer Testing. 26 (2007) 1049–1061. https://doi.org/10.1016/j.polymertesting.2007.07.006.

[337] Y.-X. Weng, L. Wang, M. Zhang, X.-L. Wang, Y.-Z. Wang, Biodegradation behavior of P(3HB,4HB)/PLA blends in real soil environments, Polymer Testing. 32 (2013) 60–70. https://doi.org/10.1016/j.polymertesting.2012.09.014.

[338] H.-S. Kim, H.-J. Kim, J.-W. Lee, I.-G. Choi, Biodegradability of bio-flour filled biodegradable poly(butylene succinate) bio-composites in natural and compost soil, Polymer Degradation and Stability. 91 (2006) 1117–1127. https://doi.org/10.1016/j.polymdegradstab.2005.07.002.

[339] G. Koronis, A. Silva, M. Fontul, Green composites: A review of adequate materials for automotive applications, Composites Part B: Engineering. 44 (2013) 120–127. https://doi.org/10.1016/j.compositesb.2012.07.004.

[340] F.P. La Mantia, M. Morreale, Green composites: A brief review, Composites Part A: Applied Science and Manufacturing. 42 (2011) 579–588. https://doi.org/10.1016/j.compositesa.2011.01.017.

[341] M.P.M. Dicker, P.F. Duckworth, A.B. Baker, G. Francois, M.K. Hazzard, P.M. Weaver, Green composites: A review of material attributes and complementary applications, Composites Part A: Applied Science and Manufacturing. 56 (2014) 280–289. https://doi.org/10.1016/j.compositesa.2013.10.014.

[342] S. Alimuzzaman, R.H. Gong, M. Akonda, Biodegradability of nonwoven flax fiber reinforced polylactic acid biocomposites, Polymer Composites. 35 (2014) 2094–2102. https://doi.org/10.1002/pc.22871.

[343] K. Oksman, M. Skrifvars, J.-F. Selin, Natural fibres as reinforcement in polylactic acid (PLA) composites, Composites Science and Technology. 63 (2003) 1317–1324. https://doi.org/10.1016/S0266-3538(03)00103-9.

[344] S. Ochi, Mechanical properties of kenaf fibers and kenaf/PLA composites, Mechanics of Materials. 40 (2008) 446–452. https://doi.org/10.1016/j.mechmat.2007.10.006.

[345] C.A. Woolnough, T. Charlton, L.H. Yee, M. Sarris, L.J.R. Foster, Surface changes in polyhydroxyalkanoate films during biodegradation and biofouling, Polym. Int. 57 (2008) 1042–1051. https://doi.org/10.1002/pi.2444.

[346] K. Cho, J. Lee, K. Kwon, Hydrolytic degradation behavior of poly(butylene succinate)s with different crystalline morphologies, Journal of Applied Polymer Science. 79 (2001) 1025–1033.

[347] J.M. Lee, J.J. Pawlak, J.A. Heitmann, Longitudinal and concurrent dimensional changes of cellulose aggregate fibrils during sorption stages, Materials Characterization. 61 (2010) 507–517. https://doi.org/10.1016/j.matchar.2010.02.007.

[348] J. Mussig, H. Fisher, N. Graupner, A. FDrieling, Testing methods for measuring physical and mechancial fibre properties (plant and animal fibres), Industrial Application of Natural Fibres: Structure, Properties and Technical Application. John Wiley & Sons, Chichester, United Kingdom. (2010) 269–309.

[349] P.V. Joseph, M.S. Rabello, L.H.C. Mattoso, K. Joseph, S. Thomas, Environmental effects on the degradation behaviour of sisal fibre reinforced polypropylene composites, Composites Science and Technology. 62 (2002) 1357–1372. https://doi.org/10.1016/S0266-3538(02)00080-5.

[350] C. Björdal, T. Nilsson, S. Bardage, Three-dimensional visualisation of bacterial decay in individual tracheids of Pinus sylvestris, 59 (2005) 178–182. https://doi.org/10.1515/HF.2005.028.

DOCTORAT BRETAGNE LOIRE SCIENCES POUR L'INGENIEUR

Université Bretagne Sud

Titre : Caractérisation multi-échelle de composites de lin biodégradables par le biais d'études structurelles, mécaniques et de vieillissement

Mots clés : Biocomposites, Fibres de lin, Propriétés mécaniques, Microstructure, Vieillissement

Résumé : La production des matériaux et la gestion des déchets sont une cause importante de nos défis environnementaux. Les fibres de lin sont des ressources biodégradables et renouvelables tout en présentant des propriétés mécaniques spécifiques, idéales pour le renforcement des composites. En outre, la transition vers des thermoplastiques biodégradables comme matrice pour les composites renforcés lin conduit à des matériaux entièrement biodégradables. Ce travail vise à étudier la faisabilité des composites thermoplastiques biodégradables à fibres de lin. Les polymères poly-(lactide) (PLA), poly-(butylène-succinate) (PBS) et un poly-(hydroxy alkanoate) (PHA), renforcés par des préformes en lin, sont étudiés dans cette thèse. Le potentiel mécanique de ces composites biodégradables est étudié à travers une approche multi-échelle, de l'adhérence aux propriétés mécaniques du composite. L'influence de la mésostructure des plis sur leurs propriétés mécaniques est ensuite analysée, en particulier la teneur en porosité, l'orientation des fibres et la présence d'anas. Enfin, en se concentrant sur l'évolution dans le temps de leur mésostructure et de leurs propriétés mécaniques, le vieillissement des composites biodégradables dans des environnements sévères est abordé : six semaines dans différentes conditions hygroscopiques et enfouis six mois dans du compost de jardin. L'ambitieux paradoxe de tels composites est en effet de conserver de bonnes propriétés mécaniques, pendant leur phase d'usage et jusqu'à leur biodégradation. Ce travail contribue à l'étude des composites biodégradables en mettant en évidence à différentes échelles leur potentiel mécanique et leurs mécanismes de dégradation.

Title: Multiscale characterisation of biodegradable flax composites through structural, mechanical and ageing investigations

Keywords: Biocomposites, Flax fibres, Mechanical properties, Microstructure, Ageing

Abstract: The production and disposal of materials is an important source of our environmental challenges. Flax fibres are interesting reinforcements for polymer composites, as they are biodegradable, renewably-sourced, and retain low density with good mechanical properties. Furthermore, transitioning to biodegradable thermoplastics as matrices for flax composites will lead to fully-biodegradable composites. This work aims to investigate the feasibility of biodegradable flax thermoplastic composites. Poly-(lactide) (PLA), poly-(butylene-succinate) (PBS) and poly-(hydroxy alkanoate) (PHA) polymers are considered in this thesis, binding a range of flax fibre preforms. The mechanical potential of these biodegradable composites is investigated through a multi-scale approach, from fibre-matrix adherence to composite mechanical properties. The influence of the ply mesostructure on composite mechanical properties is investigated, particularly porosity content, fibre orientation, and the presence of shives. Finally, the ageing of biodegradable composite is tackled, focussing on the evolution their mesostructure and mechanical properties over time in harsh environments: six weeks under hygroscopic conditions and six months buried in a garden compost. The challenging paradox that needs to be addressed is to maintain good mechanical properties over time during service, until their biodegradation upon disposal. This work contributes to the study of biodegradable composites by highlighting their mechanical potential and degradation mechanisms at several scales.